

**CRANFIELD UNIVERSITY**

**W M FAKANYA**

**DEVELOPMENT OF MULTI MARKER  
ELECTROCHEMICAL IMMUNOSENSORS FOR  
CARDIOVASCULAR DISEASE DETECTION**

**CRANFIELD HEALTH**

**PhD THESIS**

**CRANFIELD UNIVERSITY**

Cranfield Health

Advanced Diagnostics and Sensors

**PhD Thesis**

Academic Years 2009- 2012

**Wellington M Fakanya**

**Development of Multi Marker Electrochemical  
Immunosensors for Cardiovascular Disease  
Detection**

Supervisor: Dr Ibtisam E. Tothill

August 2012

This thesis is submitted in partial fulfilment of the requirements for  
the degree of Doctor of Philosophy

© Cranfield University 2012. All rights reserved. No part of this publication may  
be reproduced without the written permission of the copyright owner

## ABSTRACT

Cardiovascular disease (CVD) is the world's biggest killer, globally accounting for over 17,5 million deaths annually. Almost half of these deaths are caused by acute myocardial infarction. It is an umbrella term that encompasses several medical conditions associated with the heart and the circulatory system. It is important to detect patients with high risk of acute myocardial infarction quickly. This can help in cutting costs by screening the hospital admissions process and focusing resources to those that are specifically at risk. Biomarkers and biosensors are playing a crucial role in the diagnostic revolution of cardiovascular disease. Although significant studies have been done on electrochemically transduced biosensors for detecting CVDs, of late they have had limited commercial success. However, advances in interrelated research areas have made it possible for faster, accurate, portable and environmentally friendly electrochemical diagnostic devices to be made. This project aims to:

- Develop Immunoassays for two cardiac biomarkers which are CRP and cardiac troponin T
- Integrate the immunoassays on to screen-printed gold electrodes (SPGE) to make electrochemical immunosensors.
- Optimise the immunosensors to produce rapid, sensitive and specific devices
- Evaluate the performance of the optimised immunosensors compared to other alternative detection devices.

Some aspects of the fabrication process of screen-printed gold electrodes were investigated particularly ink compositions and curing techniques. It was found that the quality of the carbon ink affects the performance of the electrodes and that curing electrodes with conventional oven drying gave better performance to high throughput infra-red drying. Initially a plate based ELISA assay for CRP was developed before the assay was transferred onto screen-printed gold electrodes.

Antibodies were immobilised using passive adsorption and after optimisation of the screen-printed immunosensor, it managed to detect CRP with a limit of detection of  $0.52 \mu\text{g mL}^{-1}$  with a linear range up to  $20 \mu\text{g mL}^{-1}$  in spiked serum. This was within diagnostically relevant range. Comparison of the assay with a commercial alternative gave good correlation ( $R^2$  value of 0.99). A second immunosensor was developed for cardiac Troponin T (cTnT) using similar screen-printed gold electrodes. In this immunosensor, the use of self-assembled monolayers (SAMs) was employed to assist in covalent immobilisation, orientation and preservation of the capture antibody. A method for depositing the 11-mercaptoundecanoic acid (11-MUA) SAMs on the gold working electrode without compromising functionality of the other electrodes was developed. It was found that the use of self-assembled monolayers increased the sensitivity of the assay enabling it to decrease the limit of detection on the immunosensor from  $2.12 \text{ ng mL}^{-1}$  (passive adsorption) to  $1.14 \text{ ng mL}^{-1}$  (SAM assisted covalent immobilisation). It was also found that the use of SAMs enhanced the shelf life of the immobilised antibody compared to those passively adsorbed.

The use of gold nanoparticles to amplify the immunosensor signal was explored. This further improved the sensitivity of the cTnT assay. The final immunosensor setup comprising the use of 11-MUA self-assembled monolayers and 60 nm conjugated gold nanoparticles enabled the detection of cTnT with a limit of detection of  $0.51 \text{ ng mL}^{-1}$  in buffer and  $0.58 \text{ ng mL}^{-1}$  in 75% serum samples. This assay was benchmarked against a hospital analyser and a quartz crystal microbalance biosensor (QCM-1). It gave comparable results with correlation values of 0.99 and 0.95. The two developed immunosensors for CRP and cTnT can easily be integrated onto an electrochemical analyser to make a multi-marker electrochemical immunosensor for detecting cardiovascular diseases.



## ACKNOWLEDGEMENTS

I would like to express my sincere gratitude to Dr Ibatsam E Tothill for her continuous guidance, support and resourcefulness throughout the whole project. Special thanks to Professor David Cullen, Dr Huijun Zhu and Professor Naresh Magan for their delightful contributions, constructive criticism and analytical insights, during project reviews. I am grateful to DuPont Ltd, microcircuit materials department for their endless supply of screen printed electrodes and Dr WS Wassif, Consultant/Head of Department of Clinical Biochemistry and Metabolic Medicine Bedford Hospital NHS Trust for approving laboratory analysis of our samples.

I would like to thank Michael Binder for helping me see the world differently and for his friendship and advice. I would also like to thank Frederique Vanheusden for his friendship and help with the QCM-1, and all my Cranfield Health colleagues particularly, Mahomad Elras, Sejakhosi Mohale, Yildez Uludang, Faridah Salam, Zeynep Altintas and all those who were always there to share with me my Cranfield Health experience.

I would like to thank my son Mambo and my wife Margaret for their enormous patience and motivation. Without their encouragement and understanding, it would have been difficult to finish this work. Finally and most importantly, I would like to thank my parents Livingstone and Tamisa Fakanya who without complaint have always nurtured and cultivated my dreams to become reality including this project.

# TABLE OF CONTENTS

<b>ABSTRACT</b> .....	i
<b>ACKNOWLEDGEMENTS</b> .....	iii
<b>LIST OF FIGURES</b> .....	viii
<b>LIST OF ABBREVIATIONS</b> .....	xvi
<b>1 Introduction and Literature Review</b> .....	2
1.1 An Overview of Cardiovascular Disease.....	2
1.1.1 Statistics.....	2
1.1.2 Types of Cardiovascular Disease.....	4
1.1.3 General Symptoms and Risk Factors for Cardiovascular Disease.....	6
1.1.4 Modifiable Risk Factors.....	6
1.1.5 Non-Modifiable Risk Factors.....	7
1.1.6 Chest Pain Symptoms for CVD.....	8
1.1.7 Other Symptoms for CVD.....	9
1.2 Pathophysiology of Cardiovascular Disease.....	9
1.2.1 Atherosclerosis and Cardiovascular Disease.....	9
1.2.2 Inflammation and Cardiovascular Disease.....	11
1.2.3 Endothelial dysfunction.....	12
1.2.4 Growth and Development of an Atherosclerotic Lesion.....	13
1.2.5 Plaque Rupture.....	14
1.3 Biomarkers for Cardiovascular Diseases.....	15
1.3.1 General Introduction.....	15
1.3.2 Properties of an Effective Cardiac Biomarker.....	16
1.3.3 Biomarkers for Inflammation.....	18
1.3.4 Early Biomarkers for Myocyte Injury.....	22
1.3.5 Cardiac Troponins.....	23
1.3.6 Other Biomarkers.....	25
1.3.7 New Biomarkers.....	25
1.4 Current Methods for diagnosis of CVDs.....	27
1.4.1 Background.....	27
1.4.2 Electrocardiography.....	28
1.4.3 Imaging Techniques.....	30
1.4.4 Immuno Techniques.....	32
1.5 Biosensors.....	37
1.5.1 Introduction to biosensors.....	37
1.5.2 Optical Immunosensors.....	39
1.5.3 Piezoelectric/acoustic Immunosensors.....	42
1.5.4 Electrochemical Immuno-sensors.....	43
1.5.5 Detection of Cardiovascular Diseases using Biosensors.....	45
1.6 Aims and Objectives.....	49

1.6.1 Aims .....	49
1.6.2 Objectives .....	50
2 Screen Printed Electrodes, Fabrication and Characterisation .....	53
2.1 Introduction to Screen-Printed Gold Electrodes (SPGE).....	53
2.1.1 Characterisation of Screen-Printed Electrodes .....	59
2.1.2 Aims and Objectives.....	62
2.2 Materials .....	63
2.3 Methods .....	65
2.3.1 Cyclic Voltammetry for investigating different Inks .....	65
2.3.2 Cyclic Voltammetry for investigating different Curing Methods .....	66
2.3.3 Environmental Scanning Electron Microscope .....	67
2.3.4 Characterization of electrodes using Immuno Assay.....	67
2.4 Results and Discussion.....	68
2.4.1 Performance of Different Electrode Ink Compositions.....	70
2.4.2 Effect of Different Electrode Ink Curing Techniques.....	75
2.5 Conclusions .....	81
3 Development of an Electrochemical Immunosensor for C-Reactive Protein .	84
3.1 Introduction .....	84
3.1.1 Electrochemical Immunosensors .....	84
3.1.2 Role of Antibodies in Immunosensors .....	87
3.1.3 Immuno Assay Development .....	88
3.2 Materials .....	94
3.3 Methods .....	95
3.3.1 Optimisation of the ELISA micro-plate based assay .....	95
3.3.2 Optimisation of the Coating Antibody .....	95
3.3.3 Method of Optimising the CRP Assay on Screen Printed Gold Electrodes .....	98
3.3.4 Surface Modification of the Gold Electrode with Thiol group Self Assembled Monolayers (SAMs) .....	100
3.3.5 Characterisation of the chemically modified working electrode .....	101
3.3.6 Surface modification evaluation using immunoassay .....	103
3.3.7 Optimisation of the assay for antigen addition.....	104
3.3.8 SPGE Calibration Plot and Interpretation of Result.....	106
3.3.9 Comparing the Performance of the SPGE and the Optimised ELISA with a Commercial ELISA.....	107
3.3.10 Cross Reactivity Studies .....	108
3.4 Results and Discussion.....	108
3.4.1 Development of an micro plate based ELISA assay .....	108
3.4.2 Investigating the ELISA Coating Antibody Concentration.....	109
3.4.3 Optimising the Detection Antibody for CRP.....	110
3.4.4 Development of the Screen-printed immuno-sensor for CRP .....	115

3.4.5 Optimised CRP Assay on Screen-Printed Gold Electrodes.....	120
3.4.1 Exploring the use of self-assembled monolayers to enhance assay sensitivity.....	121
3.4.2 Immunoassay for Evaluating Different Immobilisation Techniques	124
3.4.1 Comparison of developed immunosensor with the commercial and Optimised ELISAs .....	127
3.5 Conclusions .....	131
4 The Development of a Gold Nanoparticle Enhanced Immunosensor for Cardiac Troponin T.....	135
4.1 Introduction .....	135
4.2 Materials .....	139
4.3 Methods .....	141
4.3.1 Preliminary characterisation of the antibodies performance using an ELISA assay.....	141
4.3.2 Method of Optimising the Cardiac Troponin T Assay on the Gold Electrodes .....	143
4.3.3 The use of self-assembled monolayers (SAMs) for capture antibody immobilisation .....	144
4.3.4 The use of gold nanoparticles in signal enhancement.....	145
4.3.5 The use of Quartz Crystal Microbalance to Investigate the Attachment of the Gold Nano particles to the Detection Antibodies .....	147
4.3.6 Immobilisation of the capture antibody on Modified surfaces of SPGE and QCM-1 chips. ....	148
4.3.7 SPGE Optimised immunosensor protocol .....	149
4.3.8 Detection of cTnT in commercial serum .....	150
4.4 Results and Discussion.....	151
4.4.1 Preliminary microplate based studies.....	151
4.4.2 Development of the screen printed immunosensor for cardiac Troponin T.....	155
4.4.3 Exploring the use of self-assembled monolayers to enhance assay sensitivity through covalent immobilisation.....	158
4.4.4 Exploring the use of gold nano-particles to increase assay sensitivity through enhanced signal.....	163
4.4.5 Generation of a standard curve using 75% serum on the optimised gold nanoparticle immunosensor .....	167
4.4.1 Comparative summary of the different assay procedures used on SPGEs .....	169
4.4.2 Detection of cTnT in commercial serum samples using the developed Immunosensor. ....	171
4.5 Conclusions .....	174
5 Stability of the Immobilised Antibodies on the Immunosensor Surface .....	178

5.1 Introduction .....	178
5.1.1 Types of biosensor stability .....	178
5.1.2 Mechanisms of the Inactivation and Preservation of Proteins .....	179
5.2 Materials .....	181
5.3 Methods .....	182
5.3.1 Method for preparing immunosensors using passive adsorption ...	183
5.3.2 Method for preserving immunosensors using covalent immobilisation .....	184
5.3.3 Method for preserving Immunosensors using Stabiliguard® .....	184
5.3.4 Batching and Storage of Immunosensors .....	185
5.3.5 Analysis of the Functionality of the Immobilised Antibodies .....	185
5.4 Results and Discussion .....	186
5.4.1 Stabilisation of immobilised antibodies .....	186
5.4.1 The environmental conditions .....	189
5.5 Conclusion .....	193
<b>6 Final Discussion and Conclusions .....</b>	<b>196</b>
6.1.1 Overview .....	196
6.1.2 Fabrication and Characterisation of Screen-printed Electrodes .....	196
6.1.3 Development of an Electrochemical Immunosensor for C-Reactive Protein .....	198
6.1.4 The Development of a Gold Nanoparticle Enhanced Immunosensor for Cardiac Troponin T .....	201
6.2 Future Work .....	205
6.3 Final Conclusions .....	207
<b>REFERENCES .....</b>	<b>209</b>

## LIST OF FIGURES

Figure 1.1: A map of the world showing numbers of deaths from coronary heart disease (W.H.O, 2011b).....	3
Figure 1.2: Global number of deaths per year due to different types of cardiovascular diseases and their age distribution (Open University, 2010). .....	3
Figure 1.3: Different types of cardiovascular diseases and their origin (W.H.O, 2011a). ....	5
Figure 1.4: Different stages of atherosclerosis (Ellertsen, 2011). ....	14
Figure 1.5: Structure of CRP fragment and the chemical structure (Science Photo Library, 2012). ....	18
Figure 1.6: CRP as a risk factor for cardiovascular disease through several stages of atherogenesis (Bisoendial <i>et al.</i> , 2010). ....	19
Figure 1.7: Summary of pathophysiology of cardiovascular diseases and potential cardiac markers including CRP (Apple <i>et al.</i> , 2005). ....	20
Figure 1.8: The schematic diagram showing the interaction of cardiac Troponins with actin and myosin (Brighthead, 2009). ....	24
Figure 1.9: The electrocardiogram at different heart activity (Muskopf, 2012)..	29
Figure 1.10: Angiogram showing a blocked coronary artery left and unblocked after surgery right (Heuser, 1999). ....	31
Figure 1.11: Schematic diagram of the CT scan showing its major components (Thim <i>et al.</i> , 2008). ....	32
Figure 1.12: Schematic diagram of the immunoglobulin structure (Invitrogen, 2012). ....	34
Figure 1.13: Diagram showing direct immunoassay set up (AMRITA, 2012). ..	35
Figure 1.14: Diagram showing indirect immunoassay set up (AMRITA, 2012). ..	35
Figure 1.15: Diagram showing indirect sandwich immunoassay set up (AMRITA, 2012). ....	36
Figure 1.16: Schematic diagram showing components of a biosensor (Solanki, 2011). ....	38
Figure 1.17: The working mechanism of a surface plasmon resonance (SPR) biosensor (Sabban, 2011). ....	41
Figure 1.18: The Triage® cardiac panel system is able to detect myoglobin, creatine kinase-MB fraction and cTnI from whole blood, Biosense Inc (2009). .....	47

Figure 1.19: The iSTAT® system for POC detection of cTnI (Abbot, 2011). ....	48
Figure 1.20: Flow chart outlining the different phases of work carried out in this study. ....	51
Figure 2.1: Schematic representation of the screen-printing process (Hobby, 1997). ....	55
Figure 2.2: The production of screen-printed electrodes on an industrial scale (Hobby, 1997). ....	56
Figure 2.3: Screen-printed electrodes used in this project. ....	57
Figure 2.4: Cyclic voltammogram recorded for a reversible redox in single potential cycle $E_{pa}$ = anodic peak potential; $E_{pc}$ = cathodic peak potential; $I_{pa}$ = anodic peak current; $I_{pc}$ = cathodic peak current. (Bard, 2001). ....	61
Figure 2.5: Voltammogram for the characterisation of the electrode screen-printed electrodes. Cyclic voltammetry using 100 $\mu$ L of 1mM $K_3[Fe(CN)_6]$ in 0.1M KCl pipetted on the gold working electrode, scan rates 30, 60, 90, 120 $mV s^{-1}$ were used scanning 3 cycles from -0.5 to 0.8 V relative to Ag/AgCl reference. (A) JA electrode, (B) JC electrode, and (C) the JD electrode...	71
Figure 2.6: Summary of the electrochemical performance of JA, JC, and JD electrodes. Cyclic voltammetry using 100 $\mu$ L of 1mM $K_3[Fe(CN)_6]$ in 0.1M KCl pipetted on the gold working electrode, scan rates 30, 60, 90, 120 $mV s^{-1}$ were used scanning 3 cycles from -0.5 to 0.8 V relative to Ag/AgCl reference, n=3, maximum CV=9.8%, Bars = standard deviation. ....	72
Figure 2.7: The Immuno assay results showing the advantage of using the JD electrode composition compared to the JC and JA variants. Electrochemical immunoassay for CRP was integrated on the different electrodes to make immunosensors and peak electrochemical signals at different CRP concentrations were used to assess electrode performance n=3. maximum CV=11.4%, Bars = standard deviation. ....	74
Figure 2.8: Voltammogram showing electrochemical performance of an alternatively dried sensor. Cyclic voltammetry using 100 $\mu$ L of 1mM $K_3[Fe(CN)_6]$ in 0.1M KCl pipetted on the gold working electrode, scan rates 20, 40, 60, 80, 100 $mV s^{-1}$ were used scanning 3 cycles from -0.8 to 0.8 V relative to Ag/AgCl reference. (A) alternatively dried electrodes, (B) Infrared dried electrode. ....	76
Figure 2.9: Summary of the Investigating effect of Alternative vs Infra-red drying techniques The R <sup>2</sup> values were obtained using a plot of the square root of the scan rates used in Figure 2.8, n=3, maximum CV=9.8%, Bars = Standard deviation. ....	77
Figure 2.10: The ESEM results showing the image and composition analysis of the gold surface of (a) alternatively dried sensors and (b) infrared dried	

sensors. The element weight information is an average of three spots on a single sensor for each drying technique. ....	78
Figure 2.11: The Immuno assay results showing the advantage of alternatively dried electrodes over infrared. The differently cured electrodes were transformed to immunosensors by integrating a CRP immunoassay; the high peak currents obtained from detecting several CRP concentrations were used to identify the best curing method. n=3, CV=11.2%, Bars =standard deviation. ....	80
Figure 3.1: Overview of the protein adsorption mechanisms on the sensor surface (Davies, 2007 ). ....	89
Figure 3.2 An Illustration showing the three components of an ordinary thiol based self-assembled monolayer (Srisombat <i>et al.</i> , 2011) ....	90
Figure 3.3: Schematic diagrams for (A) Sandwich immuno assay setup for the C-reactive protein on a screen-printed gold electrode. The antibodies are immobilised passively and the detection antibodies are conjugated with HRP. In diagram (B) the combination of TMB and H <sub>2</sub> O <sub>2</sub> with HRP enzymes results in a reaction with indirect electron transfer on the gold working electrode surface. ....	93
Figure 3.4: The chemical structures of the two compounds used to modify the surface of the gold working electrodes through creating self-assembled monolayers SAMs. ....	100
Figure 3.5: A Screen-printed gold electrode mounted on the stage of a CAM 100 Optical Contact Angle Meter. The image on the screen is for a drop of de ionised water being injected to the gold surface before measurements are taken. ....	102
Figure 3.6: The chemistry of the covalent immobilisation of the CRP antibody 1c11 on self-assembled monolayers of 3,3-dithiodipropionic acid (DTDPA) using EDC-NHS coupling method. Figure adapted from Park et al, (2004). ....	103
Figure 3.7: The standard curves showing the effect of increasing concentration of coating antibody on the signal obtained. Varying concentrations of the coating antibody (2, 4, 6 ,8 10 µg mL <sup>-1</sup> ) were investigated by matching the rest of the parameters on a plate immunoassay . n=3, maximum CV=6.2%. ....	109
Figure 3.8: The effect of increasing concentration of the detection antibody on the signal obtained. Varying concentrations of detection HRP conjugated antibody (0.1, 0.25, 0.375, 0.5 µg mL <sup>-1</sup> ) were investigated. n=3, maximum CV=6.8%. ....	111
Figure 3.9: The effect of different incubation times on assay response. A micro plate was coated with 6 µg mL <sup>-1</sup> of anti-human CRP antibody and incubated for varying times (0.25, 0.5, 1, 2, 5 hr) at 37°C as well as 16h at	



4°C, the rest of the assay parameters were synchronised, n=3, maximum CV=5.9%,bars represent standard deviation.....	113
Figure 3.10: The standards curve for optimised ELISA assay for C- reactive protein with a linear plot insert. Standard concentrations of CRP (0.1 ,0.156, 3.12, 6.25, 12.5, 25, 50, 100 ng mL <sup>-1</sup> ) were assayed using optimised parameters.n=3 ,bars = standard deviation, maximum CV=7.4., LoD=1.9 ng mL <sup>-1</sup> .	114
Figure 3.11: The effect of the different blocking agents were investigated on the sandwich assay. A plate was coated with 6 µg mL <sup>-1</sup> of coating antibody and incubated for 2 h at 37°C before being washed, three different blocking agents (300 µL of 10 % milk protein, 1% PVA, 5% BSA ) were investigated. n=3, maximum CV=5.8 %,bars represent standard deviation.	116
Figure 3.12: The optimisation of the coating and detection antibody for C-reactive protein assay on screen-printed gold electrodes (SPGEs), varying concentrations of the detection (10, 20, 30, 50, 100 µg mL <sup>-1</sup> ) and for coating (5, 10, 20, 30, 50, 100 µg mL <sup>-1</sup> ) antibody concentrations were investigated. n=3, maximum CV=4.9%, bars made using standard deviation.....	117
Figure 3.13: The effect of premixing the detection antibody with the antigen on signal performance. Electrodes were coated and blocked, in the standard assay CRP antigen concentrations were added, while for the premixed procedure, detection antibodies and the antigen were premixed at room temperature first.. n=3, maximum CV=9.4% and bars represent standard deviation.....	119
Figure 3.14:The Graph showing standard curve for the C-reactive protein assay on screen-printed gold electrodes (SPGEs). Concentrations of CRP antigen in buffer were premixed with detection antibody before an assay was done on the immunosensor. n=3, CV=9.8%, bars= standard deviation LOD=2.6ng mL <sup>-1</sup> .....	120
Figure 3.15: Cyclic voltammetry for validating the deposition and formation of Self assembled monolayers by thiol group chemicals that facilitate covalent coupling with the capture antibody. 5 scans of cyclic voltammetry were done using 1 mM potassium ferricyanide K <sub>3</sub> [Fe(CN) <sub>6</sub> ] were prepared in 0.1 M KCl at 50 mV S <sup>-1</sup> scan rate. ....	123
Figure 3.16: The impact of different covalent surface modifications to the assay performance of C-reactive protein on screen-printed gold electrodes (SPGEs).Two sets of electrodes were chemically treated with self-assembled monolayers (DTDPA and 11-MUA) to facilitate covalent coupling. Optimised electrochemical immuno-assays were done to evaluate the effect of SAMs on the assay performance. n=3, CV=9.7%,bars = standard deviation.....	125

Figure 3.17: Diagram showing possible sources of non-specific binding on SAMs, (1) unutilised reactive groups (2) imperfect monolayers and (3) surface morphology (Choi and Chae, 2010).....	126
Figure 3.18: The evaluation of three detection methods for C-reactive protein using spiked serum samples with unknown CRP concentrations. A commercial human serum stock was randomly spiked with CRP. The samples were then diluted 200 x with PBS tween before being analysed in triplicates using the different methods. n=3, CV=6.2%, bars = standard deviation.....	127
Figure 3.19:Correlation of performance between the commercial ELISA kit and the one developed In-house.....	129
Figure 3.20:Correlation of performance between the immunosensor and the commercial ELISA kit. ....	129
Figure 3.21: No significant cross reactivity between other plasma proteins and the CRP assay. The proteins ( $25 \text{ ng mL}^{-1}$ ) were assayed using the standard optimised procedures of the different methods and they did not give out a signal statistically different from the blank which showed there was no cross reaction on the tested proteins. ....	130
Figure 4.1: Schematic diagram showing gold nanoparticles being used to increase assay sensitivity for the cardiac assay, Enzymes and antibody molecules are attached to the gold nanoparticle and cause enhanced signal output that positively influence sensitivity. ....	138
Figure 4.2: Chemical formula of 11-MUA (Sigma-Aldrich, 2012).....	147
Figure 4.3: Schematic overview of the EDC:NHS coupling procedure. (I) is the Carboxylic end group attached to the (chip) surface, (II) is EDC, (III) is Oacylisourea,(IV) is NHS, (V) is N-acylisourea, (IV) is diamino-PEO coupled to the surface, (VII) is the hydrolysis reaction of O-acylisourea, (VII) is the NHS activated carboxylic group and (IX) is the hydrolysis of this activated group (Van Delden <i>et al.</i> , 1996).....	148
Figure 4.4: Micro plate based ELISA assay for selecting the best antibody and working concentration for cTnT sandwich assay, (a) plates coated with anti-cardiac troponin 9g6 and (b) plates coated with 1c11. In both assays 100 $\mu\text{L}$ of various concentrations of coating antibody used and assayed against 100 $\mu\text{L}$ of antigen concentrations (0, 10, 50, 100 $\text{ng mL}^{-1}$ ) with a detection antibody (200 $\mu\text{L}$ of $5 \mu\text{g mL}^{-1}$ ) n=3, maximum CV= 4.3%. ....	152
Figure 4.5: The effect of increasing the concentration of detection antibody on the signal, varying concentrations of the detection antibody were assayed against standards after coating the plate with (200 $\mu\text{L}$ of $10 \mu\text{g mL}^{-1}$ ) of HRP conjugated anti-cTnT (1c11), n=3, maximum CV= 3.8%. ....	153
Figure 4.6: Logarithmic scale of the optimised micro plate assay, (Inset) a liner plot of the same curve. Plates were coated with 100 $\mu\text{L}$ of $10 \mu\text{g mL}^{-1}$ of	

- 1c11 and assayed with cTnT serially diluted standard in buffer. The detection antibody was HRP conjugated anti cTnT antibody 7E7 (100  $\mu\text{L}$  of 10  $\mu\text{g mL}^{-1}$ ).n=3, maximum, bars=standard deviation,CV=4.7%...... 154
- Figure 4.7: The optimisation of the coating and detection antibody for cTnT assay on bare screen-printed gold electrodes. A 10  $\mu\text{L}$  of different concentrations of anti cTnT 1C11 coating antibody were immobilised on the gold working electrode. It was assayed with standard concentration of the cTnT antigen premixed with the detection antibody. A reverse approach was applied for investigating the detection antibody n=3, maximum CV=6.2%, error bars= standard deviation. .... 156
- Figure 4.8: Logarithmic scale of the immunosensor with no surface modifications, (Inset) a liner plot of the same curve. Bare working electrodes of SPGEs were coated and assayed with cTnT serially diluted standards in buffer. LoD 2.12  $\text{ng mL}^{-1}$ ,n=3, maximum CV=10.9%, bars=standard deviation..... 157
- Figure 4.9: Cyclic voltammetry for validating the deposition and formation of Self assembled monolayers by 11-MUA. 5 scans of cyclic voltammetry were done using 1 mM potassium ferricyanide  $\text{K}_3[\text{Fe}(\text{CN})_6]$ , 0.1 M KCl at 50  $\text{mV S}^{-1}$  scan rate. The zero current on 11-MUA coated chips signifies insulation due to the successful formation of the monolayer. .... 159
- Figure 4.10: Pictures showing the distribution of 100  $\mu\text{L}$  drop of deionised water on (left) a 11-MUA coated Chip and (right) a bare electrode..... 160
- Figure 4.11: The optimisation of the coating and detection antibody for cTnT assay on 11-MUA modified screen-printed gold electrodes, electrodes were first sensitised with 30  $\mu\text{L}$  of EDC/NHS solution before the assay. Different concentrations of anti cTnT coating and detection antibodies were investigated, n=3, CV=7.4%, error bars= standard deviation. .... 161
- Figure 4.12: Logarithmic scale of the immunosensor with 11-MUA surface modifications, (Inset), a liner plot of the same curve. Working electrodes of SPGEs were sensitised with 30  $\mu\text{L}$  EDC/NHS and were then coated with 10  $\mu\text{L}$  of 60  $\mu\text{g mL}^{-1}$  of 1c11 and assayed with cTnT serially diluted standard in buffer premixed with detection antibody HRP conjugated anti cTnT antibody 7E7 (60  $\mu\text{g mL}^{-1}$ ), n=3, maximum CV= 9.8%. .... 162
- Figure 4.13: Effect of successful conjugated gold nanoparticles on the frequency shift. The chips were reacted with either 1:10 antibody conjugated gold nanoparticles solution or 10  $\mu\text{g mL}^{-1}$  of detection antibody solution. Method was adapted from work by (Van Heusden, 2011) n=3, maximum CV=6.9%. .... 164
- Figure 4.14: The optimisation of conjugated gold nanoparticles for detection of cTnT assay on 11-MUA modified screen-printed gold electrodes. Electrodes were first sensitised with 30  $\mu\text{L}$  of EDC/NHS solution. A 10  $\mu\text{L}$  of 60  $\mu\text{g mL}^{-1}$  anti cTnT 1C11 was immobilised on the gold working

- electrode. It was assayed with standard concentration of the cTnT antigen ( $50 \mu\text{g mL}^{-1}$ ) premixed with different concentrations of the conjugated gold nanoparticles..... 166
- Figure 4.15: Standard curve of the immunosensor with 11-MUA surface modifications and detected using conjugated gold nanoparticles. (Inset) a liner plot of the same curve  $\text{LOD} = 0.51 \text{ ng mL}^{-1}$ ,  $n=3$ , maximum CV= 10.4%, error bars = standard deviation. .... 167
- Figure 4.16: Standard curve of the immunosensor with 11-MUA surface modifications and conjugated gold nano-particles for detection using antigen in 75% serum, (Inset) a liner plot of the same curve,  $\text{LOD} = 0.58 \text{ ng mL}^{-1}$ ,  $n=3$ , maximum CV= 12.8%, error bars = standard deviation..... 168
- Figure 4.17: Comparison of the calibration curves that were generated using different assay optimisation techniques. The data from the calibration curves showed that the use of gold nanoparticles significantly enhanced the signal output and assay sensitivity And that the serum standards did not perform well unless diluted..... 169
- Figure 4.18: Correlation plots showing the performance of the developed biosensor for cTnT against two other detection methods. Results from a hospital analyser (A) and QCM-1 analyser (B) were compared with those of the gold nanoparticle enhanced immunosensor. Bars indicate standard deviation..... 173
- Figure 5.1: The effect of combined polyelectrolytes and Polyhydroxyl compounds in stabilising immobilised proteins. Polyelectrolytes promotes the formation of soluble protein - polyelectrolyte complexes, polyhydroxyl compounds can then penetrate the structure more effectively leading to stabilisation (A.E.T Ltd, 2012). .... 187
- Figure 5.2: Effect of Stabiliguard® on preserving the functionality of immobilised antibodies on (A) passively adsorbed and (B) covalently immobilised using 11-MUA self-assembled monolayers. Each of the two setups had a Stabiliguard® stabilised and un stabilised variables and performance was compared over immunosensors stored in a variety of environments ( $4^\circ\text{C}$ , room temperature and vacuum dessicator),  $n=9$ . .... 188
- Figure 5.3 The effect of different storage conditions on the performance of immunosensors with (A) passively immobilised (B) covalently immobilised antibodies. Batches of immunosensors were stored in different conditions and analysed.  $n=3$ , CV=12.2%, Error bars represent standard deviation. .... 190
- Figure 5.4 The effect of time on the performance of various immunosensor compositions for cardiac troponin t stored at different conditions over 90 days. Immunosensors were stored at (A)  $4^\circ\text{C}$  (B) room temperature (C) room temperature in a vacuum. .... 192

## LIST OF TABLES

Table 1-1 Classifications of biomarkers for the detection of cardiovascular diseases (Braunwald, 2008).....	17
Table 1-2: The significant parameters of CRP as a Cardiac marker (Lemos, 2004).....	21
Table 1-3: Summary of current diagnostic devices for cardiovascular diseases .....	46
Table 2-1: The commercial organisations associated with screen-printing of electrodes.....	58
Table 2-2: The distribution of components on three sensors used in this work. All the inks used are from DuPont.....	64
Table 2-3: Parameters used in the Randel-Sevcik equation .....	66
Table 2-4: Table showing the results of the Randles-Sevcik equation. ....	73
Table 2-5: Results of the Randles-Sevcik equation on different curing techniques.....	77
Table 3-1: Summary of published work on Immuno electrochemical detection of CRP .....	86
Table 3-2: Showing the intra and inter assay reproducibility of the detected CRP spiked in serum samples, n=5.....	129
Table 4-1: Summary of published work on Immunosensors detection of cardiac troponin T .....	139
Table 4-1 The summary of the performance of various immuno assay set up on the cTnt immunosensor using screen printed electrodes. ....	170
Table 4-2: The results from the analysis of eight unknown samples using the developed immunosensor, the QCM-1 and a Hospital Laboratory Analyser .....	171
Table 5-1: Methods of Inactivation of Proteins. ....	180
Table 5-2: Summary of Methods of Protein Stabilisation.....	180

## LIST OF ABBREVIATIONS

11-MUA	11-mercaptoundecanoic acid
Ab	Antibody
Ag	Antigen
Ag/AgCl	Silver/Silver Chloride
AMI	Acute Myocardial Infarction
ANP	Atrial natriuretic peptide
ATP	Adenosine Triphosphate
Au	Gold
BHF	British Heart Foundation
BNP	Brain natriuretic peptide
BSA	Bovine serum albumin
CeVD	Cerebrovascular Disease
CK	Creatinine Kinase
CNP	C-type natriuretic peptide
COOH	Carboxyl terminal
CRP	C-reactive protein
CRP	C-Reactive Protein
cTnT	Cardiac troponin t
CU	Cranfield University
CVA	Cerebrovascular Accident
CVD	Cardio-Vascular Disease
DTDPA	3,3-dithiodipropionic acid
E (V)	Energy or Current (Volt)
ECG	Electrocardiogram
ECIS	Electro Chemical Immuno-Sensor
EDC	N-ethyl-N'-(3-dimethylaminopropyl)-carbodiimide
ELISA	Enzyme Linked immunosorbent Assay
ELISA	Enzyme linked immunosorbent assay
EU	European union
FRET	Fluorescence resonance energy transfer
GC-MS	Gas Chromatography Mass Spectrometry
GPES	General Purpose Electrochemical System
H <sub>2</sub> O <sub>2</sub>	Hydrogen Peroxide
HDL	High density lipoproteins
HPLC	High Performance Liquid Chromatography
HPLC	High Performance Liquid Chromatography
HRP	Horseradish peroxidase
Hz	Frequency unit
I (A)	Potential (Ampere)
IFN-	Interferon-gamma
IgG	Immunoglobulin G
IL	Interleukin
K <sub>4</sub> Fe(CN) <sub>6</sub>	Potassium ferrocyanide
KCl	Potassium chloride
LA	(±)-α-lipoic acid

LDL	Low density lipoproteins
LDL	Low- Low Density Lipoprotein
LOD	Limit of detection
M	Molar
mM	Milimolar
MCP-1	Monocyte chemo attractant protein
mg	Milligram
µg	Microgram
MMP	Metalloprotease
mL	Millilitre
µL	Microlitre
NHS	N-hydroxysuccinimide
NHS	National health service
NMR-MS	Nuclear Magnetic Resonance
NO	Nitric oxide
oxLDL	Oxidised low-density lipoprotein
PAD	Peripheral Artery Disease
PBS	Posphate buffer saline
PBS-T	Posphate buffer saline containing 0.05% Tween
PCR	Polymerase Change Reaction
QCM	Quartz crystal microbalance
QCM	Quartz Crystal Microbalance
ROS	Reactive Oxygen Spicies
SAM	Self Assemble Monolayer
SEM	Scanning Electron Microscope
SPGE	Screen Printed Gold Electrode
TIMP	Tissue inhibitors of matrix metalloproteinases
TMB	3,3',5,5'-tetramethylbenzidine hydrochloride
TNFα	Tumor Necrosis Factor Alfa
TNF-α	Tumor necrosis factor alpha
VCAM-1	Vascular cellular adhesion molecule
VLDL	Very Low Density Lipoprotein

# CHAPTER 1

## INTRODUCTION AND LITERATURE REVIEW



# 1 Introduction and Literature Review

The origin of this thesis was to develop an electrochemical biosensor platform for the detection of cardiac makers that will aide in the diagnosis and or prognosis of cardiovascular disease. This chapter will explain the background of the project and the need for such a biosensor. It will then show the current methods used in detecting and diagnosing cardiovascular disease, the pathophysiology of cardiovascular disease and its link to the biomarkers associated with the disease. It will also list the current biomarkers that are used in the diagnosis of cardiovascular disease and the objectives of this thesis are then described.

## 1.1 An Overview of Cardiovascular Disease

### 1.1.1 Statistics

The World Health Organization (W.H.O) lists cardio-vascular disease (CVD) as the premier cause of death globally accounting for more than 17.3 million deaths in 2008 which equates to 30 % of all deaths that year (W.H.O, 2011b). In the United Kingdom for every 1000 people, 11 are affected by some form of CVD which in turn is directly responsible for 200,000 deaths annually, slightly more than 1 in 3 deaths (W.H.O, 2011c). According to the British Heart Foundation (BHF) there are two main forms of CVD which are Coronary Heart Disease (CHD) and stroke. About half of all CVD deaths (48%) are from CHD and more than a quarter (28%) are from stroke (Allender *et al.*, 2008a). CHD causes around 94,000 deaths in the UK each year (Allender *et al.*, 2008b). Figure 1.1 shows the global distribution of the problem, although many advances have been made in the prevention, early detection and treatment of these diseases, they still remain the leading causes of death worldwide (Gerszten and Wang, 2008).

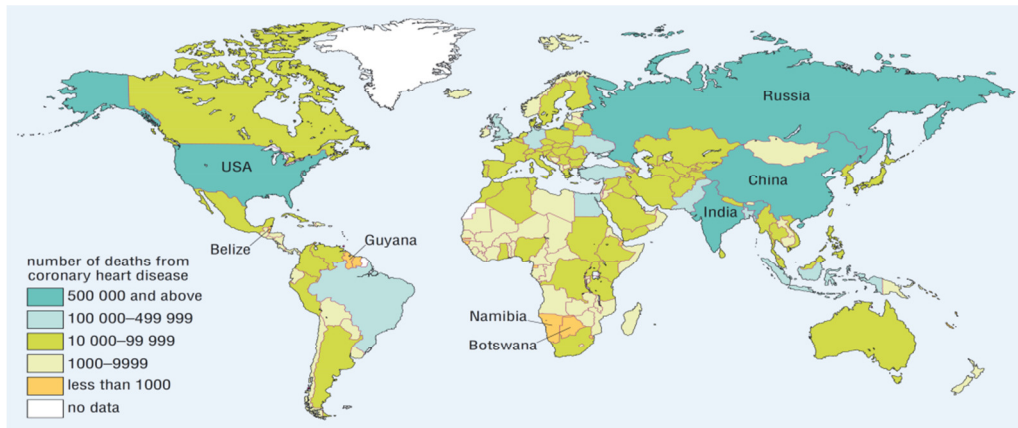


**Figure 1.1:** A map of the world showing numbers of deaths from coronary heart disease (W.H.O, 2011c)

There are indications that these figures will keep on rising and by 2030 it is estimated that almost 23.6 million people will die from CVDs, mainly from heart disease and stroke (W.H.O, 2011b) Figure 1.2 shows the current global number of deaths due to different cardiovascular diseases and the incidence at different age groups. It is clear then that cardiovascular disease prevention is an important social and clinical issue, but it is also an economic one. The CVD cost the health care system in the UK £14.4 billion in 2006 (Allender *et al.*, 2008a).

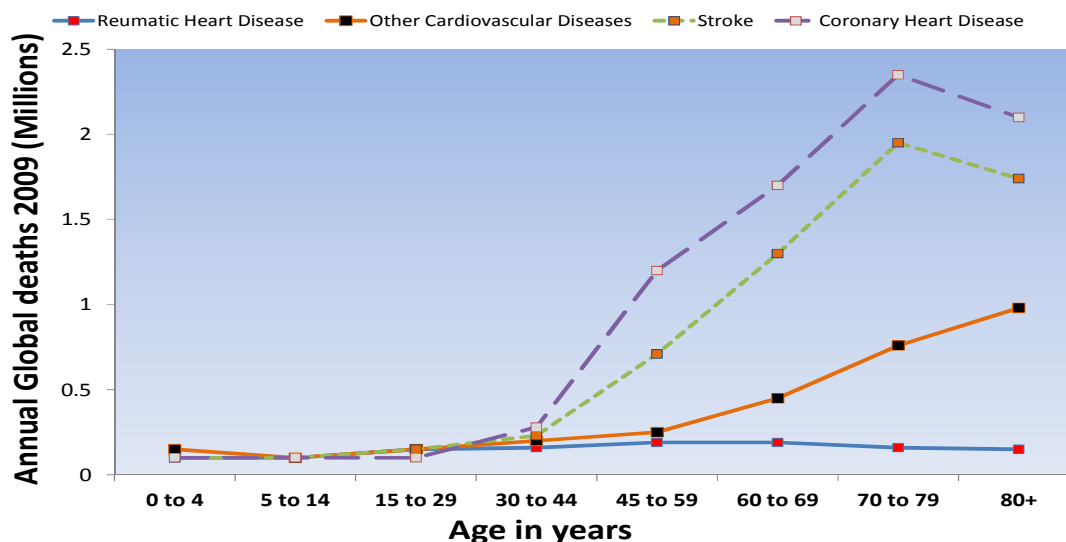


**Figure 1.2:** Global number of deaths per year due to different types of cardiovascular diseases and their age distribution (Open University, 2010).

### **1.1.2 Types of Cardiovascular Disease**

Cardiovascular disease is an umbrella term that encompasses several medical disorders of the heart and blood vessels and includes coronary heart disease (CHD) which is a disease of the blood vessels supplying the heart muscle. It is the condition, which results when the heart's blood supply is blocked or interrupted by a build-up of fatty substances in the coronary arteries. The walls of the arteries can become clogged up with fatty deposits called atheroma in a process known as atherosclerosis (W.H.O, 2011b). Cerebrovascular Disease (CeVD) is also classified under cardiovascular diseases and it is a condition that affects the blood vessels supplying the brain. Unlike CHD that is caused mainly by atherosclerosis, it is hypertension in the case of CeVD. It damages the blood vessel lining including the endothelium and thus exposes the collagen inducing platelets to aggregate and initiate a repairing process that may be incomplete and sometimes have imperfections. In the long term the sustained hypertension may permanently change the structure of the blood vessels transforming them into stiffened, deformed, narrow, and uneven which in turn makes them more vulnerable to blood pressure fluctuations. Another cardiovascular disease is peripheral arterial disease, which is a disease of blood vessels supplying the arms and legs. Other cardiovascular conditions are rheumatic heart disease, which is caused by streptococcal bacteria damage to the heart valves and muscle through rheumatic fever, congenital heart disease caused by birth defects and malformations of heart. Deep vein thrombosis and pulmonary embolism are delocalised blood clots from the leg veins, which can dislodge and move to the heart and lungs. Heart failure is the ultimate result of most unattended cardiovascular diseases. Heart failure can be classified into two types. If heart failure occurs suddenly, it is known as acute heart failure. Chronic heart failure is when heart failure happens gradually over a long period. A summary of the different types of cardiovascular diseases and their origin is highlighted in Figure 1.3

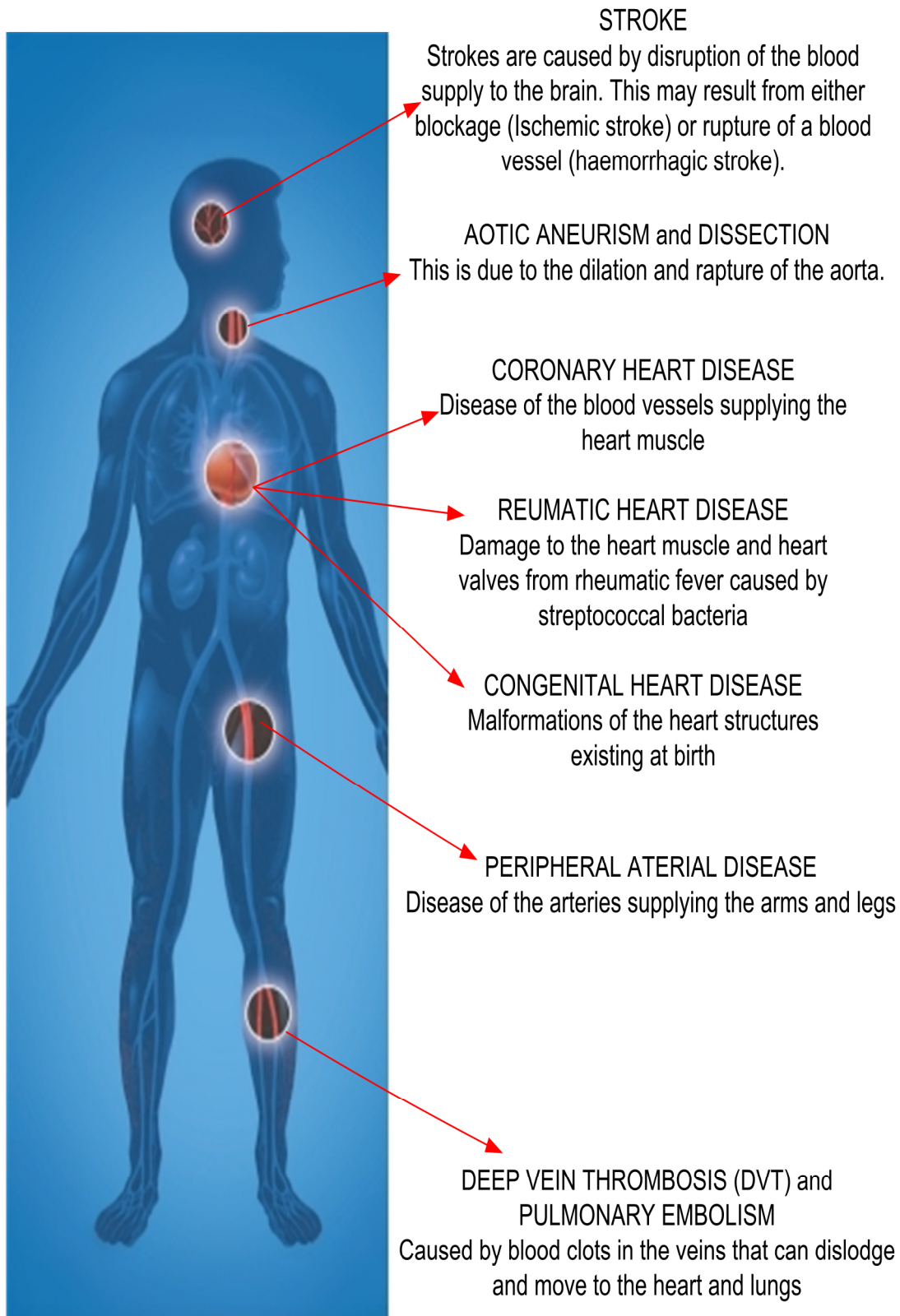


**Figure 1.3:** Different types of cardiovascular diseases and their origin (W.H.O, 2011a).

### **1.1.3 General Symptoms and Risk Factors for Cardiovascular Disease**

The evaluation of risk factors for cardiac diseases is complicated and is different to that of some diseases with clear-cut causes like infections where a single common pathogen can manifest clinically observed symptoms. This is because cardiovascular diseases do not have clear cut risk factors (Huether and McCance, 2004). There is a complex interplay involved at molecular and cellular level in the development of atherosclerosis. There are two major categories of risk factors for CVD, which are those that can be avoided called modifiable risk factors and those that cannot be changed which are called non-modifiable risk factors. It is important to highlight the fact that risk factors do not necessarily have a definitive causal role, but are justified by being statistically linked to CVD (Huether and McCance, 2004). Symptoms for coronary heart disease (CHD) are known to be both very noticeable and discrete. Several variations of CHD present different symptoms and clinical manifestations (Ahmed *et al.*, 2007).

### **1.1.4 Modifiable Risk Factors**

Cardiovascular disease is casually linked to the lifestyle of the individual and modifiable behaviours such as smoking, a sedentary lifestyle, a poor diet which are all strongly correlated to high incidence (Cotran R, 1999). In more developed and modernized economies the behaviour patterns are easily influenced by the growth of towns and cities. This has an effect of promoting a sedentary type of life as there is easy availability of transport. There have been significant levels of mechanisation and many processes are being done more efficiently with machines done instead of the traditional manual methods. People have more amenities and easy access to unhealthy diets, technology has made it possible to order fast food on the internet and have it delivered on the door step (Cotran *et al.*, 1999). These factors coupled with lack of exercise are significant factors in the pandemic of obesity in the developed world, which

is linked to CVD. The World Health Organisation estimates that 60% of the world's population is not sufficiently physically active.

Although this trend is more prevalent in the developed world, CVD is also a major growing problem in the developing world (Murray and Lopez, 1997). In the developing world the ever improving medical treatment and increasing modernisation has resulted in less malnutrition and communicable disease and thus increasing the average life span (Murray and Lopez, 1997). This has made more people in the developing countries to be more likely to die of chronic degenerative diseases associated with older age (Yusuf *et al.*, 2001). In developing countries, where increasingly Westernised lifestyles, jobs, smoking and unhealthy diets has brought about the emergence of cardiovascular disease as the major cause of morbidity and mortality after a lag period of one or two decades (Novak, 1998).

### **1.1.5 Non-Modifiable Risk Factors**

Non-modifiable risk factors include age, family history, sex and ethnicity. There is a general misconception that the cardiovascular disease is a mature onset condition that only appears later in life. This is because statistics show more victims aged above 75 to be at risk of having more chances of an attack. Some authors argue that there are strong chances that the condition could have started earlier in life taking decades to progress. According to Cotran (1999) with every decade in life there is a slightly more than a doubling in risk of developing complications like CVD. It is however difficult to define and distinguish the actual mechanism for this as old age is associated with a lot of conditions like diabetes and hypertension which are also risk factors for CVD (Ahmed *et al.*, 2007). On average men are twice as likely to have an AMI when compared to age matched pre-menopausal women. However, post-menopausal AMI statistics rise sharply; this is attributed to the absence of endogenous oestrogen which is thought to have protective effect in pre-menopausal women (Gray, 2002a).

However, this advantage is not present in stroke patients. Menopause is associated with a progressive increase in total cholesterol, with, in particular, an increase in LDL and decrease in HDL. Total cholesterol levels peak in women aged between 55-65 years; a 10 years delay compared to the peak in men (Murray and Lopez, 1997).

### **1.1.6 Chest Pain Symptoms for CVD**

There are two main types of chest pains; these can be classified as typical and atypical chest pains. Atypical chest pains are those that are often sharp and which come and go. They are normally felt on the left side of the chest, the abdominal area, back, or the arm. Atypical chest pains are more common in women (Ahmed *et al.*, 2007). On the other hand typical chest pain usually feels heavy or like someone being squeezed. It is felt under the breastbone and the pain usually occurs with strong activity or emotion, and goes away with rest or a medication like nitroglycerin. Adults with typical chest pain have a higher risk of CHD than those with atypical chest pain (Gray, 2002a). Angina pectoris is a main symptom of coronary heart disease characterised by a painful heavy feeling in the centre of the chest that is capable of expanding to the stomach, back, jaw, neck and arms. Symptoms of stable angina are triggered at times of increased physical or emotional activity. However, in unstable angina, these symptoms can manifest at any time. For the less fortunate, the first signs of a heart disease may be a heart attack or myocardial infarction (Ahmed *et al.*, 2007).

### **1.1.7 Other Symptoms for CVD**

In patients suffering from coronary heart disease, it is common to experience irregular and unusually fast heart palpitations caused by unbalanced beating of the heart. The heartbeats can be observed to beat at an irregular rhythm, usually more rapid. Each heartbeat can also be felt to beat much harder and forcefully than normal. This symptom can last for several hours and reoccur over several days while the patient can also experience unusual breathlessness, dizziness or even chest pains (Gray, 2002b). It is also worth mentioning that heart palpitations may not necessarily be a direct consequence of coronary heart disease but also a variety of other conditions. Frequent fainting also indicates that there is an insufficient supply of oxygen to the brain and could be linked to the narrowing of blood vessels (Ahmed, 2007). Fluid retention is also known as oedema in medical terms and is another risk factor linked to cardiovascular disease and heart failure. Other symptoms of CHD can include: nausea, dizziness, excessive sweating, shortness of breath, fatigue with activity (exertion), and heart attack (Ahmed, 2007). Heart attacks and strokes are usually acute events, which means that they are usually severe and immediate action need to be taken upon onset of the symptoms to avoid fatalities. Atherosclerosis is the major factor in the development of most acute cardiovascular diseases like acute Myocardial Infarction (AMI) (Laing *et al.*, 1991).

## **1.2 Pathophysiology of Cardiovascular Disease**

### **1.2.1 Atherosclerosis and Cardiovascular Disease**

Research into the pathogenesis of atherosclerosis has been fuelled by its link to cardiovascular diseases and the socioeconomic impact of CVDs. An understanding of the relationship between atherosclerosis and cardiovascular disease is essential to this project as diagnostic markers are usually embedded as part of the fabric that constitutes the pathophysiology of the diseases. It has



been discovered that the risk factors responsible for cardiovascular diseases trigger physiological changes that result in a chronic inflammatory condition of the tissue. This condition will then trigger a cascade of reactions and complex interactions between homeostatic molecules, responsible for innate and adaptive immunity resulting in a proatherogenic activity (Hanson, 2008). The presence of atherosclerotic lesions within the vasculature is virtually a prerequisite for most cardiovascular diseases. Advanced lesions within the coronary arteries can cause luminal occlusion leading to stable and unstable angina pectoris. Erosion or rupture of vulnerable lesions can lead to the atherothrombotic complications of myocardial infarction (MI): stroke, renal failure, heart failure, sudden death, and peripheral vascular disease (Hanson, 2008).

Atherosclerosis is a generalised process and there is evidence that it starts postnatal. Although patients may later present problems with arterial pathology, the disease is not localised, almost invariably everywhere, and it is the root cause of associated morbidity and mortality (Laing *et al.*, 1991). The high prevalence of atherosclerosis in the developed or westernised population and its scattered distribution in the vasculature, has made it desirable to fully understand the cellular and molecular relationships involved in the development of atherosclerosis. This will help individuals at risk of progressing to a cardiac event to be identified to facilitate possible pathways of therapeutic intervention (Mackay *et al.*, 2004). Traditionally atherosclerosis has been considered a lipid storage disease where lesion swelling and stenosis were thought to be the primary cause of ischaemic heart disease and stroke (Ross and Harker, 1976).

This generalisation was proven to be inadequate in the late 1970s and historical and current evidence supports the role of plasma lipids for example cholesterol and triglycerides. Lipoproteins like low-density lipoprotein (LDL) and very low density lipoprotein (VLDL) in atherogenesis were subsequently considered to be early markers (Kannel *et al.*, 1979; Martin *et al.*, 1986). Although hyperlipidaemia has traditionally been attributed to be the major cause of the development of atherosclerosis, it has since been shown not to be the case as

the extent of atherosclerosis is not always proportional to sustained blood lipid concentration. In reality almost half of all coronary events occur in individuals without clinical hyperlipidaemia (Braunwald, 1997). Some studies have gone all the way to show that hyperlipidaemia is only weakly related to ischaemic stroke (Shahar *et al.*, 2003). Attempts to develop an atherosclerotic lesion *in vivo* have proved to be complex, requiring persistent lipid presence, endothelial dysfunction and inflammation (Hanson, 2008). Inflammatory cells and cytokines are alleged to play a pivotal role in the development of the lesion and as such are a source of known and potential biomarkers for CVDs (Apple, 2007).

### **1.2.2 Inflammation and Cardiovascular Disease**

The pathophysiology of inflammation is a minefield for potential biomarkers for cardiovascular disease. This is because of the direct relationship between inflammation and cardiovascular disease mentioned earlier (Apple, 2007). A cascade of events result in inflammation, according to Alderman *et al* (2002) the process starts with the vasculature being exposed to LDL cholesterol in severe hyperlipaemic plasma. Upon exposure, the LDL penetrates the endothelial cell layers into the intima favouring areas of low shear stress. When conditions become favourable for oxidation for example in the presence reactive oxygen species (ROS) the LDL will transform to oxidised LDL (oxLDL). This triggers the expression of leukocyte adhesion molecules (LAM) on the surface of arterial endothelial cells (Hansson, 2005). Endothelial cells located overlying nascent atheroma have been observed to particularly show an increase in the production of vascular cell adhesion molecules-1 (VCAM-1) (Li *et al.*, 1993). The modified lipoprotein oxLDL has the ability to attach and bind to the endothelium resulting in endothelial activation (Cominacini *et al.*, 2001). Activation of the endothelium begins the process of localised inflammation, allowing leukocyte extravasation through production of cell adhesion proteins like selectins and integrins. There is a rapid externalisation of some Weibel-Palade bodies and these results in the endothelial surface to exhibit P-selectin

and E-selectin (Dong et al., 2000). These selectins then weakly attach to Lewis X-antigens on the surface of leukocytes, allowing loose interaction along the surface of the endothelial barrier. On the other hand endothelial expression of integrins such as vascular cellular adhesion molecule (VCAM-1) allows arresting adhesion of Mac-1 expressing monocytes, which can then extravagate into the tunica intima underlying the endothelium (Piqueras et al., 2000). It has been proven in animal models of atherosclerosis that VCAM-1 is expressed in large quantities by endothelial as part of the initial vascular response to cholesterol accumulation (Cybulsky and Gimbrone, 1991).

### **1.2.3 Endothelial dysfunction**

Endothelial dysfunction can be defined as 'a profound imbalance in the relative quantities of other vasoactive compounds such as angiotensin II and oxidants or a significant loss of ability of the endothelium to release the vasorelaxing compound nitric oxide (Verma and Anderson, 2002). It causes inappropriate vasomotor constriction of the vasculature resulting in aggravated luminal occlusions particularly from established atherosclerotic lesions. In most models of atherosclerotic development the significant loss of nitric oxide production by the endothelium is an important aspect of the development of pathophysiology of inflammation and other molecular processes in the vasculature (Szmitko *et al.*, 2003). The nitric oxide is also linked to the production of an anti-thrombotic atmosphere through restricting the aggregation of platelets on the endothelium. It also prevents leukocyte sticking together with the endothelium through suppressing expression of adhesion molecules as well as maintaining vascular smooth muscle in a non-proliferative state (Gauthier *et al.*, 1995). According to Ross (1999), there is a sensitive environment which is balanced in a vascular system and any changes to this environment can trigger endothelial activation.

### **1.2.4 Growth and Development of an Atherosclerotic Lesion**

The growth of an atherosclerotic lesion has been attributed to the chain reaction effect of processes stimulated in the initiation stage described earlier. Components of the inflammatory response like the interleukin 18 (IL-18) are known to play a pivotal role. They have the ability of IL-18 to interact with IL-12 and stimulate interferon-gamma (IFN- $\gamma$ ). The combination of these processes can motivate macrophage activation and present an opportunity for rapid cell death. This results in the creation of the necrotic core in advanced lesions (Ross, 1999). The growth of the plaque continues as long as the environment allows it and arterial dilation in some cases will be stretched until it reaches maximum capacity. The plaque then starts to intrude into the lumen, making it continuously narrower and this can cause an obstruction in the blood flow which in turn may reduce the production of nitric oxide in the endothelium (Ross, 1999). This consequence will create a positive feedback action as nitric oxide possesses anti-inflammatory properties through its ability to decrease cytokine-induced endothelial activation (Decaterina *et al.*, 1995). The growth of the lesion and the low levels of nitric oxide build up stress on the arterial walls resulting in smooth muscle cells to produce proteoglycans. These proteoglycans are responsible for attracting and retaining more LDL molecules thus refueling the cycle and making the lesion grow bigger and bigger as illustrated in Figure 1.4 (Decaterina *et al.*, 1995).

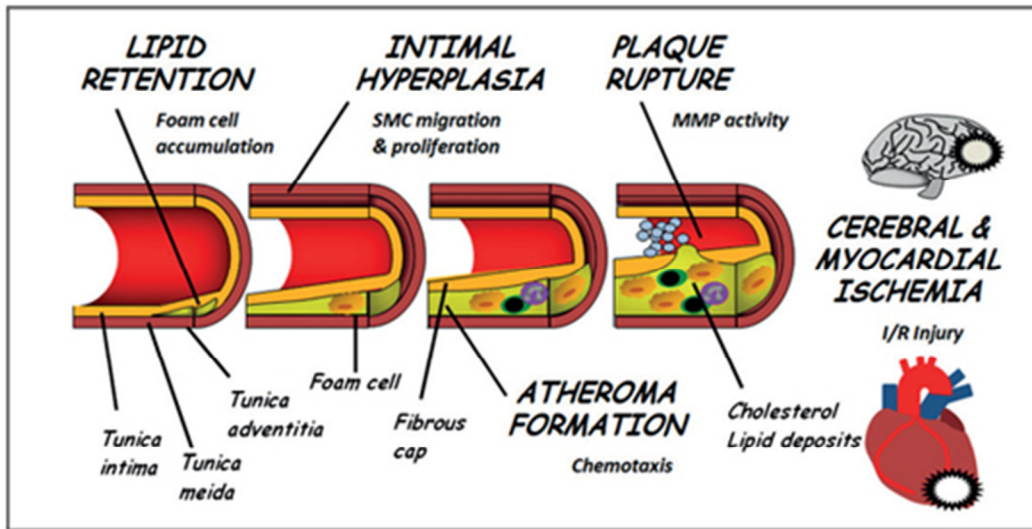


**Figure 1.4:** Different stages of atherosclerosis (Ellertsen, 2011).

### 1.2.5 Plaque Rupture

It is important to understanding the underlying mechanisms of plaque rupture because it is the major clinical implication of atherosclerosis and is the most common precursor to cardiovascular accidents and acute myocardial infarctions (Thim *et al.*, 2008). Plaques which are prone to rupture have been identified to be generally consisting of thin fibrous caps and large necrotic lipid rich centres. The rupture can only occur when the thinned fibrous cap can no longer withstand the intensity of the force placed on it by the athermanous material behind. This causes the thrombogenic material to be released into the arterial lumen causing atherothrombosis because of the fact that the plaques usually accumulate in regions of non-laminar flow, some hemodynamic factors will put mechanical stress on the plaque thus providing a mechanism for erosion of the endothelial layer and increase the probability to rupture. The lack of fibrous material in the necrotic core also means that stress is focused only across the fibrous cap increasing its liability to rupture (Fernandez-Ortiz *et al.*, 1995).

It is important to point out that atherothrombosis does not always lead to an acute myocardial infarction. Sometimes the thrombus is too small and acts to plug and repair the rupture in process called superimposed thrombosis (Lee *et*

*al.*, 2001). However, the implications of superimposed thrombosis are very serious as the new thrombus on the plaque has a tendency to encourage platelet adhesion and the thrombus can grow into the lumen causing stenosis. To add to this the plaque is also very vulnerable to subsequent ruptures as the cap has a very heterogeneous composition and is significantly weakened by previous ruptures (Thim *et al.*, 2008). Some other processes can be responsible for plaque rupture for example hemorrhages in high pressured vessels may result in plaque contained hematoma capable of exerting pressure on the cap and causing a large plaque rupture (Cotran *et al.*, 1999). Another way which can lead to rupture is when arteries calcify making them brittle and developing small fissures which grow resulting in plaque rupture or aneurysm (Gray, 2002b). The events of plaque rupture and subsequent thrombosis have been found to be the main cause of up to 50% of ACS and myocardial infarction cases (Schroeder and Falk, 1996).

## **1.3 Biomarkers for Cardiovascular Diseases**

### **1.3.1 General Introduction**

Developments in the identification of biomarkers that can identify individuals most at risk of cardiovascular diseases have been reported, they are mainly associated with inflammation or damage to cardiac tissues (Jaffe *et al.*, 2006; Apple, 2007; McDonnell *et al.*, 2009). These include established markers that are used to aid in the diagnostics of cardiovascular diseases like Creatine-kinase MB (CK-MB), Myoglobin, Troponin I, and T and other novel markers which are still being investigated like, C reactive protein (CRP), B-type natriuretic peptide (BNP), and many others which will be discussed in detail later in this Chapter, (Babu L, 2005; Jaffe *et al.*, 2006; Apple, 2007; da Silva and Moresco, 2011). Although these biomarkers provide important clinical information about a patient's condition and can aid in the prognosis, there are still some limitations in their use (Szmitko *et al.*, 2003; Anderson, 2005). They do not always give adequate information and they lack on providing insight on

location of the atherosclerotic plaque, its composition, and its liability to rupture and develop other major heart complications (Melanson and Tanasijevic, 2005; Jaffe *et al.*, 2006). They also work better as a panel of several biomarkers so that they can complement each other in aiding diagnosis (Apple, 2007). These limitations, however, are far outweighed by the benefits as biomarkers make it possible for faster and more accurate diagnosis to be carried out at Point of care without the need for highly skilled personnel unlike the conventional ECG and other laboratory-based tests (McDonnell *et al.*, 2009; da Silva and Moresco, 2011).

### **1.3.2 Properties of an Effective Cardiac Biomarker**

A cardiac marker is a biological analyte that is detectable in elevated levels in the blood upon the onset or progression of CVD including myocardial damage (Azzazy, 2002). It is important that an ideal cardiac marker exhibit several crucial characteristics due to the high risks of misdiagnosis that may result in fatalities. These desirable characteristics include: high clinical sensitivity and specificity, quick release for early diagnosis, suitable diagnostic window, ability to be assayed quantitatively, reasonable costs, and time-efficiency (Panteghini, 2004). It is necessary to have these factors to aid in diagnosis, prognosis, monitoring, and risk stratification as well as guiding therapeutic decision of suspected cardiovascular diseases patients (Azzazy, 2002). There is currently no single cardiac marker on the market which has managed to deliver all the characteristics mentioned above (Braunwald, 2008), thus there are strong recommendations for a multi marker approach when diagnosing cardiovascular disease using biomarkers. Table 1.1 shows some of the biomarkers used in combination with each other to diagnose cardiovascular disease. This section will introduce some of these typical cardiac markers that are currently used and their clinical applications in diagnosing CVD.

**Table 1-1** Classifications of biomarkers for the detection of cardiovascular diseases (Braunwald, 2008).

<b>Cardiovascular biomarker classification group</b>	<b>Selected example</b>
<b>Inflammation</b>	CRP, TNF- $\alpha$
<b>Oxidative stress</b>	Oxidised LDL, Myeloperoxidase
<b>Extracellular matrix remodellers</b>	MMP, TIMP
<b>Neurohormones</b>	Renin, Angiotensin, Arginin vasopressin
<b>Myocyte Injury</b>	cTnT, cTnI, CK-MB, Myoglobin
<b>Myocyte stress</b>	Natriuretic peptides ANP, CNP and BNP
<b>Potential new markers</b>	Copeptin, Growth differentiation factor-15

KEY (CRP): C-reactive protein,(TNF- $\alpha$ ):tumor necrosis factor alpha, (LDL): low density lipoproteins,.(ANP): atrial natriuretic peptide, (BNP): brain natriuretic peptide ,(CNP): C-type natriuretic peptide, (MMP): metalloproteinase,(TIMP): tissue inhibitors of matrix metalloproteinases

As highlighted in Table 1.1 there are wide arrays of biomarkers that can be used in the diagnosis and monitoring of specific antecedents to cardiovascular diseases. Although these markers can be incorporated onto in vitro diagnostic tests in most central laboratories, there is a selected few that are dominant in the point of care setting POC that this project is aligned to. Novel markers constantly under investigation may end up playing an integral part in the future diagnosis of CVDs. However the current position requires *in vitro* diagnosis be carried out using the analysis of established markers that are discussed below.



### 1.3.3 Biomarkers for Inflammation

The first class consists of biomarkers for general inflammation. Even though they lack specificity. This class has biomarkers that can act as independent predictors of adverse outcomes and identify asymptomatic patients with CVDs (Braunwald, 2008). C-reactive protein (CRP) which is one of the most established markers for CVD and general inflammation is part of this group. Figure 1.5 shows the structure of CRP with the chemical composition.

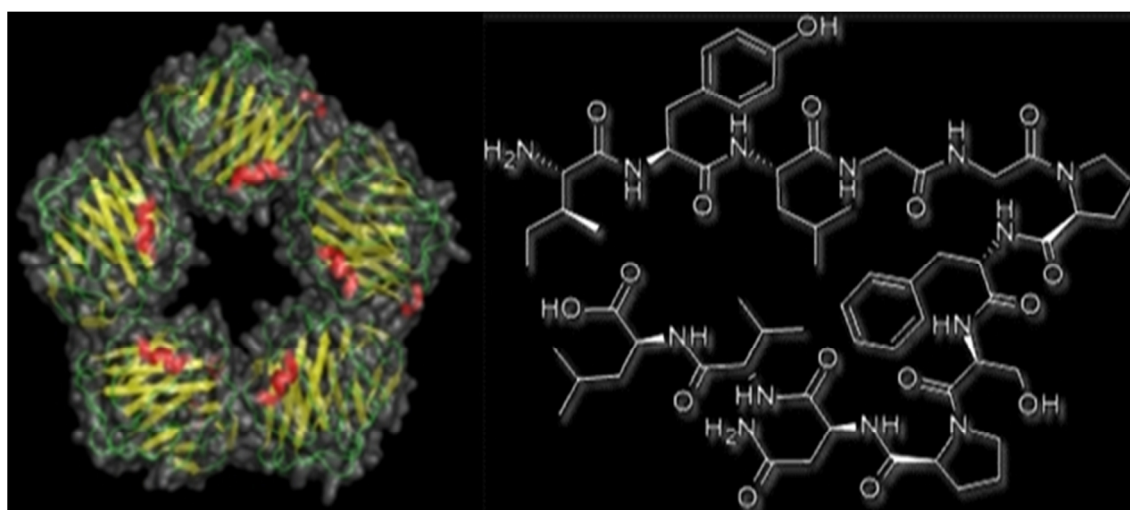


**Figure 1.5:** Structure of CRP fragment and the chemical structure (Science Photo Library, 2012)

It was first discovered by Tillett and Francis (1930) and was the first acute-phase protein to be described. It is an exquisitely sensitive systemic marker of inflammation and tissue damage (Zhang *et al.*, 1999; Pepys and Hirschfield, 2003). Although it is considered a non-specific biomarker, its level rises steeply sometimes 1000 times over the base line, as a result of tissue damage caused by infections and other acute inflammatory events including autoimmune diseases and malignancy, hence monitoring is considered very useful for screening and also disease management (McBride, 2008).

CRP has evolved from being a postulated marker that can possibly predict cardiovascular events and mortality to a proven direct partaker in the pathogenesis of atherosclerotic cardiovascular disease (Bisoendial *et al.*, 2010; Nagai *et al.*, 2011). Figure 1.6 shows how CRP is involved in several atherosclerotic stages.

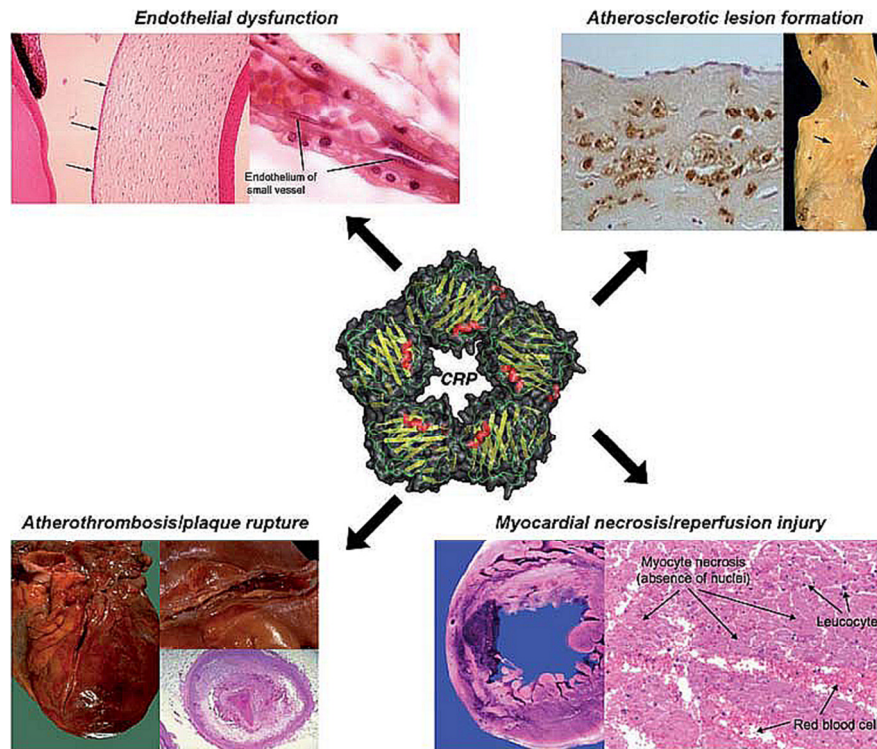


**Figure 1.6:** CRP as a risk factor for cardiovascular disease through several stages of atherogenesis (Bisoendial *et al.*, 2010).

Research developments in this arena have proved that CRP is instrumental in the initiation of several pathogenic pathways which can cause atherosclerosis a precursor to cardiovascular disease (Sattler *et al.*, 2005; Sun *et al.*, 2005; Scirica, 2009), although some are still not convinced of its pathogenic role (Anand and Yusuf, 2010). Figure 1.7 shows the pathophysiology which results in the production of several proteins that can be used as potential biomarkers for cardiovascular diseases.

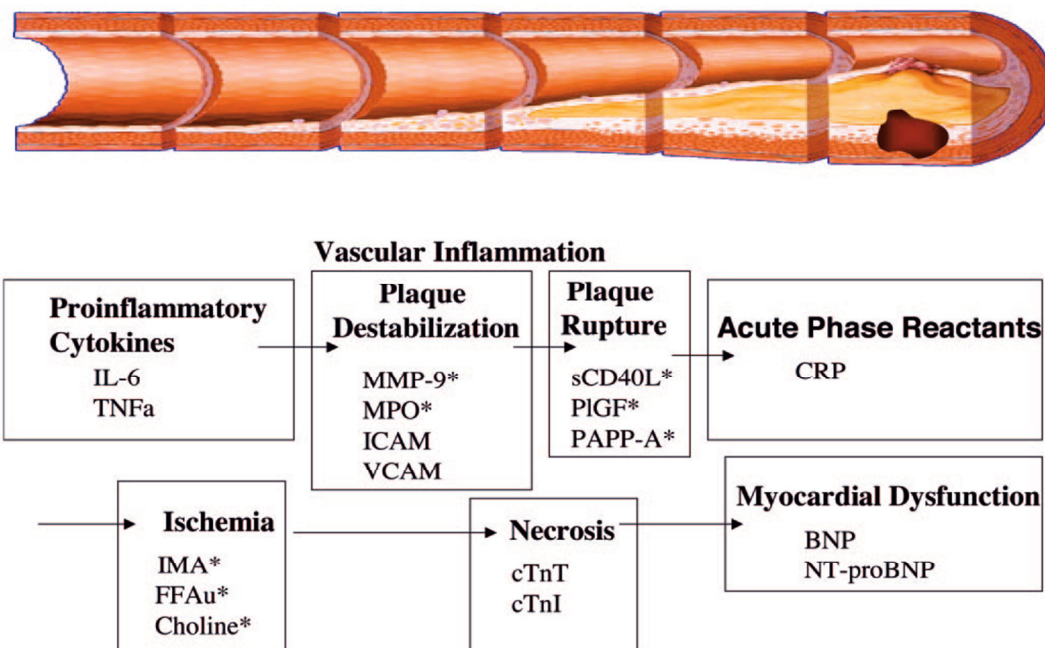


**Figure 1.7:** Summary of pathophysiology of cardiovascular diseases and potential cardiac markers including CRP (Apple *et al*, 2005).

Several researchers have used CRP as a general marker for inflammation and later for predicting cardiovascular diseases (Anand *et al.*, 2005; Schulz and Heusch, 2011). CRP is also significantly associated with the risk of stroke after cardiac surgery and may be involved in the inflammatory processes in post-cardiac surgery stroke (Grocott *et al.*, 2005). In vitro experiments with human aortic endothelial cells have shown that increased levels of CRP levels have an implication for atherothrombosis due to the generation of pro inflammatory cytokines and consequently the decrease of the TPA activity (Pepys and Hirschfield, 2003; Miller *et al.*, 2005). Table 1-2, shows the characteristics of CRP protein and how it can be used as a marker for predicting the risk of a cardiovascular event. The cut off parameters for defining the level of potential risk are also highlighted. The overall concentration of CRP measured in the plasma varies from person to person, with the age and with lifestyle, for instance diet, alcohol consumption, smoking and physical activity. The levels of CRP are also influenced by several diseases, such as diabetes.

**Table 1-2:** The significant parameters of CRP as a Cardiac marker (Lemos, 2004).

Parameter	CRP Specifications
Clinical reference range	$< 1 \text{ mg L}^{-1}$ low $1-3 \text{ mg L}^{-1}$ intermediate $> 3 \text{ mg L}^{-1}$ high relative risk
Diurnal variation	No
Correlation of levels over time	$R=0.6$
Fasting sample required	No
Commercially available assay	Yes
Assay standardized	Partially
Half life	19 hours

In healthy young adult volunteer blood donors, the median concentration of CRP is  $0.8 \text{ mg L}^{-1}$ , the 90th percentile is  $3 \text{ mg L}^{-1}$ , and the 99th percentile is  $10 \text{ mg L}^{-1}$ , but, following an acute-phase stimulus, values may increase from less than  $50 \text{ } \mu\text{g L}^{-1}$  to more than  $500 \text{ mg L}^{-1}$ , that is, 10000 fold. De novo hepatic synthesis starts very rapidly after a single stimulus, serum concentrations rising above  $5 \text{ mg L}^{-1}$  by about 6 hours and peaking around 48 hours (Rifai, 2001; Pepys and Hirschfield, 2003). Because of the fact that CRP is an acute phase reactant, it is highly associated with cytokines that are involved in the development of the immune response (Rifai, 2001). Among these cytokines are interleukin-6 and tumour necrosis factor- $\alpha$  which subsequently belong in the same class. These will not be mentioned in detail, as their role in cardiovascular events is less significant than that of CRP.

### 1.3.4 Early Biomarkers for Mycosite Injury

This category is the host of the most widely used biomarkers for the diagnosis of cardiovascular diseases. This is because of the sensitivity that the biomarkers in this group possess in flagging myocardial damage. Some of the pioneering biomarkers for CVD are part of in this group namely myoglobin and creatine kinase MB fraction (Braunwald, 2008; Hochholzer, 2010b). Myoglobin was the first non-enzymatic protein used for diagnosis of acute myocardial infarction and it was first used in the 1970s (Storrow and Gibler, 1999). A small molecule is quickly released into circulation as early as 2 h after the onset of symptoms of myocardial infarction. It has been found to have high sensitivity and high negative predictive value that makes it a valuable early screening test for myocardial infarction (Brogan *et al.*, 1994). It peaks at 6-8 hours before returning to normal in 20-36 hrs after myocardial infarction. The major limitation which myoglobin carries is its low clinical specificity. This is because of its abundant presence in not only in myocardial but also in skeletal muscle cells. Injury in skeletal muscle as well as renal failure may also trigger an elevation in the plasma concentration of myoglobin thus lowering its clinical specificity (Storrow and Gibler, 1999).

The Creatine Kinase enzyme has three known isoforms and these are found in different locations including heart muscle (CK-MB), skeletal muscle (CK-MM), and brain (CK-BB). Creatine kinase is increased in over 90% of myocardial infarctions (Christenson, 1998). Among the three isoenzyme forms of creatine kinase, CK-MB is highly sensitive in diagnosis of acute myocardial infarction and had been previously regarded as the “gold standard” in the 1980s until about 1995 (Christenson, 1998). The diagnostic specificity of CK-MB is limited because CK-MB is also present in skeletal muscle just like myoglobin. This means that it may increase during muscle trauma, physical exertion, postoperatively, convulsions, delirium tremens, and other conditions. Another limitation is that once the CK-MB is released into the blood stream it doubles its

concentration within 5–6h after the onset of chest pain and peaks in 12–24h (Males *et al.*, 2001). This gives a narrow time window that makes it difficult for CK-MB to be used as an early marker. However it is possible to use CK-MB assays for the diagnosis of persistent or re-infarctions (Panteghini *et al.*, 1998). It is because of this reason that CK-MB is so clinically useful in multi-marker panels.

### **1.3.5 Cardiac Troponins**

These are relatively recently discovered biomarkers of myocyte injury (Braunwald, 2008). Cardiac Troponin T and I are cardiac isoforms of contractile proteins of the myofibril. They are very specific for cardiac injury and are not present in serum from healthy people. Due to their great sensitivity and specificity for myocardial cell damage, cardiac troponins (cTnI and cTnT) have been considered as the “gold standard” for AMI diagnosis (Alpert *et al.*, 2000; Babuin, 2005). Figure 1.8 shows the different sub units that make the troponin complex and how they interact with actin and myosin. They are released in 2–4 hours and remains in circulation for up to 8-10 days after the onset of the event. Current guidelines from the American College of Cardiology Committee state that cardiac troponins are the preferred markers for detecting myocardial cell injury. There is a striking resemblance in the kinetics of the cardiac Troponin and the CK-MB. They are both released early following AMI and like CK-MB it take several hours for both of troponins to be released into circulation before being detectable, hence both cardiac Troponins cannot be used as early markers.

According to Jeremias (2005), the specificity of troponins for ACS is questionable because of other clinical situations like sepsis, hypervolemia and renal failure which may also cause an increase in Troponin levels. Despite these limitations Troponins are currently the most cardiac-specific markers with an added advantage of offering the widest temporal diagnostic window as they

remain abnormal for 4–10 days after the onset of AMI (Martins *et al.*, 1996). Another advantage is that the peak concentration of the Troponin closely correlated with the infarct size that makes it a more quantitative diagnostic tool (Licka *et al.*, 2002). Troponin is released during MI from the cytosolic pool of the myocytes. The degradation of actin and myosin filaments is responsible for prolonging the subsequent release. There are several conditions that are diagnosed with troponins and these include acute infarction, severe pulmonary embolism causing acute right heart overload, heart failure, and myocarditis (Christenson, 1998).

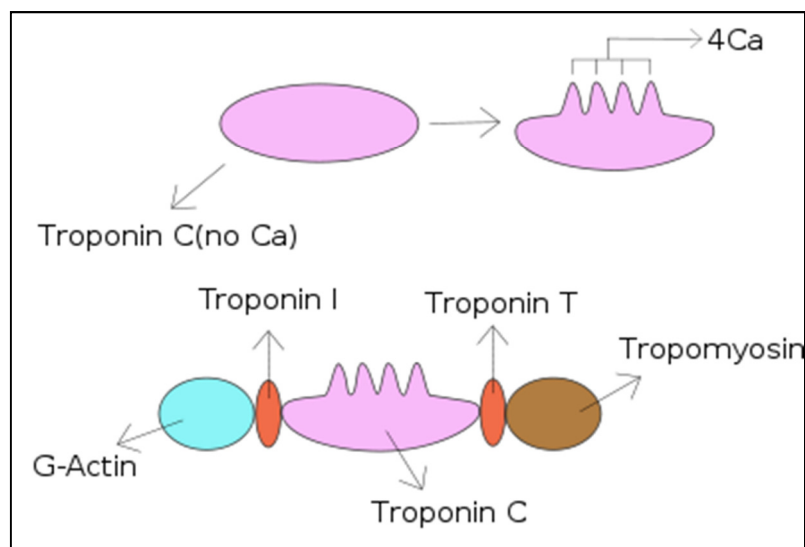


**Figure 1.8:** The schematic diagram showing the interaction of cardiac Troponins with actin and myosin (Brighthub, 2009).

The general cut off values for troponins was debatable until the National Academy of Clinical Biochemistry guidelines and measurement platforms stepped in with some recommended standards cardiac Troponin T values below  $0.05 \text{ ng mL}^{-1}$  are indicative of negative TnT, and those values between  $0.05$  to  $< 0.1 \text{ ng mL}^{-1}$  indicates low TnT. However those values that lie between  $0.1$  and  $2.0 \text{ ng mL}^{-1}$  indicate myocardial damage and values  $> 2.0 \text{ ng mL}^{-1}$  indicate massive myocardial damage (Christenson, 1998).

### 1.3.6 Other Biomarkers

Another source of cardiac biomarkers is the process of myocyte stress that is responsible for production of biomarkers like the natriuretic peptides. These can be narrowed down to three major peptides which are, Atrial natriuretic peptide (ANP), brain natriuretic peptide (BNP) ,and C-type natriuretic peptide CNP (Braunwald, 2008). ANP is prevalent in the atria whereas BNP is produced in the ventricles as a counteraction to stress. However, C-type natriuretic peptide CNP is derived primarily from endothelial cells and is rarely associated with CVD diagnosis (Iwanaga, 2010). The natriuretic peptides provide a linear relationship between diagnosis and mortality that can be adopted in the field of theranostics. The limitation is that the stability of these markers is poor stability in serum. This problem is, however, being overcome through the use of enzymatically digested regions originating from their precursor proteins that are more stable (Emdin, 2011). The process of oxidative stress is another minefield for potential biomarkers that can be used for the detection of cardiovascular diseases. Biomarkers like oxidised LDL and myeloperoxidase belong to this group. Myeloperoxidase has a stimulating effect on the formation of foam cells and atherosclerotic plaque formation as is an enzyme that helps in the oxidation of lipids (Hochholzer, 2010b). These markers however lack specificity and there are no direct measurement assay that can quantify them accurately (Braunwald, 2008).

### 1.3.7 New Biomarkers

There is a need to discover and develop new biomarkers for diagnosis and management of acute myocardial infarction for three principal reasons which are to achieve early diagnosis, better prognosis and risk stratification (Jaffe *et al.*, 2006). According to Wu (2005) two approaches can be used for the search for novel biomarkers which are the pathophysiology and the use of proteomics. The study of the pathophysiology as mention earlier can play a pivotal role in the discovery and development of new biomarkers. The diagram in Figure 1.7



shows potential markers in each stage of the pathophysiology of acute myocardial infarction. A good example for the use of proteomics in biomarker discovery is the discovery of choline as a promising marker for ACS through evaluation of the NMR spectroscopy of human blood plasma (Jaffe *et al.*, 2006). The current biomarkers used in the diagnosis of acute myocardial infarction are mostly indicators of necrosis.

It is important to discover and utilise information from other markers that reflect earlier components of the physiopathology chain (Panteghini, 2004; Jaffe *et al.*, 2006). Investigations managed by Jaffe *et al.* (2006) and Braunwald (2008) give overviews of some future cardiac biomarkers that may have potential to identify the patients at risk. Braunwald (2008) identified key prospects in markers like myeloperoxidase, metalloproteinase-9, soluble CD40 ligand, pregnancy-associated plasma protein A, choline, ischemia-modified albumin, unbound free fatty acids, glycogen phosphorylase isoenzyme BB, and placental growth factor. He acknowledged them as having demonstrated promise and need to be more thoroughly evaluated for commercial development for implementation into routine clinical and laboratory practice. Some of these markers have since been dismissed as too general to be used for cardiovascular disease diagnosis. Prospective biomarkers are constantly being investigated and the recent developments have brought about several prospective markers although these are still being debated on and their potential being truly evaluated.

Growth differentiation factor 15 (GDF-15) is one of the rising stars in the potential cardiac biomarker hunt. GDF-15 is a growth factor  $\beta$  cytokine (Kempf, 2007). It was originally used to predict miscarriage in pregnancy because of its high concentrations in the placental tissue (Tong, 2004). However discovered that increased levels of GDF-15 can also be found in activated macrophages to counteract pathological or environmental stress (Brown, 2002; Kempf, 2007). Another study conducted by Kempf *et al.* (2009) identified the best risk

stratification strategies, found that there was synergy when GDF-15 was combined with BNP as the result improved the identification of high-risk patients compared with the individual markers.

Another potential marker that was recently identified is copeptin; a non-functional protein which is located on the same precursor as arginine vasopressin (Hochholzer, 2010a). Increased levels of arginine vasopressin have been correlated with risk of CVD, and the same has been done for copeptin which shares the same precursor with it. Copeptin was shown to be able to predict adverse outcome especially when it was used in combination with the amino-terminal of the BNP precursor (Khan, 2007). Another fantastic attribute is that it has been proven to be able to distinguish patients with an acute myocardial infarction from those with other causes of chest pain (Reichlin, 2009). Unlike arginine vasopressin which is stable in serum the copeptin is vulnerable with a short half-life and a great affinity for binding to other proteins, which makes it difficult to measure (Stoiser, 2006).

## **1.4 Current Methods for diagnosis of CVDs**

### **1.4.1 Background**

There is no standard way in which CVD is diagnosed; this is in part due to the disease being clinically silent until serious complications occur (Grainger, 2006). The current diagnosis of CVD is dominated by either expensive imaging techniques or risky invasive techniques. Sophisticated imaging techniques like the magnetic resonance imaging (MRI) or ultrafast computerized tomography (CT) require expensive equipment and highly skilled staff. The same problem applies to invasive techniques such as coronary or cerebrovascular angiography (Apple, 2007). The invasive procedures are known to have associated risks making them not ideal for mass screening. Some affordable, user friendly and less invasive diagnostic approaches have been developed as

alternatives but these come with their own limitations. A more clinical diagnostic approach is presented by scoring methods like the Framingham study or the Prospective Cardiovascular Münster Study (PROCAM) which considers several simple risk factors and classical symptoms of myocardial ischemia. The combinations of several obtained risk factors is believed to create a synergy and thus give better predictive power but a huge number of patients at high risk go undetected (Grainger, 2006).

Current protocol stipulates medical professionals to focus their resources on all people with chest pains reporting at emergency department as having a potential AMI (Apple, 2007). This strains on the precious resources, and can lead to situations where patients with a milder CVD like angina are unnecessarily admitted and tested for possible heart attack. For this reason much recent research has focused on identifying individuals most at risk of primary cardiovascular events at the point of care (McDonnell *et al.*, 2009). This makes it quick to administer effective prophylaxis, such as aspirin, beta blockers and statins, as well as give appropriate advice on lifestyle choices on an outpatient basis, and has the advantages of freeing up hospital beds and admitting only patients with a high probability of having an imminent AMI (Apple, 2007; da Silva and Moresco, 2011). This section will look at some of the currently used diagnostic techniques for Cardiovascular Diseases. It will highlight the advantages and challenges associated with the current methods and will then give examples and discuss the need for the shift to point of care methods.

#### **1.4.2 Electrocardiography**

It the most commonly used diagnostic apparatus for cardiovascular diseases, as it is affordable and widely available. It is based on the electrical changes that occur temporally as the heart completes its usual cycle. These changes can be monitored in healthy sate and vary when compared to those in certain disease states (Breathnach and Westphal, 2006). There are two major tests that are

done using the electrocardiogram which are the resting and the exercise testing. Resting testing is commonly used to rule out rather than rule in CHD as it has relatively low sensitivity (Gray H, 2002). The exercise testing is also known as the stress testing is performed under conditions that aim to exasperate stenosis. Patients will usually perform the ECG under pharmacologically induced stress or a treadmill. This procedure is important in the diagnosis of Angina (Gray H, 2002). Exercise tests are usually performed following an indicative resting ECG or to aid risk assessment and disease state following AMI to allow the clinician to tailor rehabilitation and management for the individual patients. The clinician will monitor the patient's condition not only by examining the graphical data as shown in Figure 1.9 but by observation of the patient's physical condition (Breathnach and Westphal, 2006).

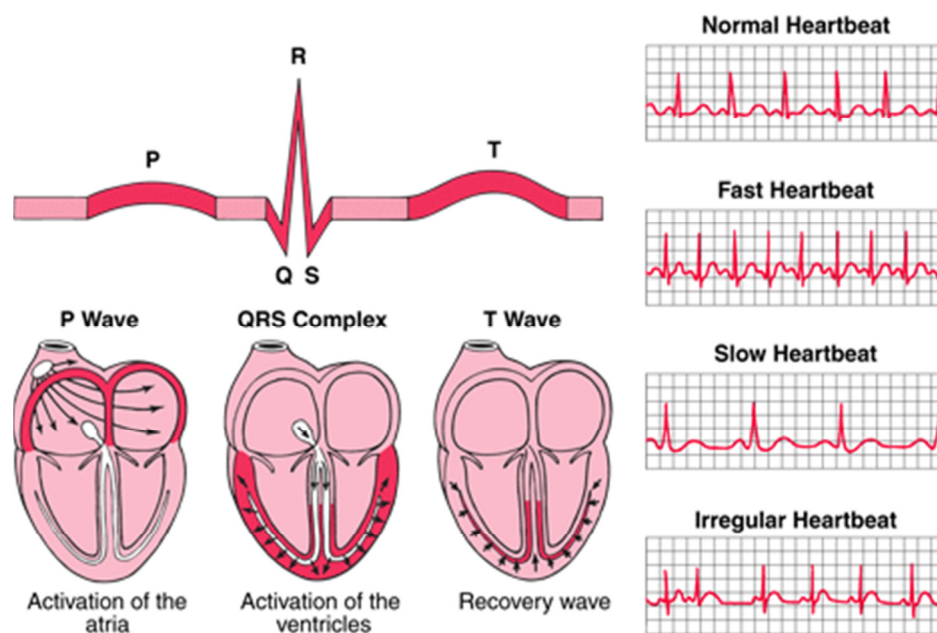


**Figure 1.9:** The electrocardiogram at different heart activity (Muskopf, 2012).

### 1.4.3 Imaging Techniques

Magnetic resonance imaging MRI is an imagining technique that has significant benefits in the diagnosis of CVD as it is capable of providing information on plaque composition. According to Adame *et al* (2006) there are many applications of MRI in CVD diagnosis, contrast-enhanced magnetic resonance angiography (CE-MRA) uses materials such as gadolinium which has desirable magnetic properties to give greater contrast to vasculature clearly denoting stenosis. Another MRI technique such as vessel wall MRI (VW-MRI) which can be used to detect vascular remodeling has proven to be an excellent diagnostic tool (Adame *et al.*, 2006). MRI can also give insight into the pathological state of an atheromatous plaque as well as elements of composition and thickness of the fibrous cap thus it can be used to more definitively identify patients at high risk of AMI or CVA (Cai *et al.*, 2005). The major drawback of MRI is the cost. It is not suitable for patients with metallic stents or pacemakers as it utilizes a strong magnet (Adame *et al.*, 2006).

Computed tomography also commonly known as a CT scan is routinely used in the diagnosis of cardiovascular diseases. It combines multiple X-ray images obtained from a ring of rotating x rays with the aid of a computer to produce cross-sectional views of the body. Cardiac CT is a heart-imaging test that uses CT technology to visualize the heart anatomy, coronary circulation, and great vessels (Heuser, 1999; Cai *et al.*, 2005). Figure 1.10 shows a CT angiograph of the heart taken from the back of the muscle.



**Figure 1.10:** Angiogram showing a blocked coronary artery left and unblocked after surgery right (Heuser, 1999).

The quality of the results obtained is similar to those of the MRI. A modified variation of Ct, which is becoming more popular with the diagnosis of cardiovascular diseases is the Ultra-Fast Computer Tomography (UFCT), also called the electron beam CT. It varies from conventional CT scans because it does not have a rotating x-ray assembly; it has a ring of fixed crystal detectors and another fixed ring of tungsten x-ray targets, which act together (Thim et al., 2008). A major disadvantage of the CT scan to its rival the MRI is that it uses X rays which have long been associated with cancer a schematic diagram for the components of such a device are shown in Figure 1.11.

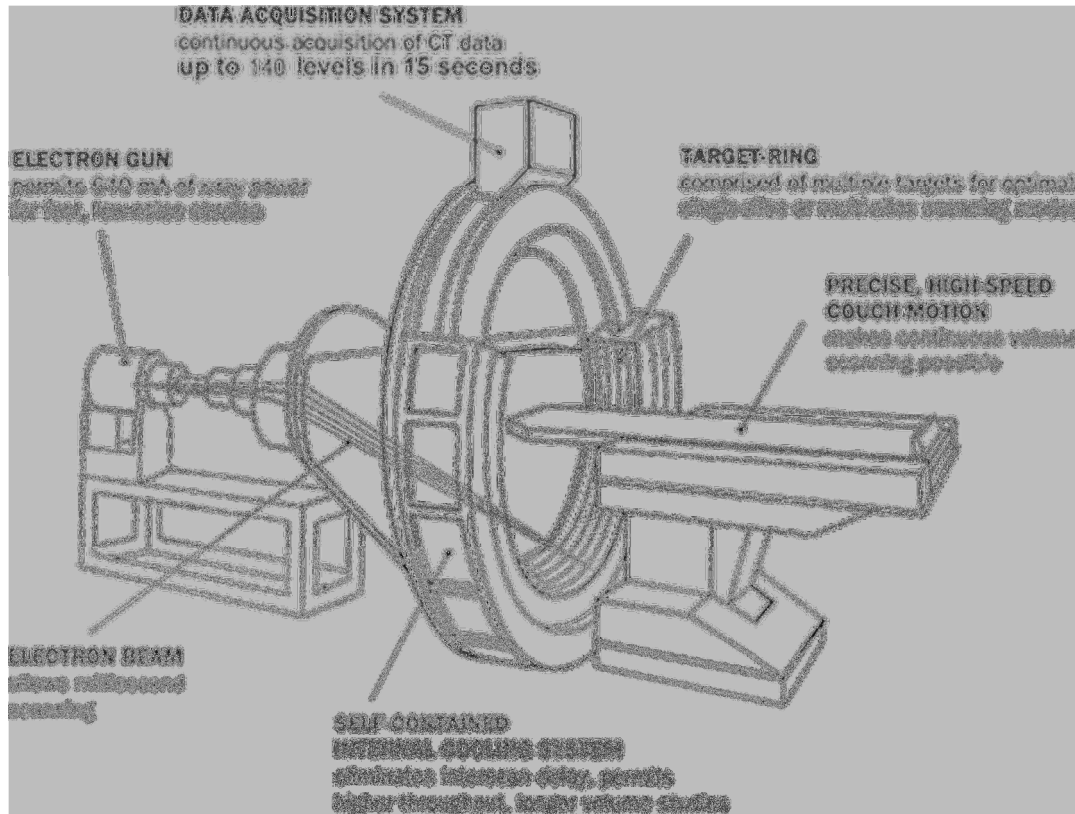


**Figure 1.11:** Schematic diagram of the CT scan showing its major components (Thim *et al.*, 2008).

#### 1.4.4 Immuno Techniques

The analysis of cardiovascular markers can be carried out using immunology based methods like immunoassays. These utilise the specificity of immuno reactive components mostly antibodies, in binding to a specific pathogen, to qualitatively and quantitatively confirm the presence or absence of the antigen. The most common immuno assay is the enzyme-linked immuno sorbent assays (ELISAs). The enzyme linked immunosorbent assay (ELISA) is a method for detecting and quantifying a specific protein in a complex mixture. It was originally described by Engvall and Perlman (1971). In this method, the visualisation of the target antigen is realised through a colour-generating enzyme, covalently linked to a specific antibody. The colour formation is proportional to the concentration and can be used for quantification by analysing the absorbance. The ELISA method was made possible because of

scientific advances in a number of related fields, including the production of antigen-specific monoclonal antibodies by Kohler and Milstein (1976), and the ability to chemically link antibodies to biological enzymes whose activities can be measured as a signal (Avrameas, 1969). Besides the ELISA, there are several other immuno assay formats that were developed earlier including radioimmunoassay which use antibodies labelled with radioisotopes. It was first used before alternatives were sought because of health risks associated with radiation. Several variations have been made to the original ELISA with most changes being made on the method of transduction. A general term 'immuno assays' is more universally accepted.

Focus will be placed on ELISA as the immunosensors developed in this work are based on the modification of the transduction of a sandwich ELISA. It is important to understand the structure and function of antibodies as they play a major role in immuno assays. Antibodies are produced by B-cells as part of the immune response system that identify and neutralise foreign objects such as bacteria and viruses known collectively as pathogen. The antibody recognises a unique part of the pathogen. Antibodies have been used as recognition elements in immunoassay and subsequently immunosensor development because of their high affinity, high specificity, versatility and commercial availability (Ricci, 2007). Antibodies derived from separate cell lines that recognise various regions on the immunogen are termed as polyclonal antibodies, and those derived from single cell line are monoclonal antibodies. There are five major classes of antibodies, which are, IgG, IgD, IgE, IgA, and IgM. Of all these the IgG is the most abundant class in serum has been used in immunoassay development for half a century. Figure 1.12 show the IgG antibody structure that consist of four polypeptide chains - two gamma,  $\gamma$  heavy chains and two kappa,  $\kappa$  chains connected by disulphide bonds.



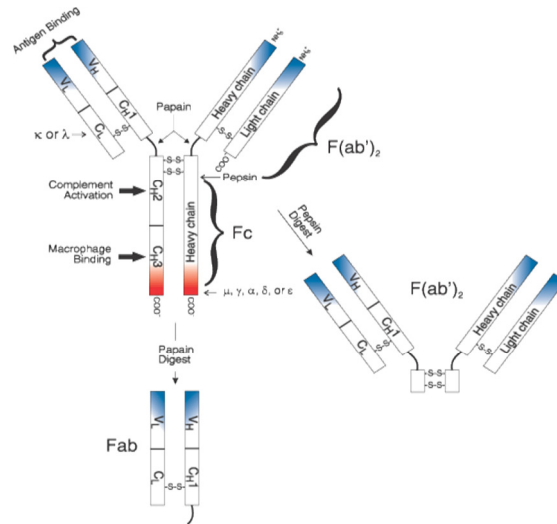


**Figure 1.12:** Schematic diagram of the immunoglobulin structure (Invitrogen, 2012).

There are four main types of Immuno assay protocols for the detection of proteins: direct, indirect, competitive, and “sandwich” Immuno assays. The basic principles for the assays are similar and they include, the capture of the protein of interest, blocking of non-reacted surface, and recognition of the protein (Kemeny and Chantler, 1989). Direct Immuno assay is the simplest form of protein detection. It involves immobilising the protein of interest to the surface this is followed by a washing step and drying and blocking before a specific labelled antibody for the protein is added for detection. Figure 1.13 shows an illustration of a direct immuno assay.

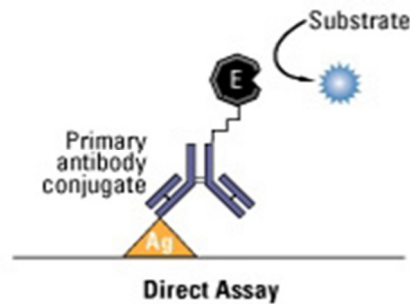


**Figure 1.13:** Diagram showing direct immunoassay set up (AMRITA, 2012).

The other format called indirect immuno assay has the ability to improve the sensitivity of the detection in this method the protein of interest is bound to a specific antibody after immobilisation onto the surface. A labelled secondary antibody against this primary antibody is then incubated for detection purposes as shown in Figure 1.14. It is important that the secondary antibody be raised in another species than the primary antibody to avoid non-specific binding (Kemeny and Chantler, 1989).

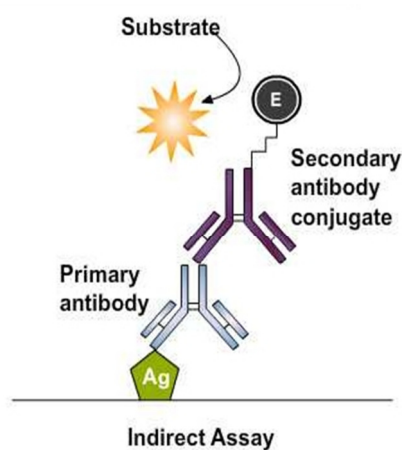


**Figure 1.14:** Diagram showing indirect immunoassay set up (AMRITA, 2012).

By far the most common type of immuno assay detection is achieved by applying two specific antibodies for the protein in a “sandwich” format immuno assay. Antibody-sandwich immuno assays may be the most useful of the immuno-sorbent assays for detecting antigen because they are frequently between 2 and 5 times more sensitive than those in which antigen is directly bound to the solid phase (Law, 1996). An illustration of the sandwich assay is shown in Figure 1.15. The antigen being investigated is actually “sandwiched” between two antibodies which are the coated antibody immobilised on a surface and the detection antibody which is usually conjugated to a marker that can cause a quantifiable response which is proportional to its concentration (Kemeny and Chantler, 1989).

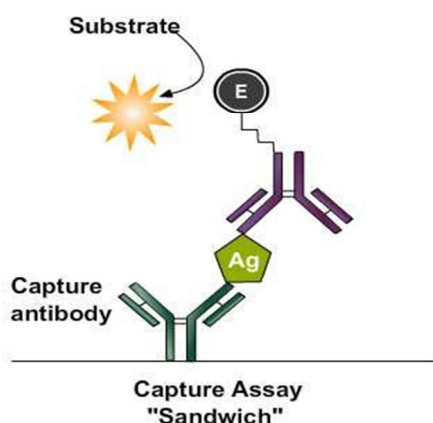


**Figure 1.15:** Diagram showing indirect sandwich immunoassay set up (AMRITA, 2012).

This assay format will be used in this work since the biomarkers to be detected have a molecular weight suitable for a sandwich assay format. Another type of immunoassays called competitive immunoassays, which is used for detecting very small molecules is not covered in this work since it is not relevant in detecting large molecule antigens.

## 1.5 Biosensors

### 1.5.1 Introduction to biosensors

A key area that can be improved in cardiovascular biomarker research is the use of new and novel sensors to detect the established biomarkers. There have been several developments in the field of biosensors and several formats are shown to be capable of detecting and quantifying cardiac markers (Jaffe *et al.*, 2006). One of the first descriptions of a device with bio sensing capabilities was described in 1962. The device utilized the enzyme glucose oxidase coupled to an oxygen sensor to determine the concentration of glucose in the samples from patients during and after surgery (Clark and Lyons, 1962). A biosensor can be defined as a device which converts chemical information into a quantifiable electrical signal (Turner *et al.*, 1987). It is an analytical device that is made up of a biological material such as microorganisms, tissue, enzymes, antibodies or biologically derived material that acts as the recognition molecules. These have to be utilised in conjunction with or attached to a transducer that can give an electronic signal proportional to the concentration of a specific analyte or group of analytes (Tothill and Turner, 1998).

The recognition of the specific analytes can be a binding process, for instance involving an antibody in case of affinity based biosensors or an enzymatic, biocatalytic reaction (Thevenot *et al.*, 2001; D'Orazio, 2003). The signal can be an end-point measurements or continuous but this is easily configured depending on the regulatory and market requirements. The advances in technology and the high expectation from the market especially for miniaturised, cost effective and environmentally friendly has resulted in biosensors becoming relevant in a wide range of analysis. The analytical capabilities of biosensors have been improved as faster microprocessors are constantly being developed (Newman and Turner, 1994). Figure 1.16 shows a schematic diagram for a biosensor.

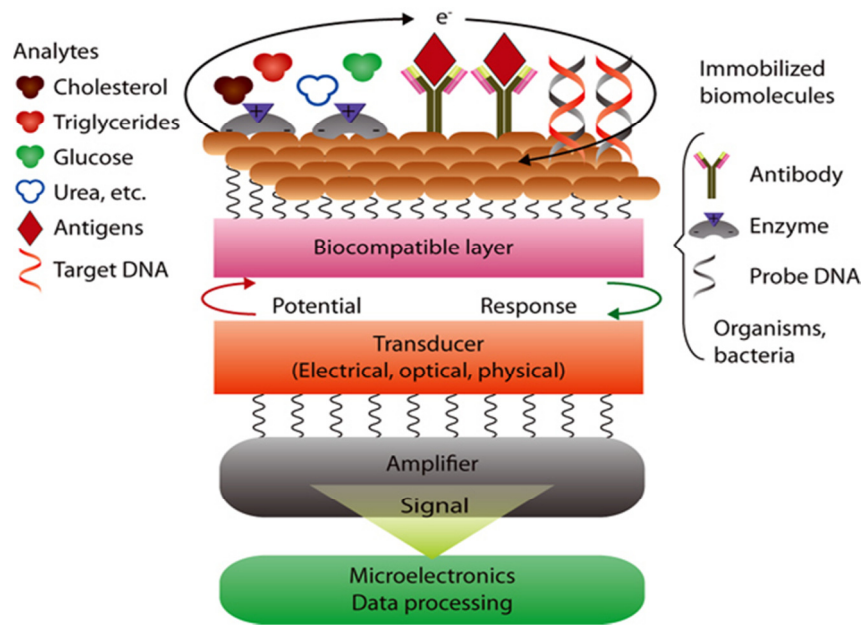


**Figure 1.16:** Schematic diagram showing components of a biosensor (Solanki, 2011).

The classification of biosensors is usually according to the type of transducer thus there are categorized into electric, radiant or optical, thermal, magnetic, and mechanical, frequency transducer (Spichiger-Keller, 1998). According to D'Orazio, (2003) biosensors offer an almost unlimited range of applications in many different kinds of disciplines due to the incorporation of a biological component with its selectivity and specificity.

Today, the applications of biosensors span from applied research to commercially available sensors. There are a wide range of applications from agriculture (Velasco-Garcia and Mottram, 2003) to the measurement of blood metabolites routinely in the laboratory or as point-of-care devices (Tothill, 2009). Considering electrochemical transduced biosensors, potentiometric and amperometric biosensors are the most described in the literature. However, affinity biosensors have generally proved more amenable to optical detection methods (Tothill and Turner 2003).

Immunosensors are a specific subset of biosensors at large and they are distinguishable because they consist of immuno-reagents as the biological sensing elements or receptors. These are mainly antibody or antigen immobilised in close contact with physicochemical transducers for example electrodes and optical fibres. The Measurement of the analyte in the sample is achieved by the selective transduction of the bonding of the receptor-target for example antibody-antigen reaction, resulting in a quantifiable electrical or optical signal (Tothill and Turner 2003). Immunosensors have made it possible for continuous detection to be achieved for a wide variety of analytes. The electrochemical immunosensor is particularly suited for situations where real time monitoring capabilities are required. Where the antibody-antigen interaction conventional immunoassay methods may require duration of several minutes to several hours, such interactions in electrochemical immunosensors are completed within microseconds to minutes. Immunosensors have the advantages of sensitivity and selectivity inherent to the use of immunochemical interactions (Tothill, 2009). The limitation of the immunochemical sensors rise from the fact that the regeneration of the immuno surface is often difficult thus they are mostly require single use disposable components. There is also an issue of cross-reactivity or interference. This can be both a blessing and a curse depending on the application of the immunosensor as well as the type of the target analyses (Tothill and Turner 2003).

### **1.5.2 Optical Immunosensors**

Optical methods are among the oldest and best-established techniques for sensing biochemical analytes. They generally consists of a light source, modulating agent, and a photo-detector for processing the optical signal (Mendelson, 2000). Surface plasmon resonance (SPR) is a good example of an optical immunosensor. It is based on a phenomenon that occurs when light is reflected off thin films of metal and can be verifies by the arrangement based on the Kretschmann configuration (Liedberg *et al.*, 1995). It is one of the first

examples of the demonstration of the functionality of affinity sensors based on optical transducer and is still popular (Perkins and Squirrell, 2000). It involves immobilising antibodies to the surface of a thin metal film for example gold deposited on the reflecting surface of a glass prism. Interaction of antigens with immobilised antibodies to the surface will elicit a change in the refractive index as variations in light intensity, reflected from the back of the film proportionally to the mass of antigens bound to the surface. When light is shone onto the grating at a certain angle of incidence, the momentum of the photons is converted into a collective motion of the electrons in the metal called surface plasmons (Liedberg *et al.*, 1995).

This results in a decrease in the intensity of the reflected light. The angle of incidence at which resonance occurs depends on the optical thickness (essentially refractive index) of the layer that is within 300nm of the diffraction component surface (the evanescent field), and thus, the SPR-based sensors facilitate direct label-free detection (Iwasaki *et al.*, 2001). SPR measurements in the laboratory are often made with the chip in a flow cell to allow for controlled delivery of reagents and sample. The use of SPR for cardiovascular biomarkers is in its self not novel as some studies have already been done. Some SPR sensors have been reported based on immuno-sensors for biomarkers of cardiovascular diseases including for C-reactive protein (Meyer *et al.*, 2006) and for myoglobin and cardiac Troponin I (Masson *et al.*, 2004). The SPR commercial scene is currently dominated by the BIAcore system, and since the introduction of BIAcore a number of more sensitive SPR instruments have been launched (McDonnell, 2001). One such machine is the AutoLab Spirit® which, unlike the BIAcore, the reflection is measured as a function of the incident angle of the light beam (Dutra and Kubota, 2007). Figure 1.17 shows the working mechanism of an SPR biosensor.

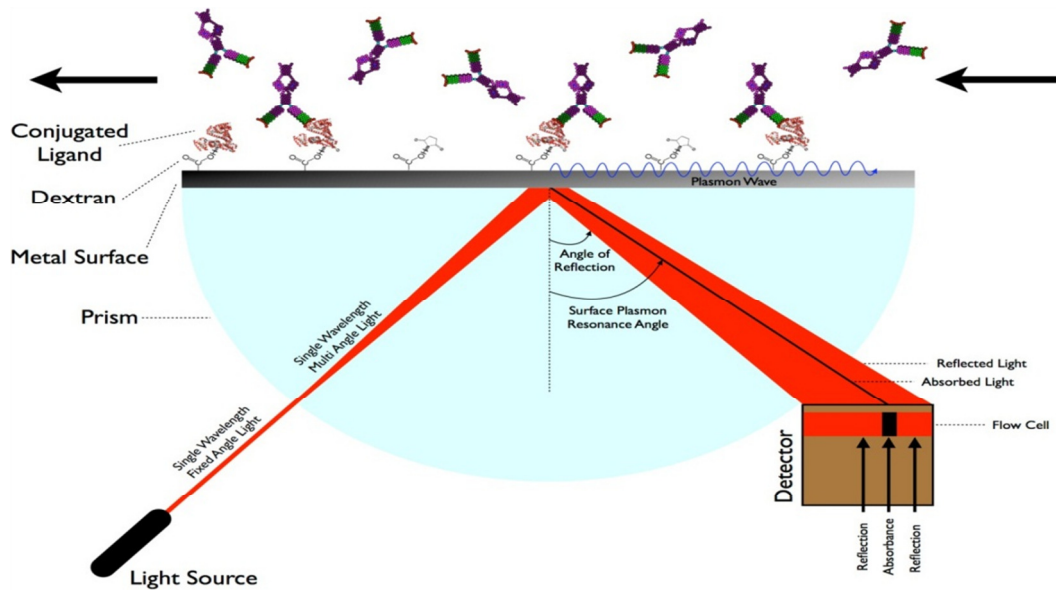


**Figure 1.17:** The working mechanism of a surface plasmon resonance (SPR) biosensor (Sabban, 2011).

The use of fibre optics in immuno biosensors for cardiovascular disease is another classical example of recent developments in optical immuno-biosensors (Kwon, 2003). Other novel optical immuno-sensing techniques are being developed for the early detection of myocardial infarction. One such technique is called fluorescence resonance energy transfer (FRET). It involves utilizing the distance-dependent chemical transduction method of fluorescence resonance energy transfer. The FRET process requires two fluorophores termed the donor and the acceptor. When in close proximity, the donor absorbs energy from the excitation source and non-radioactively transfers the energy to the acceptor, which in turn emits fluorescent energy. This distance-dependent property is utilised to detect conformational changes when antibodies combine with their respective antigens. This technology has already been used in detecting biomarkers for cardiovascular diseases (Grant *et al.*, 2004).



### 1.5.3 Piezoelectric/acoustic Immunosensors

The Quartz Crystal Microbalance (QCM) is an extremely sensitive mass sensor, capable of measuring mass changes in the nanogram range. QCMs are piezoelectric devices fabricated of a thin plate of quartz with electrodes affixed to each side of the plate. Piezoelectric ceramic materials can be produced by a less expensive process, however the ceramics are limited by their lack of long term stability compared to single crystal materials which are less sensitive but when carefully handled have a significantly long-term stability (Bunde *et al.*, 1998). Single crystal materials are quartz, tourmaline and gallium phosphate. Of the two it is the quartz crystals which are common type of single crystal materials used in analytical application due to their electrical, mechanical, and chemical properties (Bunde *et al.*, 1998).

The resonant frequency of the quartz crystal depends on several parameters, for instance the size, the density, the shear modulus, but also the cut. Quartz Crystal Microbalance (QCM) is a special sensor that has acoustic impedance detector by mass loading. Piezoelectric also known as acoustic immunosensor such as the quartz crystal microbalance (QCM) and other surface acoustic devices are classified as direct immunosensor, when immuno-reagent is used as the receptor. Quartz crystal immunosensors are dependent on the immobilisation of antigen or antibody at the surface of a piezo-electric material (Uludag and Tothill, 2010). The natural vibration frequency of the support is changed when there is a significant immunochemical recognition reaction. The applications of QCM are diverse and many commercial piezoelectric detectors are now available. They have been proven to show the possibility of developing faster diagnosis assays compared to traditional detection methods for cardiovascular diseases (Wong-ek, 2009).

### 1.5.4 Electrochemical Immuno-sensors

The electrochemical transduction appears to be the fastest growing trend in the development of biosensors. This growth is linked to the benefits it offers like miniaturisation, specificity and sensitivity as well as the success story of the blood glucose biosensors, which has emerged to be the leading commercial biosensor of all time (Apple, 2007). Electrochemical transduction based immunosensors have been used in the detection of a range of analytes (Salam and Tothill, 2009; Kadir and Tothill, 2010). The detection of cardiovascular biomarkers using immuno-electrochemical assays has been attempted for cardiac troponins (Mohammed and Desmulliez, 2011) and for myoglobin (Suprun *et al.*, 2011). It is on this basis that immuno electrochemical biosensor platform was developed for this work.

Electrochemical immunosensors are based on conventional antibody based enzyme immunoassays that are typical of most ELISA platforms. Immunoassay-based sensors have been developed to exploit the high degree of specificity and affinity of antibodies for specific antigen. Their mechanism catalysis of substrates by an enzyme conjugated to an antibody produces products such as ions, pH change or In this particular application, a given chemical, metabolite, or modified protein can act as the antigen, and an EC response linked to antibody binding with the antigen (Darain *et al.*, 2003). The Direct immuno-electrochemical detection without the use of labelling can be performed by cyclic voltammetry, chronoamperometry, impedimetry, and by measuring the current during potential pulses, a process called pulsed amperometric detection. These methods are able to detect a change in capacitance or resistance of the electrode induced by binding of protein. Despite having a lot of variety in the label free immnoelectric sensor platforms, it is the labelled amperometric immunosensor, which is popular (Darain *et al.*, 2003).

The principle of electrochemical immunosensor using amperometric transducer in detecting cardiac biomarkers is similar to that of other applications in the field. In principle the antibody or analyte of interest is immobilised on a membrane and the analyte is measured by signal derived from a conjugated tag that is attached to either the antibody or analyte (Piras and Reho, 2005). Two types of immunoassays are generally employed which are competitive or sandwich assay. Both are characterised by the coupling the electrode to the antibodies raised against the biomarker of choice to an electron transport chain via low molecular weight mediators. These are redox species that transfer electrons between the electrode and redox active bio-molecules via an alternate oxidation/reduction reaction (Kadir and Tothill, 2010).

There are several of such species including peroxides, phosphatases, urases, and glucose oxides mediated electron transfer (Piras and Reho, 2005). Peroxidase is a good enzyme label in this application. When given a suitable substrate like 3, 3', 5, 5'- tetramethylbenzidine hydrochloride (TMB) and hydrogen peroxide it is capable of producing an oxidised product that can be electrochemically reduced to produce electrons. These electrons are responsible for generating a catalytically enhanced current which is easily detected if a constant potential is applied (Darain *et al.*, 2003). These approaches are essentially conventional binding assays which used enzyme label to detect the reaction and involve multistep procedures of incubating and washing that often found in traditional immunoassay formats based on microtitre plates (Darain *et al.*, 2003). Improvements in assay development for immuno-electrochemistry for example the use of gold nanoparticles have made this a common research area with potential commercial outcomes (Luo *et al.*, 2006; Saha *et al.*, 2012). This study will include the development of immuno-electrochemical biosensors for cardiovascular diseases. Since this technique will be used in these assays, a more comprehensive cover of the method will be discussed in the specific sections required in the work.

### **1.5.5 Detection of Cardiovascular Diseases using Biosensors**

Laboratory analysers are an invaluable resource but have several limitations, they are more suited for a hospital setting where there are trained personnel who can operate the machine and interpret the results accurately as well as phlebotomists who can take blood and supply the sample. Effective intervention of cardiovascular disease strongly relies on a rapid turnaround time (Apple, 2007). This is the time taken between taking the blood sample from the patient until the results are obtained. The standard for chest pain diagnosis that is ideally it should be between 30 minutes to one hour, with 30 minutes or less being the optimum and this is not always possible if tests are performed in a centralised laboratory (O'Regan, 2003). Recent market demand devices that are more compact and can be used independently by the end user.

There are no known over the counter devices for cardiovascular disease diagnosis but a step towards this has been achieved through the point-of-care devices. Bench top analysers are an example of such devices and are usually modified main laboratory analysers that have been miniaturised. They usually resemble larger systems and are capable of offering an array of tests that can assist in the diagnosis of a particular area of interest. A good example is the analysers that have a cardiac panel that enables them to test a single sample for a multitude of cardiac markers. This type of analysers also have the ability to use a variety of analytical methods including enzyme activity measurements, spectrophotometric substrates, haematological particle counting, immunoassay and biosensors (Luppa *et al.*, 2011 ). A summary of such devices have been summarised in Table 1-3. Figure 1.18 shows the triage bench analyser. The triage is one of the pioneering compact analysers for cardiovascular disease. It was launched in 1998 and while all the other machines were laboratory based the triage had approval to be used as a point of care device. It is capable of detecting three cardiac markers, which are Troponin I, Myoglobin, and CK-MB. It is based on optical transducer which detects an output from a cartridge which employs the lateral flow technique (Christenson, 1998).

**Table 1-3:** Summary of current diagnostic devices for cardiovascular diseases

Supplier	Biosite	Response Biomedical/ Roche	Roche	First Medical	Dade Behring	Biomerieux	Abbot
<b>Product</b>	Triage Cartridge	RAMP cardiac marker system	Cardiac reader	Alpha DX	Stratus	Vidas CK-MB	I-start
<b>Analysis type</b>	Fluorescent microfluidics	Fluorescence and microfluidics, read on table top reader	Dried down strip with gold labelled antibodies and table top analyser	Disk analysed in tablet op reader	Fluorometric analyser machine	Fluorometric analyser machine	Hand held Immunosensor based analyser
<b>Readout time</b>	15 min	10-12 min	12 min	18 min	13 min	30 min	10 min
<b>Limit of Detection Tns</b>	1ng mL <sup>-1</sup>	0.3 ng mL <sup>-1</sup>	0.05 ng mL <sup>-1</sup>	0.5 ng mL <sup>-1</sup>	0.3 ng mL <sup>-1</sup>	0.11 ng mL <sup>-1</sup>	0.008 ng mL <sup>-1</sup>
<b>Dynamic Range Tns</b>	1-80 ng mL <sup>-1</sup>	0.3 -50 ng mL <sup>-1</sup>	1-40 ng mL <sup>-1</sup>	0.5-100 ng mL <sup>-1</sup>	0.3-150 ng mL <sup>-1</sup>	0.01-30 ng mL <sup>-1</sup>	0.008- 50 ng mL <sup>-1</sup>
<b>Markers detected</b>	TroponinI	Myoglobin	TroponinT,	Troponin I	TroponinT and I,	Myoglobin	Cardiac troponin I
	Myoglobin	CKMB	Myoglobin	Myoglobin	Myoglobin,	CKMB	CKMB
	CKMB		CKMB	CKMB and CK	CKMB		BNP



**Figure 1.18:** The Triage® cardiac panel system is able to detect myoglobin, creatine kinase-MB fraction and cTnI from whole blood, Biosite Inc (2009).

The triage has several advantages, which has made it a success, The major ones being that the transduction and output device can work on any specified antigen. This means that it is not limited to detecting just cardiac markers but other blood proteins like haemoglobin 1C. The second advantage is that it uses whole blood that means it does not require sample pre-treatment at all. It uses capillary action that will draw blood from the sample port to a filtration membrane before exposing the Serum to the lateral flow device in the cartridges. The downside for the triage and most other analysers is the expensive costs. The costs associated with buying the machine around £3800 when launched and cartridges at around £8 per test, are too high for home users and the amount of blood which is required need to be drawn out by a trained phlebotomist hence it cannot be used as an over the counter test. Great strides are being made towards eliminating these obstacles as demonstrated by launched iSTAT® which is a hand held device from Abbot shown in Figure 1.19 .



**Figure 1.19:** The iSTAT® system for POC detection of cTnI (Abbot, 2011).

This device utilises a dual-site coupled onto an electrochemical sensor. An alkaline phosphatase-conjugated secondary antibody is used to recognise and bind to the immobilised antigen before substrate is applied. The substrate is then catalysed by the alkaline phosphatase and electrons are produced that can be transduced to a proportional concentration of the analyte immediately. Test results can be remotely sent and be integrated into lab information systems (Abbott, 2011).

## 1.6 Aims and Objectives

### 1.6.1 Aims

The world is becoming more environmentally aware and as such miniaturisation is the general trend in medical diagnostics as with most consumer electronic goods (Newman and Turner, 1994). The demand for diagnostic products that can be accessed by the less developed countries without consistent power supplies and in some cases technical knowhow of operating some big laboratory based instruments. This has promoted research to focus on the development of portable low powered and easy to use diagnostic equipment capable of Point of care testing (McDonnell *et al.*, 2009). Cardiovascular disorders remain one of the leading causes of death worldwide. The amount of individuals affected is increasing constantly. Especially in developing countries, a dramatic increase has occurred during the last decades (World Health Organisation 2011).

Recent research focus on diagnosis of cardiovascular disease is centred on trend of identifying not only fast, accurate, reliable, and affordable diagnostic tools which are robust and compact but also capable of facilitating a predictive function for prognosis and risk stratification (da Silva and Moresco, 2011). Electrochemically transduced biosensors are capable of providing a solution to this problem, if they are designed to detect specific cardiac markers (Silva *et al.*, 2010). The use of immunosensors particularly those that use screen-printed electrodes is the cheapest and most effective way of doing this. Screen printed electrodes are capable of being commercially produced in bulk at very low cost and offer other desirable characteristics like miniaturisation, disposability and ease of use (Garcia-Gonzalez, 2008; Tothill, 2009). This project aims to achieve this by developing immuno-electrochemical assays and incorporate them on to screen-printed gold electrodes to make multi marker immuno-based biosensors for the detection of cardiovascular diseases.



### **1.6.2 Objectives**

Immunoassays in the form of ELISA assays were developed for selected cardiac markers, which are cardiac Troponin T (cTnT) and C-reactive protein. This provided a learning platform for the assay setup and feasibility before it was transferred onto screen-printed electrodes. This is because ELISA plates are easier to work with in terms of high volume investigations as they can accommodate 96 wells. This makes it easier to develop and optimise assays. The next step was to transfer the optimized ELISA assay to the immuno-sensor platforms in the hope that the optimised parameters for the plate assay will have a similar performance on the electrode surface.

A manufacturing perspective was investigated in this project to identify appropriate ink compositions and curing techniques for making competent electrodes that provide a platform immunosensor development. This was complemented with the investigations on the best surface chemistries for optimised binding and blocking of biosensor surfaces.

An evaluation of current protein stabilization techniques was made with particular reference to the preservation of immobilised active proteins. Attempts to formulate new ways were made. The evaluation of the biosensor developed was done to test measurement of cTnT and CRP. Comparisons of the performance of the developed immuno-sensors against other commissioned methods and devices was made. A systematic summary of the objectives of this project is given by Figure 1.20.

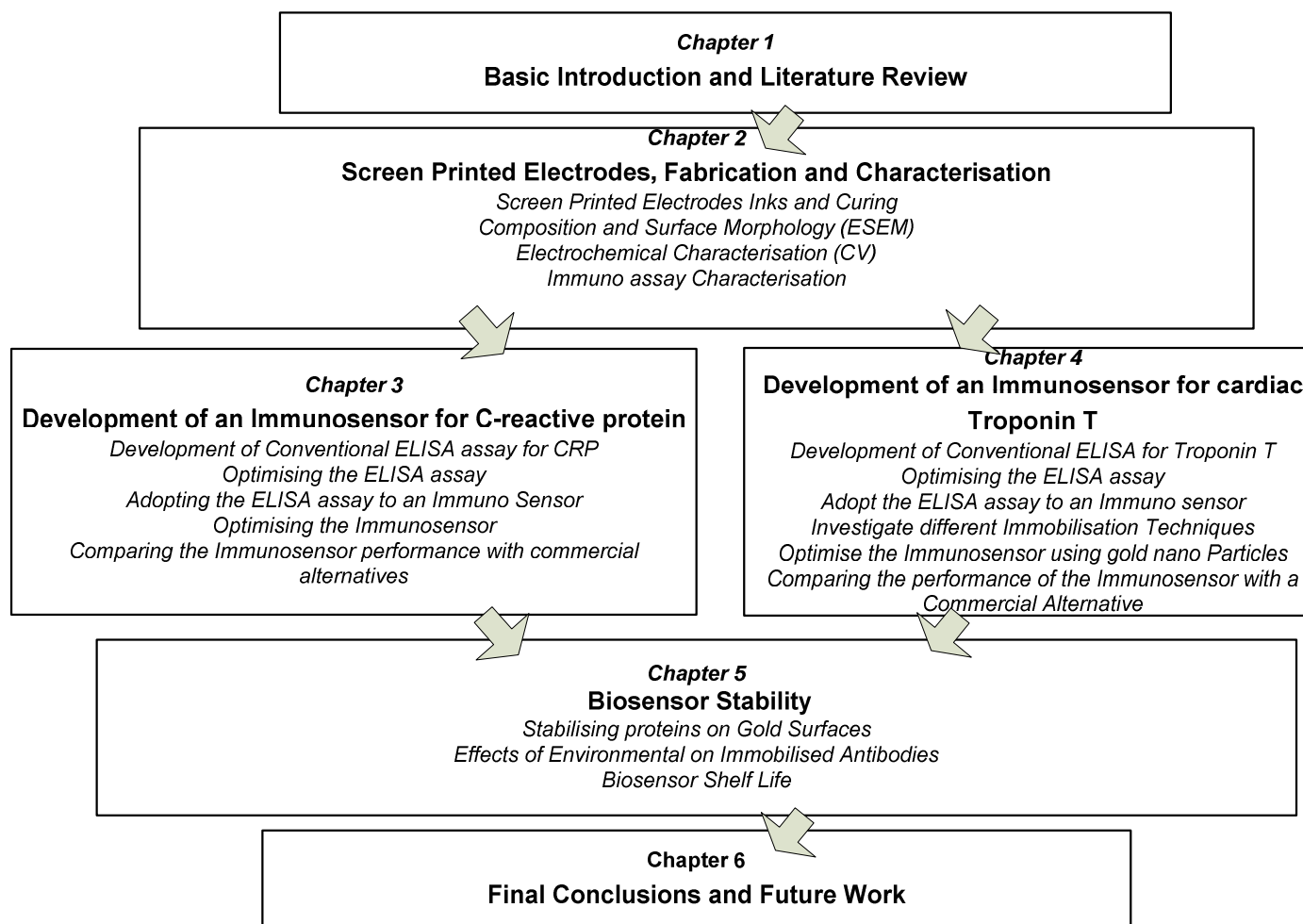


**Figure 1.20:** Flow chart outlining the different phases of work carried out in this study.

## CHAPTER 2

# SCREEN PRINTED ELECTRODES, FABRICATION AND CHARACTERISATION

## 2 Screen Printed Electrodes, Fabrication and Characterisation

This section discusses screen-printed electrodes and their role in electrochemical transduced sensors with particular reference to immuno-sensors. It will give an insight into material compositions and the methods of manufacturing. Some experiments conducted in an attempt to improve the performance of the electrodes before they can be used as immuno sensors will be shown and discussed.

### 2.1 Introduction to Screen-Printed Gold Electrodes (SPGE)

The general market trends in the diagnostics and analytical devices are undoubtedly oriented towards miniaturisation. Across fields of the analytical trade, it is evident that the interfacial nature of measurements favours the fabrication of miniaturised analytical devices. According to Garcia-Gonzalez (2008) it is because of this context that the thin and thick-film technology are of great utility to the diagnostic and analytical trade. Screen-printing is a well-known thick film technique that is now widely used for the mass-production of disposable electrochemical sensors. Generally screen-printed electrodes are made from templates which allow for the simultaneous production of usually three tracks which will become the working, reference and auxiliary electrodes (Erlenkotter, 2000). This potentiostatic system allows them to be used as single use drop-on sensors in a static mode or in flow systems (Alvarez *et al.*, 2002; Santos *et al.*, 2004). The advantages of a single-use disposable sensor include the elimination of problems associated with carryover of contamination and sterilisation and also minimises the fear of expensive damage often associated with a re-usable sensor (Erlenkotter, 2000). Sensor micro-fabrication technologies such as thick film screen-printing, thin-film lithography, silicon technology, optical sensor technology can provide a pathway for the simple and inexpensive mass production of disposable electrodes. Screen-printed

electrodes (SPEs) rely on planar carbon or gold working electrodes and a silver reference electrode that are printed on an expensive plastic or ceramic support. Hence, each strip can be considered as a disposable electrochemical cell onto which the sample droplet is placed (Alvarez *et al.*, 2002).

Different electrode geometries can be fabricated using suitable patterned photo masks or stencils. Electrode structures with 0.5  $\mu\text{m}$  dimensions can be produced with modern micro lithographic processes, while larger (75-100  $\mu\text{m}$ ) structures can be achieved using screen-printing (Wang, 1995). Screen-printing is a printing technique that uses a woven mesh to support an ink-blocking stencil. The attached stencil forms open areas of mesh that transfer ink or other printable materials. A roller or squeegee is moved across the screen stencil, forcing or pumping ink past the threads of the woven mesh in the open areas forming a sharp-edged image onto the substrate as shown in Figure 2.1. The paste-films have a typical thickness between 10 and 50  $\mu\text{m}$ . The performance of sensors fabricated by thick-film technology depends critically on the applied materials and the manufacture. There is a wide range of inks and substrate materials that can be used to produce low cost sensor strips. Commercial carbon and good metal conductors like platinum and gold are used in Ink formulations for printing the working electrodes, whereas silver-based inks are used for obtaining the reference electrode (Wang, 1995).

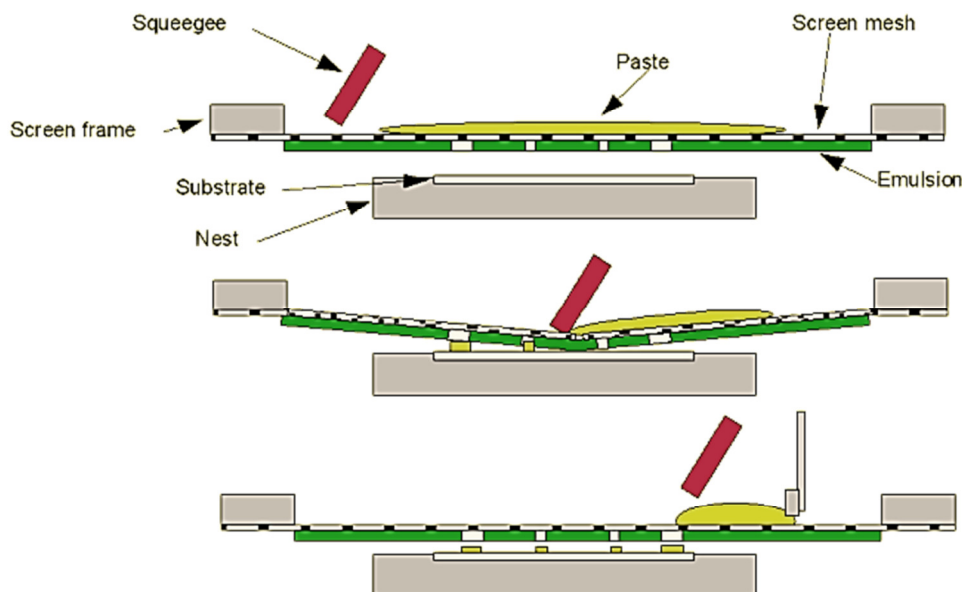


**Figure 2.1:** Schematic representation of the screen-printing process (Hobby, 1997).

There are several significant advantages of thick film technology, which have attractive option for the fabrication of sensors and biosensors. These include flexibility of design and choice of materials, easy integration with electronic circuits, low cost in infrastructure and mass production, the possibility of automation of the fabrication process as shown in Figure 2.2, a low barrier for technological transfer from thick-film to other technologies (Alvarezicaza and Bilitewski, 1993). Miniaturisation is feasible, along with a high degree of electrochemical activity of the devices deriving from their high specific area and microporous structure. However, thick-film technology also has its own drawbacks.

This technology mostly has problems related to compatibility between the different materials, and between the materials and the manufacturing process (Erlenkotter, 2000). Other shortcomings are related to sensor-fabrication processes, such as the need of complicated curing cycles with high temperatures and long times, and low reproducibility of the constructed devices resulting, for example, from evaporation of solvents in the paste formulation (Galan-Vidal, 1998).



**Figure 2.2:** The production of screen-printed electrodes on an industrial scale (Hobby, 1997).

Several commercial companies are capable of making screen-printed electrodes for immuno-sensing applications and commercially sell them. Other companies are only capable of making the inks that can be used to make the electrodes. The table below shows the companies that are associated with the production of inks or the manufacturing of screen-printed electrodes.

The sensors used in this project were designed by Cranfield University and fabricated using screen printing facilities at Dupont, the inks used in the fabrication of these electrodes were supplied by Dupont. Figure 2.3 shows the set-up of the screen-printed electrodes from Dupont used in this project.

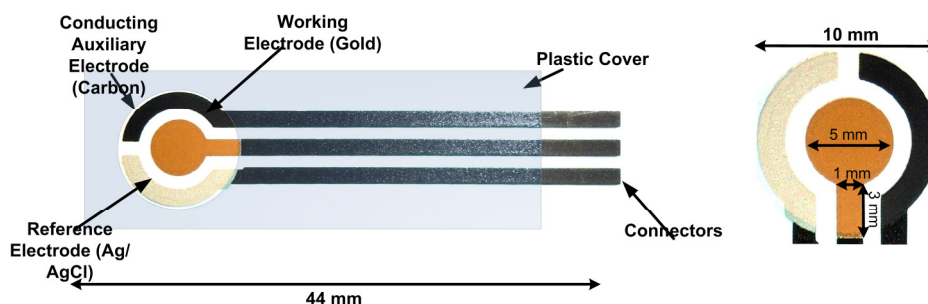







**Figure 2.3:** Screen-printed electrodes used in this project.

The quality of the sensor inks is a significant factor that contributes the overall quality of the electrodes. Carbon inks are however, still relevant for sensing applications because they are relatively inexpensive and lead to low background currents and a wide potential range. Such inks are composed of graphite particles, a polymeric binder and other additives that play a role in the dispersion, printing and adhesion processes (Garcia-Gonzalez, 2008). The exact formulations are treated as proprietary information that helps them gain a competitive advantage over competition. Such differences in the ink composition like the size of particles, and in the printing and curing conditions, may strongly affect the overall analytical performance of the resulting sensors. Materials with more desirable characteristics like gold are now getting significant research interests. This is because of the good electrical conductivity and its ability to form strong Au-S bonds with self-assembled monolayers (SAMs) (Bain, 1989). The strong bond between gold and SAMs brings forth the enormous possibilities of immobilisation of bio-molecules on its surface, which resulted in wide application in bio-sensing technologies.

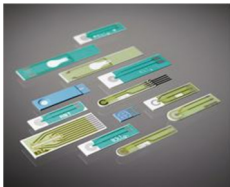


**Table 2-1:** The commercial organisations associated with screen-printing of electrodes.

Company Name	Location	Description	Products
<b>BST Bio Sensor Technology GmbH</b>	Germany	The design, development and production of thick film based biosensors	
<b>VT Technologies</b>	Czech Republic	Research and development of new types of electrochemical sensors and biosensors.	  
<b>University of Florence</b>	Italy	The group of Prof. Marco Mascini from the University of Florence produces screen printed electrodes (SPE) on a plastic base	
<b>Dropsens</b>	Spain	Innovative Technology-Based Firm specialised in the design and manufacture of instruments for Electrochemistry Research.	
<b>Ercon</b>	USA	Biomedical and Electrochemical sensor Materials	Silver/Silver Chloride Carbon Graphite Platinum, Gold, Catalyst Insulayer™ FIP Microporous Media™
<b>Kanichi</b>	UK	Knowledge based company that specialises in developing custom-made electrodes for advanced sensor systems	Contract research, Electrochemical sensors, nanoparticles , custom synthesis
<b>Gwent Group</b>	UK	Consultancy and industrial fabrication of diagnostic biosensors	Fabrication equipment, Consultancy, Research, Manufacturing
<b>Dupont</b>	USA, UK	Suppliers of Inks and screen printing facilities for Biosensors applications	Silver/Silver Chloride Carbon Graphite Platinum, Gold, Catalyst Insulation layers, Fabrication facilities

### 2.1.1 Characterisation of Screen-Printed Electrodes

There are many publications reported about the electrochemical characteristics of screen-printed electrodes (Osborne *et al.*, 1996; Cui *et al.*, 2001a; Cui *et al.*, 2001b; Grennan *et al.*, 2001; Morrin *et al.*, 2003). Screen-printed gold electrodes SPGEs have been mentioned to be the basis of most sensors for heavy metals detection (Noh and Tothill, 2006). They have also become popular as immunosensors in recent years (Salam and Tothill, 2009; Kadir and Tothill, 2010; Heurich, 2011) which will be their main function in this project. Many important chemical processes occur at the surface of a solid. Some examples include catalysis, electrochemistry and adhesion. Understanding these processes requires an understanding of the composition and structure of the surfaces. The analytical techniques that can selectively characterize solid surfaces can be divided into two categories: techniques that are primarily used for elemental analysis at surfaces, and techniques primarily used for surface imaging (Garcia-Gonzalez, 2008).

Several methods are used to try to characterise and understand the surface chemistries of immuno-sensor. These help to validate batch-to-batch consistency as well as to assess the viability of the electrodes. The most common optical method is the use of the electron microscopy. Electron microscopy is an imaging technique that used an electron beam to probe a material. Since the wavelength of an electron is much smaller than the wavelength of visible light, diffraction effects occur at much smaller physical dimensions (Kimseng and Meissel, 2001). The imaging resolution in electron microscopy is approximately 1 nm, which is much better than the  $\mu\text{m}$  resolution of light microscopy. When electrons penetrate a sample, they are diffracted to form a diffraction pattern. This diffraction pattern can be transformed with a lens to obtain the sample image. The use of electron beams requires that the sample be placed in a vacuum chamber for analysis. A variable of this kind of machine are the Scanning electron microscopy (SEM) and the environmental Scanning

electron microscopy (ESEM). The instruments are used for studying surface morphology. Nonconductive samples will need to be treated by evaporated gold or graphite coating over the sample to prevent charging effects. These charging effects are capable of distorting the electric fields in the electron microscope and thus affecting the quality of the image. A recent innovation in scanning electron microscopy is the environmental scanning electron microscopy (ESEM), it uses several stages of differential pumping between the electron gun and the sample, which is placed in a vacuum of a few torr. This allows imaging of samples that would quickly vaporise in a high-vacuum environment (Kimseng and Meissel, 2001). This method will be used to characterize the surface composition and morphology of the working electrodes used in this work.

Cyclic voltammetry is the most widely used technique for acquiring qualitative information about electrochemical reactions. It consists of scanning a potential on a stationary working electrode in an unstirred solution so that the measured current is limited by analyte diffusion at the electrode surface. The electrode potential is swept between two values at a fixed rate, when the potential reaches the second value, the scan reverse back to the starting voltage. A basic shape of the current response for a cyclic voltammetry experiment is shown in Figure 2.4. For a fully reversible reaction, the forward sweep curve is similar to that of linear sweep voltammetry. On reversing the scan direction, electrons are withdrawn from electrode and the material reduced in the forward sweep are oxidized back (Bard, 2001). The cyclic voltammogram is characterized by several important parameters. Two peak currents and two peak potentials provide the basis for the diagnostics developed for analysing the cyclic voltammetric response as shown in Figure 2.4.

The anodic and cathodic peaks  $E_{pa}$  and  $E_{pc}$  respectively play a major role as well as the peak currents ratio  $i_{pa}$  and  $i_{pc}$ . In this, experiment the  $i_{pa}$  values that were used in the Randles-Sevcik equation. In cyclic voltammetry, the Randles-Sevcik equation describes the effect of scan rate on the peak current (Gosser, 1993). For simple redox events such as the ferrocene/ferricenium couple, the peak current depends on both the concentration and diffusional properties of the electro-active species and the scan rate. Using the relationships defined by this equation, the diffusion coefficient of the electro active species can be used to determine the active surface area of the working electrode (Bard, 2001).

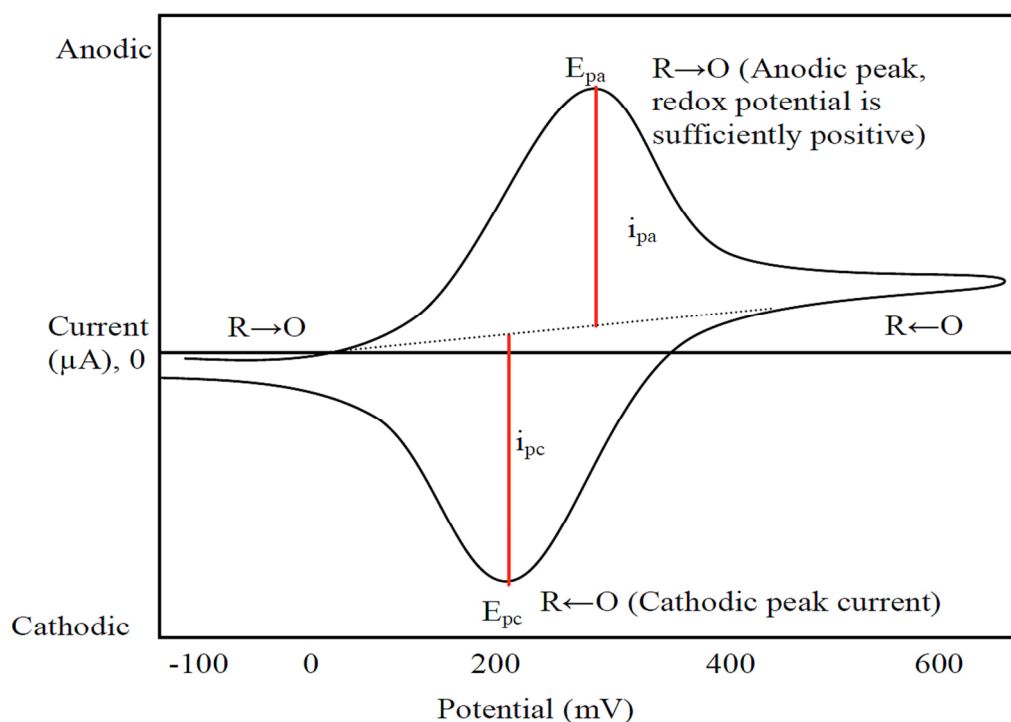


**Figure 2.4:** Cyclic voltammogram recorded for a reversible redox in single potential cycle  $E_{pa}$  = anodic peak potential;  $E_{pc}$  = cathodic peak potential;  $i_{pa}$  = anodic peak current;  $i_{pc}$  = cathodic peak current. (Bard, 2001).

The analysis of the electrodes using cyclic voltammetry is based on the fact that a cyclic voltammogram of a fully reversible system will display a known set of characteristics governed by a series of equations (Gosser, 1993). One of the major equations is the Randles-Sevcik equation which at room temperature is.

$$I_p = (2.69 \cdot 10^5) \cdot A \cdot C \cdot \sqrt{n^3 \cdot D \cdot \nu}$$

**Equation 2-1**

Where  $n$  is the number of electrons,  $A$  the electrode area in  $\text{cm}^2$ ,  $C$  the concentration in  $\text{mol}/\text{cm}^3$ ,  $D$  the diffusion coefficient in  $\text{cm}^2/\text{s}$ , and  $\nu$  the scan rate (in  $\text{V}/\text{s}$ ). The equation can be used to estimate the percentage of the active surface of the working electrode (Bard, 2001).

### **2.1.2 Aims and Objectives**

The aim of the work described in this chapter was to define the composition of the final electrodes that will be used in the development of biosensors for cardiovascular diseases. There were many combinations of inks that could have been used and this search was narrowed down to three compositions that had to be investigated to find the electrode with the best combinations. This was done through primarily cyclic voltammetry but an immuno assay was also carried out on the chosen different electrode combinations to validate the results of the cyclic voltammetry.

A secondary aim was to investigate the effect of the method of curing on the performance of the electrodes. Investigations were conducted to evaluate the performance of electrodes cured using a conventional technique that utilised oven drying a more faster alternative that used infra-red IR drying. This was

done by monitoring the electrochemical behaviour using cyclic voltammetry. The experiment was complimented with the evaluation of the curing techniques to the surface chemistry and morphology. This was determined using environmental scanning electron microscope E-SEM.

## 2.2 Materials

Potassium chloride (KCl), potassium ferricyanide ( $\text{K}_3\text{Fe}(\text{CN})_6 \cdot 3\text{H}_2\text{O}$ ), TMB (3, 3', 5, 5'- tetramethylbenzidine hydrochloride), PBS (phosphate buffered saline) containing 0.137M sodium chloride, and phosphate buffer, 0.01M, pH 7.4 in tablet form, citrate phosphate buffer (0.05 M, pH 5.5) tablets, hydrogen peroxide, sodium hydroxide (NaOH) and sodium chloride (NaCl), bovine serum albumin (BSA) were purchased from Sigma-Aldrich (Poole, UK). Micropipettes were purchased from Eppendorf, UK. Pipette tips and 1.5mL tubes were purchased from Fisher Scientific (Loughborough, UK). Anti-Human C- Reactive protein capture antibody, Mouse monoclonal c6 to C reactive protein: ab 8272, Anti-Human C- Reactive protein, HRP Conjugated Detection Antibody were bought from (Abcam, Cambridge, UK). skimmed milk protein (KPL Ltd, UK), Reverse Osmosis (RO, Ultrapure) water ( $18 \text{ M } \Omega\text{cm}^{-1}$ ) was obtained from Milli-Q water system (Millipore Corp., Tokyo, Japan). Glassware and volumetric materials were of analytical grade.

All measurements were conducted with Palmsens® portable electrochemical analyser (Palm instruments BV, Houten, Netherlands) or a four channels of an Autolab Electrochemical Analyser with general-purpose electrochemical software GPES 4.9 was purchased from Metrohm (Utrecht, Netherlands). The electrodes were connected to an edge connector and then connected to the electrochemical analyser using a modified connector (Maplin UK). An environmental scanning electron microscope was used to measure the surface morphology and composition on the working electrode. A XL30 SFEG scanning electron microscope (SEM) (FEI Company, Holland) was used to characterise

the surface of bare electrode. The analysis was done based on the XLFEF/SFEG scanning electron microscope operating instruction manual AnalySIS 3.0 software. The electrodes used in this project were designed by Cranfield University and fabricated using the facilities at DuPont. The gold working electrode was circular with a 22.6 mm<sup>2</sup> planar area, a complementary carbon counter electrode and an Ag/AgCl reference electrode. The substrate material used is PET 125 µm Autotype HT5. Three types of electrodes JC, JA and JD were prepared with different Ink combinations. The Table 2-2 summarises the compositions of the electrodes.

**Table 2-2:** The distribution of components on three sensors used in this work. All the inks used are from DuPont.

Type of Sensor	JA	JC	JD
Type of Carbon Ink	7102	7102	BQ221
Type of Gold Ink	BQ331	BQ331	BQ331
Type of Ag/AgCl	5870	5880	5880
Encapsulation	5036-blue	5036-blue	5036-blue

The carbon electrode has an approximate dried thickness of 7 µm, while the gold and Ag/AgCl electrodes both have an approximate thickness of 18 µm. The encapsulation of 5036 blue had an approximate thickness dried of 4 µm. All inks are available from Dupont, UK. For the curing experiments, two sets of electrodes were fabricated, one set where the gold working electrode was cured using the conventional drying method and the other using infra-red technique. Different inks were also used from those that fabricate the JA, JC and JD.

## 2.3 Methods

### 2.3.1 Cyclic Voltammetry for investigating different Inks

Gold electrodes were first baked in an oven at 120 °C and washed with reverse-osmosis water before use. Stock solutions of 1 mM potassium ferricyanide  $K_3[Fe(CN)_6]$  were prepared in 0.1 M KCl. The electrodes were then tested using Cyclic Voltammetry (CV) to characterize the performance of the electrodes prior to any modifications thus to examine the initial performance of the electrodes. The electrochemical behaviour of potassium ferricyanide was measured using cyclic voltammetry at varying scan rates. Measurements were performed with electrodes being in a horizontal position and 100  $\mu$ L of solution was pipetted on the gold working electrode. Scan rates of 30  $mVs^{-1}$ , 60  $mVs^{-1}$ , 90  $mVs^{-1}$ , and 120  $mVs^{-1}$  were used. Measurements were obtained by scanning 5 cycles from -0.5 to 0.8 V relative to Ag/AgCl reference electrode.

The cyclic voltammetry (I-E) curves for the reduction of ferricyanide (1 mM) to ferrocyanide in a supporting electrolyte solution of 0.1M KCl at a pre-treated screen-printed gold electrode were obtained. Five electrodes were examined for each test using a Palmsens® portable electrochemical analyser (Palm instruments BV, Houten, Netherlands). The effect of different scan rates on the electrochemical behaviour of ferrocyanide toward the electrodes was observed. The relationship between the oxidation and reduction peaks, to the square root of the scan rate was calculated, and the percentage of the active surface area on the working electrode was estimated using the Randles-Sevcik equation. The parameters used in the calculation are shown in Table 2-3.



**Table 2-3:** Parameters used in the Randel-Sevcik equation

Equation Parameter	Used Values	Units
Scan Rate (V)	0.05	[V/s]
Area (A)	0.226	[cm <sup>2</sup> ]
Concentration (C)	0.001	[mol/cm <sup>3</sup> ]
Diffusion Coefficient (D)	7.60E-06	[cm <sup>2</sup> /s]
Anodic Peak (I <sub>pa</sub> )	X	[A]

### 2.3.2 Cyclic Voltammetry for investigating different Curing Methods

Two different curing methods for drying the ink on the substrate after screen-printing were investigated. The first involved curing the electrodes in a static/box oven with a set temperature of 130°C for 20 min. The second technique involved drying the sensors for 4 min in a conveyor belt drier that utilise both Infra-Red (IR) and convection heat. Cyclic voltammetry was used to investigate the electrochemical behaviour of the two sets of electrodes. Measurements were performed with electrodes being in a horizontal position and 100  $\mu$ L of solution was pipetted on the gold working electrode, Scan rates of (20mV/s, 40mV/s, 60mV/s, 80mV/s and 100mV/s) were used and measurements were obtained by scanning 3 cycles from -0.5 to 0.8 V relative to Ag/AgCl reference electrode. The electrodes were connected to an edge connector plugged on a multi-channel AUTOLAB electrochemical instrument (Ecochemie, Utrecht, Netherlands) using electrochemical GPES 4.7 software.

### **2.3.3 Environmental Scanning Electron Microscope**

A XL30 SFEG scanning electron microscope (FEI Company, Holland), was used to characterize the surface of bare gold working electrode. The sensors were first baked at 120°C for 30 min before being washed and dried with a gentle nitrogen stream. The analysis was done based on the XLFEG/SFEG scanning electron microscope operating instruction manual. The software, AnalySIS 3.0 was used for determining the composition the gold working electrode surface.

### **2.3.4 Characterization of electrodes using Immuno Assay**

In Order to validate and complement the cyclic voltammetry results the sensors were also characterised using the immuno assay immobilised on the electrode surface. After choosing, the best electrodes from previous experiments an optimised immuno assay details of which are described in Chapter 3 were used. Three different concentrations of the antigen (C –Reactive protein from Human serum) were used on in triplicates for each of the sensors. The electrodes were then washed and connected to an edge connector, which is connected with a multi-channel Ecochemie electrochemical instrument from AUTOLAB, (Utrecht, Netherlands). All measurements were performed by adding 100 µl of 4mM TMB and 0.06% H<sub>2</sub>O<sub>2</sub> in 0.05 M citrate phosphate buffer plus 0.1 M KCL with chrono-amperometry methods at constant current and run for 200s using electrochemical GPES 4.7 software. A cross section was made at 80seconds and all the current measured at this time was averaged.

## 2.4 Results and Discussion

This section describes the findings from the experiments that were conducted in an attempt to characterise the electrodes that were manufactured and used in this work, and the evaluation of electrode performance against two different curing techniques. Major emphasis of the characterisation was put on the three component inks for the electrodes that were, the gold colloid ink, the carbon counter and track ink, and the silver/silver chloride ink for the reference. Three different electrode configurations were produced using different ink compositions. Cyclic voltammetry of the electrodes was done to distinguish the best electrode combination to be used in this work. Potassium ferricyanide solution was used as it is capable producing a reversible reaction where one electron transfer [Fe (III) to Fe (II)] could be characterised by a peak separation between the anodic and cathodic peaks and a linear relationship between peak current versus scan rate is observed. This is because since one electron is used for each  $\text{Fe}^{3+}$  to reduce at the electrode, therefore the rate of reaction could be monitored by controlling the availability of electrons on the through the voltage (Cui *et al.*, 2001a).

The voltamograms produced were then compared to each other to find the ones that were providing superior performance in terms of producing the highest current peaks and reproducibility on a fixed voltage. It is expected that there will be characteristic sigmoidal shaped curves exhibiting oxidation and reduction peaks, the peaks are expected to vary proportional to the scan rates. The analysis of the peaks obtained can be done using two methods the first and simple one being based on a relationship between the oxidation and reduction peaks to the square root of the scan rate (Morrin *et al.*, 2003). This relationship is important, as it is linearity shows the effectiveness of the diffusion of the electrolytes on the sensor surface. This is a good indicator for the quality of the electrode particularly when unstirred highly electrolytic solutions are used.

The second assessment was done using the Randal-Sevcik equation that is highlighted in the introduction. By inputting known values of the electrode area, concentration of a known reversible redox electrolyte, its diffusion coefficient, and the scan rate used, the percentage of the active surface on the working electrode can be estimated. This is directly proportional to the electro active behaviour of the electrode and thus has a significant impact on quality. A further validation of the obtained results was done using an immuno assay developed for the electrodes. This was done later on in the project when the JD sensor had already been chosen using the cyclic voltammetry results. The experiment was done to justify whether the right decision had been made earlier. The immuno assay used was for the CRP assay, which is discussed in detail in Chapter 3.

For the evaluation of the drying techniques cyclic voltammetry was also used, also a complementary imaging experiment was done which used an environmental scanning electron microscope to analyse the surface composition of the working electrodes. This analysis is based on energy dispersive X-ray microanalysis (EDAX) of gold (Au), carbon (C) and oxygen (O) component of the gold electrode surface as well as particle size. Besides providing the chemical composition of the surface, the environmental scanning electron microscope is also capable of enabling visualization of the surface on a micro scale. The roughness of the surface and granule form of gold particle on the working electrode surface was visually inspected. Correlations were made between the performance and surface roughness, which were consistent with literature.

## **2.4.1 Performance of Different Electrode Ink Compositions**

### **2.4.1.1 Cyclic Voltammetry**

The formulations of the inks used in the screen-printing of electrodes are a big business and the composition of such inks is proprietary knowledge that remains guarded as a close secret. Different inks are made by mixing different combinations of the ink composition material for example a carbon ink may contain carbon, alcohol, substrate in different proportions. The performance of the inks differs with each formulation and the intended application. In this experiment, three types of electrodes were assembled with different ink combinations they were then tested for their electrochemical performance using cyclic voltammetry and an immuno-assay. The results of the cyclic voltamograms are shown in Figure 2.5.

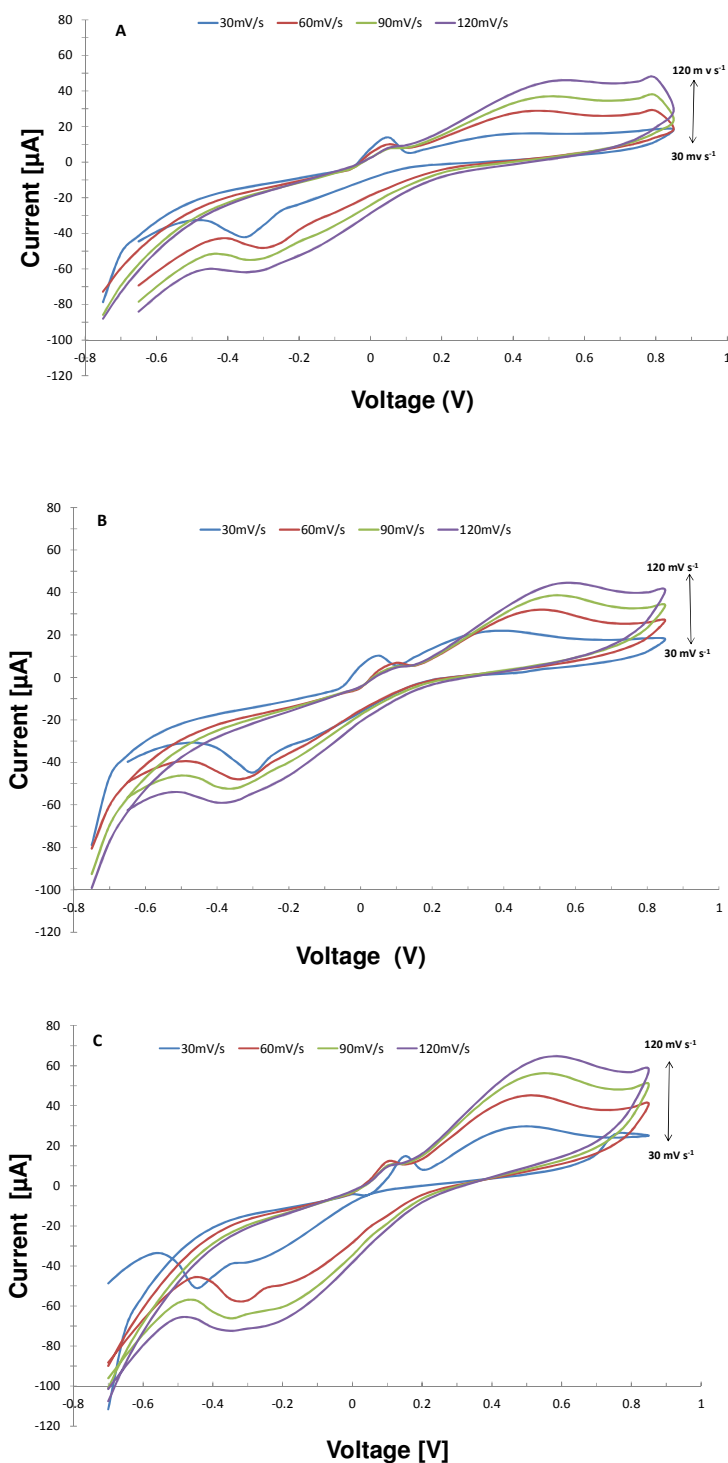


**Figure 2.5:** Voltamogram for the characterisation of the electrode screen-printed electrodes. Cyclic voltammetry using 100  $\mu\text{L}$  of 1mM  $\text{K}_3[\text{Fe}(\text{CN})_6]$  in 0.1M KCl pipetted on the gold working electrode, scan rates 30, 60, 90 ,120  $\text{mV s}^{-1}$  were used scanning 3 cycles from -0.5 to 0.8 V relative to Ag/AgCl reference .(A) JA electrode, (B) JC electrode, and (C) the JD electrode.

The three diagrams show the voltamograms obtained after cyclic voltammetry of 1 mM potassium ferricyanide solution made in 0.1M KCL solution. The oxidation and reduction peaks are visible in all three electrodes, however the JD electrodes show more response as it has the highest peaks for any given scan rate as compared to the other two electrodes. A clear comparison can be made with the aid of the summary shown in Figure 2.6. The results obtained showed a similarity between the performance of the electrodes JC and JA. This shows that both variants of the Ag/AgCl, namely 5880 and 5870 yielded similar performance on the electrodes. The experiments also showed that JD showed superior performance on the electrochemical testing. This may be because of the different carbon used BQ221, the results show that the BQ221 carbon performs better than the 7102 variant.

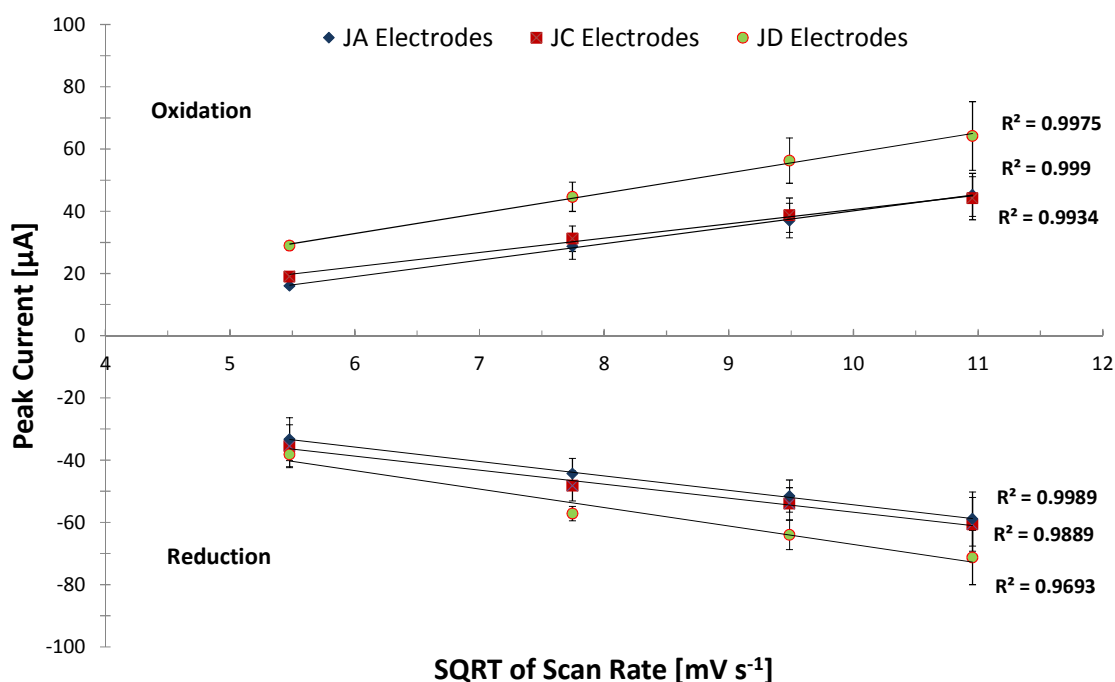


**Figure 2.6:** Summary of the electrochemical performance of JA, JC, and JD electrodes. Cyclic voltammetry using 100  $\mu\text{L}$  of 1mM  $\text{K}^3[\text{Fe}(\text{CN})_6]$  in 0.1M KCl pipetted on the gold working electrode, scan rates 30, 60, 90, 120  $\text{mV s}^{-1}$  were used scanning 3 cycles from -0.5 to 0.8 V relative to Ag/AgCl reference,  $n=3$ , maximum CV=9.8%, Bars = standard deviation.

Using Randles-Sevcik equation the surface area of the working electrode was estimated. The highest scan rate of 0.12 V/s was used and the results obtained are shown in Table 2-4. The results showed that JD had the highest calculated active area on the working electrode; the values of the JC and JA were almost similar.

**Table 2-4:** Table showing the results of the Randles-Sevcik equation.

Sensor Type	JA	JC	JD
Calculated Active Area [cm <sup>2</sup> ]	0.18	0.17	0.25
Relative Calculated Active Area [%]	81.41	76.26	111.24

#### 2.4.1.2 Immuno Assay Test

The current optimised CRP assay was done on each of the three electrodes, JA, JC and JD. Three different concentrations of the antigen (C –Reactive protein from Human serum) were used on in triplicates for each of the sensors. A hydrogen peroxide /TMB substrate was used to transduce immobilised HRP conjugated antibodies from the final step of the assay and produce electrons. The electrons were then measured as current using a Palmsens® portable electrochemical analyser (Palm instruments BV, Houten, Netherlands). The results obtained are shown in Figure 2.7 .



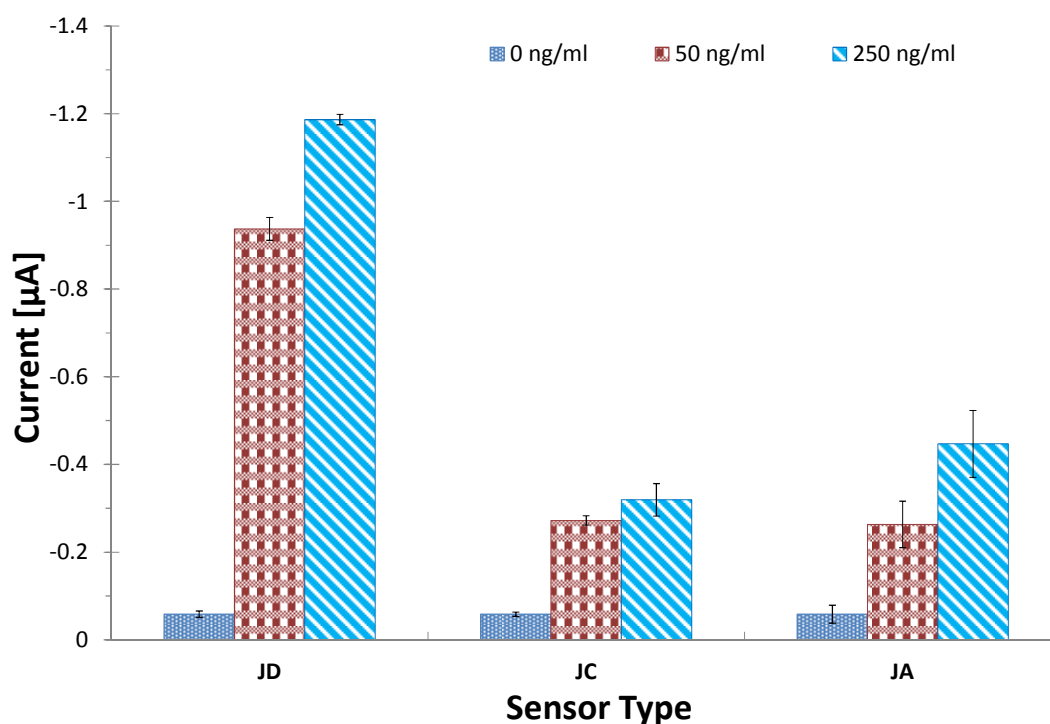


**Figure 2.7:** The Immuno assay results showing the advantage of using the JD electrode composition compared to the JC and JA variants. Electrochemical immunoassay for CRP was integrated on the different electrodes to make immunosensors and peak electrochemical signals at different CRP concentrations were used to assess electrode performance  $n=3$ . maximum CV=11.4%, Bars =standard deviation.

The results confirmed those obtained by the cyclic voltammetry that there was a superior advantage on the performance of the JD sensor compared to the JA and JC. Higher signals were obtained on non-reference samples from the JD electrodes; this may be because it contained better carbon ink BQ221 while other contained the 7102 variant.

## **2.4.2 Effect of Different Electrode Ink Curing Techniques**

### **2.4.2.1 Cyclic Voltammetry**

Two main methods are used when curing screen-printed inks. These are the alternative drying which is drying the electrode in an oven with a temperature of around 120 °C for 2hrs. Another method involves using infra-red drying chambers which makes the inks to dry faster at higher temperatures without compromising the substrate. Infrared dryers were used to dry the screen-printed inks for 15 min at 200 °C. The effects of drying strategies have been known to affect the performance of the sensor. Figure 2.8 shows the results obtained in the analysis of the performance after different drying strategies of the immuno-sensor inks. The results show that there is a major distinction in the performance of the different drying techniques. By using CV to characterise the electrodes the results showed that the electrodes which were alternatively dried gave higher oxidation and reduction peaks thus making them more sensitive than the infra –red (IR) dried sensors. There was better reproducibility on the alternatively dried sensors than the IR sensors. This is highlighted by the relatively high error bars (IR sensors CV=9.8% compared to AD CV 4.2%) in Figure 2.9.

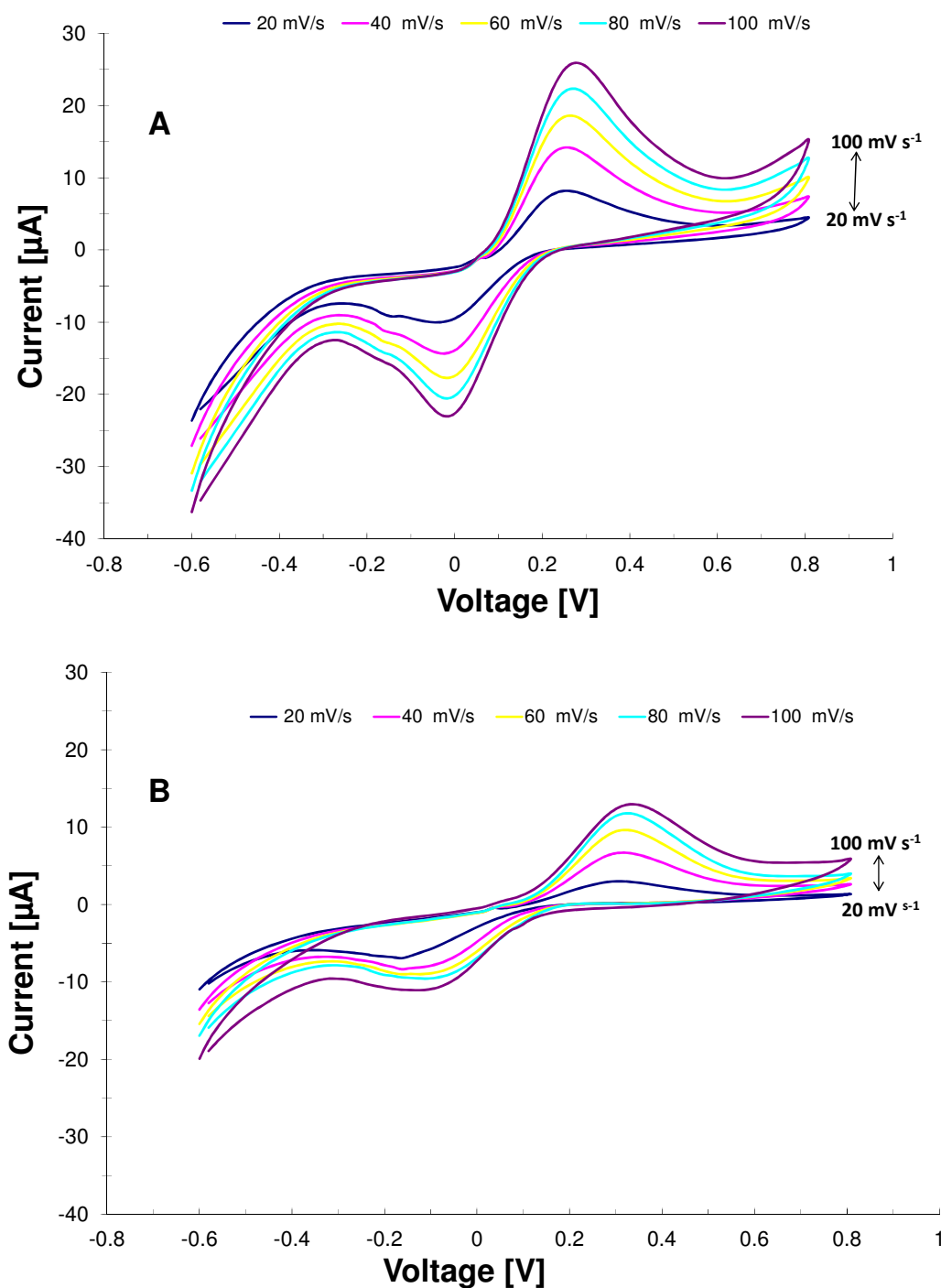


**Figure 2.8:** Voltammogram showing electrochemical performance of an alternatively dried sensor. Cyclic voltammetry using 100  $\mu\text{L}$  of 1mM  $\text{K}^3[\text{Fe}(\text{CN})_6]$  in 0.1M KCl pipetted on the gold working electrode, scan rates 20, 40, 60, 80, 100  $\text{mV s}^{-1}$  were used scanning 3 cycles from -0.8 to 0.8 V relative to Ag/AgCl reference. (A) alternatively dried electrodes, (B) Infrared dried electrode.

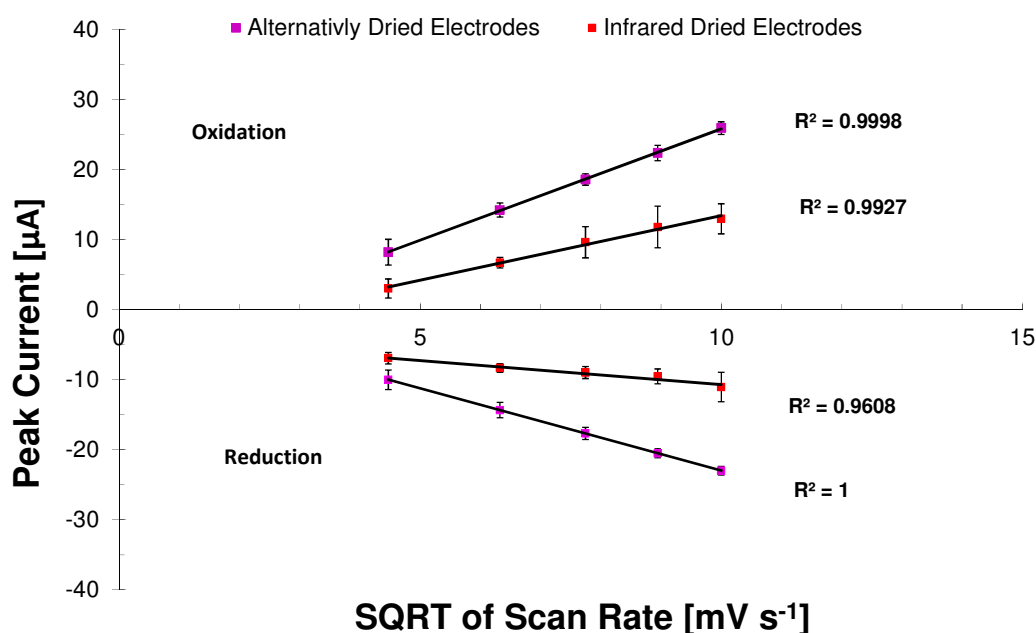


**Figure 2.9:** Summary of the Investigating effect of Alternative vs Infra-red drying techniques The R2 values were obtained using a plot of the square root of the scan rates used in Figure 2.8, n=3, maximum CV=9.8%, Bars = Standard deviation.

Using Randles-Sevcik equation the surface area of the working electrode was estimated. The highest scan rate of 0.1 V/s was used and the results obtained are shown in Table 2-5. The results show that there was relatively higher active surface area on the working electrode of the alternatively dried electrodes, almost double of that of the infra-red dried electrodes. This showed that the alternatively dried electrodes were electrochemically more active than infrared dried electrodes.

**Table 2-5:** Results of the Randles-Sevcik equation on different curing techniques.

Sensor Type	AD	IR
Calculated Active Area (cm <sup>2</sup> )	0.11	0.05
Relative Calculated active area (%)	48.84	24.44

### 2.4.2.2 Environmental Scanning Electron Microscopy (ESEM)

The Environmental Scanning Electron Microscopy (ESEM) confirmed the electrochemical results obtained through cyclic voltammetry. Figure 2.10 shows the results of the ESEM. There was a clear difference in both the chemical composition and the morphology of the constituent particles on the gold surface. Considering that the same ink was used and it was fairly homogeneous when printing occurred it is expected that the composition of the elements on the working electrode will be uniform.

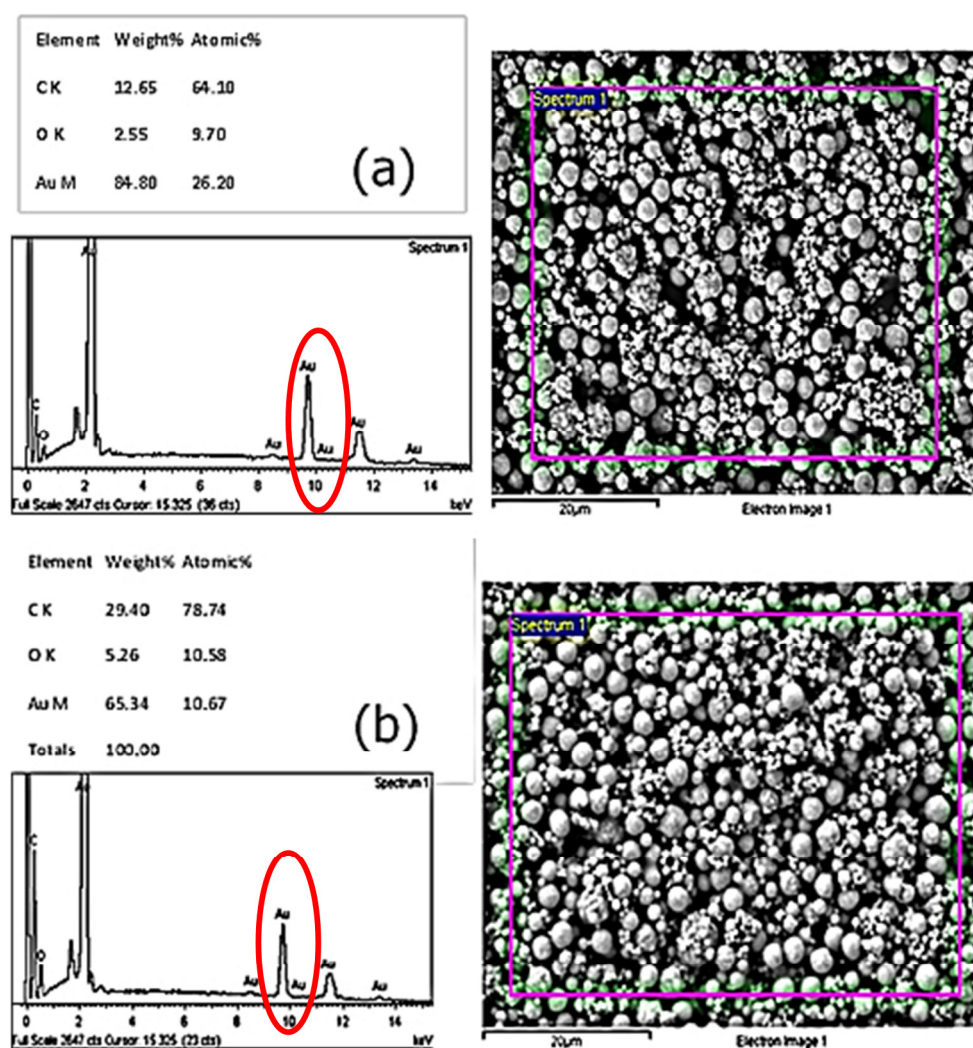


**Figure 2.10:** The ESEM results showing the image and composition analysis of the gold surface of (a) alternatively dried sensors and (b) infrared dried sensors. The element weight information is an average of three spots on a single sensor for each drying technique.

Electrodes were baked for 120°C for 30 min before being washed with reverse osmosis de ionised water and gently dried with a nitrogen spray. The working electrodes were then analysed using an ESEM. The results showed that the curing techniques affected the distribution of the ink composition of the working electrode. More pinholes were observed to be clearer on the alternatively dried sensors than the infrared dried sensors. This means that the surface was more smoother with the infrared dried sensors hence small surface area was exposed. This was confirmed by the spectrums obtained that showed the amount of exposed gold higher in the convention-dried sensors (84.8%) than the Infrared dried sensors (65.34%). This had a knock on effect on performance and could justify the performance highlighted by cyclic voltammetry.

#### **2.4.2.3 Immuno Assay**

The immuno assay validated the results of the cyclic voltammetry and the environmental scanning electron microscopy. It is evident in the results shown by Figure 2.11 that there was a higher signal response from alternatively dried electrodes than Infra-red dried electrodes.

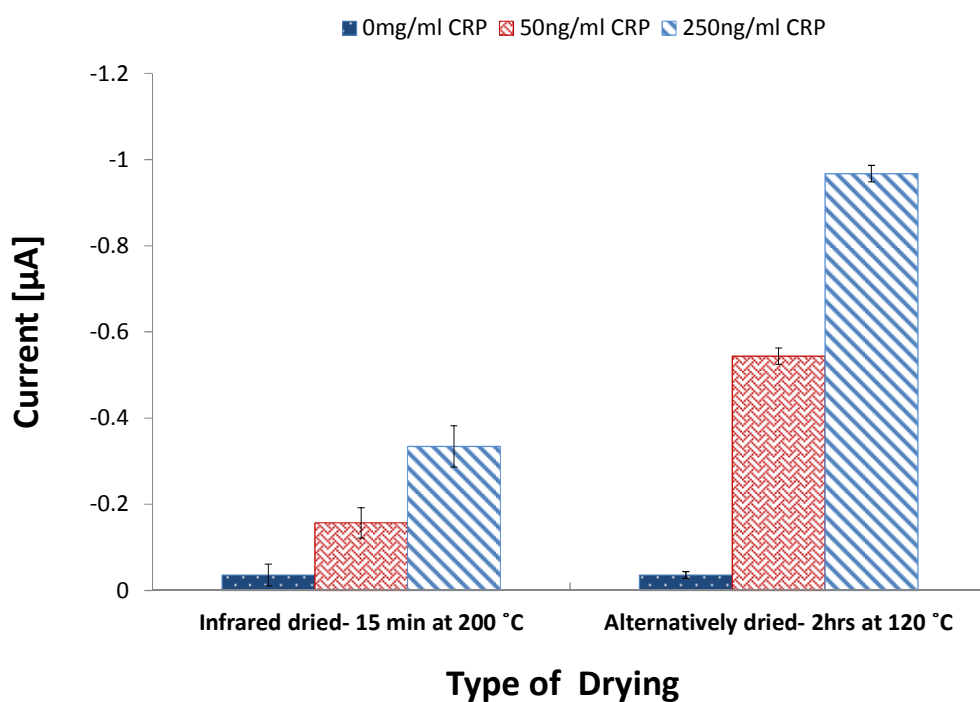


**Figure 2.11:** The Immuno assay results showing the advantage of alternatively dried electrodes over infrared. The differently cured electrodes were transformed to immunosensors by integrating a CRP immunoassay; the high peak currents obtained from detecting several CRP concentrations were used to identify the best curing method.  $n=3$ ,  $CV=11.2\%$ , Bars =standard deviation.

## 2.5 Conclusions

Several results were obtained that brought understanding on the type of electrodes that was most suitable to be used in this project. From a selection of three electrodes with different ink compositions the JD electrode was used because it showed superior performance in both electrochemical and immuno assay evaluations. The major difference between the JD and the other electrodes was that it had a superior carbon ink. The carbon in this design of electrode plays a major role as it constitute more than 80 per cent of the total ink coverage on an electrode (Morrin *et al.*, 2003). This is because besides being used for the counter electrode it is also used for tracking the other electrodes to complete the circuit. As discussed earlier the actual compositions of the inks are regarded as proprietary information so there are major restrictions to what can be discussed regarding its composition.

The results obtained showed a similarity between the performance of the electrodes JC and JA. This shows that both variants of the Ag/AgCl, namely 5880 and 5870 yielded similar performance on the electrodes. This information is helpful in deciding the cost as different inks are made from different formulations that have different costs. In this instance, it would be advisable to choose the cheaper alternative between the two formulations as they do not make a significant difference in terms of performance in this case. However, it is important to consider other factors like shelf life especially where the reference electrode is concerned as well as the effect of assay conditions particularly the Ag may be removed from the electrode and interfere with the assay as in the case of acidic conditions. The JD electrode was chosen as the appropriate platform for the design of the immunosensor. The decision was vindicated by the immuno-assay results obtained after the development of the immuno sensor that showed that it was the right electrode to use to develop the sensor.



Three experiments were conducted to evaluate the effect of different curing conditions on the performance of the electrode. The curing (drying) conditions of an electrode play a major role in the rate and cost of production of electrodes (Hobby, 1997). Different techniques are constantly being investigated to improve the production process by finding fast and cheaper curing alternatives. The two curing methods that were investigated in these experiments differ mainly in that the Infra-red drying is a faster and cheaper method than the conventional oven drying. The results from all three experiments showed that the conventional drying resulted in better performing electrodes. The electrochemical results from the cyclic voltammetry confirmed this. The results from the scanning electron microscope showed that although the same ink was used for the working electrodes there were differences in the surface composition of the electrodes after curing them differently. This may have been caused by temperature variations and humidity conditions (Grennan *et al.*, 2001).

There was a clear difference in both the chemical composition and the morphology of the constituent particles on the gold surface. Considering that, the same ink was used and it was homogeneous when printing occurred it is expected that the composition of the elements on the working electrode will be uniform. The E-SEM showed that the amount of the exposed gold on the infra-red dried sensors was less than that from the conventionally dried electrodes, conventionally-dried sensors (84.8%) than the infrared dried sensors (65.34%). This may explain the superior electrochemical behaviour of the conventionally dried electrode as shown by the cyclic voltammetry and the immuno assay results. Although the IR drying may have commercial advantages on speeding the production line, it is evident that this has an impact on the quality. The results show that the conventional oven drying of the working electrode with relatively lower temperatures results in better performing gold electrodes and thus the electrodes used in this project were cured using the conventional drying method

## CHAPTER 3

### DEVELOPMENT OF AN ELECTROCHEMICAL IMMUNOSENSOR FOR C-REACTIVE PROTEIN

## **3 Development of an Electrochemical Immunosensor for C-Reactive Protein**

### **3.1 Introduction**

This chapter will focus on the development of an immunosensor for C reactive protein using screen-printed gold electrodes. An assay was initially developed on a micro plate ELISA platform before it was adopted and optimised to make screen-printed electrode based immunosensors. The performance of the immunosensors was then compared to a commercially available ELISA assay.

#### **3.1.1 Electrochemical Immunosensors**

Electrochemical immunosensors are fast becoming a major contender in the race for robust immuno based biosensors because of their simplicity, high sensitivity and good reproducibility (Tothill and Turner 2003; Salam and Tothill, 2009). They are analytical tools based on the interaction of antibody and antigen complex on an electrode transducer (Kadir and Tothill, 2010). The production of electrodes has become a booming business and several companies mentioned in the previous chapter are moving forward with the research and development of electrodes suitable for immuno sensing applications. Immuno sensors offer a long term economic viability as they are capable of being easily fabricated, inexpensive and reproducible manufacturing is possible for large quantities thus this can result in development of low cost electrochemical immunosensors (Turner, 1998).

The success of some commercial biosensors like the Exactech® glucose pen has raised the hopes of screen-printed fabrication technology on biosensor applications. Screen-printed electrodes have been used for the development of chemical sensor and immuno sensor applications for more than a decade (Parker *et al.*, 2009). The basis of most electrochemical immunosensor systems is the ability of some enzymes to catalyse a substrate in a manner that can

generate an electrical signal on the electrode surface. Many of the commercially available electrochemical biosensors use enzymes that work on a substrate through a redox reaction. This results in either the generation or utilisation of electrons. Some examples of the enzymes include horseradish peroxidase, glucose oxidase, glutamate oxidase and lactate oxidase, these are mostly used in amperometric detection which is the most popular electrochemical technique (Shan *et al.*, 2008; Salam and Tothill, 2009). Amperometric detection involves a measure of current from the oxidation-reduction of an electro active molecule when a constant potential is applied to an electrode measured against a reference electrode. The density of the measured current will be proportional to the concentration of the redox species in the solution (Dzyadevych *et al.*, 2008; Kadir and Tothill, 2010). The redox reactions of the electro active molecules take place on the working electrode, which in this case is gold. The reference electrode will then define the potential against which other potentials could be measured because it has a known and constant potential at a given temperature. The counter electrode is responsible for draining all the excess current on the working electrode to prevent it from passing through the reference electrode. The potential of a working electrode vs. a reference electrode is usually made either more positive or negative by applying an appropriate potential (Salam and Tothill, 2009).

Some drawbacks of the electrochemical method are that it is unable to detect direct interaction between an antibody and antigen. This may cause slight inconsistencies as small changes in enthalpy and physical conformation on antigen antibody binding occur (Dzyadevych *et al.*, 2008). These may then result in unexpressed signal for some antigen. This is however, a generic problem that affects all immuno based diagnostic systems and the changes are often negligible. Other electrochemical methods that try to base the transduction on the direct interaction of the antibody and antigen complex have been used in the form of potentiometric and impedimetric platforms (Hu *et al.*, 2003; Sun *et al.*, 2011; Mao *et al.*, 2012). The indirect method that utilises an enzyme has an

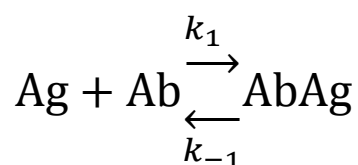
advantage that it is exempted from the high ionic and electrical interference that affect other methods. This has an impact on the quality of the results, thus an indirect detection technique based on a sandwich immuno assay that uses horseradish peroxidase labelled enzymes was used in this project. Another limitation of amperometric transducers is interference from electroactive compounds, particularly those that may originate from reagents (Garcia-Cardena *et al.*, 2001). C reactive protein has been detected using immuno electrochemical transduction in various assays that used a wide variety of electrochemical methods. Table 3-1 show some of the work that has been reported and achievements using these methods

**Table 3-1:** Summary of published work on Immuno electrochemical detection of CRP

Detection Technique	Assay Range	Reference
Amperometry	0.3 to 100 $\mu\text{g mL}^{-1}$	(Shaolin <i>et al.</i> , 2011)
Electrochemical Impedance	0.12 to 1.5 $\mu\text{g mL}^{-1}$	(Hennessey <i>et al.</i> , 2009)
Electrochemical Impedance	0.1 to 20 $\mu\text{g mL}^{-1}$	(Chen <i>et al.</i> , 2008)
Electrochemical Impedance	5 to 25 $\mu\text{g mL}^{-1}$	(Zhu <i>et al.</i> , 2003)
Electrochemical Impedance	0.04 to 5.84 $\mu\text{g mL}^{-1}$	(Rajesh <i>et al.</i> , 2010)
Square wave A/ Stripping	0.5 to 200 $\mu\text{g mL}^{-1}$	(Zhou <i>et al.</i> , 2010)

### 3.1.2 Role of Antibodies in Immunosensors

Antibodies have been used as the bioreceptor molecules for immuno sensors as they are a natural product of the immune system. They poses high affinity, specificity, versatility and commercial availability , which makes them suitable for this role (Ricci, 2007). Antigen- antibody interactions involve non-covalent binding of an epitope to the variable region of the immunoglobulin chains. The interactions include hydrogen bonding, ionic bonds, hydrophobic interactions, and Van der Waals forces in a fashion known as induced fit hypothesis. The strength of these interactions is weak compared to that of a covalent bond and it depends on the very close fit between the antigen and the antibody, which attributes the characteristic responsible for the high degree of specificity (Ricci *et al.*, 2007). The affinity and avidity are two common measures of the strength of Ab-Ag interaction, avidity is a measure of the stability of the complex that is formed from the binding of an antigen and antibody and affinity is the strength of the attraction. Low affinity antibodies bind weakly to the antigen and can easily dissociate, however high affinity antibodies will bind a close fit that is tight and thus stronger and more durable. The equation below summarises the association between antibody and antigen during binding.



In this formular ,  $k_1$  is the forward association rate constant and  $k_{-1}$  is reverse dissociation rate constant. The ratio of the two constants ( $k_1/k_{-1}$ ) is the association constant, which is used to define the affinity. Several external factors can affect the overall association constant and these include temperature, pH and motion.

### 3.1.3 Immuno Assay Development

The development of the assay component of the immunosensor development was based on the working principles of the ELISAs. Although many variants of ELISA have been developed and used in different applications, they all depend on the same basic principles that are coating, blocking, detection, and signal measurement. These elements have to be optimised to improve on the capabilities of the assay. With the hope of later transferring the optimised ELISA assays on to the electrodes to make the immuno sensors, this was done in this project. Sandwich ELISA assays for C-reactive protein was developed and optimised, the sandwich was chosen as earlier work by Salam and Tothill (2009) identified the sandwich method as the most suitable for the type of the electrode design that were worked on. Another factor was that sandwich assays are relatively straightforward and there are several examples of miniaturised diagnostic devices that utilise them. The sandwich ELISA has more sensitivity in its detection and it offers a more direct quantification. In electrochemical immunosensors, the stability of the immobilised immuno reagents on the sensor surface is crucial.

There is a wide range of enzymes that can be used in the indirect electrochemical transduction of immunosensors. A qualifying criterion is that they have to poses some redox properties that make them capable of catalysing the reduction or oxidation of a substrate to generate or consume electrons. Some good examples of such enzymes are the oxidases, peroxidases and reductases. These enzymes have been used in the past the development of redox based signal transduction. Horseradish peroxidases have been used in both optical and electrochemical capacities on redox based intermediation because it has the ability to catalyse reactions that change colour and generate electrons at the same time. This enzyme has a high substrate turnover rate and is tolerant of its substrate. Its active site is also close to the external surface of the protein, thus creating direct and mediated optical and electrochemical

transduction processes that are more efficient. In this project, it was used on both capacities as the ELISA platform used in the preliminary studies was optically detected and the immunosensors developed were electrochemically detected.

The immobilised antibody on a sensor surface act as both a capturing antibody and also as the detector surface (Oh, 2005). Several methods can be used to immobilise antibodies on sensor surfaces. These include passive adsorption, the avidin–biotin system and self-assembled monolayers (SAMs). The antibody immobilisation step is critical in the development of immunosensors as it supports the backbone or foundation of immunosensor (Newman and Turner, 1994). It also defines and gives the sensor its identity. If immobilised material is not well integrated to the sensor surface, it will affect the consistency and dependability of the sensor, even more so when intended to be reusable (Tothill, 2009). The diagram below Figure 3.1 shows the different mechanisms proteins like antibodies can be incorporated on to a sensor surface.

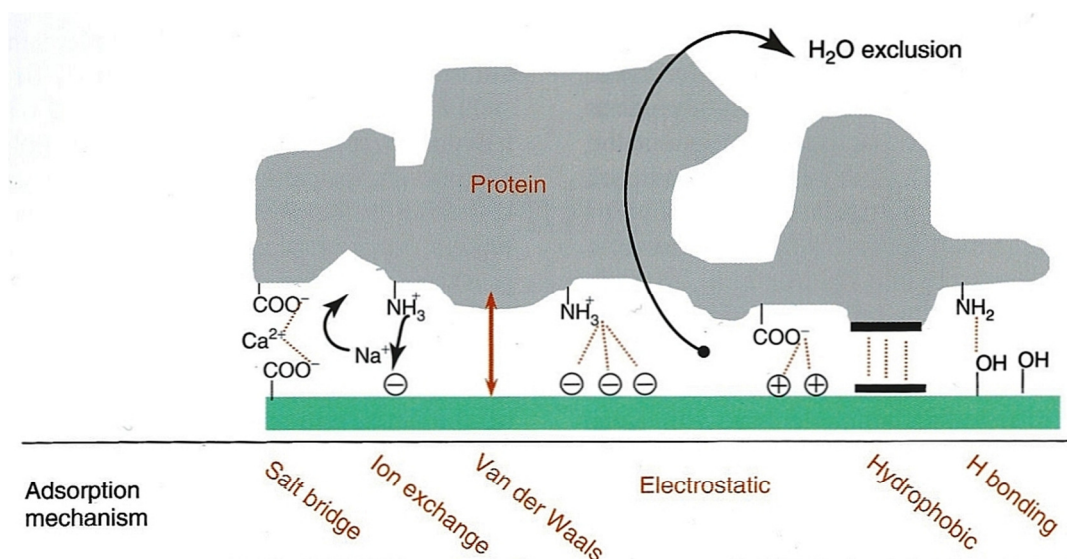


**Figure 3.1:** Overview of the protein adsorption mechanisms on the sensor surface (Davies, 2007 ).



The strength of the interaction between the immobilised antibody and the surface should be stable enough to perform one or more assays. The ability to withstand the force exerted by the fluids in the washing step in the assay is required as this procedure increases the risk of remobilising the antibodies and consequently dismantling the assay. The functionality of the antibodies is also compromised if the coating procedure is not done properly. The orientation of the antibodies is very important for its binding ability. This means that an irregular orientation of antibodies is less favourable than a meticulously directed immobilisation strategy that ensures the exposure of the binding region to the right orientation above the surface (Turner *et al.*, 1987). To improve on the immobilisation of the antibodies techniques like the use of self-assembled monolayers may be used. Self-assembled monolayers (SAMs) are a good example of covalent immobilisation and can be formed by means of sulphur containing groups on oxidised and hydroxylated surfaces and by means of thiols on metal surfaces (Srisombat *et al.*, 2011; Altintas *et al.*, 2012). The thiol molecules, usually alkanethiols, consist of three parts as shown in Figure 3.2 and these include: a head group (S-H group), a spacer or hydrocarbon chain, and a tail group which is active and specific.

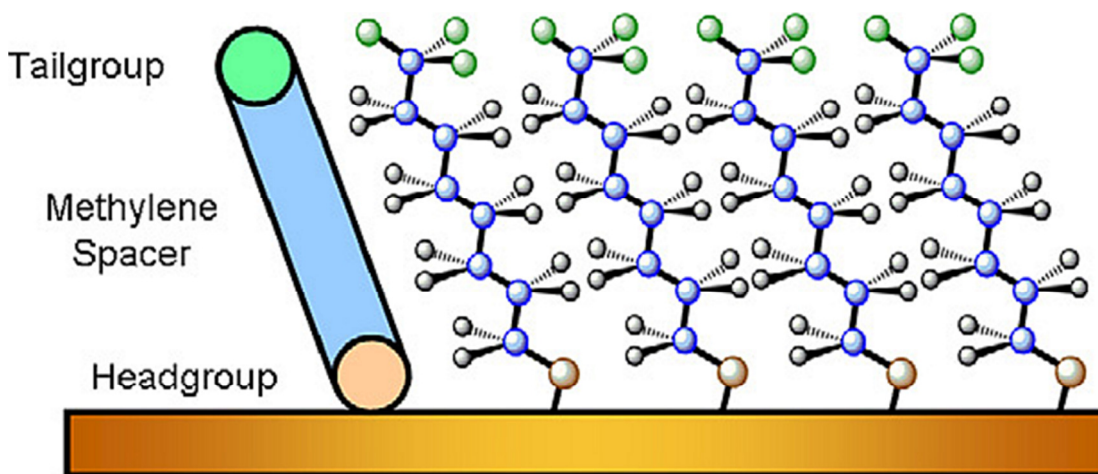


**Figure 3.2** An Illustration showing the three components of an ordinary thiol based self-assembled monolayer (Srisombat *et al.*, 2011)

Alkanethiols with amine and carboxyl end groups have been reported for use in to immobilise proteins on sensor surfaces (Arya *et al.*, 2010; Altintas *et al.*, 2012). The high affinity of the sulphur atom to noble metal surfaces is responsible for spontaneous formation of semi-covalently bounds. As a result of this there is a tendency for van der Waals forces to form between the hydrocarbon chains which then stabilize the structures and create an ordered monolayer. The terminal group of the molecule is responsible for the surface characteristics of the monolayer. For example to obtain hydrophobic  $-\text{CH}_3$  and  $-\text{CF}_3$  terminal groups are used and consequently  $-\text{COOH}$ ,  $-\text{NH}_2$  or  $-\text{OH}$  groups yield hydrophilic surfaces. SAMs can be formed on surfaces either by simply immersing the metal substrate in a dilute solution of thiol /silane or alternatively they can be formed by vapour deposition (Schreiber, 2000). If a metal substrate is immersed in dilute thiol solution, a disorganised monolayer spontaneously forms and then slowly the molecules are evenly organised due to van der Waals forces. The quality of the assembled monolayer depends on the cleanliness of the metal substrate, the purity of the alkanethiol solutions used and the length and composition of the alkanethiol. The head group of the alkanethiol is critical to obtain a monolayer with the required functionality. Many alkanethiols with different head groups are commercially available for the immobilisation of biological recognition elements on biosensor surfaces such as  $-\text{COOH}$ ,  $-\text{NH}_2$ ,  $-\text{OH}$ , -biotin, and (NHS),-N-hydroxysuccinimide (Altintas *et al.*, 2012). The use of SAMs in immunosensors for CRP have been reported before (Rajesh *et al.*, 2010) but mostly for electrochemical impedance measurements.

After the successful immobilisation, other areas that need to be investigated are finding a suitable blocking agent. These are designed to fill in any gaps on the immobilised protein surface that can later result in non-specific binding of the antigen. Several solutions can be used for blocking; these include known concentrations of proteins like bovine serum albumin (BSA), and skimmed milk solutions. Polyvinyl acetate (PVA) has also been reported for use as a blocking agent (Kadir and Tothill, 2010), as well as some commercial products with

protected recipes like Stabilicoat® (Surmodicks, Minnesota). A suitable blocking agent will need to be investigated and it needs to possess some characteristic that enable it to perform well without interfering with the electrochemical processes. The blocking step is crucial to the development of viable immuno assays, according to Péterfi (2000), the importance of blocking in affinity assays is paramount and as such it cannot be overlooked. This is because the surfaces designed for the immobilisation of proteins are inherently sticky because of their modified surface chemistry. This makes them prone to permit nonspecific adsorption and thus excessive protein-surface interaction which results in the loss of activity (Sentandreu *et al.*, 2007).

The aim of this chapter is to describe how an immunosensor was developed for the C-reactive protein (CRP) biomarker. The clinical reference ranges for predicting cardiovascular events using CRP assay are  $\geq 1 \mu\text{g mL}^{-1}$  low risk,  $1-3 \mu\text{g mL}^{-1}$  is medium risk and  $\leq 3 \mu\text{g mL}^{-1}$  is high risk (Rifai, 2001). The work that was done in the development of an electrochemical immunosensor for CRP was based on optimised parameters first developed on the ELISA platform. The parameters were then transferred on to screen-printed gold electrodes (JD variant). These electrodes were chosen after an evaluation study was conducted on different types of electrodes described in chapter two. The adopted parameters from the ELISA were then further optimised to enhance the performance of the electrochemical immuno sensors, including investigating the effect of using covalent immobilisation techniques. The performance of the optimised immunosensors was then compared to that of the in house ELISA and a commercially acquired ELISA kit using spiked serum samples. The assay sensitivity was also explored using several plasma proteins. A direct sandwich ELISA format was developed and optimised for human C-reactive protein. Two types of mouse anti- human CRP monoclonal antibodies were used. One was conjugated to horseradish peroxidase (HRP) and was used as the detection antibody, and the other was immobilised as the capture antibody. Horseradish peroxidase was chosen because it is an enzyme with high substrate turnover

rate, its active site is in close proximity to the surface and thus it is capable of efficient electrochemical transduction process that aid sensitive detection (Schumacher, 2001).

A commercially acquired chromogenic substrate based on 3,3', 5,5'-tetramethylbenzidine dihydrochloride (TMB) and  $\text{H}_2\text{O}_2$  solution was used on the ELISA and self-made alternative was used on the immunosensor. The ELISA format used is shown in Figure 3.3. The electrochemical detection was done using chronoamperometry at -200 mV on the JD screen-printed immunosensors that have on board gold working electrode and an integrated Ag/AgCl pseudo-reference electrode. The applied potential was selected through recommendations from work done on similar reagents and electrodes (Salam and Tothill, 2009).

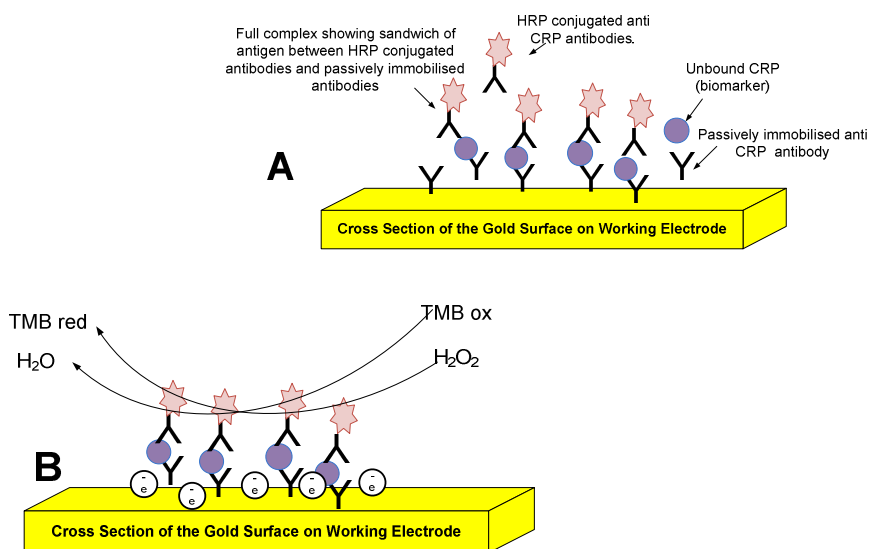


**Figure 3.3:** Schematic diagrams for (A) Sandwich immuno assay setup for the C-reactive protein on a screen-printed gold electrode. The antibodies are immobilised passively and the detection antibodies are conjugated with HRP. In diagram (B) the combination of TMB and  $\text{H}_2\text{O}_2$  with HRP enzymes results in a reaction with indirect electron transfer on the gold working electrode surface.

Standard curves were generated using immuno sensors on standards with known concentrations of CRP in both buffer and spiked serum. The results were then fitted using a four-parameter curve fit which was used to extrapolate unknown concentrations (Warwick, 1996). The results of the unknown concentrations were then compared with those obtained on the same samples using a commercial ELISA.

### 3.2 Materials

Potassium chloride (KCl), potassium ferricyanide ( $K_3Fe(CN)_6 \cdot 3H_2O$ ), TMB (3, 3', 5, 5'- tetramethylbenzidine hydrochloride), PBS (phosphate buffered saline) containing 0.137 M sodium chloride, and phosphate buffer, 0.01 M, pH 7.4 in tablet form, citrate phosphate buffer tablets, hydrogen peroxide, sodium hydroxide and sodium chloride, bovine serum albumin (BSA), 11-mercaptoundecanoic acid (11-MUA), and 3,3-dithiodipropionic acid (DTDPA), were purchased from Sigma-Aldrich (Dorset, UK). Micropipettes were purchased from Eppendorf, UK. Pipette tips and 1.5 mL tubes, were purchased from Fisher Scientific (Loughborough, UK). Anti-Human C- Reactive protein capture antibody and mouse monoclonal c6 to C reactive protein: AB 8272, Anti-Human C- Reactive protein, HRP conjugated detection antibody were bought from (Abcam, Cambridge, UK). Skimmed milk protein, (KPL Ltd, Gaithersburg, USA). Reverse Osmosis (RO, Ultrapure) water ( $18\text{ M }\Omega\text{cm}^{-1}$ ) was obtained from Milli-Q water system (Millipore Corp., Tokyo, Japan). Glassware and volumetric materials were of analytical grade.

ELISA tests were first developed using a micro well polystyrene plates, MaxiSorp® plates purchased from Fisher Scientific, Loughborough, UK. An incubator/shaker from Labsystem iEMS® was used for temperature control incubation. A Florostar® plate reader was used which was set at appropriate wavelengths, BMG, UK. The electrodes used in this project were the JD type

designed by Cranfield University and fabricated using the facilities at DuPont (Bristol, UK). The gold working electrode was circular with a 1.3 cm<sup>2</sup> planar area, a complementary carbon counter electrode and an Ag/AgCl reference electrode. The substrate material used is PET 125 µm Autotype HT5. The carbon electrode has an approximate dried thickness of 7 µm, while the gold and Ag/AgCl electrodes both have an approximate thickness of 18 µm. The encapsulation of 5036 blue had an approximate thickness dried of 4 µm. Inks used in the construction of the sensors are BQ221 carbon ink, BQ331 gold ink and the 5880 Ag/AgCl and are available from DuPont (Bristol, UK). Autolab Electrochemical Analyser with general-purpose electrochemical software GPES 4.9 was purchased from Metrohm (Utrecht, Netherlands). The electrodes were connected to an edge connector and then connected to the electrochemical analyser using a modified connector (Maplin UK).

### **3.3 Methods**

#### **3.3.1 Optimisation of the ELISA micro-plate based assay**

Detailed description of how the micro plate based ELISA assay was developed for C-reactive protein. The optimum coating and detection antibodies were investigated, several other parameters including experiments for discovering the best blocking solutions and incubation times were conducted and are discussed in this section.

#### **3.3.2 Optimisation of the Coating Antibody**

Antibody immobilisation on the micro plate was achieved through passive absorption. The optimisation of the coating antibody was carried out first to select the optimal concentration of the capture antibody to use for coating. A checkerboard concentrations method was used to optimise and select both the coating and the detection antibodies. A generic protocol for this method was adapted from Salam and Tothill (2010) was initially used but parameters were

optimised for the CRP antigen. A new ELISA plate was air brushed with nitrogen to clean it and then coated with various concentrations of the capture antibody (100  $\mu\text{L}$ ) mouse monoclonal anti human CRP antibody ab 8272 (Abcam, Cambridge, UK ) dissolved in 0.05 M carbonate-bicarbonate buffer pH 9.6. Different concentrations of the coating antibody (2, 4, 6, 8, 10  $\mu\text{g mL}^{-1}$ ) were then deposited in triplicates and allowed to incubate overnight at 4  $^{\circ}\text{C}$ .

The plate was then gently washed with Phosphate buffer saline plus 0.05 % Tween 20 (PBS-T) three times and dried by inverting and blotting the plate on paper towel. The plates were then blocked for 60 minutes at 37  $^{\circ}\text{C}$  with 300  $\mu\text{L}$  of 1:10 dilution of milk protein (KPL Ltd., UK) in PBS. The plates were then washed in a similar manner as described above and standard concentration of the antigen 100  $\mu\text{L}$  of (0, 0.5, 1, 10, 50  $\text{ng mL}^{-1}$ ) was added to the well and it was incubated for 1 h at 37  $^{\circ}\text{C}$ . The plate was then washed again and a conjugated rabbit monoclonal anti human CRP antibody with HRP Ab 8296 (Abcam, Cambridge, UK). A concentration of 0.375  $\mu\text{g mL}^{-1}$  in PBS with milk was added to the plate and incubated for 1 hour at 37  $^{\circ}\text{C}$ . The plate was finally washed 4 times and a 100  $\mu\text{L}$  solution of TMB based chromogenic substrate was added and incubated for 30 min before the reaction is stopped by 100  $\mu\text{L}$  of 1 N sulphuric acid solution.

#### **3.3.2.1 Investigating Appropriate ELISA Blocking Solution.**

The investigation of the most suitable blocking solution was done between three recommended choices from previous work at Cranfield Health. Three blocking solutions were investigated for the C-reactive protein assay. These included blocking agents previously reported in literature including a 1 in 10 dilution of skimmed milk protein in PBS (Salam and Tothill, 2010), 1% PVA (Kadir and Tothill, 2010) and BSA which is a traditional blocking agent. This was done by running the assay using the method described in Section 3.3.2.4. Using plates coated with 6  $\mu\text{g mL}^{-1}$  of coating antibody and running three concentrations (0, 25, 50  $\text{ng mL}^{-1}$ ) of antigen in triplicate for each of the blocking solution.

### 3.3.2.2 Optimisation of the ELISA Detection Antibody

A new Elisa plate was air bushed with nitrogen to clean it and it was labelled and coated in triplicated with 100  $\mu\text{L}$  the optimised capture antibody concentration of 6 $\mu\text{g}/\text{ml}$  of mouse monoclonal anti human CRP antibody ab 8272 (Abcam, Cambridge, UK ) and allowed to incubate overnight at 4  $^{\circ}\text{C}$ . The plate was then gently washed with Phosphate Buffer Saline plus 0.05% Tween 20 (PBS-T) for three times and dried by inverting and blotting on paper towel. The plates were then blocked for 60 minutes at 37  $^{\circ}\text{C}$  with 300  $\mu\text{L}$  of 1:10 dilution of skimmed milk in PBS. The plates were then washed in similar manner described above and standard concentrations of the antigen 100  $\mu\text{L}$  of (0, 0.5, 1, 5, 10, 20, 40, 60, 80, 100  $\text{ng mL}^{-1}$ ) were added to the microwells and it was incubated for 1 h at 37  $^{\circ}\text{C}$ . The plate was then washed again before 100  $\mu\text{L}$  of different concentrations of conjugated rabbit monoclonal anti human CRP antibody were added. The antibodies were diluted with PBS to give final concentrations of 0.1, 0.25, 0.375, 0.5  $\mu\text{g mL}^{-1}$  and incubated for 1 hour at 37  $^{\circ}\text{C}$ . The plate was finally washed six times and a 100  $\mu\text{L}$  solution of TMB based chromogenic substrate was added and incubated for 30 min before the reaction was stopped by 100  $\mu\text{L}$  1 N sulphuric acid solution.

### 3.3.2.3 Optimisation of the ELISA Incubation Times

After successfully selecting optimum coating and detection antibody concentrations, Investigations were done to find the best incubation time for the assay. The first experiments were done for the optimum incubation time for the coating antibody. The assay was completed as described in Section 3.3.2.4 but several incubation times were tried for the coating (15 min, 30 min, 1 h, 2 h, 5 h) at 37  $^{\circ}\text{C}$  and for overnight coating (16 h 4 $^{\circ}\text{C}$ ). The other assay parameters were kept constant. For the antigen and the detection antibody limited times were investigated because of the known strength of the antibody antigen thus only incubation times of 15 min, 30 min, 1h, 2 h were investigated.



### **3.3.2.4 Detection of CRP using the Optimised Micro Plate ELISA**

Taking into account the best conditions in the investigations for the optimisation of the ELISA assay a protocol was devised that was used for determining the final standard curve and interpreting unknown concentrations in the samples. In this final protocol, 100  $\mu\text{L}$  of the optimised capture antibody concentration of 6  $\mu\text{g mL}^{-1}$  of mouse monoclonal anti human CRP antibody was used for coating and this was allowed to incubate for 2 h at 37°C. The plate was then gently washed three times with phosphate buffer saline plus 0.05% Tween 20 (PBS-T) and dried by inverting and blotting on paper towel. The plates were then blocked for 60 minutes at 37 °C with 300  $\mu\text{L}$  of 1:10 dilution of skimmed milk in PBS. The plate was then washed and dried again and standard concentrations of the antigen 100  $\mu\text{L}$  (0, 0.5, 1, 5, 10, 20, 40, 60, 80, 100  $\text{ng mL}^{-1}$ ) were added to the microwells and it was incubated for 1 h at 37 °C. The plate was washed again and 100  $\mu\text{L}$  of 0.1  $\mu\text{g mL}^{-1}$  HRP conjugated rabbit monoclonal anti human CRP antibody was added to the plate and incubated for 1 hour at 37 °C. The plate was finally washed six times and a 100  $\mu\text{L}$  solution of TMB based chromogenic substrate was added and incubated for 30 min before the reaction is stopped by 100  $\mu\text{L}$  of 1 N sulphuric acid solution. The curves were fitted using a four-parameter curve fitting described in Section 3.3.8.

### **3.3.3 Method of Optimising the CRP Assay on Screen Printed Gold Electrodes**

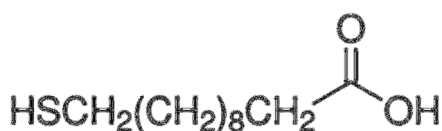
The immuno assay for CRP was optimised to function on the electrode surface. The method used for the optimisation of the gold electrode was adapted from a procedure described by previous work on development of a biosensor for Salmonella detection by Salam and Tothill (2009). Antibody immobilisation on the gold working electrode was carried out using passive absorption and it was this processes which was optimised first to get the best concentration of the capture antibody to use for coating. As usual, the electrode strips were first baked at a temperature of 120 °C for 30 minutes, washed and rinsed with

distilled water to remove any particle contaminants. The working electrode was then coated with a drop of 10  $\mu\text{L}$  of mouse monoclonal antibody dissolved in 0.05 M carbonate-bicarbonate buffer pH 9.6. Different concentrations of the coating antibody (5, 10, 20, 50, 100  $\mu\text{g mL}^{-1}$ ) were deposited in triplicates and allowed to incubate overnight at 4  $^{\circ}\text{C}$ . The electrode surface was then gently washed with PBS-Tween, two times, rinsed with distilled water and air-dried with nitrogen.

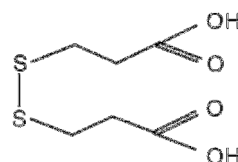
The working electrodes surface was then blocked for 30 minutes at 37  $^{\circ}\text{C}$ . The blocking solution was a 1:10 skimmed milk dilution in PBS. The electrodes were then washed in similar manner described above, standard concentration of the antigen (20  $\mu\text{L}$  of 1  $\mu\text{g mL}^{-1}$ ) was added to the working electrode and it was incubated for 2 h at 37  $^{\circ}\text{C}$  in a moist Petri dish. The electrode was washed again and a conjugated rabbit monoclonal antibody with HRP (20  $\mu\text{g mL}^{-1}$ ) in PBS with milk was added to the electrode and incubated for 1 hour at 37 $^{\circ}\text{C}$ . The electrodes were then connected to an edge connector, which is connected with a multi-channel AUTOLAB electrochemical instrument from Metrohm (Utrecht, Netherlands). All measurements were performed by adding 100  $\mu\text{L}$  of 4 mM TMB and 0.06%  $\text{H}_2\text{O}_2$  in 0.05 M citrate phosphate buffer plus 0.1 M KCL combined in a 1:1 ratio, with chronoamperometry methods at -200 mV constant current and run for 200 to 300 s using electrochemical GPES 4.7 software. Similarly, the same was done for the optimisation of the conjugate and a reverse approach was done where the capture antibody was chosen to remain constant at 60  $\mu\text{g mL}^{-1}$  and the antigen remained at 1  $\mu\text{g mL}^{-1}$  but HRP conjugated antibody was varied between (10, 20, 30, 50, 100  $\mu\text{g mL}^{-1}$ ). Incubation conditions for the coating antibody were also investigated by varying time and temperature.

### 3.3.4 Surface Modification of the Gold Electrode with Thiol group Self Assembled Monolayers (SAMs)

Self-assembled monolayers were made using two chemicals, 11-mercaptoundecanoic acid (11-MUA) and 3,3-dithiodipropionic acid (DTDPA) that have long and short carbon spacers respectively. This was done by baking the JD electrodes in an oven at 120 °C for 30 min before plasma cleaning them in oxygen free nitrogen at 50w for 2.5 minutes (Emitech K 1050X, EM Technologies, Kent, UK), at a power of 50 W with a bleed vacuum trip of  $3 \times 10^{-1}$  mbar and an ashing time of 1 minute. The working electrodes were then washed with ethanol using a pipette. For the 11-MUA monolayer, of 2mM of 11-mercaptoundecanol solution was made and the electrode were deposited in it ensuring that the working electrodes faced up and they were not on top of each other. The working electrodes were incubated in the dark at room temperature overnight. The electrodes were then washed with deionised water and dried using nitrogen gun with a gentle flow.



*11-mercaptoundecanoic acid*



*3,3-dithiodipropionic acid (DTDPA)*

**Figure 3.4:** The chemical structures of the two compounds used to modify the surface of the gold working electrodes through creating self-assembled monolayers SAMs.

For the DTDPA monolayer, 3% w/v of 3,3-dithiodipropionic acid in ethanol was made and the added to the working electrodes, ensuring that the working electrodes faced up and they were not on top of each other. The working electrodes were incubated in the dark at room temperature overnight before being washed and dried. These methods were based on direct translation of the optimised surface modification of QCM-1 chips using similar chemicals that was done by our colleagues (Uludag and Tothill, 2010).

### **3.3.5 Characterisation of the chemically modified working electrode**

The thiol modified gold electrodes were characterised using contact angle measurements and cyclic voltammetry. The measurement of contact angle is an invaluable basic technique used to assess the interaction of a surface with a standard liquid solution. The Young Dupree equation is used to calculate and quantify this relationship and it is based on adhesion and surface tension (Kumar and Prabhu, 2007). The contact angle measurements were done first as they did not alter the modified surface and thus the electrodes could be used again for the cyclic voltammetry analysis. For the contact angle measurement, three modified electrodes from each of the two chemical modification used as well as the bare electrodes were investigated, the electrodes were gently dried with a nitrogen gun and mounted on the stage of a CAM 100 Optical Contact Angle Meter from KSV instruments (Helsinki, Finland). A drop of Millipore water was added on the surface of the working electrode and the contact angle was analysed using the CAM 100 software and the average contact angle was automatically calculated. Figure 3.5 below shows the setup of a contact angle measurement using a CAM 100 Optical contact angle meter.



**Figure 3.5:** A Screen-printed gold electrode mounted on the stage of a CAM 100 Optical Contact Angle Meter. The image on the screen is for a drop of de ionised water being injected to the gold surface before measurements are taken.

The surface modified electrodes were then characterised using cyclic voltammetry. This was conducted by placing 100  $\mu\text{L}$  of solution (1 mM potassium ferricyanide  $\text{K}_3[\text{Fe}(\text{CN})_6]$  prepared in 0.1 M KCl) on the electrode surface. The electrochemical behaviour of potassium ferricyanide was measured using cyclic voltammetry at  $50 \text{ mVs}^{-1}$ , measurements were obtained by scanning 5 cycles from -0.5 to 0.8 V relative to Ag/AgCl reference electrode using a multi-channel AUTOLAB electrochemical instrument.

### 3.3.6 Surface modification evaluation using immunoassay

A 20  $\mu\text{L}$  of an equal volume of EDC–NHS (0.4M EDC and 0.1M NHS prepared in distilled water) was applied to activate the electrode surface for 15 min at room temperature. The two chemicals are capable of activating the carboxylic groups on the exposed side of the SAMs to enable reaction with the ligand. The chemistry behind this is explained in literature (Vaughan *et al.*, 1999) and is summarised in Figure 3.6.

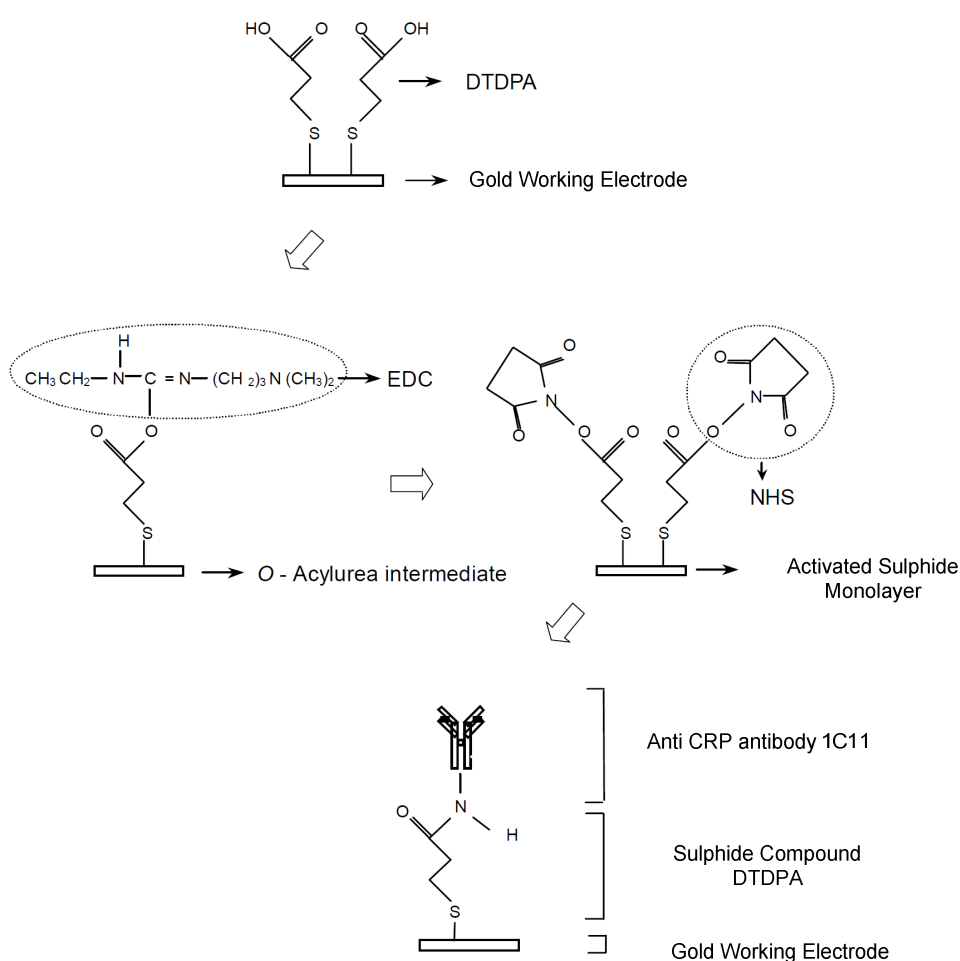


**Figure 3.6:** The chemistry of the covalent immobilisation of the CRP antibody 1c11 on self-assembled monolayers of 3,3-dithiodipropionic acid (DTDPA) using EDC-NHS coupling method. Figure adapted from Park et al, (2004).

The electrodes were then subsequently washed again and gently dried using  $N_2$  flow. A 10  $\mu\text{L}$  of the antibody solution ( $50\text{ }\mu\text{g mL}^{-1}$ ) of mouse monoclonal antibody against Human CRP dissolved in 0.05 M carbonate bicarbonate buffer pH 9.6 was deposited over the surface for immobilisation. Exposed ester groups were then blocked with 20  $\mu\text{L}$  of 1Methanolamine–HCl. The electrodes were then washed in similar manner described above and 20  $\mu\text{L}$  of standard concentrations of the antigen (0, 25, 50, and 100  $\text{ng mL}^{-1}$ ) were added to the working electrodes and it was incubated for 1 hrs at 37 °C in a moist Petri dish. The electrodes were washed and a HRP conjugated mouse monoclonal antibody against human CRP ( $20\text{ }\mu\text{g mL}^{-1}$ ) in 1:40 dilution milk protein was added to the electrode and incubated for 30min at 37 °C. The electrodes were then washed and connected to an edge connector, which is connected with a multi-channel AUTOLAB electrochemical instrument from Metrohm (Utrecht , Netherlands).

### **3.3.7 Optimisation of the assay for antigen addition**

Two methods for introducing the antigen were investigated which are the standard procedure and the premixed procedure. Both methods start with the passive immobilisation of the antibodies on the working electrode followed by blocking. This was done by first baking the electrodes in the oven at 120 °C for 30 min and washing and drying and drying them before being coated with 20  $\mu\text{L}$  of  $60\text{ }\mu\text{g mL}^{-1}$  coating antibody solution in carbonate bicarbonate buffer pH 9.6. The electrodes were then incubated for 2 h at 37 °C. The electrode surface was then gently washed with phosphate buffer saline with 0.05% Tween 20 two times and rinsed with distilled water before air-drying with nitrogen. The working electrodes surface was blocked (30 min at 37 °C with 50  $\mu\text{L}$  milk protein diluted with PBS) in a controlled humid condition, the electrodes were then washed and air-dried. The following steps then differed depending on the antigen addition method used.

The first method was the systematic (step-by-step) assay in which the antigen and the detection antibody are introduced separately with a washing step in between. In this procedure after blocking, standard concentrations of the antigen 20  $\mu\text{L}$  of (0, 12.5, 50 and 100  $\mu\text{g mL}^{-1}$ ), were added to the working electrodes of different sensors in triplicates. They were then incubated for 1 h at 37  $^{\circ}\text{C}$  in a moist petri dish before being washed and a conjugated mouse monoclonal antibody with HRP 20  $\mu\text{L}$  of 30  $\mu\text{g mL}^{-1}$  in 1:40 dilution milk protein was added to the electrode and incubated for 1 h at 37 $^{\circ}\text{C}$ . The electrodes were then washed and connected to an edge connector, which is connected with a multi-channel AUTOLAB electrochemical instrument. The substrate was added and measurements were done.

For the premixed procedure, the antigen was mixed in solution with the conjugated mouse monoclonal antibody for 1 h. The solutions were made to ensure that the concentration of both the antigen (0, 12.5, 50 and 100  $\mu\text{g mL}^{-1}$ ) and the detection antibody (30  $\mu\text{g mL}^{-1}$ ) were not compromised by the premixing. Compensatory calculations for the concentrations were done that the final premix well has the suitable concentrations. The mixture was then incubated for 1h on a Stuart SB3 rotator (Appleton Woods, Birmingham, UK), with the rotator at a 10 $^{\circ}$  inclination angle. A 20  $\mu\text{L}$  of the solution of the premix was then deposited on the blocked working electrodes and incubated for another 1 h. For both methods the electrodes were then washed and connected to an edge connector, which is connected with a multi-channel AUTOLAB electrochemical instrument. All measurements were performed by adding 100  $\mu\text{L}$  of 4 mM TMB and 0.06 %  $\text{H}_2\text{O}_2$  in 0.05 M citrate phosphate buffer plus 0.1 M KCL with chronoamperometry methods at -200 mV potential and run for 200 s to 300 s using electrochemical GPES 4.7 software.



### 3.3.8 SPGE Calibration Plot and Interpretation of Result

After discovering that the premixed antigen addition gave favourable results, It was adopted for used in the optimised immunosensor protocol. The exact pre mixed procedure described in Section 3.3.7 was to create a standard curve that would be later used to quantify spiked serum samples with unknown CRP concentrations. Serial diluted concentrations of the standards (0.1 , 0.156, 3.12, 6.25, 12.5, 25, 50, 100 ng mL<sup>-1</sup>) were tested using Both the immunosensor and ELISA methods and calibration curves were fitted by non-linear regression using the following four parameter logistic function (Warwick, 1996 ).

$$y = \frac{a - d}{\left[1 + \left(\frac{x}{c}\right)^b\right]} + d \quad \text{Equation 3-1}$$

In this equation y is response or current obtained, a and d , are the maximum and minimum values of calibration curve, respectively, x is the concentration at c = inflection point and b is the slope. The limit of detection (LoD) is defined as the minimum concentration of an analyte that can be detected with statistical confidence. There are many ways of estimating LoD and they depend on the level of confidence required. In this work the LoD of CRP was defined as that equivalent to three times the value of standard deviation ( $\sigma$ ) of the blank signal. This was calculated based on the following equation 3-2 where  $\sigma$  becomes the standard deviation of the zero value (Warwick, 1996).

$$LOD = x \left[ \frac{a - d}{(a - d) - 3\sigma} \right]^{-\frac{1}{b}} \quad \text{Equation 3-2}$$

In this equation a= minimum asymptote of the estimated response at zero concentration, d= maximum asymptote of the estimated response at infinity concentration, x represents the concentration of the analyte and b is the slope of the curve at c. Another important parameter to consider is the limit of quantification. While this depends on the level of confidence required to be presented on the assay, the U S Food and drug administration F.D.A defines it as the mean of the blank plus 10 times standard deviation (F.D.A, 2001).

### **3.3.9 Comparing the Performance of the SPGE and the Optimised ELISA with a Commercial ELISA**

The developed CRP assay on the screen-printed gold electrodes and the optimised ELISA assay were compared to a commercially acquired human CRP immuno assay that was purchased from immunology consultants laboratory (Newburg, USA). The three techniques were used to detect the amount of CRP antigen spiked in commercial serum. The assays were performed according to their optimised protocols described in sections 3.3.2.4 and 3.3.8. For the commercial ELISA a protocol incorporated in the kit was followed closely. This consisted of re-suspending lyophilised controls and standards with sample diluent buffer as directed. All samples were to be diluted 200 times with the sample diluent buffer. A 100  $\mu\text{L}$  of the standards, samples and controls were pipetted to the provided pre-coated micro plate and incubated for 1 hr. The next step was washing with appropriately diluted washing buffer that was provided, before putting 100  $\mu\text{L}$  of the 10 times diluted detection antibody and incubating for 30 min. The plate was then washed again and 200  $\mu\text{L}$  of chromogenic substrate was added in each used well and the plate was incubated at room temperature in the dark for 15 min. A stopping solution was then added to each well (100  $\mu\text{L}$ ) and the plate was read on the fluorostar® plate reader at 450 nm wavelength.

Six samples with unknown concentrations of CRP were made by spiking a random amount of antigen into commercially acquired serum. The serum samples were then inter diluted ensuring that the concentrations of the antigen in them will be different. The spiked serum samples were then analysed in triplicates using the optimised and commercial ELISAs as well as the optimised immuno sensor. Standard curves were plotted and the unknown concentrations of CRP in the samples were interpolated and results compared, the limit of detection of all the methods was established.

### **3.3.10 Cross Reactivity Studies**

Cross reactivity is a measure of the specificity of the antibodies to the antigen of interest. Although this was confirmed by the antibody manufacturers there is always a need to verify the claims if the resources are available. In this experiment, other proteins were used to investigate the specificity of the developed immuno assays on the optimised ELISA and the immunosensor platform. Commercial serum was spiked with antigens to make three solutions with 25 ng mL<sup>-1</sup> of CRP, cardiac troponin t and prostate specific antigen (PSA). These solutions were then assayed in triplicate using the three methods analysed using the methods described in Sections 3.3.2.4 , 3.3.9 and 3.3.8. For the commercial ELISA a protocol incorporated in the kit was followed closely. Standard curves were plotted and the signal from the various proteins was interpolated and normalised against the highest output based on the positive control of the commercial ELISA.

## **3.4 Results and Discussion**

### **3.4.1 Development of an micro plate based ELISA assay**

The checkerboard method was used to optimise the ELISA assay. The optimized coating antibody was investigated first and a Nunc Microtittre flat-bottomed plate was used as it has enhanced binding abilities due to its surface chemistries with more exposed carboxyl groups. The detection antibody was then investigated followed by other assay parameters like incubation times and blocking reagents. The optimised micro plate based ELISA was then compared to a commercial alternative and the developed immunosensor.

### 3.4.2 Investigating the ELISA Coating Antibody Concentration

Various coating antibody concentrations were investigated (2, 4, 6, 8, and 10  $\mu\text{g mL}^{-1}$ ) and the results are shown in Figure 3.7. The results showed that there was an increase in the signal output with an increase in the concentration of the coating antibody for the CRP assay. This trend was however consistent until 6  $\mu\text{g mL}^{-1}$  concentration after which there was no major difference observed with subsequent increases in the coating antibody. This indicate that the optimum coating concentration is around 6  $\mu\text{g mL}^{-1}$  as any further increase did not give any advantage to the signal output. The results also showed that there was saturation at around 15  $\text{ng mL}^{-1}$ , this may have been caused by the fact that the detection antibody concentration was not yet optimised and the provisionally used concentration of 0.375  $\mu\text{g mL}^{-1}$  was probably too concentrated.

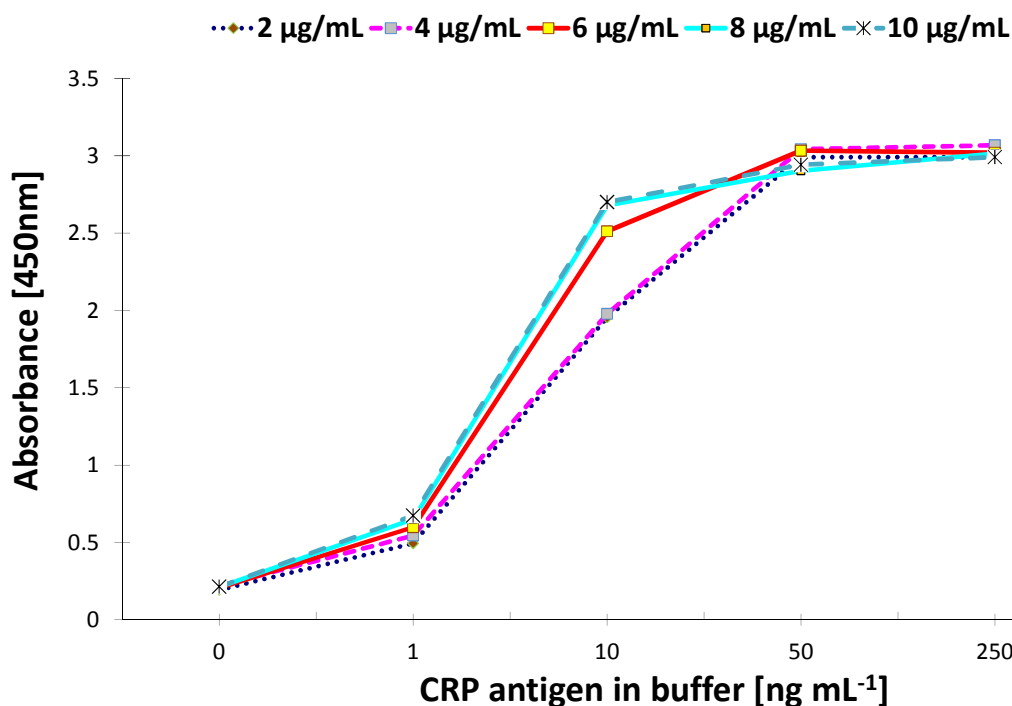


**Figure 3.7:** The standard curves showing the effect of increasing concentration of coating antibody on the signal obtained. Varying concentrations of the coating antibody (2, 4, 6, 8, 10  $\mu\text{g mL}^{-1}$ ) were investigated by matching the rest of the parameters on a plate immunoassay.  $n=3$ , maximum CV=6.2%.

### 3.4.3 Optimising the Detection Antibody for CRP

After obtaining the optimum coating antibody of  $6 \mu\text{g mL}^{-1}$ , the next step was to investigate the best concentration of the detection antibody. It was discovered in preliminary experiments that the HRP conjugated anti human CRP used in this experiment was very active and saturation was being achieved prematurely thus resulting in a low dynamic range. The experiment was designed to focus on concentrations below  $0.5 \mu\text{g mL}^{-1}$  as these were more feasible and dilute enough not to saturate the assay. The results are shown in Figure 3.8, they show that there is a relationship between increasing the signal and the concentrations of the anti CRP HRP conjugate. However, the relationship ceases to exist at  $0.375 \mu\text{g mL}^{-1}$ , where any increase in the concentration of the detection antibody did not give any further advantage. The best dynamic range was given by the least concentrated detection antibody concentration ( $0.1 \mu\text{g mL}^{-1}$ ) which was the only one capable of detecting up to  $100 \text{ ng mL}^{-1}$  CRP concentrations.

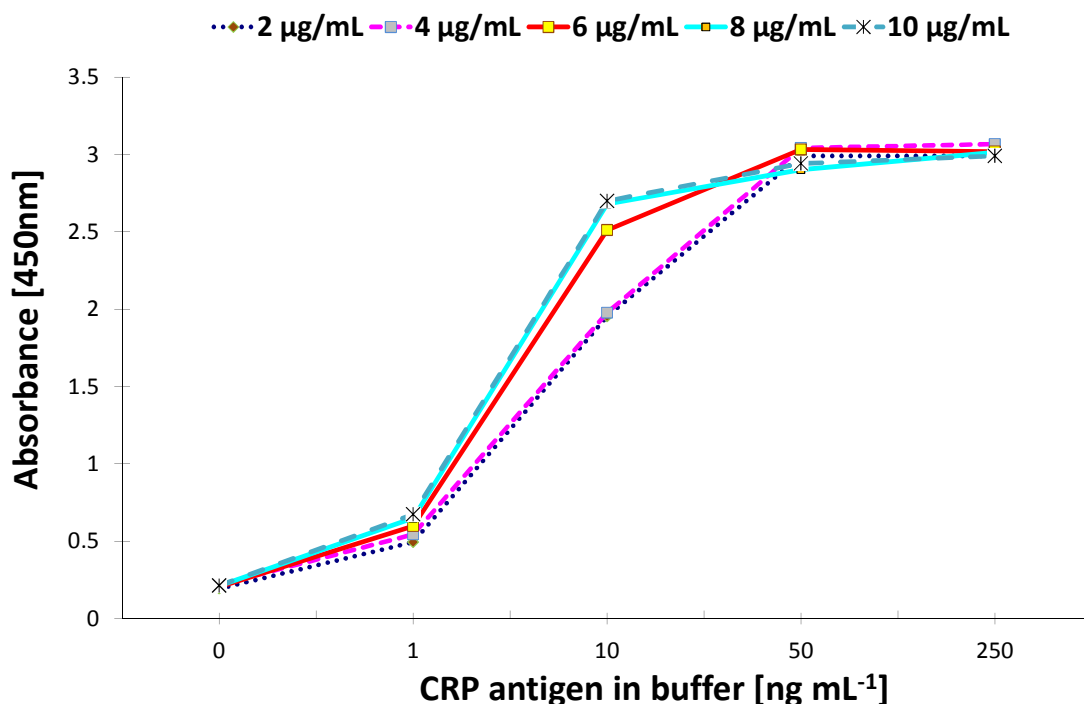


**Figure 3.8:** The effect of increasing concentration of the detection antibody on the signal obtained. Varying concentrations of detection HRP conjugated antibody (0.1, 0.25, 0.375, 0.5  $\mu\text{g mL}^{-1}$ ) were investigated.  $n=3$ , maximum CV=6.8%.

#### 3.4.3.1 Optimising the Blocking Buffer

Three blocking solutions were investigated for the C-reactive protein assay. These included blocking agents previously reported in literature including a 1 in 10 dilution of skimmed milk protein in PBS (Salam and Tothill, 2010), 1% PVA (Kadir and Tothill, 2010) and BSA which is a traditional blocking agent. This was done by running the assay using the method described in Section 3.3.2.4. Using plates coated with 6  $\mu\text{g mL}^{-1}$  of coating antibody and running three antigen concentrations (0, 25, 50  $\text{ng mL}^{-1}$ ) of antigen in triplicate for each of the blocking solution.

The results of this experiment showed that the 10 % skimmed milk protein gave the best blocking with good consistency and limited nonspecific binding. Figure 3.11 shows that the columns representing no antigen reading (blank) gave the lowest reading when compared with bovine serum albumin (BSA) and PVA polyvinyl acetate (PVA). The standard deviation of the wells with 10 % milk was also much smaller and more consistent than that for the other blocking agents that were investigated. It was decided to continue to use the 10 % milk protein for future immuno-assays.

#### **3.4.3.2 Optimising the Incubation Time for the ELISA Coating Antibody**

The coating of the plate is arguably a very important step as it can directly affect the results of the assay. A performance study was done to identify the optimum incubation time, which ensures that the maximum capture antibody was bound onto the solid state. Figure 3.9 indicates that there is an increase in the signal with increasing the incubation times. This increase however reaches a plateau between 1 and 2 h of incubation time. The results also show that there is no major benefit of incubating overnight to that of 2 h. The incubation of 2 h was thus adopted for the coating antibody for all future assays.

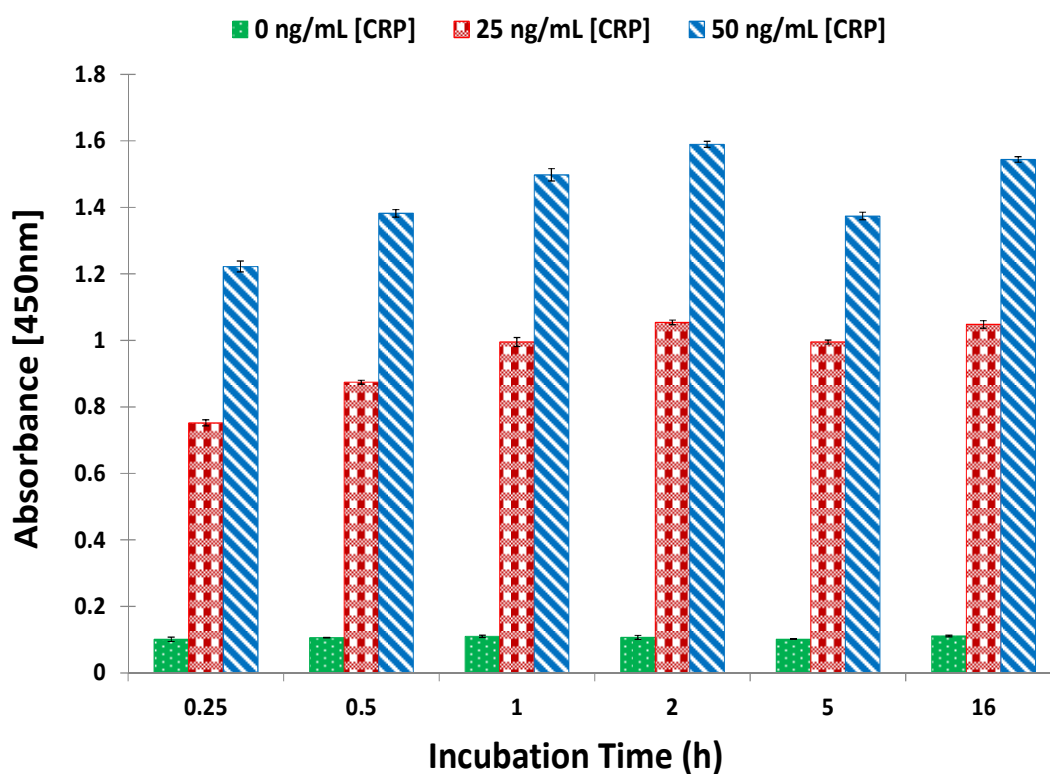


**Figure 3.9:** The effect of different incubation times on assay response. A micro plate was coated with  $6 \mu\text{g mL}^{-1}$  of anti-human CRP antibody and incubated for varying times (0.25, 0.5, 1, 2, 5 hr) at  $37^\circ\text{C}$  as well as 16h at  $4^\circ\text{C}$ , the rest of the assay parameters were synchronised,  $n=3$ , maximum  $\text{CV}=5.9\%$ , bars represent standard deviation.



### 3.4.3.3 Standard Curve for the optimised ELISA

Taking into account the best coating antibody concentration ( $6 \mu\text{g mL}^{-1}$ ) and the best detection antibody concentration ( $0.1 \mu\text{g mL}^{-1}$ ) a standard curve was constructed to show the full capabilities of the CRP Elisa Assay. The results in Figure 3.10, shows the optimised standard curve of the CRP assay.

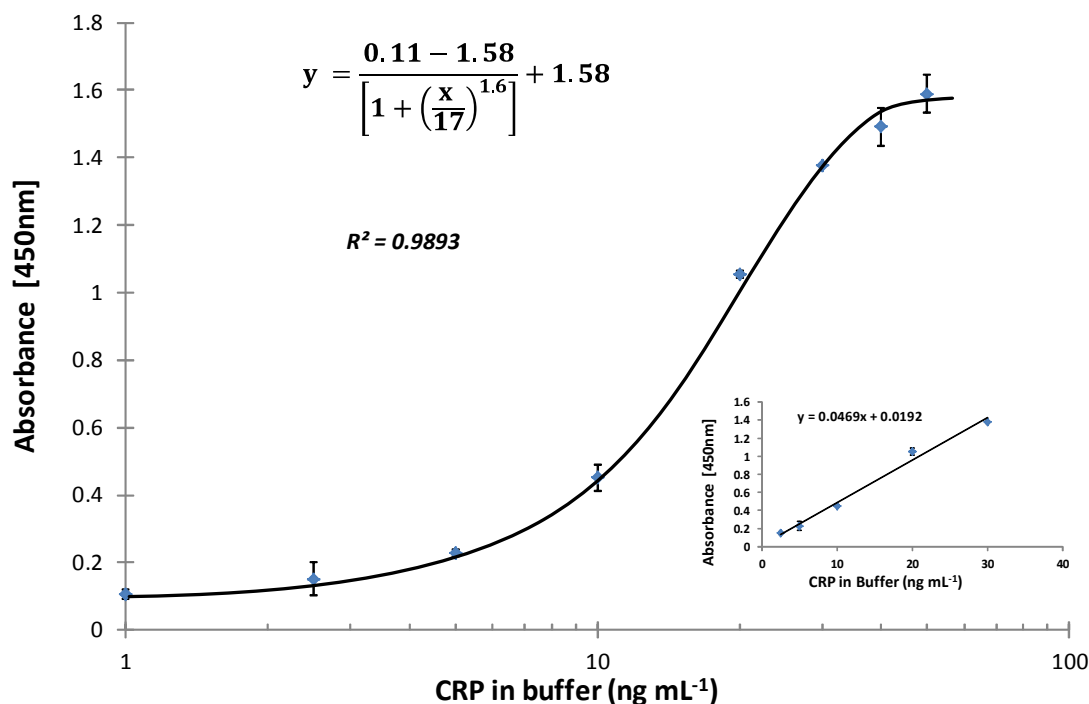


**Figure 3.10:** The standards curve for optimised ELISA assay for C- reactive protein with a linear plot insert. Standard concentrations of CRP (0.1 ,0.156, 3.12, 6.25, 12.5, 25, 50, 100  $\text{ng mL}^{-1}$ ) were assayed using optimised parameters.  $n=3$  ,bars = standard deviation, maximum CV=7.4., LoD=1.9  $\text{ng mL}^{-1}$ .

Figure 3.10 shows that the standards curve for the optimised ELISA assay for CRP. The calculated limit of detection for the assay was  $1.9 \text{ ng mL}^{-1}$  and this was calculated by extrapolating the calculated signal of adding the background absorbance to a value three times the standard deviation from its replicates. This is was a good result as it is capable of distinguishing low risk from high-risk patients, thus making this assay suitable for inclusion in a biomarker diagnostics test for risk of cardiovascular disease. The targeted dynamic range was  $0.5$  to  $50 \text{ ng mL}^{-1}$  and this result is comparable to other kits on the market.

### **3.4.4 Development of the Screen-printed immuno-sensor for CRP**

The optimisation of the assay carried out on the ELISA was then transferred to the biosensor platform. The differences in the surface chemistry, sample volumes and other factors like limited surface area for binding meant that the assay required optimisations on to the screen-printed electrodes in order to achieve optimal results. Far more concentrated antibody solutions would be required to give detectable signals especially if high sensitivity is to be achieved.

#### **3.4.4.1 Optimising the coating and detection antibodies**

Both the coating and the detection antibody concentrations had to be investigated on the screen-printed electrode platform. Different concentrations (5, 10, 20, 30, 50, 100  $\mu\text{g mL}^{-1}$ ) of coating antibody (10  $\mu\text{L}$  of mouse monoclonal antibody dissolved in 0.05 M carbonate-bicarbonate buffer pH 9.6) were investigated. The coating antibody were deposited in triplicates and allowed to incubate overnight at 4  $^{\circ}\text{C}$ , before an electrochemical assay was done as described in Section 3.3.8 using at 1  $\mu\text{g mL}^{-1}$  CRP antigen standard and 20  $\mu\text{g mL}^{-1}$  detection antibody concentration. Similarly, the same was done for investigating the optimised detection antibody. The coating antibody was standardised at the optimum concentration 60  $\mu\text{g mL}^{-1}$ ) and the antigen was also fixed at 1  $\mu\text{g mL}^{-1}$  but the detection antibody concentrations were used (10, 20, 30, 50, 100  $\mu\text{g mL}^{-1}$ ) to find the optimum. The electrodes were then washed and connected to an edge connector to a multi-channel AUTOLAB electrochemical instrument from Metrohm (Utrecht, Netherlands).

The results obtained for these experiments are shown in Figure 3.12. The general trend showed that the peak for the coating antibody concentration is around the 60  $\mu\text{g mL}^{-1}$ . The drop in the signal after the peak can be due to packing impedance or steric hindrance. There was an increase in signal with increasing concentration of the detection antibody. This appears to reach a plateau at 30  $\mu\text{g mL}^{-1}$  concentration, where the highest signal was achieved.

This plateau is caused by several factors including the fact that there is saturation of the antigen with the HRP conjugated detection antibody. There may also be a possibility that the applied voltage can only yield a maximum of the peak current given the type of the electrode and the quality of the immune-assay.

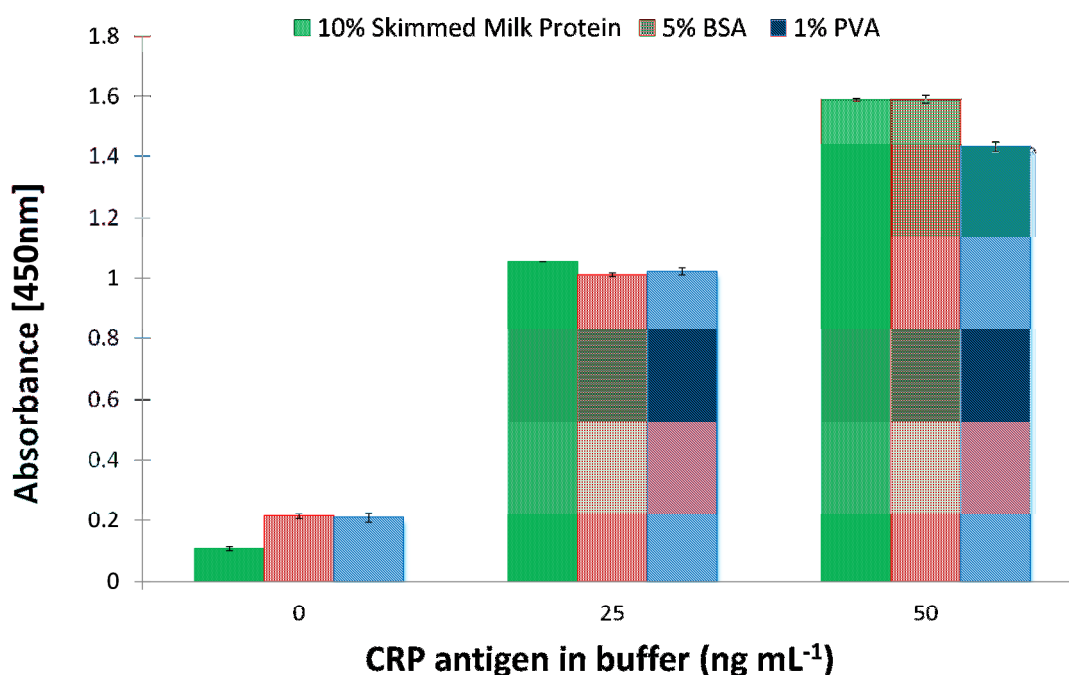


**Figure 3.11:** The effect of the different blocking agents were investigated on the sandwich assay. A plate was coated with 6  $\mu\text{g mL}^{-1}$  of coating antibody and incubated for 2 h at 37 °C before being washed, three different blocking agents (300  $\mu\text{L}$  of 10 % milk protein, 1% PVA, 5% BSA ) were investigated.  $n=3$ , maximum CV=5.8 %, bars represent standard deviation.

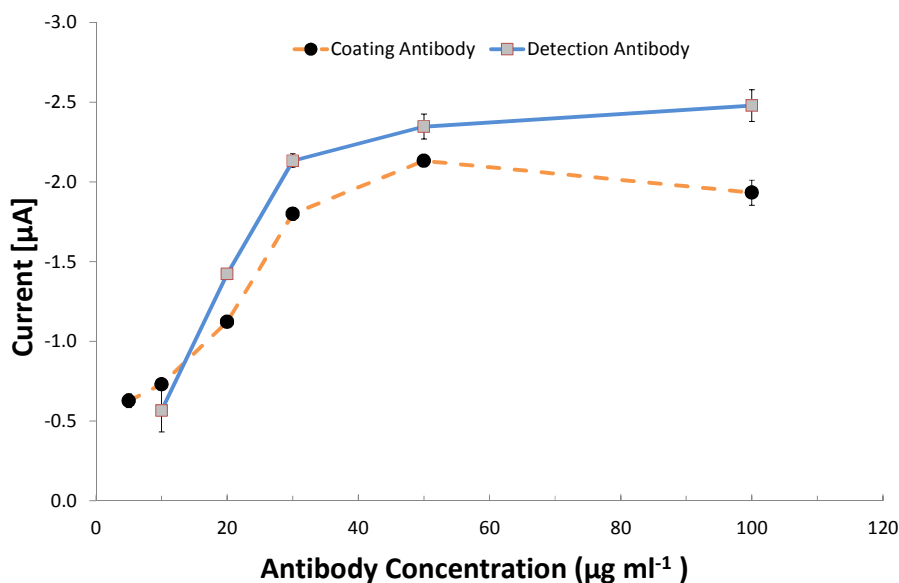


**Figure 3.12:** The optimisation of the coating and detection antibody for C-reactive protein assay on screen-printed gold electrodes (SPGEs), varying concentrations of the detection (10, 20, 30, 50, 100  $\mu\text{g mL}^{-1}$ ) and for coating (5, 10, 20, 30, 50, 100  $\mu\text{g mL}^{-1}$ ) antibody concentrations were investigated.  $n=3$ , maximum CV=4.9%, bars made using standard deviation.

#### 3.4.4.2 Optimisation of the Method of Antigen addition

Immuno assays are enhanced by several factors that include the orientation of the assay procedure particularly concerning the introduction of the antigen. From a product development point of view it is more beneficial to have an assay which performs better with an setup which involves the detection antibody interacting with the antigen before being introduced to the immobilised capture antibody. This will simulate the procedure that is employed by most lateral flow devices. While plate immuno-assays with the exception of competitive ones operate on an step by step application it is more desirable to have a premixed antigen antibody complex as this may save on assay time and may improve on the assay sensitivity.

In this experiment, the incubation of the HRP conjugated antibody with the antigen-capture complex is compared to an alternative setup where the two (antigen and detection antibody) are premixed in free solutions. It was also important to synchronize the contact time of the assay in order to make sure that the concentrations of the reagents were not compromised through dilution.

In both methods, the electrodes were coated with 20  $\mu\text{L}$  of 60  $\mu\text{g mL}^{-1}$  coating antibody solution in carbonate bicarbonate and incubated for 2 h at 37 °C. The working electrodes surface was washed and blocked (30 minutes at 37 °C with 50  $\mu\text{L}$  milk protein diluted with PBS) in a controlled humid condition, the electrodes were then washed and air-dried. For the standard procedure, CRP standard concentrations (20  $\mu\text{L}$  of 0, 12.5, 50 and 100  $\mu\text{g mL}^{-1}$ ) were added to the working electrodes in triplicates. They were then incubated for 1 h at 37 °C in a moist petri dish before being washed and a conjugated mouse monoclonal antibody with HRP 20  $\mu\text{L}$  of 30  $\mu\text{g mL}^{-1}$  in 1:40 dilution milk protein was added to the electrode and incubated for 1 hr at 37°C. In the case of the premixed procedure, the detection antibodies and the compensatory antigen concentration were premixed in solution with the conjugated mouse monoclonal antibody and incubated at room temperature for 1h, with a Stuart SB3 rotator (Appleton Woods, Birmingham, UK) with the rotator at a 10° inclination angle. A 20  $\mu\text{L}$  of the solution of the premix was then deposited on the blocked working electrodes and incubated for another 1 h. The electrodes were then washed and connected to an edge connector, which is connected with a multi-channel AUTOLAB electrochemical instrument. The substrate was added and measurements were done by adding 100  $\mu\text{L}$  of 4 mM TMB and 0.06 %  $\text{H}_2\text{O}_2$  in 0.05 M citrate phosphate buffer plus 0.1 M KCL with chronoamperometry methods at -200 mV potential and run for 200 s to 300 s using electrochemical GPES 4.7 software.

Figure 3.13 shows the results obtained, the premixed assay showed there was increase in sensitivity than the standard systematic setting. This could be attributed to the fact that before the antigen was captured directly on the sensor surface it had more flexibility to interact and bind to the detection antibody in solution. Unlike the systematic set up where the antigen will already be immobilised by the time the detection antibody is introduced. Another disadvantage of the systematic method is that the excess antigen will have been washed away before getting a chance to bind to the detection antibody, This may explain the enhanced signals and the proportional response shown in Figure 3.13.

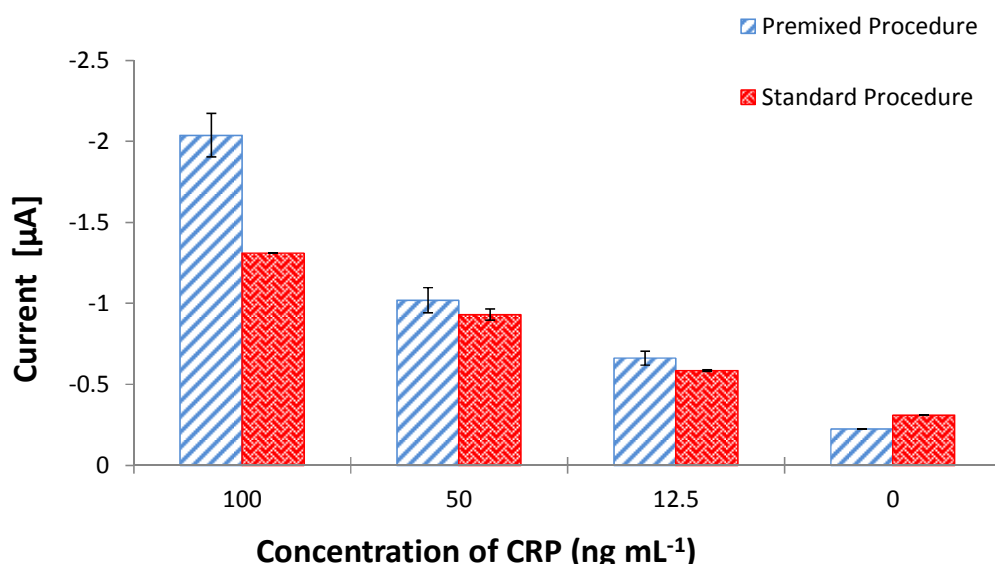


**Figure 3.13:** The effect of premixing the detection antibody with the antigen on signal performance. Electrodes were coated and blocked, in the standard assay CRP antigen concentrations were added, while for the premixed procedure, detection antibodies and the antigen were premixed at room temperature first..  $n=3$ , maximum CV=9.4% and bars represent standard deviation.

### 3.4.5 Optimised CRP Assay on Screen-Printed Gold Electrodes

A standard curve was constructed using the optimised assay described in section 3.3.8. The standard curve obtained is shown in Figure 3.14. The assay was done using the method described in section 3.3.8 and the calibration plot was used to extrapolate CRP from spiked serum samples. The comparative studies of samples and cross reactivity were conducted using this curve. The final developed SPGE immunosensor exhibited working ranges from 2.2 to 100 ng mL<sup>-1</sup>. This is well in range for the detection limit required for the standard use of CRP, thus the immuno-sensor demonstrated the feasibility of electrochemical detection of CRP using screen-printed gold electrodes.

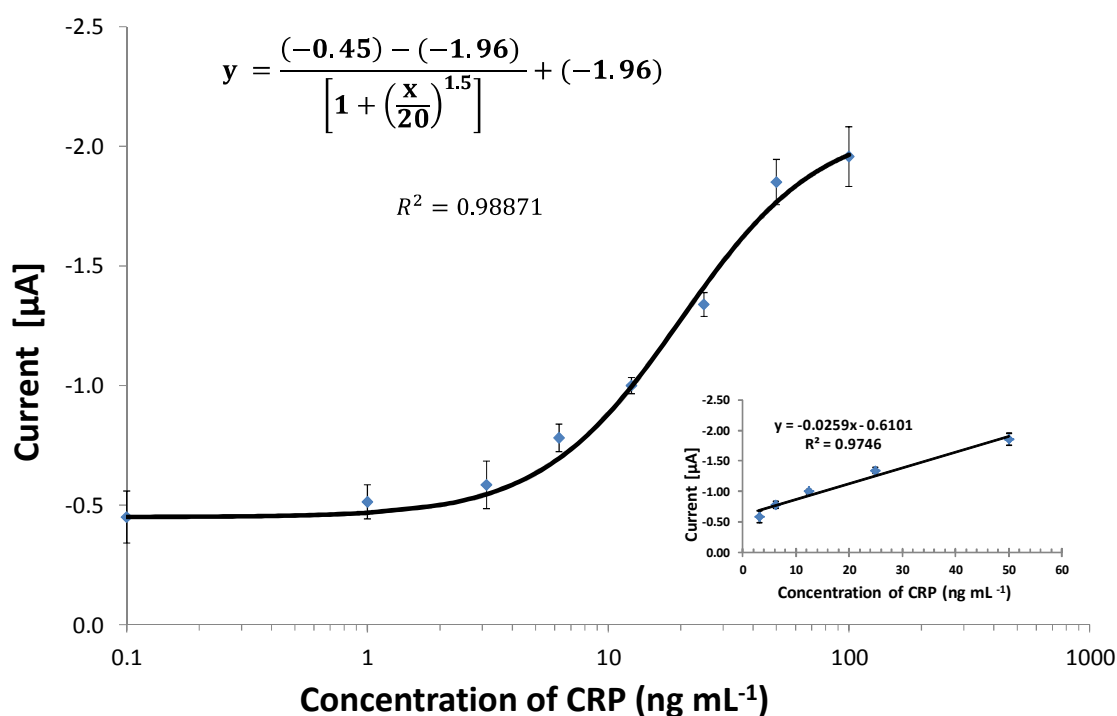


**Figure 3.14:** The Graph showing standard curve for the C-reactive protein assay on screen-printed gold electrodes (SPGEs). Concentrations of CRP antigen in buffer were premixed with detection antibody before an assay was done on the immunosensor.  $n=3$ ,  $CV=9.8\%$ , bars= standard deviation  $LOD=2.6\text{ ng mL}^{-1}$ .

### **3.4.1 Exploring the use of self-assembled monolayers to enhance assay sensitivity**

Although the optimised immunosensor that was developed using passive adsorption was competent to meet the diagnostic assay parameters, there was need to investigate on other immobilisation methods that could potentially improve the antibody immobilisation on the sensor surface. The antibody immobilisation plays a crucial role in the fabrication of immunosensor, and the immobilization and orientation of the antibody on transducer surfaces like gold has become another focus of study in the biosensor field (Hao *et al.*, 2009). Regardless of the kind immobilisation procedures chosen, it is important that more antibodies are immobilized on the transducer surface (Furuya *et al.*, 2006). Furthermore, functionality of antibodies should be preserved and that more active sites should be accessible. Immobilisation methods could be classified into covalent and non-covalent combinations. Several covalent coupling methods are available to immobilise the antibody depending on the specific reactive groups. The amine ( $-\text{NH}_2$ ), thiol ( $-\text{SH}_2$ ) and aldehyde ( $-\text{COOH}$ ) coupling chemistries are well-established procedures. Covalent coupling is stable and, in general, does not need any modification of the antibody. The immobilization level is easily controlled and the ligand consumption is low. (Choi and Chae, 2010).

Self-assembled monolayers (SAMs) are monolayers of well-defined structural and chemical properties. There are a variety of SAMs made by chemical adsorption, such as alkylchlorosilanes with long alkyl chains and organosulfur compounds like thiols, disulfide, and sulphides (O'Dwyer *et al.*, 2004). Alkanethiol SAMs are widely used bioreceptor linker molecules because they offer two major advantages which are abundant functional groups to immobilize bioreceptors and a fully packed monolayer that results in limited nonspecific binding (Chaki and Vijayamohanan, 2002; Salam and Tothill, 2009). The stability of the SAM has been linked to the size of the carbon spacer and the longer the chain the more stable the SAM (Love *et al.*, 2005). For this reason larger molecules like 11-mercaptoundecanoic acid (11-MUA) have been



favourites for the making of SAMs (Chaki and Vijayamohanan, 2002). However other authors have argued that short carbon spacers have advantages of lowering non-specific binding and thus increasing sensitivity (Bolduc and Masson, 2008).

In this experiment self-assembled monolayers were made using two chemicals, 11-mercaptoundecanoic acid (11-MUA) and 3,3-dithiodipropionic acid (DTDPA) that have long and short carbon spacers respectively. This was done by baking and plasma cleaning electrodes. The working electrodes were then washed with ethanol using a pipette, for the 11-MUA monolayer, electrodes were dipped in a 2mM of 11-mercaptoundecanol solution overnight in the dark at room temperature. For the DTDPA monolayer, 3% w/v of 3,3-dithiodipropionic acid in ethanol was used in the same conditions. The electrodes were then washed with water and gently dried with a nitrogen gun.

#### **3.4.1.1 The Characterisation of the chemically modified working electrodes**

After the preparation of the self-assembled monolayer, cyclic voltammetry was used to determine the integrity of the method used to deposit the self-assembled monolayers. After their deposition, it is physically impossible to see they had been formed and to what extent the coverage. The results obtained are shown in Figure 3.15. The results showed that there was very limited conductivity on the modified surfaces as shown by near flat cyclic voltamograms. The voltamograms for the bare electrode showed the most conductivity and there was limited conductance on the 11-MUA compared to the bare electrode. The DTDPA surface had the least conductance, which may translate to impedance being caused by the monolayer. The contact angle measurements were done to confirm this. The results showed decreased wettability on modified surfaces compared to the bare electrode. This could be attributed to the increased lyophobicity of the surface by the chemicals.

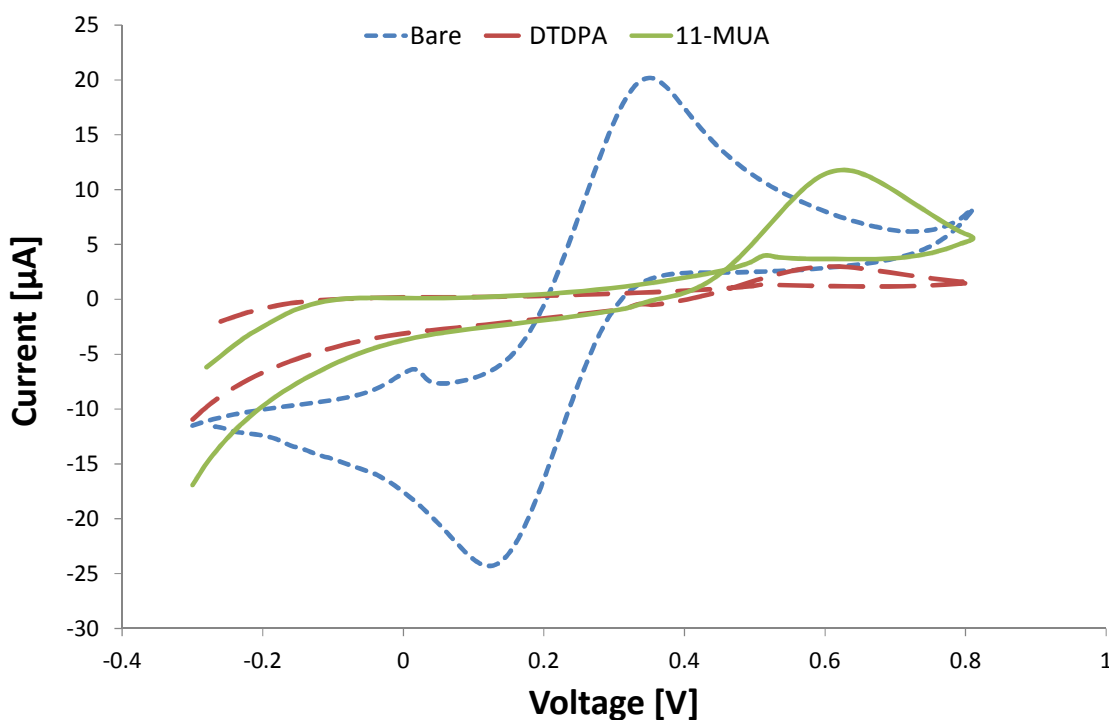


**Figure 3.15:** Cyclic voltammetry for validating the deposition and formation of Self assembled monolayers by thiol group chemicals that facilitate covalent coupling with the capture antibody. 5 scans of cyclic voltammetry were done using 1 mM potassium ferricyanide  $K_3[Fe(CN)_6]$  were prepared in 0.1 M KCl at  $50 \text{ mV S}^{-1}$  scan rate.

The average contact angle for bare screen-printed electrodes was  $39.88^\circ \pm 0.72$ , and the modified surfaces gave a higher angle measurement with  $47.81^\circ \pm 1.90$  for 11-MUA and  $45.98^\circ \pm 1.90$  for DTDPA. The monolayers of 11-MUA and DTDPA are capable of depolarising the gold surface thus making it more water repellent.

### 3.4.2 Immunoassay for Evaluating Different Immobilisation Techniques

Immuno assays were carried out to evaluate the effectiveness of the covalent coupling due to the two thiol group chemicals (11-MUA and DTDPA). The coupling is a result of the activation of the carboxyl groups by NHS and EDC via carbodiimide chemistry is one of the most popular methods (Park *et al.*, 2004; Salam and Tothill, 2009). This method is based on the formation of NHS esters that will react with nucleophilic groups of the antibody under elimination of NHS and formation of a covalent bond. As mentioned earlier there have been reported improvements in the orientation and packing of the coating antibody due to the use of chemical compounds like 11-MUA and DTDPA (Uludag and Tothill, 2010). The two compounds were tried against a conventional passive immobilisation technique and the obtained results are shown in Figure 3.16.

The results showed that the bare electrode gave a better consistent signal than the covalent immobilisation methods. Several factors may explain these unexpected results, the first being that there may have been damages to the electrodes when they got in contact with ethanol during washing or formation of the covalent surfaces. Ethanol was used as a solvent as 11-MUA is not water-soluble. The electrodes used have an on board Ag/AgCl reference electrode that can be easily eroded away by volatile solvents like ethanol.

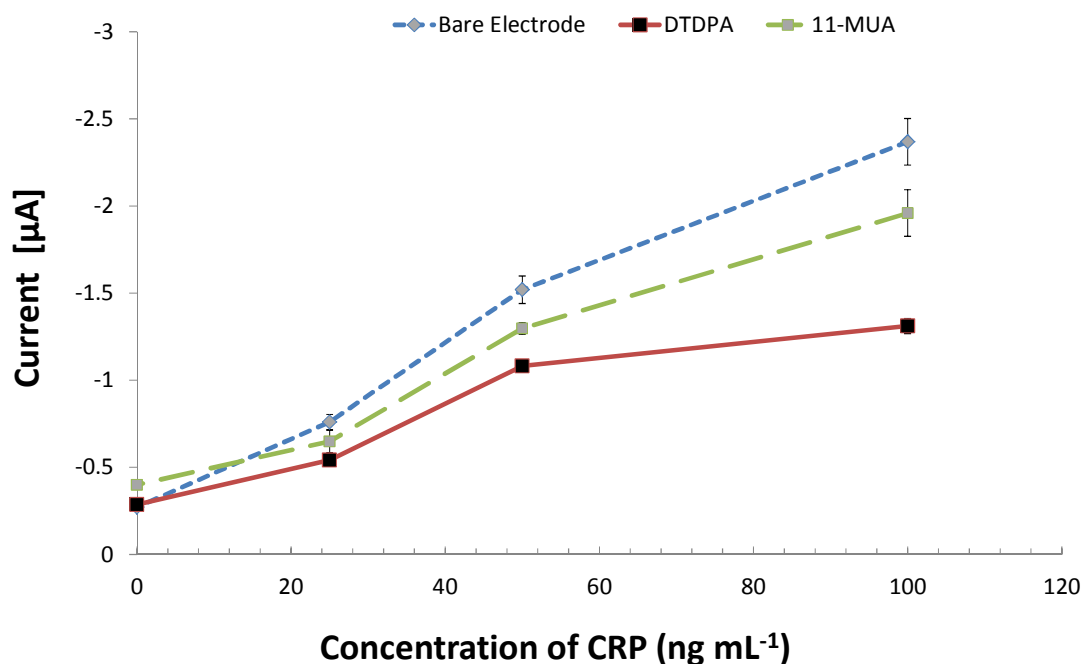


**Figure 3.16:** The impact of different covalent surface modifications to the assay performance of C-reactive protein on screen-printed gold electrodes (SPGEs). Two sets of electrodes were chemically treated with self-assembled monolayers (DTDPA and 11-MUA) to facilitate covalent coupling. Optimised electrochemical immuno-assays were done to evaluate the effect of SAMs on the assay performance.  $n=3$ ,  $CV=9.7\%$ , bars = standard deviation

The results showed non-specific binding on the 11-MUA coated chips. The control signal of 11-MUA coated chips was relatively higher than for other immuno sensors (Bare and DTDPA), this may have been caused by molecules trapped in the lattice of the 11-MUA monolayer. The 11-MUA monolayer has long carbon spacers due to its chemical structure, this means there is a considerable distance between its reactive groups and this in turn influences the distance between the sensor surface and the ligand. Unlike smaller molecules like DTDPA with short carbon spaces, Long chain SAM molecules that have been proven to trap proteins non-specifically in several ways (Love *et al.*, 2005).

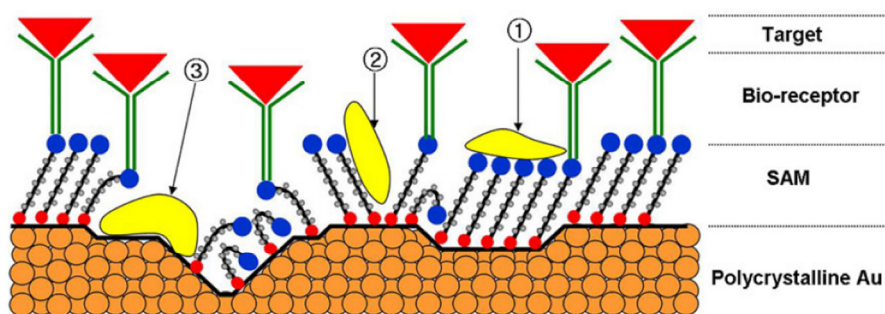


**Figure 3.17:** Diagram showing possible sources of non-specific binding on SAMs, (1) unutilised reactive groups (2) imperfect monolayers and (3) surface morphology (Choi and Chae, 2010).

Bio sensing surfaces functionalized with alkanethiol SAMs suffer from non-specific binding. The three main reasons are non-immobilized bio receptors like antibodies, imperfectly formed monolayers and polycrystalline gold grain structure (Love *et al.*, 2005). Non-specific binding on the activated head group of the SAM where antibodies are not immobilized and reactive surfaces are exposed and unutilised they can attach non-specifically (Figure 3.17, 1). Several techniques have been tried to control this, especially through deactivating the head group with ethanolamine-HCl (O'Dwyer *et al.*, 2004; Furuya *et al.*, 2006). This was done in this experiment, although non-specific binding was still observed. Non-specific on the 11-MUA coated chips binding may also have been caused by imperfect monolayers form on polycrystalline gold surfaces as shown in (Figure 3.17 , 2 ), and unevenly distributed gold surface (Figure 3.17, 2 and 3 ). As the performance of passive absorption was meeting the diagnostic requirements for a CRP assay no further input on covalent immobilisation was pursued for the development of this immunosensor.

### 3.4.1 Comparison of developed immunosensor with the commercial and Optimised ELISAs

Comparative studies were done to ascertain the quality of the developed electrochemical immunosensors and the in-house micro-plate based ELISA assay for CRP. This was done by triangulating the two developed methods with a commercially acquired ELISA assay.

#### 3.4.1.1 Assay Performance

The performance of immunosensor was tested against that of the commercial ELISA from Immunology Consultants Limited as well as the in-house developed ELISA assay. The results showed that all the three methods were capable of detecting the unknown CRP concentrations in the spiked serum with slight variations in signals produced.

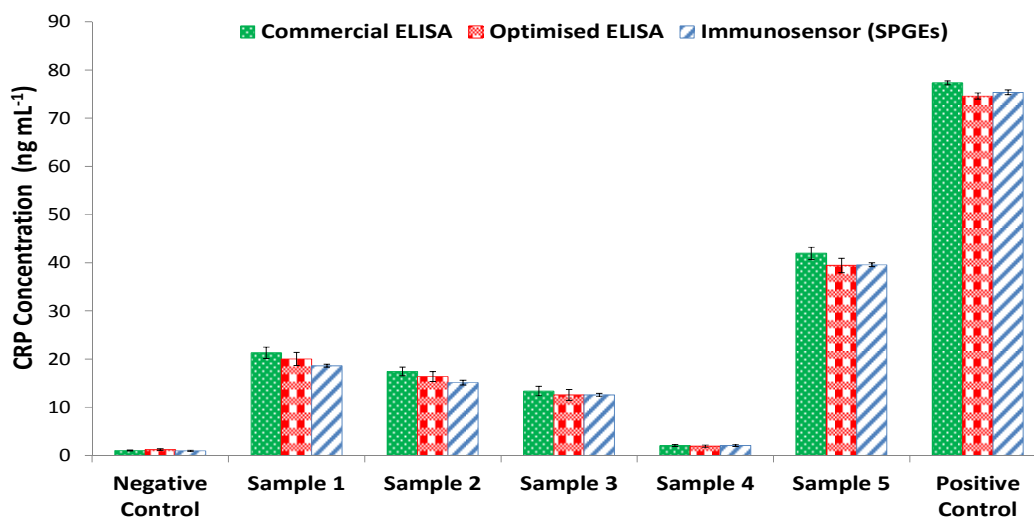


**Figure 3.18:** The evaluation of three detection methods for C-reactive protein using spiked serum samples with unknown CRP concentrations. A commercial human serum stock was randomly spiked with CRP. The samples were then diluted 200 x with PBS tween before being analysed in triplicates using the different methods.  $n=3$ ,  $CV=6.2\%$ , bars = standard deviation.

The results obtained are summarised in Table 3-2 which showed consistency in the determination of the unknown CRP concentrations with acceptable correlations between the methods. Both intra and inter assay analysis showed acceptable reproducibility expected of most commercial for diagnostic assays which is between  $\geq 15\%$ . The intra assay variation is the percentage error due to the differences in the interpolated quantities of an analyte in a sample run several times on a single assay. In this experiment, this was achieved after running 5 reps of a sample and interpolating the unknown against a single standard curve assayed concurrent with the samples. For results that are more accurate far more reps were needed but the resources permitted limited choices on this. For all the three methods used, the highest intra-assay variation on the unknown samples was 13.8% and this was from the in-house ELISA. The rest of the methods had fewer values than this, which was encouraging. The inter assay variation on the samples was below 7 % on all the methods used, which meant that there was close agreement between the different methods that were used. In this case inter assay variation is being defined as the level of error against the agreement of interpolated values between the three different assays. **Error! Not a valid bookmark self-reference.** showed the correlated performance between the commercial and the in-house ELISA, and Figure 3.20 shows the one between the developed electrochemical immunosensor and the commercial ELISA. Both correlations were exceptional with  $R^2$  values around closely approaching 1.

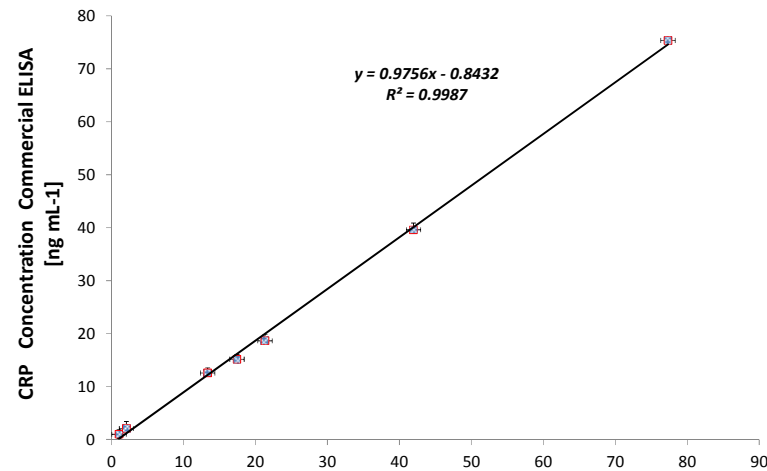


**Figure 3.20:**Correlation of performance between the immunosensor and the commercial ELISA kit.

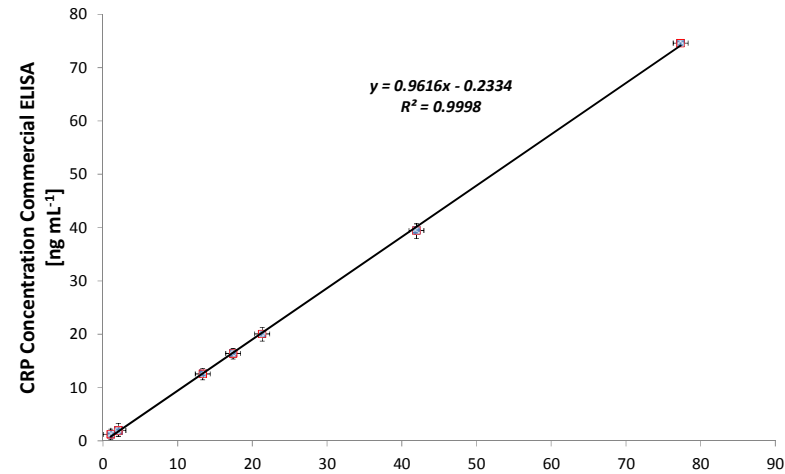


**Figure 3.19:**Correlation of performance between the commercial ELISA kit and the one developed In-house.

Table 3-2:Showing the intra and inter assay reproducibility of the detected CRP spiked in serum samples, n=5.

Sample	Commercial ELISA (ng mL <sup>-1</sup> )	Optimised ELISA (ng mL <sup>-1</sup> )	Immunosensor (SPGEs) (ng mL <sup>-1</sup> )	Commercial ELISA CV (%)	Optimised ELISA CV (%)	Immunosensor (SPGEs) CV (%)
Negative Control	1.05	1.23	0.98	8.57	13.82	11.22
Sample 1	21.32	20.04	18.64	5.48	6.76	1.61
Sample 2	17.43	16.38	15.13	5.21	6.43	3.19
Sample 3	13.36	12.56	12.57	7.24	8.94	2.41
Sample 4	2.07	1.94	2.09	9.48	11.83	9.59
Sample 5	41.96	39.44	39.58	3.03	3.74	1.02
Positive Control.	77.32	74.58	75.36	0.53	0.88	0.64



### 3.4.1.2 Cross Reactivity Studies

Cross- reactivity generally refers to assay specificity, which is the possibility of an assay to react with other unintended antigens. It occurs in cases where several antigens carry the same antigenic determinant as that of the one used in raising the antibody used in the immuno assay. Specificity is dependant mostly on the quality of the antibodies and it is an important analytical parameter for measuring the reliability of an immunosensor (Kawaguchi *et al.*, 2007; Salam and Tothill, 2009). The significance of cross-reactivity in immunosensors is that with higher cross-reactivity equates to more false positive tests (Jongh-Leuvenink *et al.*, 2005).

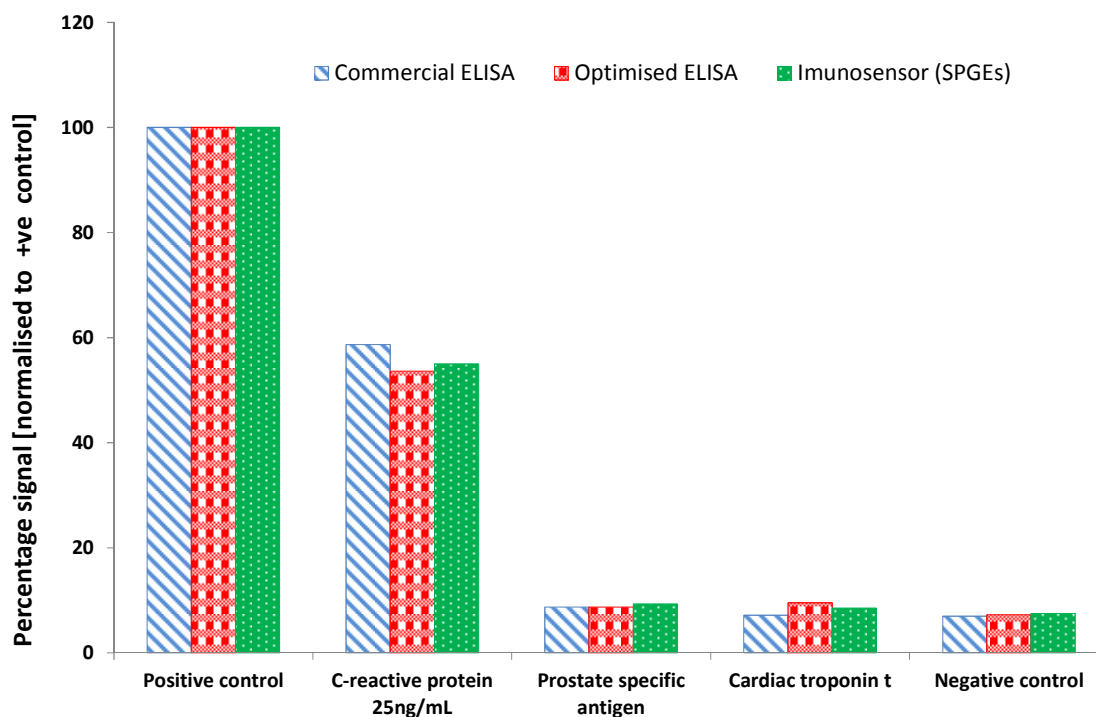


**Figure 3.21:** No significant cross reactivity between other plasma proteins and the CRP assay. The proteins ( $25 \text{ ng mL}^{-1}$ ) were assayed using the standard optimised procedures of the different methods and they did not give out a signal statistically different from the blank which showed there was no cross reaction on the tested proteins.

The results of the cross reactivity studies were normalised against the positive control reading of each of the three assays. The results visibly showed that the antibodies did not have non-specific affinity for other plasma proteins that were investigated.

### 3.5 Conclusions

An electrochemical immunosensor based on a gold working electrode made using screen-printing technology was developed for the detection and analysis of CRP in serum samples. The clinical reference ranges for CRP assay are  $\geq 1 \mu\text{g mL}^{-1}$  low risk,  $1\text{--}3 \mu\text{g mL}^{-1}$  is medium risk and  $\leq 3 \mu\text{g mL}^{-1}$  is high risk. The performance of the CRP immunosensor was competent to satisfy these parameters as the developed electrochemical immunosensor has a LOD of  $2.6 \text{ ng mL}^{-1}$  and spans a dynamic up to  $100 \text{ ng mL}^{-1}$ , however when the dilution factor was factored in, the final dynamic range of the immunosensor was  $0.52 \mu\text{g mL}^{-1}$  to  $20 \mu\text{g mL}^{-1}$ . The need to dilute all serum samples 200 times with PBS- tween played a significant role in the attainment of the diagnostic objectives of the assay mainly for two reasons which are removing the matrix effect and ensuring high levels of CRP can be detected easily.

Compared to in-house optimised ELISA, the performance of the commercial ELISA was superior to both the electrochemical immunosensor and the in-house optimised ELISA. This is because the commercial ELISA had the lowest calculated lower limit of detection of  $1.1 \text{ ng mL}^{-1}$ , unlike  $1.91 \text{ ng mL}^{-1}$  for the in-house ELISA and  $2.2 \text{ ng mL}^{-1}$  achieved by the immunosensor. A correlation curve was plotted using randomly spiked samples between a commercial ELISA kit a correlation with a  $R^2$  value of 0.998 was achieved. The in-house immunosensor had an  $R^2$  value of 0.999 against the commercial ELISA. The data for comparing the three methods is however interesting, as there is no statistical difference in performance when it comes to detecting the random

samples that were tested. This is because the inter assay variation between the two methods is within the accepted coefficient of variation of most diagnostic devices which is below 10%.

Although a direct transfer of the immuno assay first developed on the ELISA platform was not possible, some valuable lessons and skills were transferable on the optimisation of the immuno sensor. The major difference between the two developed platforms was that the concentration of the antibodies needed. For the immunosensor, the higher concentrations of antibodies had to be used for both the coating and detecting than the ELISA platform. This was because there is need to counteract for the limited volumes used by the biosensor, as there are containment concerns. Unlike the microwells that can easily accommodate 300  $\mu\text{L}$ , the screen-printed gold working electrode surface can take a maximum of 35  $\mu\text{L}$  before the liquid overflows to other electrodes.

The most effective concentration of the coating antibody was identified to be 60  $\mu\text{g mL}^{-1}$ , which was exactly ten times the concentration of the ELISA. It is important to note that this does not mean the immunosensor used more antibodies than the ELISA, although it used more concentrated antibody solutions it required far less volumes than the ELISA did. The experiments showed that at 60  $\mu\text{g mL}^{-1}$  antibody concentration there is the highest peak response to a standardized antigen concentration. It was observed that there was a characteristic tailing of the curve with concentrations of the coating antibody above 60  $\mu\text{g mL}^{-1}$ . This could be attributed to steric hindrance and other factors associated with the change in behaviour of highly concentrated antibodies. While the prospect of increasing signal with increasing the concentration of the antibodies were plausible, trade-offs were made to take into account the performance and costs relationship.. Experiments showed that although it was an interesting field to explore , there was no need to utilise covalent coupling in the CRP immunosensor as it managed to meet the clinical

reference range need for diagnosing cardiovascular diseases using CRP easily though passive adsorption. This option was however left for further exploration in future assays as the advantages of covalent coupling have been demonstrated to be phenomenal (Salam and Tothill, 2009). The method used in the surface modification may have been unfriendly to the electrodes, this was primarily because of the prolonged exposure of the electrode to ethanol which is a relatively strong solvent considering the materials on board the electrode. The electrode contains and on board Ag/AgCl reference electrode that is sensitive to ethanol, as such a new method with limited or no exposure of the ethanol to Ag/AgCl reference may improve the viability of utilising solvent-based surface modification techniques. This task however was left for further scrutiny in the next chapters. The detection antibody exhibited similar characteristics as shown on the optimisation of the capture where there was increasing signal with increasing concentration of the antibody.

The data showed that the concentration of  $30 \mu\text{g mL}^{-1}$  was the optimum for the detection antibody. The investigation of finding out the best method for the detecting the antigen showed that there are better results if the antigen is premixed with the detection antibody before being exposed to immobilised capture antibody. This is because both the antigen and the detection antibody are free in solution they have a better chance of binding in line with Brownian motion laws. Generic assay parameters were investigated on the ELISA platform instead of the immunosensors to curb on cost and to enjoy increased flexibility the micro plate offers in assay development. Reagents such as the blocking solutions, and appropriate buffers were selected from literature, and there was enough literature to ascertain that the current blocking solution of 1 to 10 milk protein in PBS was competent enough for assays on screen printed gold electrodes (Salam and Tothill, 2009; Heurich, 2011).

## CHAPTER 4

# THE DEVELOPMENT OF A GOLD NANOPARTICLE ENHANCED IMMUNOSENSOR FOR CARDIAC TROPONIN T

## 4 The Development of a Gold Nanoparticle Enhanced Immunosensor for Cardiac Troponin T

This chapter discusses the development of a gold nanoparticle enhanced electrochemical immunosensor for the detection of cardiac troponin T (cTnT). The development stages mimicked those described in the previous chapter for CRP. Two major distinctions in the development of this immunosensor are the use of gold nanoparticles (AuNPs) and the incorporation of self-assembled monolayers (SAMs) to aid in the immobilisation process. This was done in response to the challenges presented by the requirements of very low limit of detection for diagnostic cardiac troponin assays. A different protocol to that described in Chapter 3 was adopted for the development of SAMs, which increased their performance and applicability for use on the cardiac troponin Immunosensor.

### 4.1 Introduction

Gold nanoparticles have been recently gaining increasing attention in their use for enhancing immunoassays (Ambrosi *et al.*, 2009; Salam and Tothill, 2009). This could be of a combination of factors including unique structure, as well as electronic, magnetic, optical, and catalytic properties. These attributes have made them a striking material for use in the development of biosensor systems and bioassays, including several other interesting applications in the field of electrochemical sensors (Pumera *et al.*, 2005; Salam and Tothill, 2009). Due to their excellent biocompatibility, AuNPs have increasing application as signal enhancers (Stoeva *et al.*, 2006; Saha *et al.*, 2012).

Direct adsorption of biological molecules on metal surfaces generally has a detrimental effect of denaturing them or facilitates extensive loss of function. This is mainly caused by the fact that most interactions between biomolecules and metal surfaces are very weak. This relationship however changes in the case of nano scale metals in which case the biocompatibility is improved, and as such allows for stronger adsorption of biomolecules without denaturation or loss of bioactivity (Hu *et*

*al.*, 2003). The nanoparticles have large surface areas with high free energy. This allows biological molecules like enzymes and antibodies to be strongly adsorbed onto their surface easily (Ansari *et al.*, 2010). Gold nanoparticles take advantage of two basic chemical interactions that have been developed for forming nanoparticle/protein conjugates these include the reaction of protein sulfhydryl's with functionalized phosphine-groups and electrostatic interaction of proteins with citrate-passivated colloidal gold (Ackerson *et al.*, 2006; Luo *et al.*, 2006). They have considerable advantages when used in screen-printed electrodes. This is because they are capable of facilitating electron transfer reactions as well as increase the rate of reactions on the electrode. This enables lower working electrode potentials to be used and marked improvements in both the sensitivity and the stability of biological components on the working electrode (Jubete *et al.*, 2009). Another advantage is where enzymes are used, they are unable to have direct electrical communications with electrodes surface as they will be mounted on nanoparticles and their centers are insulated with protein shells that block the electron transfer to the electrodes. They also benefit from their ability to be miniaturised with a diameter of 1–100 nm and are capable of being part of very small devices without compromising on function and microfluidic processes. AuNPs confer miniaturisation, signal improvement, and sensitivity amplification (Luo *et al.*, 2006; Jubete *et al.*, 2009; Tothill, 2009).

In this chapter, methods of improving assay sensitivity will be explored with particular reference to two methods that are the use of gold nanoparticles, and the use of self-assembled monolayers (SAMs) for antibody immobilisation. The use of self-assembled monolayers in improving stability and orientation of immobilised antibodies for immuno sensors was partially discussed in Chapter 3. They are a good example of covalent immobilisation and can be formed by means of sulphur containing groups on oxidised and hydroxylated surfaces and by means of thiols on metal surfaces (Altintas *et al.*, 2012). The thiol molecules, usually alkanethiols consist of three parts including: a head group (S-H group), a spacer or hydrocarbon chain), and a the tail group specific which is active and specific. Alkanethiols with amine and carboxyl end groups are have been reported for use in to immobilise

proteins on sensor surfaces (Arya *et al.*, 2010; Altintas *et al.*, 2012). The high affinity of the sulphur atom to noble metal surfaces is responsible for spontaneous formation of semi-covalently bounds. Because of this, there is a tendency for van der Waals forces to form between the hydrocarbon chains that then stabilize the structures and create an ordered monolayer.

The terminal group of the molecule is responsible for the surface characteristics of the monolayer. For example to obtain hydrophobic surfaces  $-\text{CH}_3$  and  $-\text{CF}_3$  terminal groups are used and consequently  $-\text{COOH}$ ,  $-\text{NH}_2$  or  $-\text{OH}$  groups yield hydrophilic surfaces. SAMs can be formed on surfaces either by simply immersing the metal substrate in a dilute solution of thiol /silane or alternatively they can be formed by vapour deposition (Schreiber, 2000). If a metal substrate is immersed in dilute thiol solution, a disorganised monolayer spontaneously forms and then slowly the molecules are evenly organised due to van der Waals forces. The quality of the assembled monolayer depends on the cleanliness of the metal substrate, the purity of the alkanethiol solutions used and the length and composition of the alkanethiol. The head group of the alkanethiol is critical to obtain a monolayer with the required functionality. Many alkanethiols with different head groups are commercially available for the immobilisation of biological recognition elements on biosensor surfaces such as  $-\text{COOH}$ ,  $-\text{NH}_2$ ,  $-\text{OH}$ , -biotin, and -N-hydroxysuccinimide (Altintas *et al.*, 2012). These methods were adopted for used in the development of an immunosensor for the detection of cardiac troponin T, a cardiovascular disease biomarker. There is great need for increased assay sensitivity as the diagnostic requirements for the detection of cardiac troponin t for diagnosis of cardiovascular disease are more challenging. The diagnostic range for cTnT needs performances of detection of up to 99th percentile cut point of the base line values. This equates to detecting very low concentrations of the biomarker, around  $30 \text{ pg mL}^{-1}$  of antigen with a significant signal variation from that of the control. Furthermore, cardiac troponin assays should work toward a goal of total CV of 10 % with a 1-h or less turnaround time (Azzazy, 2002). Surface immobilisation techniques described earlier in chapter 3 were investigated to see their effect on gold conjugated assays. Figure 4.1 shows a schematic diagram of the set up for gold nanoparticles enhanced cardiac troponin assay.



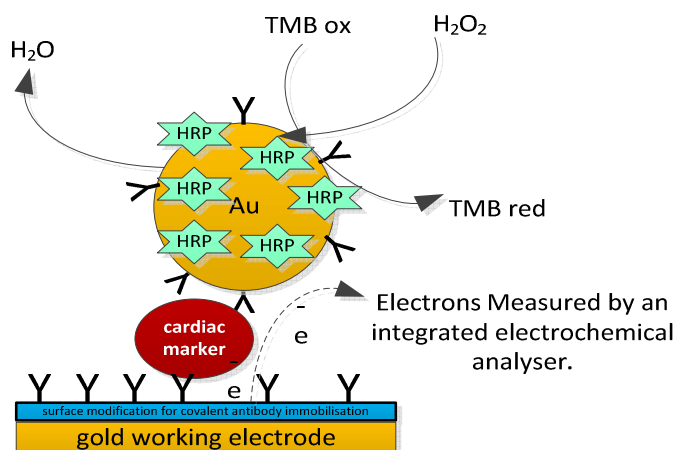


**Figure 4.1:** Schematic diagram showing gold nanoparticles being used to increase assay sensitivity for the cardiac assay, Enzymes and antibody molecules are attached to the gold nanoparticle and cause enhanced signal output that positively influence sensitivity.

An enhanced immunosensor for cardiac troponin T (cTnT), that utilises gold nanoparticles and covalently immobilised capture antibodies using self-assembled monolayer (11-MUA), will be presented in this chapter. Work conducted on a Quartz Crystal Microbalance (QCM) system for validating the conjugation of gold nanoparticles to antibodies will also be presented. Comparative studies of the performance of the electrochemical immunosensor against the QCM assays and hospital analyser were also conducted. Table 4.1 below summarises some published work for immunosensors for cardiac troponin T

**Table 4-1:** Summary of published work on Immunosensors detection of cardiac troponin T

Detection Technique	Assay Range	Reference
Electrochemical SPE immunosensors with a streptavidin and avidin system for signal amplification	0.1-10 ng mL <sup>-1</sup>	(Silva <i>et al</i> , 2010)
Electrochemical detection immunosensors using carbon nanotubes on the sensor surface for signal amplification.	0.1-10 ng mL <sup>-1</sup>	(Gomes-Filho <i>et al.</i> )
SPR immunosensor for human cardiac troponin T based on self-assembled monolayers for signal amplification.	0.05- 4.5ng mL <sup>-1</sup>	(Dutra <i>et al</i> , 2007)
Dual quartz crystal microbalance for human cardiac troponin T in real time detection	LoD 0.008ng mL <sup>-1</sup>	(Dutra <i>et al</i> , 2007)
A nanostructured piezoelectric immunosensor (QCM) for detection of human cardiac troponin T.	0.003 to 0.5 ng mL <sup>-1</sup>	(Fonseca <i>et al</i> , 2011)

## 4.2 Materials

Potassium Chloride (KCl), Potassium Ferricyanide ( $K_3Fe(CN)_6 \cdot 3H_2O$ ), TMB (3, 3', 5, 5'- tetramethylbenzidine hydrochloride), PBS (phosphate buffered saline) containing 0.137 M sodium chloride, and phosphate buffer, 0.01 M, pH 7.4 in tablet form, citrate phosphate buffer (0.05 M, pH 5.5) tablets. Hydrogen peroxide, sodium hydroxide (NaOH) and sodium chloride (NaCl), bovine serum albumin (BSA), 11-mercaptoundecanoic acid (11-MUA) were purchased from Sigma-Aldrich (Dorset, UK). Potassium chloride (KCl) were purchased from Fisher Scientific (Loughborough, UK). Primary (batch 1c11), secondary antibody (batch 9g6 HRP conjugated) and (7E7 non conjugated), and human cTnT (Molecular Weight (MW) = 36 kDa) were obtained from (Abcam, Cambridge, UK). Skimmed milk protein, (KPL Ltd, Gaithersburg, USA ). Reverse Osmosis (RO, Ultrapure) water (18 M  $M\Omega cm^{-1}$ ) was obtained from Milli-Q water system (Millipore Corp., Tokyo, Japan). Glassware and volumetric materials were of analytical grade.

ELISA tests were first developed using a micro well polystyrene plates, MaxiSorp® plates purchased from Fisher Scientific, Loughborough, UK. An incubator/shaker from Labsystem iEMS® was used for temperature control incubation. A Florostar® plate reader was used which was set at appropriate wavelengths, BMG, UK. Glassware and volumetric materials were of analytical grade. Pipettes and tips from Eppendorf®. The electrodes used in this project were the JD type designed by Cranfield University and fabricated using the facilities at DuPont (Bristol, UK). The gold working electrode was circular with a  $0.226 \text{ cm}^2$  planar area, a complementary carbon counter electrode and an Ag/AgCl reference electrode. The substrate material used is PET 125  $\mu\text{m}$  Autotype HT5. The carbon electrode has an approximate dried thickness of 7  $\mu\text{m}$ , while the gold and Ag/AgCl electrodes both have an approximate thickness of 18  $\mu\text{m}$ . The encapsulation of 5036 blue had an approximate thickness dried of 4  $\mu\text{m}$ . Inks used in the construction of the sensors are BQ221 carbon ink, BQ331 gold ink and the 5880 Ag/AgCl and are available from DuPont (Bristol, UK). Gold nanoparticles with a diameter ranges from 20-100 nm were purchased from BBInternational Ltd (Cardiff, UK). QCMA-1 system and QCMA-1 chips with dual chambers for simultaneous sample and reference evaluation were obtained from (Sierra Sensors GmbH, Hamburg, Germany). Emitech K 1050X plasma cleaner (EM Technologies, Kent, UK).

## **4.3 Methods**

### **4.3.1 Preliminary characterisation of the antibodies performance using an ELISA assay**

Experiments were conducted to evaluate the performance of different antibodies that were commercially available for troponin T in order to select the best performing combinations for use on the immunosensor.

#### **4.3.1.1 Selection of the coating antibody and the optimal concentration on the ELISA platform**

Two antibodies, mouse anti human cardiac troponin t variables 9g6 and 1c11 were chosen as potential coating antibodies. These were investigated for their performance to identify the best working concentration to apply in the assay. In order to do that, a new ELISA plate was air bushed with nitrogen to clean it and then labelled and coated with various concentrations of the capture antibodies (2, 4, 6, 8, 10, 12  $\mu\text{g mL}^{-1}$ ) to be investigated. A 100  $\mu\text{L}$  of the antibody solutions dissolved in 0.05 M carbonate-bicarbonate buffer pH 9.6 were then deposited in triplicate (for each antibody type and concentration), and allowed to incubate overnight at 4 °C. The Plate was then gently washed with phosphate buffer saline plus 0.05 % Tween 20 (PBS-T) three times and dried by inverting and blotting the plate on paper towel. The wells were then blocked for 60 minutes at 37 °C with 300  $\mu\text{L}$  of 1:10 dilution of milk protein (KPL Ltd., UK) in PBS. The Plates were washed and standard concentrations of the antigen (100  $\mu\text{L}$  of 0, 10, 50, 100  $\text{ng mL}^{-1}$  of cTnT) were added to the wells and it was incubated for 1 h at 37 °C. The Plate was then washed again and a HRP conjugated mouse monoclonal anti human cTnT (7E7) was added (100  $\mu\text{L}$  of 5  $\mu\text{g mL}^{-1}$ , in PBS with 1:40 skimmed milk) was added to the plate and incubated for 1 hour at 37 °C. The plate was finally washed six times and a 100  $\mu\text{L}$  solution of TMB based chromogenic substrate was added and incubated for 30 min before the reaction is stopped by 100  $\mu\text{L}$  1 N sulphuric acid solution.

#### **4.3.1.2 Selection of the detection antibody concentration on the ELISA platform**

Having realised that the 1C11 was a superior coating antibody, a working concentration of  $10\text{ }\mu\text{g mL}^{-1}$  was used for coating in an attempt to investigating a suitable detection antibody concentration. A  $100\text{ }\mu\text{L}$  solution of  $10\text{ }\mu\text{g mL}^{-1}$  antibody (1c11) solution dissolved in  $0.05\text{ M}$  carbonate-bicarbonate buffer pH 9.6 were deposited in microwells of a cleaned plate and allowed to incubate for 2h at  $37^{\circ}\text{C}$ . The plate was then gently washed with phosphate buffer saline plus 0.05% Tween 20 (PBS-T) for three times and dried by inverting and blotting on paper towel. The plates were then blocked for 60 minutes at  $37^{\circ}\text{C}$  with  $300\text{ }\mu\text{L}$  of 1:10 dilution of skimmed milk in PBS. The Plates were then washed in similar manner as described above and standard concentrations of the antigen ( $100\text{ }\mu\text{L}$  of 0, 50,  $100\text{ ng mL}^{-1}$  of human cardiac troponin t), were added to different wells and the plate was incubated for 1 h at  $37^{\circ}\text{C}$ . The plate was then washed again and several solutions of different concentrations of HRP conjugated mouse monoclonal anti human cardiac troponin antibody (7E7) were added ( $100\text{ }\mu\text{L}$  of 5, 7, 10,  $12\text{ }\mu\text{g mL}^{-1}$ ) to the plate and incubated for 1 hour at  $37^{\circ}\text{C}$ . The plate was finally washed six times and a  $100\text{ }\mu\text{L}$  solution of TMB based chromogenic substrate was added and incubated for 30 min before the reaction is stopped by  $100\text{ }\mu\text{L}$  1 N sulphuric acid solution.

#### **4.3.1.3 Standard curve for the cardiac troponin Assay on the ELISA platform**

Taking into account the best conditions in the investigations for the optimisation of the ELISA assay a protocol was devised that was used for determining the final standard curve. In this final protocol,  $100\text{ }\mu\text{L}$  of the optimised capture antibody concentration of  $10\text{ }\mu\text{g mL}^{-1}$  of mouse monoclonal anti human cardiac troponin t (1c11) antibody was used for coating and allowed to incubate for 2 h at  $37^{\circ}\text{C}$ . The plate was then gently washed three times with Phosphate Buffer Saline plus 0.05% Tween 20 (PBS-T) and dried by inverting and blotting on paper towel. The plates were then blocked for 60 minutes at  $37^{\circ}\text{C}$  with  $300\text{ }\mu\text{L}$  of 1:10 dilution of skimmed milk in PBS. The plates were then washed and dried again, standard concentrations of the antigen human cardiac troponin T ( $100\text{ }\mu\text{L}$  of 0, 1, 5, 10, 20, 30, 50,  $100\text{ ng}$

mL<sup>-1</sup>) were added to the microwells, and it was incubated for 1 h at 37 °C. The Plate was then washed again and 200 µL of 7 µg mL<sup>-1</sup> HRP conjugated mouse monoclonal anti human cardiac troponin t (7E7) antibody was added to the plate and incubated for 1 hour at 37 °C. The plate was finally washed three times and a 100 µL solution of TMB based chromogenic substrate was added and incubated for 30 min before the reaction is stopped by 100 µL of 1 N sulphuric acid solution. The curves were fitted using a four-parameter curve fitting described in Chapter 3.3.8.

### **4.3.2 Method of Optimising the Cardiac Troponin T Assay on the Gold Electrodes**

The immunoassay for cardiac troponin T was then optimised on the electrodes surface. This was done in order to select the optimal concentrations of the assay reagents for sensor development. Experiments conducted on ELISA platform were limited to validate functionality of the reagents. The method used for the optimisation of assay on the gold electrodes was adapted from previous work conducted to develop a biosensor for Salmonella detection (Salam and Tothill, 2009) which has been mentioned earlier in Chapter 3. Antibody immobilisation on gold working electrode with the passive absorption method was followed here and it was this procedure which was optimised first to achieve the best concentration of the capture antibody to use for coating the sensor surface. Experiments were conducted for the optimisation of both bare and 11-MUA modified working electrodes. Finally the conjugated gold nanoparticles were investigated.

#### **4.3.2.1 Optimisation of the coating and detection antibody**

The JD electrode strips were first baked at a temperature of 120 °C for 30 minutes, washed and rinsed with distilled water to remove any particle contamination. The working electrode was then coated with a drop of 10 µL of mouse monoclonal anti cTnT (1C11) dissolved in 0.05 M carbonate-bicarbonate buffer pH 9.6. Different concentrations of the coating antibody (10, 30, 60, 90, 120 µg mL<sup>-1</sup>) were deposited in triplicates and allowed to incubate overnight at 4 °C. The electrodes surface were

then gently washed with Phosphate Buffer Saline with 0.05% Tween 20 (PBS-T), two times, rinsed with distilled water and air-dried with nitrogen. The working electrodes surface was then blocked for 30 minutes at 37 °C. The blocking solution was a 1:10 skimmed milk dilution in PBS. The electrodes were then washed in similar manner as described above. A standard concentration of the antigen was premixed with the detection antibody to give a mixture comprising of a 50 ng mL<sup>-1</sup> antigen concentration and 50 µg mL<sup>-1</sup> of conjugated mouse monoclonal anti human cardiac troponin T antibody. The mixture was incubated to premix for 1h on a rotter away from sunlight. It was then added on top of the the blocked electrodes and incubated for 1hr at 37°C. The electrodes were then connected to an edge connector, which is connected with a Palmsens® portable electrochemical analyser (Palm instruments BV, Houten, Netherlands. All measurements were performed by adding 100 µL of 4 mM TMB and 0.06% H<sub>2</sub>O<sub>2</sub> in 0.05 M citrate phosphate buffer plus 0.1 M KCL combined in a 1:1 ratio, with chronoamperometry at -200 mV constant current and run for 100 to 200 s. Similarly, the same was done for the optimisation of the conjugated detection antibody. A reverse approach was done where the capture antibody was chosen to remain constant at 90 µg mL<sup>-1</sup> and the antigen remained at 50 ng mL<sup>-1</sup> in mixture with a variable detection antibody concentrations (30, 60, 90, 120 µg mL<sup>-1</sup>).

#### **4.3.3 The use of self-assembled monolayers (SAMs) for capture antibody immobilisation**

Self-assembled monolayer was used to functionalise the gold working electrodes using 11-mercaptoundecanoic acid (11-MUA) .The procedure used in chapter 3 was modified in order to counteract on the performance limitations caused by the solvents on the Ag/AgCl and the rest of the sensor. The major change was the controlled administration of the solvent on to the sensor surface, and an increase in the concentration of the 11-MUA to compensate for the smaller volumes that were being used. A retrospective comparison of the two methods showed that the modified method described here performed much better than the previously described method in Chapter 3.

In the new procedure, the electrodes were baked in an oven for 120 °C for 30 min before being plasma cleaned with the gold facing up in oxygen free nitrogen for 2.5 minutes (Emitech K 1050X, EM Technologies, Kent, UK ). After this, the working electrode was washed with deionized water and coated with 2 x 50 $\mu$ L of 4mM 11-MUA placed three hours apart in an overnight incubation step at 4 °C in darkness. This allowed the 11-MUA to form a self-assembled monolayer on the sensor surface. It is important to prevent rapid evaporation of the ethanol on the 11-MUA solution.

After making, the 11-MUA modified working electrode using the procedure described above, it was validated using the methods described earlier in Chapter 3.3.8. The cyclic voltammetry of the surface modified electrodes was conducted by placing 100  $\mu$ L of solution (1 mM potassium ferricyanide  $K_3[Fe(CN)_6]$  in 0.1 M KCl) on the electrode surface. The electrochemical behaviour of potassium ferricyanide was measured using cyclic voltammetry at 50 mVs<sup>-1</sup>. Measurements were obtained by scanning 5 cycles from -0.5 to 0.8 V relative to Ag/AgCl reference electrode using a multi-channel AUTOLAB electrochemical instrument. The contact angle measurements were also taken by drying a bare and a modified electrode with a nitrogen gun and mounting them on the stage of a CAM 100 Optical Contact Angle Meter, before applying a drop of Millipore water to the surface of the working electrode. The contact angle was analysed using the CAM 100 software and the average contact angle was calculated.

#### **4.3.4 The use of gold nanoparticles in signal enhancement**

To improve the detection limit of the sandwich immunoassay, the use of gold nanoparticles was employed. Gold nanoparticles can act as a carrier of specific detection antibody and significantly higher amounts of peroxidase enzymes (Ansari *et al.*, 2010). The higher enzyme label in the assay will accelerate the rate of reaction where small antigen concentration exist in the sample and thus increase the assay sensitivity (Saha *et al.*, 2012).



#### **4.3.4.1 Conjugation of Gold Nanoparticles with Antibodies and HRP**

Gold nano- particles with average diameter of approximately 60 nm were purchased from (BBInternational, Cardiff, UK). The colloidal gold solution was stored at 4°C in the dark, as they were stored in distilled water they were used directly without any pre-treatment. The particle size of colloidal gold was  $60 \pm 4.2$  nm and the number of particle is about  $6.2 \times 10^{11}$  particles  $\text{mL}^{-1}$ . The antibody- colloid gold conjugate was prepared according to the procedure described by (Liu *et al.*, 2010). In this experiment, gold nano-particles were conjugated with horse radish peroxidase (HRP) and anti cTnT 7E7 (unconjugated). Two eppendorfs were each filled with 1 mL of gold nanoparticles solution and 5  $\mu\text{L}$  of 0.2 M NaOH was added in each vial before gently mixing well. A 10  $\mu\text{L}$  solution of  $1\text{mg mL}^{-1}$  HRP in water was then added to each eppendorf vial and incubated at 22°C for 60 minutes on a Stuart SB3 rotator (Appleton Woods, Birmingham, UK) with the rotator at a 10° inclination angle. After this a 5  $\mu\text{L}$  solution of  $2\text{mg mL}^{-1}$  of detection antibody mouse monoclonal anti human cTnT 7E7 and incubate for 20 min on the rotor. The two eppendorfs were then centrifuged at 4°C for 25 minutes at 8000 rpm using the Heraeus Fresco 21 centrifuge system, (Loughborough, UK). After extraction of the supernatant from the eppendorfs, the pellet was then re-suspended in a 3:1 with 0.05% PBS-Tween 20, concentrated milk blocking diluents solution to obtain a total volume of 100  $\mu\text{L}$ .

#### **4.3.4.2 Quality control of conjugated Gold Nano particles**

To check if the conjugation was successful, 20  $\mu\text{L}$  of 2.5M NaCl was added to 200  $\mu\text{L}$  solution of 1 in 10 diluted modified gold colloid solution and checked for flocculation. If flocculation occurs, it indicates the modification is not successful and will need to be repeated (Saha *et al.*, 2012). The concentration of the remaining gold nanoparticles after the conjugation procedure can be estimated by measuring the absorbance of the modified gold colloid solution and by comparing it with the standard concentration, which has known amounts of the nanoparticles.

### 4.3.5 The use of Quartz Crystal Microbalance to Investigate the Attachment of the Gold Nano particles to the Detection Antibodies

In this work, the fully automated QCMA-1 system (Sierra Sensors GmbH, Hamburg, Germany) was used to validate antibody conjugation to gold nanoparticles through detecting cTnT using conjugated and unconjugated antibodies. An optimised cardiac troponin t assay described by Vanheusden (2011) was used. A dilutions series of cTnT in PBS containing 10% concentrated milk blocking proteins was made to have a final concentration range between 1 and 100 ng mL<sup>-1</sup>. Dilution series were stored at 4 °C and thawed immediately before use. A volume of 250 µl of the different cTnT concentrations were applied to both spots of the coated sensor chip. A sandwich immunoassay was performed by adding 200 µL of a 20 µg mL<sup>-1</sup> detection antibody solution or a solution of the gold nanoparticles coated with detection antibody to the bound cTnT. The frequency shift was measured using the QCMA-1 analyser software. The surface of the sensor chip was regenerated after each concentration with a short washing step with 0.1 M HCl. After the last concentration, the sensor chip regenerated again using a 20 mM NaOH solution.

#### 4.3.5.1 Preparation of QCMA-1 sensor chips

The QCM gold sensor chips were cleaned prior to coating by nitrogen plasma etching (Emitech K 1050X, EM Technologies, Kent, UK) at a power of 50 W with a bleed vacuum trip of  $3 \times 10^{-1}$  mbar and an ashing time of 1 minute. After this, the sensor chip surface was coated with an insulating layer of 11-MUA. This was done by immersing the chips with the gold surface up in a 2mM 11-MUA solution in pure ethanol overnight at 22 °C in darkness. Figure 4.2 shows the chemical structure of 11-MUA.

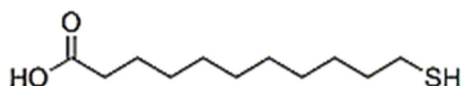


**Figure 4.2:** Chemical formula of 11-MUA (Sigma-Aldrich, 2012)

This allowed the 11-MUA to form a self-assembled monolayer on the sensor surface. Cyclic voltammetry (CV) was used to assess the extent of the coating. A chip was used as working electrode in a CV setup with an Ag/AgCl reference electrode and a carbon counter electrode. Analysis was performed by applying a 100  $\mu$ l volume of a 1 mM potassium ferricyanide on the working electrode and measuring the current produced by the redox reaction occurring after application of an external voltage sweep as described in Section 4.3.3.

#### 4.3.6 Immobilisation of the capture antibody on Modified surfaces of SPGE and QCM-1 chips.

Covalent coupling of the cTnT (1C11) antibodies on to the gold surface of both the QCMA-1 chips and the screen printed gold electrodes was facilitated by the free carboxylic group 11-MUA using an EDC:NHS protocol as described by Uludag (2010). The exact chemistry of the EDC:NHS interaction is described in other publications (Van Delden *et al.*, 1996). Figure 4.3 summarizes the chemistry used in the sensitization of the modified surfaces.

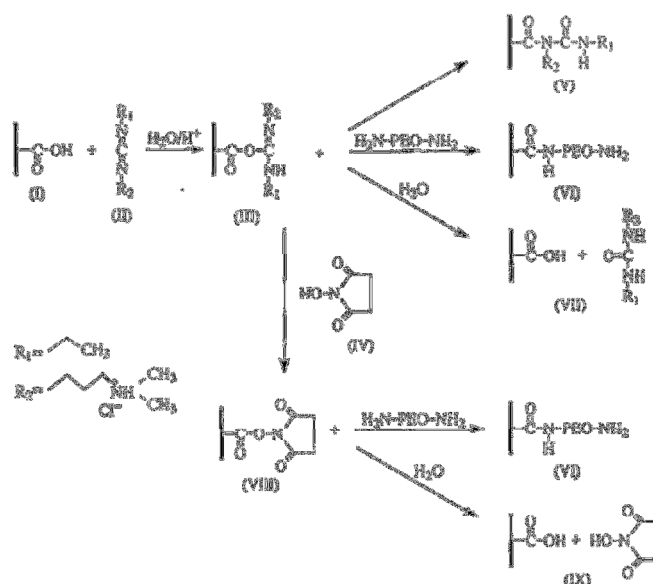


**Figure 4.3:** Schematic overview of the EDC:NHS coupling procedure. (I) is the Carboxylic end group attached to the (chip) surface, (II) is EDC, (III) is Oacylisourea, (IV) is NHS, (V) is N-acylisourea, (IV) is diamino-PEO coupled to the surface, (VII) is the hydrolysis reaction of O-acylisourea, (VII) is the NHS activated carboxylic group and (IX) is the hydrolysis of this activated group (Van Delden *et al.*, 1996).

In these experiments two solutions a 400 mM EDC and 100 mM NHS solution in deionized water were mixed in a 1:1 rate and applied to the surfaces immediately after mixing them. For the SPGE, the solution was applied by adding 30  $\mu\text{L}$  and incubating for 10 min, for the QCMA-1 system a total volume of 150 $\mu\text{L}$  was applied to pass through the sensor chip spots at a flow rate of 50 $\mu\text{L}$  per min. After this, a short washing step was performed with PBS buffer was performed for both methods. The next step was the attaching of the capture antibody. On the SPGE, this was done by adding 20  $\mu\text{L}$  of 80  $\mu\text{g mL}^{-1}$  1c11 anti human cardiac troponin t antibody on the working electrode and incubating for 2 hrs at 37 °C in a humid environment control chips were coated with anti-ochratoxin A antibody in the same conditions.

For the QCM-1 chips since each chip contained two measurement spots, the cTnT specific antibody was attached to the active spot and an antibody non-specific for cTnT (anti-ochratoxin A) was attached to the control spot. The optimum concentrations of these antibodies were provided by the method developed (Van Heusden, 2011). In this method 30  $\mu\text{g mL}^{-1}$  and 10  $\mu\text{g mL}^{-1}$  of appropriate antibodies dissolved in sodium acetate buffer with 1% concentrated milk blocking diluents (KPL, Wembley Middlesex, UK) for the active and control, respectively. For both methods, the next step is washing off excess antibodies and blocking twice. First the free space on both spots was covered using 10% milk blocking proteins dissolved in PBS. Lastly, non-reacted EDC:NHS molecules were covered by a 1M ethanol amine solution.

#### **4.3.7 SPGE Optimised immunosensor protocol**

The optimised cardiac troponin t assay on screen-printed gold electrodes was based on the immuno assay that used gold nanoparticles. This assay consists of several steps that include the modification of the working electrode as described in Section 4.3.3 and the sensitisation and coating of the working electrode as described in section 4.3.6. The optimum coating antibody concentration was found to be (60  $\mu\text{g mL}^{-1}$  of 1C11) and this was incubated for 2 h at 37 °C in a humid environment. During

blocking, appropriate mixtures of the antigen and the conjugated gold nanoparticle solutions are made to premix for 1 h in a gently spinning rotor. The conjugated gold nanoparticles (60nm) are diluted to a ratio of 1:10 in antigen solutions. It is essential that the working concentrations of both the antigen and the gold nanoparticles be uncompromised through dilution. After the excess blocking solution had been washed and the electrodes have been dried, 20  $\mu\text{L}$  of the mixture of gold nanoparticles and the antigen standard were deposited on the electrodes and they are incubated for a further 1 h. The electrodes were then washed and connected to an edge connector, which is connected with a multi-channel AUTOLAB electrochemical instrument.

#### **4.3.8 Detection of cTnT in commercial serum**

A standard curve was plotted using standards with 75% commercial serum spiked with appropriate cardiac troponin t (cTnT). Thus was done to synchronise the standard curve with the same level of interference that would be in the spiked serum samples that were intended to be analysed and their cTnT concentrations interpolated using the curve. Although in an ideal world standard curve generated in whole serum would be desirable, In this case the sensitivity of the assay was severely compromised by interfering proteins and a compromise of 75% spiked serum was reached basing on the recommendations of work by department colleagues (Uludag and Tothill, 2010).

In this experiment, commercialised human serum samples (Sigma-Aldrich) were diluted with 25%v/v PBS-T with additives to give a 75% v/v serum solution. The additives (0.5 M NaCl, 200  $\mu\text{g mL}^{-1}$  BSA and 500  $\mu\text{g mL}^{-1}$  dextran) had been proven to help with lowering non-specific binding (Uludag and Tothill, 2010). The 75% serum solution was used to make standards as well as samples spiked with unknown concentrations of cTnT.

## 4.4 Results and Discussion

### 4.4.1 Preliminary microplate based studies

ELISA tests were developed on the microplate in order to investigate the best antibody combinations as well as their performance for troponin t detection. A standard curve was done to show the basic performance of the cTnT assay on a micro plate.

#### 4.4.1.1 Antibody combinations and coating antibody concentrations

In order to investigate the optimal antibody combinations for the ELISA assay as well as the working concentration of the coating antibody. A generic ELISA protocol as described in Section 4.3.1.1 was conducted. The results obtained are shown in Figure 4.4, and these indicate that the antibody combinations of the 1C11 and 7E7 gave better responses compared to those of 7E7 and 9g6. This different performance can be attributed to two factors that are antigenic affinity and the proximity of the epitopes on the antigen surface responsible for the generation of the antibodies (both detection and coating). There is a possibility that there may be superior antigenic affinity of the 1C11 coating antibody as compared to the 9g6, this will result in higher numbers of the antigen forming stronger bonds with the 1C11 antibody that in turn is expressed as higher signal when the detection antibody is used. Another explanation could be that there could be close proximity between the epitopes responsible for the generation of the antibodies 9g6 (coating) and 7E7 (detection). Monoclonal antibodies made from epitopes in close proximity can have an inhibitory effect when associating with the antigen (Law, 1996; Wild, 2000). This is because that the first antibody to associate with the antigen (in this case the coating antibody 9g6) may provide a physical barrier for other antibodies for example those used for detection (7E7) to access their binding site on the antigen (Dickason *et al.*, 1994; Law, 1996). The results of this experiment also showed that there was an increase in signal with increasing concentration of the coating antibody. A  $10 \mu\text{g mL}^{-1}$  coating concentration for the micro plate based ELISA assay was chosen as the optimum. This is because it gave a high proportional yield competently achieved the requirements of the assay, without compromising on costs. The antibody

combination of 1c11 and 7E7 were chosen to be used for further experiments and a coating concentration of  $10 \mu\text{g mL}^{-1}$ .

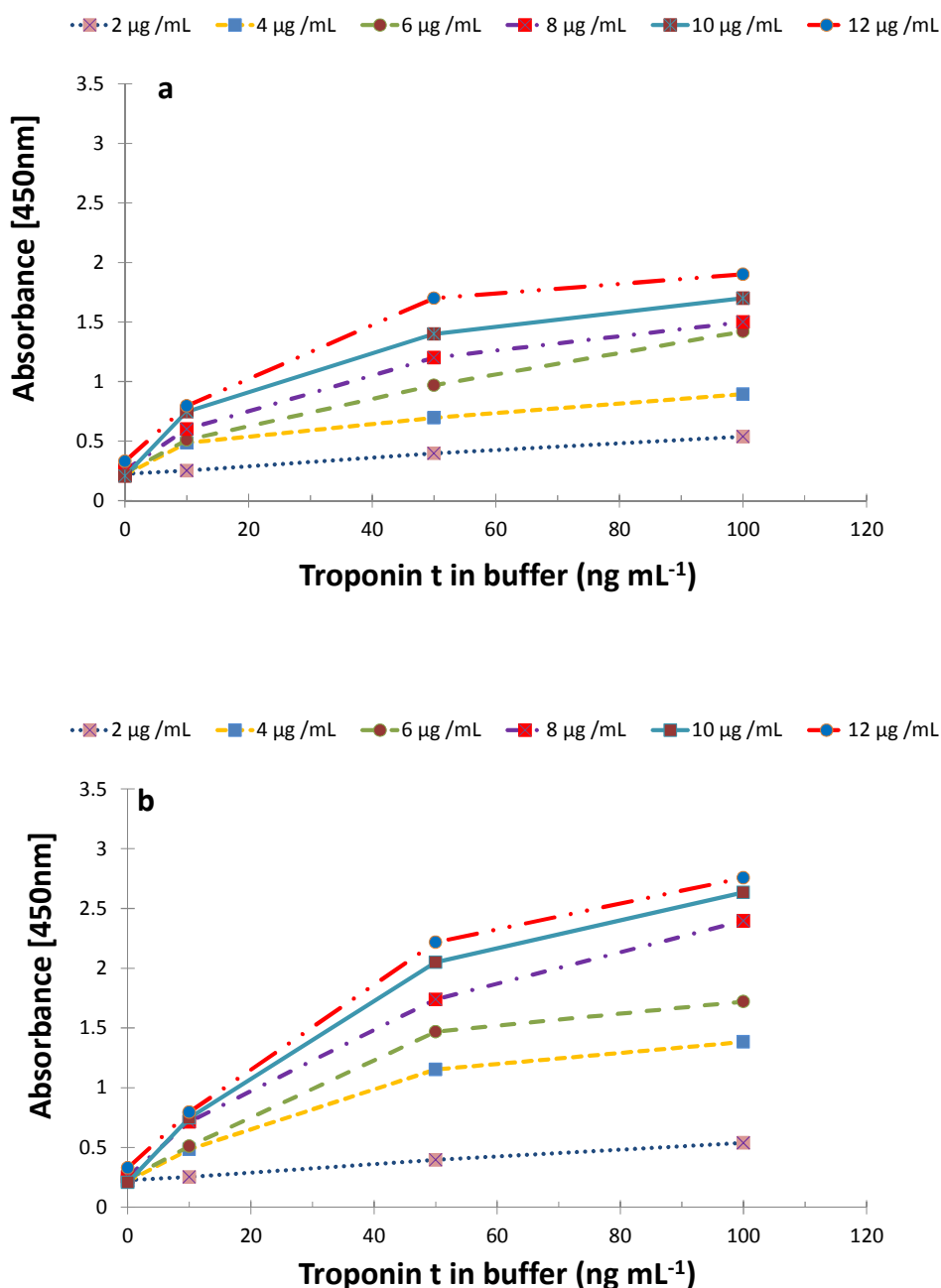


**Figure 4.4:** Micro plate based ELISA assay for selecting the best antibody and working concentration for cTnT sandwich assay, (a) plates coated with anti-cardiac troponin 9g6 and (b) plates coated with 1c11. In both assays 100  $\mu\text{L}$  of various concentrations of coating antibody used and assayed against 100  $\mu\text{L}$  of antigen concentrations (0, 10, 50, 100  $\text{ng mL}^{-1}$ ) with a detection antibody (200  $\mu\text{L}$  of 5  $\mu\text{g mL}^{-1}$ )  $n=3$ , maximum CV= 4.3%.

#### 4.4.1.2 Detection antibody concentrations

After selecting the coating antibody to be 1c11 and choosing its concentration to be  $10 \mu\text{g mL}^{-1}$  the next challenge was to optimise the detection antibody. A microplate was coated with coating antibody ( $100 \mu\text{L}$  of  $10 \mu\text{g mL}^{-1}$  1c11) and assayed with standard concentration of cTnT ( $0, 10, 50, 100 \text{ ng mL}^{-1}$ ) and four concentrations of detection antibody 7E7 were investigated ( $5, 7, 10, 12 \mu\text{g mL}^{-1}$ ). The results obtained are shown in Figure 4.5

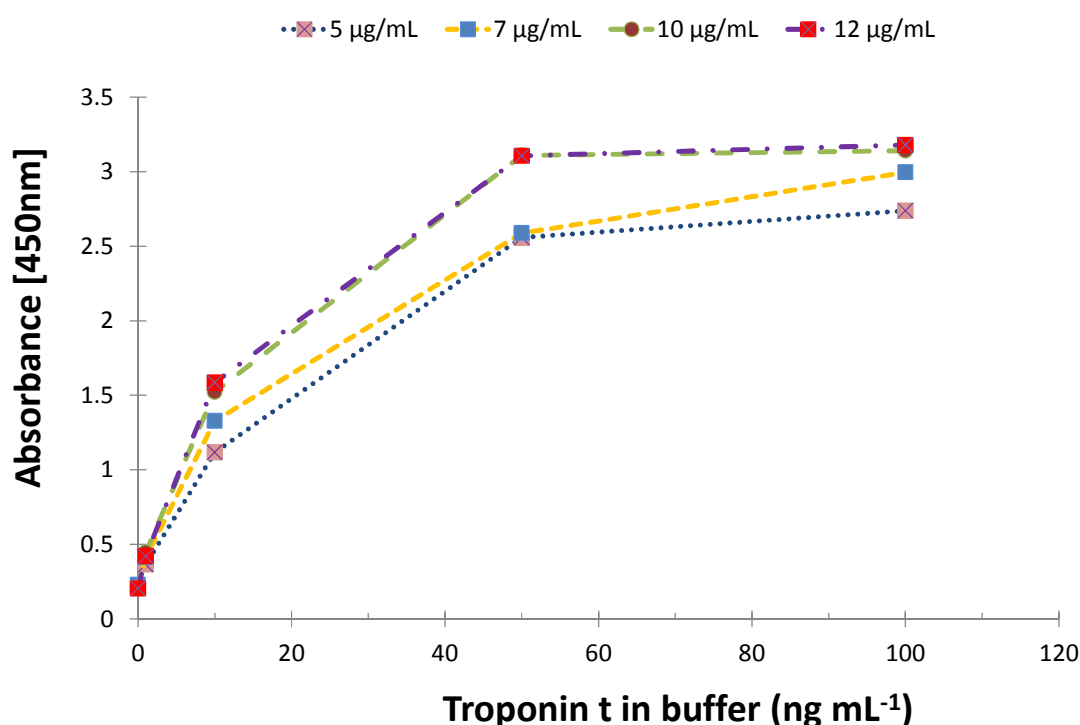


**Figure 4.5:** The effect of increasing the concentration of detection antibody on the signal, varying concentrations of the detection antibody were assayed against standards after coating the plate with ( $200 \mu\text{L}$  of  $10 \mu\text{g mL}^{-1}$ ) of HRP conjugated anti-cTnT (1c11),  $n=3$ , maximum CV= 3.8%.



The results show that increasing signal was achieved with increasing detection antibody concentration. This relationship was shown to cease at  $10 \mu\text{g mL}^{-1}$  where further increases in HRP conjugated 7E7 anti cTnT antibody, did not yield any significant enhancement of the signal. A concentration of  $10 \mu\text{g mL}^{-1}$  was adopted to be suitable for the microplate assay.

#### 4.4.1.3 Standard curve of cTnT on micro plate assay

After optimising the reagents concentrations of the ELISA assay, a standard curve for cTnT was plotted using the optimised conditions.

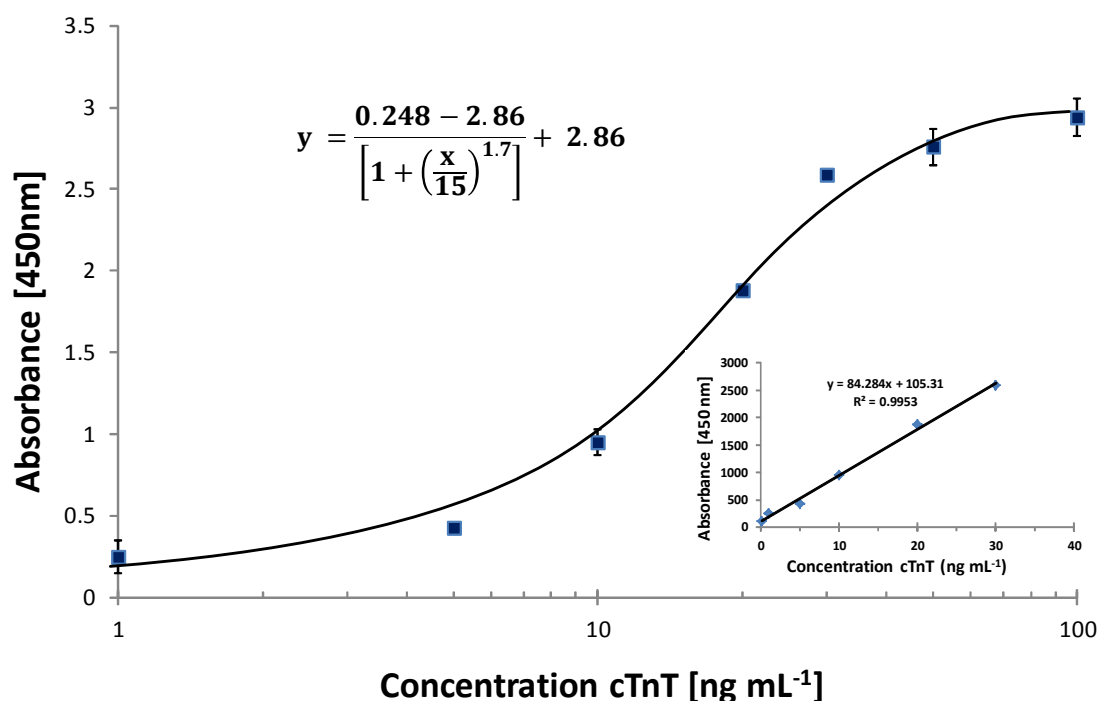


**Figure 4.6:** Logarithmic scale of the optimised micro plate assay, (Inset) a liner plot of the same curve. Plates were coated with 100  $\mu\text{L}$  of  $10 \mu\text{g mL}^{-1}$  of 1c11 and assayed with cTnT serially diluted standard in buffer. The detection antibody was HRP conjugated anti cTnT antibody 7E7 ( $100 \mu\text{L}$  of  $10 \mu\text{g mL}^{-1}$ ).  $n=3$ , maximum, barrs=standard deviation,  $\text{CV}=4.7\%$ .

The assay had a lower limit of detection L.O.D of  $2.2 \text{ ng mL}^{-1}$ , which higher than the baseline values of cTnT which are  $< 0.03 \text{ ng mL}^{-1}$  (Licka *et al.*, 2002; Babuin L, 2005). Further optimisation of the assay parameters may result in better detection limit. However, since the aim is to develop an immunosensor, it was decided to move the assay to screen- printed electrodes as these were known to give higher sensitivity than ELISA tests (Tothill, 2009).

#### **4.4.2 Development of the screen printed immunosensor for cardiac Troponin T**

This section describes work that was done to develop an immunosensor for cardiac Troponin T based on screen-printed electrodes. The first optimisation was done on the bare electrodes and the next step utilised the surface modification of the working electrode using self-assembled monolayers SAMs. An enhanced alternative procedure for application of SAMs on working electrodes, which does not interfere with the electrodes in a manner described in Chapter 3 is offered. The final step of the optimisation involved the use of both SAMs and gold nanoparticles on the immunosensors. Gold nanoparticles were responsible for enhancing the signal output and thus increasing on the sensitivity of the immunosensor.

##### **4.4.2.1 Optimisation of the coating and detection antibodies on the bare electrodes**

The concentration of the antibodies both coating and detection play a major role in the functionality of the immunosensor. In an attempt to find the optimum concentrations for use on this version of the immunosensor , different concentrations of were used in the assays on the sensor surface. The results of the experiments are shown in Figure 4.7. The results show that there was rising signal with increasing concentration of the coating antibody. This rise in signal however curtailed and lost gradient after the  $90 \text{ ng mL}^{-1}$  and there was no significant changes with higher concentrations in the coating antibody. The best coating antibody on the bare electrode was thus shown to be  $90 \text{ } \mu\text{g mL}^{-1}$ . The detection antibody showed a similar

trend that only that the optimum was at  $60 \mu\text{g mL}^{-1}$ . The results showed that although there was still an increase in signal with increased detection antibody after  $60 \mu\text{g mL}^{-1}$ , the increase in signal output was limited and not justify the use of higher amount of antibodies.

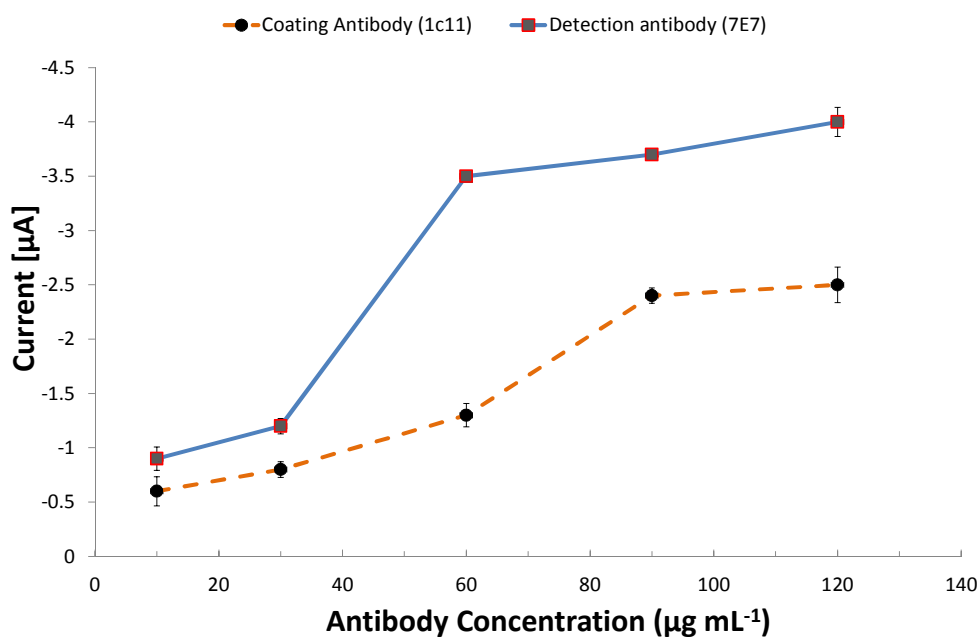


**Figure 4.7:** The optimisation of the coating and detection antibody for cTnT assay on bare screen-printed gold electrodes. A  $10 \mu\text{L}$  of different concentrations of anti cTnT 1C11 coating antibody were immobilised on the gold working electrode. It was assayed with standard concentration of the cTnT antigen premixed with the detection antibody. A reverse approach was applied for investigating the detection antibody  $n=3$ , maximum CV=6.2%, error bars= standard deviation.

The optimised parameters of coating antibody ( $90 \mu\text{g mL}^{-1}$  of 1C11) and detection antibody ( $60 \mu\text{g mL}^{-1}$  of 7E7) were used next to prepare a standard curve for the optimised assay. The standard curve obtained is shown in Figure 4.8.

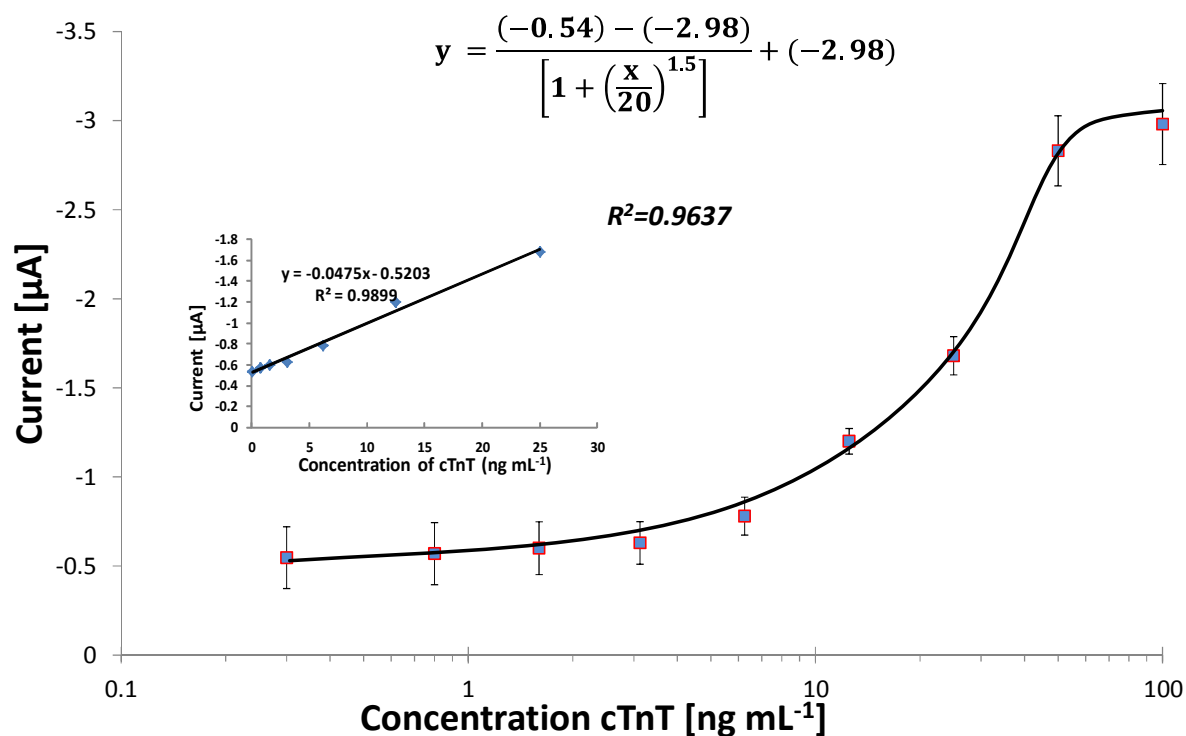


**Figure 4.8:** Logarithmic scale of the immunosensor with no surface modifications, (Inset) a liner plot of the same curve. Bare working electrodes of SPGEs were coated and assayed with cTnT serially diluted standards in buffer. LoD  $2.12 \text{ ng mL}^{-1}$ ,  $n=3$ , maximum CV=10.9%, bars=standard deviation

The standard curve for the cTnT using this immunosensor format had a lower limit of detection of  $2.12 \text{ ng mL}^{-1}$ . This was higher and much further from the detecting baseline values of below  $0.03 \text{ ng mL}^{-1}$  as required. The results showed that there was need to continue improving the immuno sensor and thus further optimisation such as the use of self-assembled monolayers was incorporated in the next immunosensor design.

#### **4.4.3 Exploring the use of self-assembled monolayers to enhance assay sensitivity through covalent immobilisation**

As discussed earlier, self-assembled monolayers SAMs play a crucial role in the immobilization and orientation of the antibody on the transducer surface like gold and has become another focus of study in the biosensor field (Hao *et al.*, 2009). There are a variety of SAMs available but in this study the monolayers were made using 11-mercaptoundecanoic acid (11-MUA). This is because the stability of the SAM has been linked to the size of the carbon spacer and the longer the chain the more stable the SAM is (Love *et al.*, 2005). For this reason larger molecules like 11-mercaptoundecanoic acid (11-MUA) have been favourites for the making of SAMs functionalised surfaces for sensor application (Chaki and Vijayamohanan, 2002).

The screen printed electrode surfaces were modified by first baking the electrodes in an oven for 120 °C for 30 min, followed by plasma cleaning them in oxygen free nitrogen at 50w for 2.5 minutes (Emitech K 1050X, EM Technologies, Kent, UK). The power settings were 50 W with a bleed vacuum trip of  $3 \times 10^{-1}$  mbar and an ashing time of 1 minute. After this, the working electrode was washed with deionized water before being coated with 2 x 50 $\mu$ L of 4mM 11-MUA in an overnight incubation step at 4°C in darkness. After making, the 11-MUA modified working electrode using this procedure the surfaces were validated using cyclic voltammetry. This was done by placing 100  $\mu$ L of solution (1 mM potassium ferricyanide  $K_3[Fe(CN)_6]$ , 0.1 M KCl) on the electrode surface. The electrochemical behaviour of potassium ferricyanide was measured using cyclic voltammetry at 50 mVs<sup>-1</sup>, measurements were obtained by scanning 5 cycles from -0.5 to 0.8 V relative to Ag/AgCl reference electrode using a multi-channel AUTOLAB electrochemical instrument. The obtained results are shown in Figure 4.9.

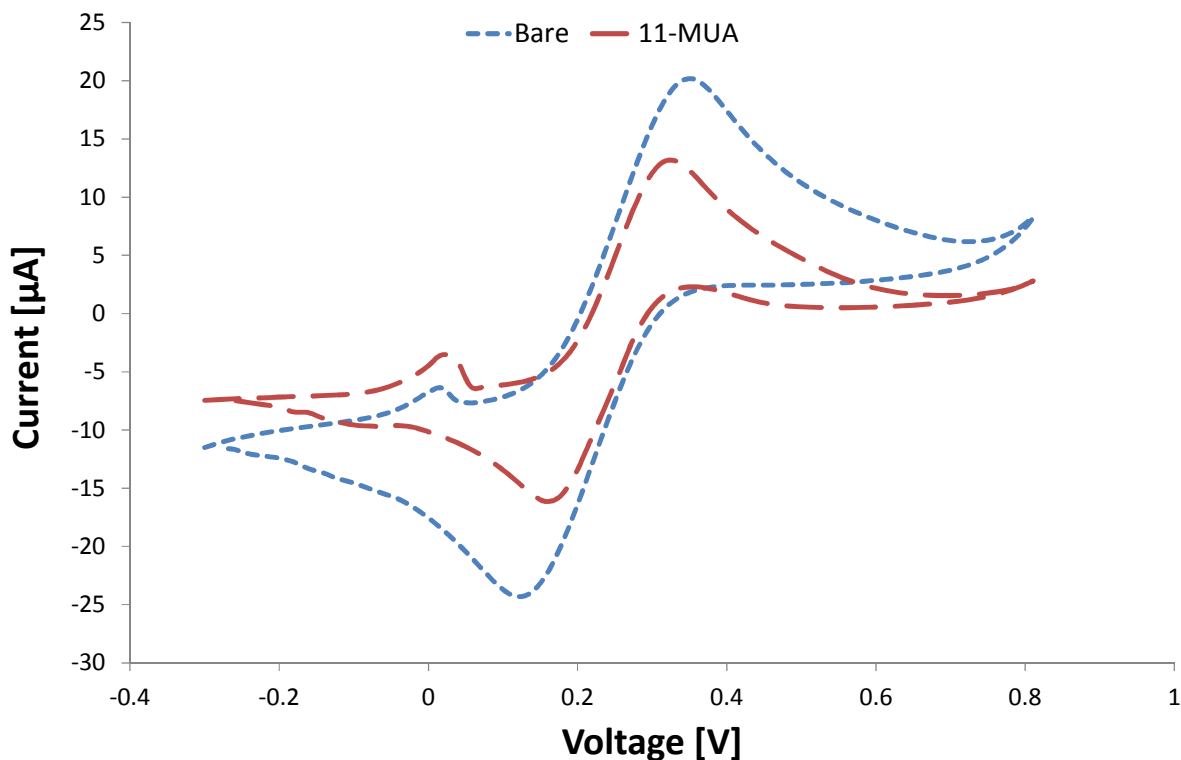


**Figure 4.9:** Cyclic voltammetry for validating the deposition and formation of Self assembled monolayers by 11-MUA. 5 scans of cyclic voltammetry were done using 1 mM potassium ferricyanide  $K_3[Fe(CN)_6]$ , 0.1 M KCl at  $50 \text{ mV S}^{-1}$  scan rate. The zero current on 11-MUA coated chips signifies insulation due to the successful formation of the monolayer.

There were changes to the experimental procedure, from that described in Chapter 3, for the method for making the 11-MUA SAM on the working electrode and the new method had improved conductivity. As discussed in Chapter 3, there was very limited conductivity on the modified surfaces. The cyclic voltamograms of the 11-MUA modified electrodes when compared to that of the bare electrodes clearly showed this shortfall in conductivity. In this experiment, the voltamograms for the bare electrode showed the most conductivity, however the 11-MUA surface coated electrodes performed electrochemically better than those made using the previous method. The change in the method of making the monolayer improved the conductivity of the electrode which meant that the monolayer formation would not impede on the flow of electrons. This was shown by the relatively higher oxidation and reduction peaks on the SAM modified surface compared to those achieved in

Chapter 3. The contact angle measurements were done to confirm the formation of the monolayer and the results from their measurements are illustrated in Figure 4.10.

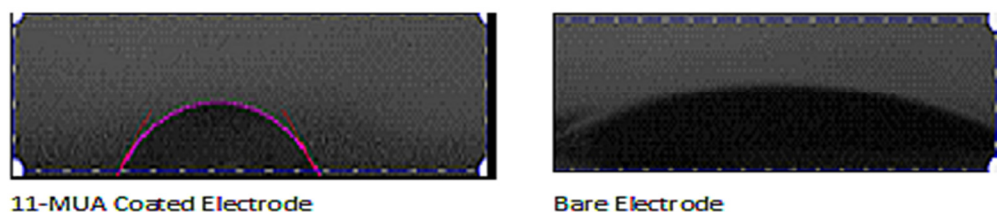


**Figure 4.10:** Pictures showing the distribution of 100  $\mu\text{L}$  drop of deionised water on (left) a 11-MUA coated Chip and (right) a bare electrode.

The difference in the contact angle between the surface and the liquid shows polarisation properties of the surfaces. The results showed decreased wettability on modified surfaces (left) compared to the bare electrode (right). This could be attributed to the increased lyophobicity of the surface by the use of SAMs surface. As discussed in Chapter 3, the monolayers of 11-MUA are capable of depolarising the gold surface thus making it more water repellent.

#### 4.4.3.1 Optimisation of the coating and detection antibodies on the 11-MUA modified electrodes

A similar procedure to that described in Section 4.3.6 was employed to investigate the detection and coating antibody for the immuno sensors that were coated with 11-MUA. The procedure consisted of a surface sensitisation step that employs the use of the EDC/NHS coupling chemistries. In the procedure, 400 mM EDC and 100 mM NHS solution in deionized water were mixed in a 1:1 rate and 30  $\mu\text{L}$  were applied to the surfaces immediately after mixing. Immobilisation of the coating antibody 1C11 the follows followed by two blocking steps one of 1M ethanolamine for blocking un occupied active groups and anther with 1:10 milk protein. The remainder of the procedure is standard as described in Section 4.4.2.1. The obtained results are shown in Figure 4.11.

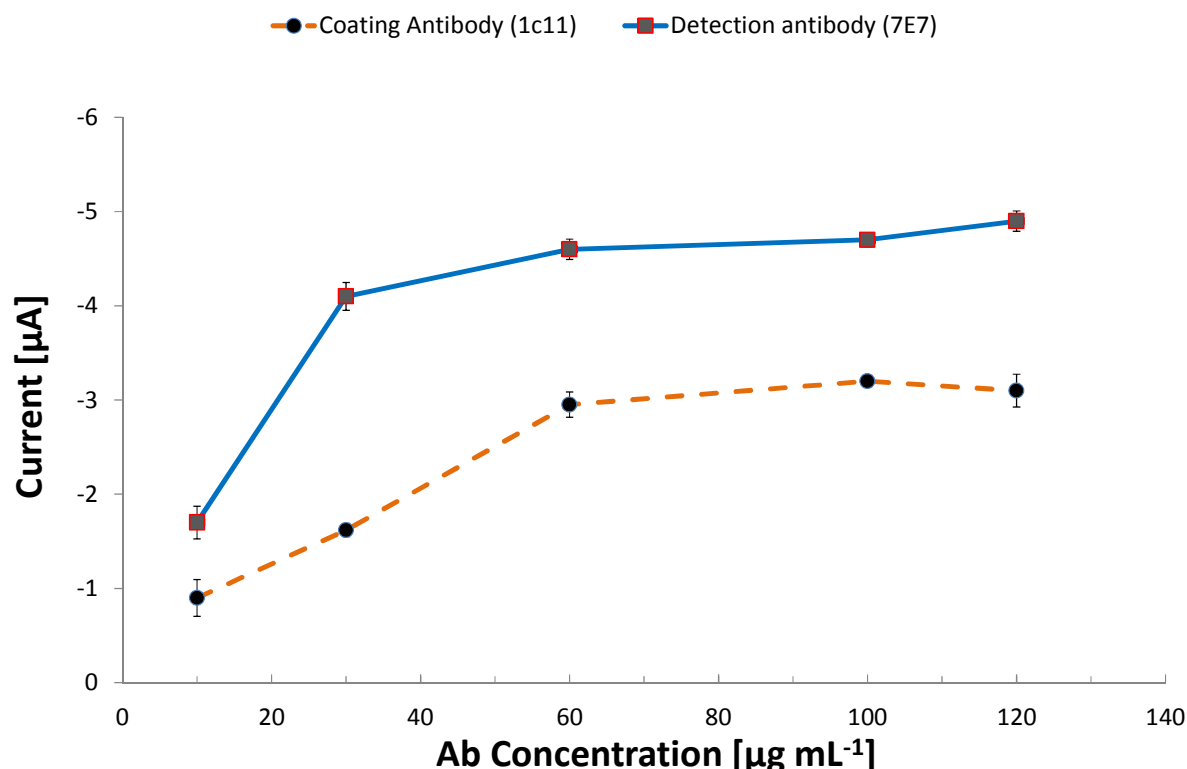


**Figure 4.11:** The optimisation of the coating and detection antibody for cTnT assay on 11-MUA modified screen-printed gold electrodes, electrodes were first sensitised with 30  $\mu\text{L}$  of EDC/NHS solution before the assay. Different concentrations of anti cTnT coating and detection antibodies were investigated,  $n=3$ ,  $\text{CV}=7.4\%$ , error bars= standard deviation.

The results showed the expected trend of increasing signal with increasing antibody concentrations. The peak antibody concentrations for the 11-MUA modified surfaces were less than for the bare electrodes. The optimum coating concentration was 60  $\mu\text{g mL}^{-1}$  and the detection antibody was 30  $\mu\text{g mL}^{-1}$ . These values were incorporated on to an assay and a standard curve was developed for the 11-MUA modified surface immunosensor for cTnT, this curve is shown in Figure 4.12.



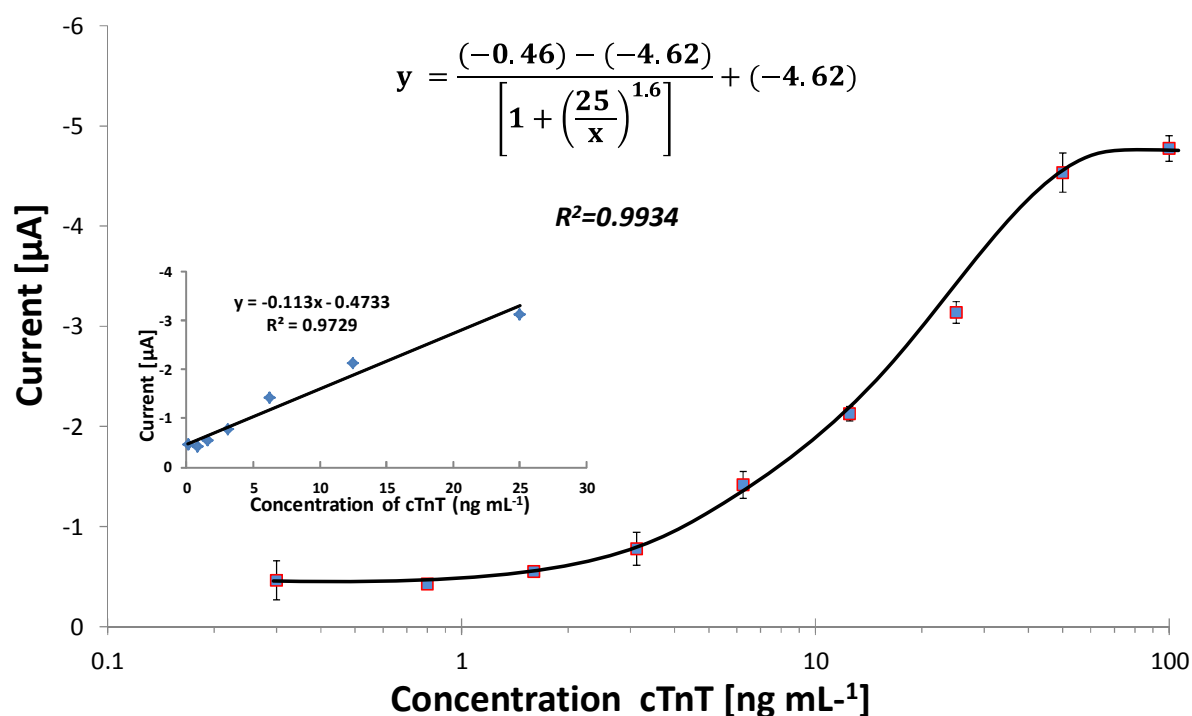


**Figure 4.12:** Logarithmic scale of the immunosensor with 11-MUA surface modifications, (Inset), a liner plot of the same curve. Working electrodes of SPGEs were sensitised with 30  $\mu\text{L}$  EDC/NHS and were then coated with 10  $\mu\text{L}$  of 60  $\mu\text{g mL}^{-1}$  of 1c11 and assayed with cTnT serially diluted standard in buffer premixed with detection antibody HRP conjugated anti cTnT antibody 7E7 (60  $\mu\text{g mL}^{-1}$ ),  $n=3$ , maximum CV= 9.8%.

The calibration plot generated showed better sensitivity than both the bare electrode based assay and the micro plate based ELISA assay. The maximum current output was higher than that of the comparable bare electrode immunosensor and the gradient of the linear slop was steeper which showed that there was improved sensitivity. It had a LOD of 1.14  $\text{ng mL}^{-1}$ . Although this was still higher than the baseline values for cTnT in healthy individuals, it was better than the previous assays. This showed the 11-MUA SAMs had a significant effect in improving the assay performance on the immunosensor. However, there was need to improve the assay further and thus the use of gold nanoparticles was employed in the next assay setup.

#### **4.4.4 Exploring the use of gold nano-particles to increase assay sensitivity through enhanced signal**

Gold nanoparticles (60 nm), were conjugated with horseradish peroxidase (HRP) and anti cTnT 7E7 antibody using a procedure described in Section 4.3.4.1. After making them, the success of the conjugation was confirmed by checking for flocculation after 20 µl of 2.5M NaCl was added to 200 µL solution of 1 in 10 diluted modified gold colloid solution. If flocculation occurs, it means the modification is not successful and will need to be repeated. However, this generic method does not give detail as to whether or not any antibody has been conjugated on to the gold nanoparticles. As it is impossible to visually see and quantify the success of the conjugation of the antibodies on the gold surfaces an automated biosensor based the Quartz Crystal Microbalances (QCMs) techniques for the detection of biomolecules. It is quicker than the conventional immuno assay and does not require a label. Gold nanoparticles were conjugated with detection antibody using a procedure described in Section 4.3.5 and QCM experiments were conducted to validate this conjugation. Figure 4.13 shows how the QCM was used to validate successful conjugation of the detection antibody on to the gold nanoparticles. This was done in the hope that comparing the performance of conjugated and unconjugated detection antibodies on immuno assays done of quartz crystals will ascertain any successful conjugations. The QCM-1 device used in this project is a biosensor capable of detecting low antigen concentrations. It could be used as an alternative technology for comparative studies to the electrochemical immunosensor that was being developed. Quartz Crystal Microbalance (QCM) is a special sensor that has acoustic impedance detector by mass loading, when an external voltage is applied to a quartz crystal the crystal starts oscillating at a specific frequency. This frequency changes when the crystal is loaded with extra mass (Freymuth and Sauebray, 1963; Uludag and Tothill, 2010). This relationship is shown by the Sauebray equation below.

$$\Delta f = \frac{1}{C_{QCM}} \Delta m$$

**Equation 3-1**

In this equation the frequency change ( $\Delta f$ ) is proportional to the mass ( $\Delta m$ ) of the adsorbed molecules per unit area. The  $C_{QCM}$  is the mass sensitivity and equal to  $V\rho/2f^2$  ( $f$  is the resonance frequency,  $V$  and  $\rho$  are the shear modulus and density of quartz, respectively (Freymuth and Sauebray, 1963). This equation was used to show the proportionality between mass and the shift in frequency at the crystal surface and in assays for cardiac troponin T before (Wong-ek *et al.*, 2010).

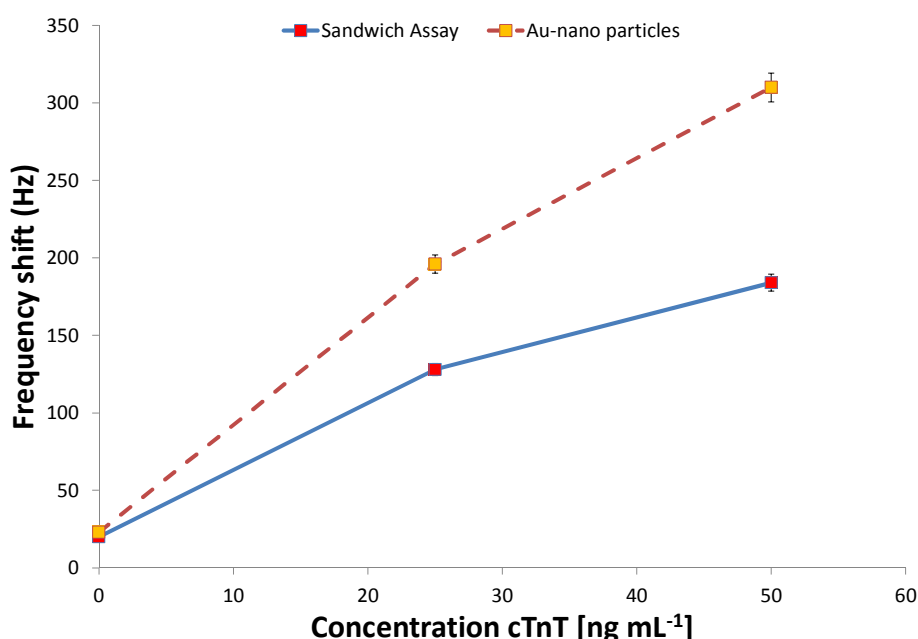


**Figure 4.13:** Effect of successful conjugated gold nanoparticles on the frequency shift. The chips were reacted with either 1:10 antibody conjugated gold nanoparticles solution or  $10 \mu\text{g mL}^{-1}$  of detection antibody solution. Method was adapted from work by (Van Heusden, 2011)  $n=3$ , maximum CV=6.9%.

There was high frequency shift on QCM assay with the use of gold nanoparticles compared to the basic sandwich assay shows that the antibodies were successfully conjugated to gold nanoparticles. After the successful conjugation of the gold nanoparticles had been proven, the next step was to investigate the optimum concentration of the conjugated gold nanoparticle for use in the immunosensor.

#### 4.4.4.1 Optimisation of the gold nano particles concentration

The optimisation of gold nanoparticles is different from other methods described earlier for the passive adsorption and 11-MUA assay setups that utilised HRP conjugated antibody for detection. This is because the precise amounts of HRP and antibody bound on the gold surface were unknown. These amounts vary with the degree of conjugation effectiveness and the surfaces that are presented by the nanoparticles. Estimations of the amount of antibodies bound on the gold surface can be done but this requires some complex imaging techniques and thus this avenue was not explored. The concentration of the gold nanoparticles was based on the dilution from the stock formed after conjugation. Photometric analysis of the final product (100 $\mu$ L of conjugated gold nanoparticles) was done to compare the quantity of the gold nanoparticles before and after conjugation. This gave a number that can be used as concentration for the gold nanoparticles, however most of the times there was strong correlation between the before and after conjugation spectrophotometric readings and thus a simple fraction dilution series was opted in this experiment.

The optimum coating antibody for the 11-MUA modified surface (10  $\mu$ L of 60  $\mu$ g mL<sup>-1</sup> 7E7) was adopted and after sensitisation of the surface with EDC/NHS, different dilutions of the conjugated gold nanoparticle stock were assayed. Several concentrations of the conjugated gold nanoparticles (Neat, 1:2, 1:5, 1:15, and 1:20) were made and pre incubated with 50ng mL<sup>-1</sup> antigen for 1 h on a rotor. A 10  $\mu$ L of this was then deposited on the surface of the, 11-MUA modified, sensitised, coated and blocked electrodes and left to incubate for 1h before being washed and analysed using an electrochemical analyser (Metrohm, Ultech, Netherlands) The results obtained are shown in Figure 4.14. The results showed the expected trend of increasing signal with increasing concentration of the gold nanoparticles. However the peak of the trends was exhibited on the 1:10 dilution where the highest signal was achieved. Any further increases in the concentration beyond this point did not yield an expected proportional signal enhancement.

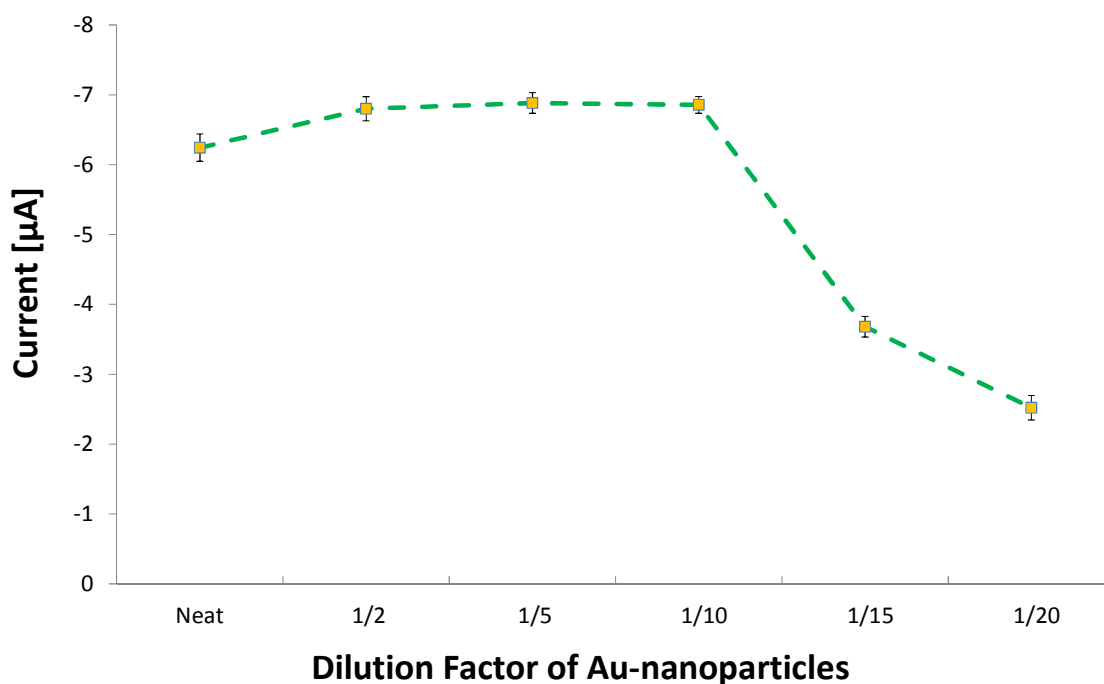


**Figure 4.14:** The optimisation of conjugated gold nanoparticles for detection of cTnT assay on 11-MUA modified screen-printed gold electrodes. Electrodes were first sensitised with 30  $\mu\text{L}$  of EDC/NHS solution. A 10  $\mu\text{L}$  of 60  $\mu\text{g mL}^{-1}$  anti cTnT 1C11 was immobilised on the gold working electrode. It was assayed with standard concentration of the cTnT antigen (50  $\mu\text{g mL}^{-1}$ ) premixed with different concentrations of the conjugated gold nanoparticles.

After the determination of the appropriate concentration of the conjugated gold Nanoparticles to use in the detection of the immuno assay, a standard curve was made using the optimum conditions. The optimised parameters of coating antibody (60  $\mu\text{g mL}^{-1}$  of 1C11) on sensitised MUA modified working electrode surface, and detection utilising gold nanoparticles conjugated with HRP and 7E7 antibody (1:10 dilution with the antigen) were used and a standard curve was plotted to show the capabilities of the immunosensor (Figure 4.15). The highest current output (-7.23  $\mu\text{A}$ ) was generated using gold nanoparticles. This assay set up had the most sensitivity basing on the high gradient of the slope. It was on this basis that the assay setup was adopted as the optimum and another standard curve was plotted using 75% serum for use in determining some unknown concentration of cTnT spiked in commercial serum.

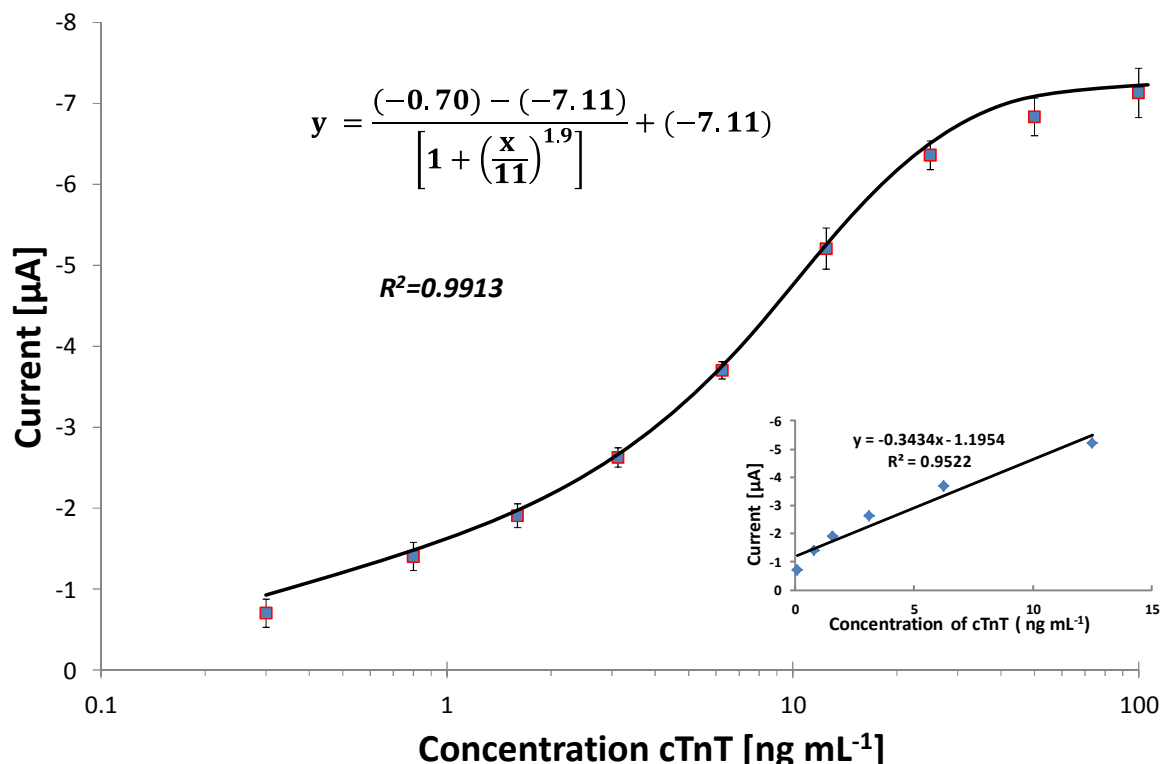


**Figure 4.15:** Standard curve of the immunosensor with 11-MUA surface modifications and detected using conjugated gold nanoparticles. (Inset) a liner plot of the same curve LOD = 0.51 ng mL<sup>-1</sup>, n=3, maximum CV= 10.4%, error bars = standard deviation.

#### 4.4.5 Generation of a standard curve using 75% serum on the optimised gold nanoparticle immunosensor

Biological samples consist of a complex mixture of compounds, including abundant proteins that tend to adsorb non-specifically to surfaces. When other abundant nonspecific proteins are present, however, it is extremely challenging to detect target biomarkers (Bolduc and Masson, 2008). This means that effective standard curves must be made using standards imbedded in the same material as the intended samples. This is even more important on assays that do not have a comprehensive dilution steps to take away the matrix effect of interfering proteins. In an attempt to accommodate interference expected from real serum samples in commercial diagnostic devices. Commercialised human serum samples purchased from (Sigma-Aldrich) were used as standards.

Attempts to construct a standard curve using undiluted serum standards yielded undesirable results with high margins of error due to lack of reproducibility. The purchased serum was diluted with 25% v/v PBS-T with additives to give a 75%v/v serum solution that was used to make standards. The additives (0.5 M NaCl, 200  $\mu\text{g mL}^{-1}$  BSA and 500  $\mu\text{g mL}^{-1}$  dextran) had been proven to help with lowering non-specific binding in earlier work by colleagues (Uludag and Tothill, 2010). The 75% serum solution was then used to make standards as well as samples spiked with unknown concentrations of cTnT.

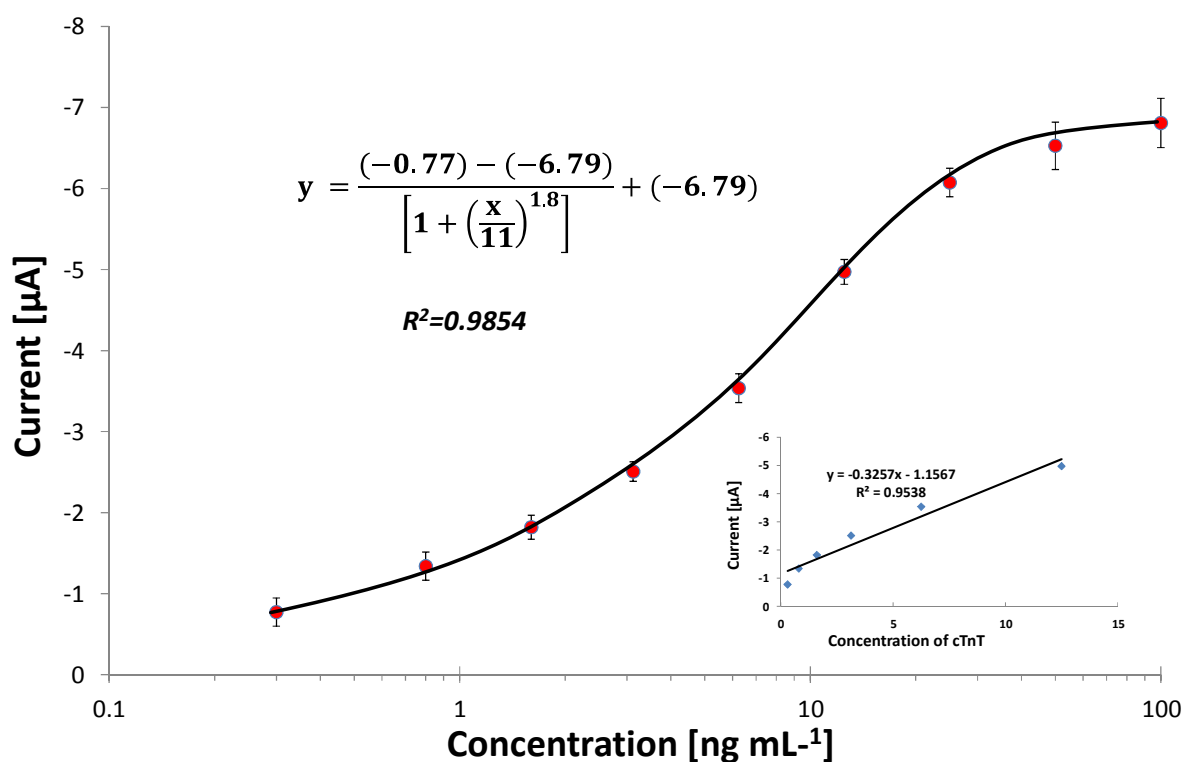
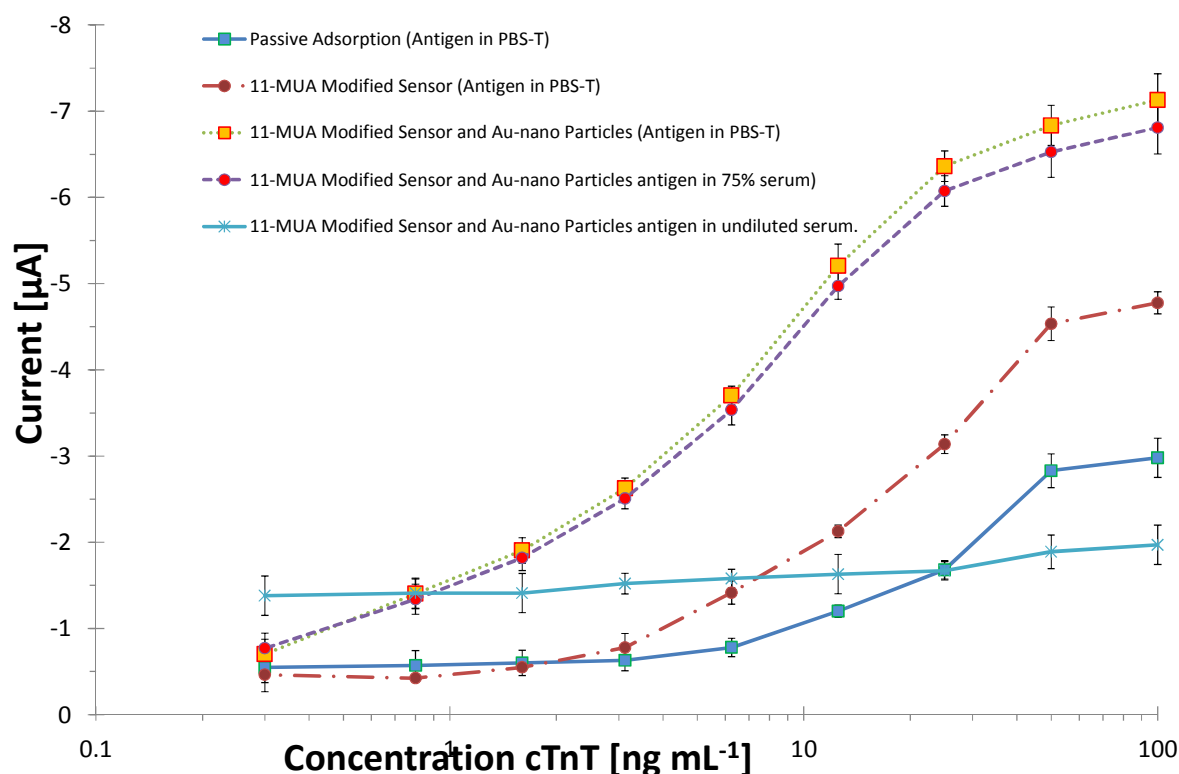


**Figure 4.16:** Standard curve of the immunosensor with 11-MUA surface modifications and conjugated gold nano-particles for detection using antigen in 75% serum, (Inset) a linear plot of the same curve, LOD=0.58  $\text{ng mL}^{-1}$ ,  $n=3$ , maximum CV=12.8%, error bars = standard deviation.

The curve resembled that of the same immunosensor format done for standards in buffer (Figure 4.15) but exhibited a lower maximum peak current. It was the curve that was used to interpolate the unknown concentrations of cTnT in spiked commercialised serum samples.

#### 4.4.1 Comparative summary of the different assay procedures used on SPGEs

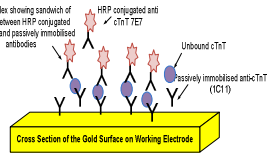
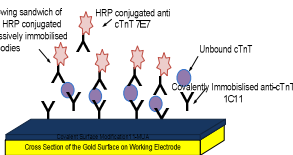
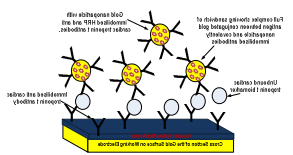
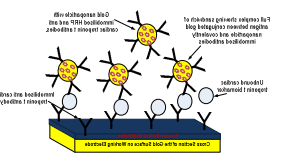
The four immunoassay set-ups used on screen-printed gold electrodes in this study were used to construct standard curves as described earlier. These standard curves were then compared against each other; Figure 4.17 and Table 4-2 shows the comparison of the standard curves of the three methods



**Figure 4.17:** Comparison of the calibration curves that were generated using different assay optimisation techniques. The data from the calibration curves showed that the use of gold nanoparticles significantly enhanced the signal output and assay sensitivity. And that the serum standards did not perform well unless diluted.



**Table 4-2** The summary of the performance of various immuno assay set up on the cTnt immunosensor using screen printed electrodes.

	Passive Adsorption	11-MUA Modified Sensor	11-MUA Modified Sensor + 60 nm gold nanoparticles	11-MUA Modified Sensor + 60 nm gold nanoparticles 75% Serum standards
Setup				
Calculated LOD	$2.12 \text{ ng mL}^{-1}$	$1.14 \text{ ng mL}^{-1}$	$0.51 \text{ ng mL}^{-1}$	$0.58 \text{ ng mL}^{-1}$
LOQ	$6.8 \text{ ng mL}^{-1}$	$4.2 \text{ ng mL}^{-1}$	$1.4 \text{ ng mL}^{-1}$	$1.7 \text{ ng mL}^{-1}$
Equation	$y = -0.0475x - 0.5203$ $R^2 = 0.9899$	$y = -0.113x - 0.4733$ $R^2 = 0.9729$	$y = -0.3434x - 1.1954$ $R^2 = 0.9522$	$y = -0.3279x - 1.1416$ $R^2 = 0.9532$
Coefficient of Variance	10.9%	9.8%	10.4%	12.8%

#### 4.4.2 Detection of cTnT in commercial serum samples using the developed Immunosensor.

Serum samples spiked with unknown concentrations of cardiac troponin t (cTnT) were made from human whole serum purchased from Sigma (Dorset, UK). The serum was diluted with 25% v/v PBS-T with 0.5 M NaCl, 200  $\mu\text{g mL}^{-1}$  BSA and 500  $\mu\text{g mL}^{-1}$  dextran. These additives were intended to reduce non-specific binding. The serum was then aliquoted into eight randomly labelled vials and spiked with unknown concentrations of cTnT that were controlled not to exceed 100  $\text{ng mL}^{-1}$  as this was the known upper limit of detection on the calibration curve. The vials were further aliquoted into three sets' the first set was analysed using the developed immunosensor using the calibration curve plotted in Figure 4.16. the remaining two sets were analysed using other devices that were intended to validate on the developed immunosensor. One was sent to the NHS Bedford Hospital where they were analysed using a clinical laboratory analyser, the other was analysed using the QCM-1 analyser using a method developed by a colleague (Van Heusden, 2011). Table 4-3 shows the results obtained.

**Table 4-3:** The results from the analysis of eight unknown samples using the developed immunosensor, the QCM-1 and a Hospital Laboratory Analyser

	Developed Immunosensor	Hospital Analyser	QCM-1
<b>Sample 1</b>	6.5 $\text{ng mL}^{-1}$	5.3 $\text{ng mL}^{-1}$	3.8 $\text{ng mL}^{-1}$
<b>Sample 2</b>	22.8 $\text{ng mL}^{-1}$	25.3 $\text{ng mL}^{-1}$	17.9 $\text{ng mL}^{-1}$
<b>Sample 3</b>	3.2 $\text{ng mL}^{-1}$	3.2 $\text{ng mL}^{-1}$	Not detected
<b>Sample 4</b>	15.4 $\text{ng mL}^{-1}$	13.8 $\text{ng mL}^{-1}$	9.2 $\text{ng mL}^{-1}$
<b>Sample 5</b>	55.4 $\text{ng mL}^{-1}$	47.9 $\text{ng mL}^{-1}$	33.7 $\text{ng mL}^{-1}$
<b>Sample 6</b>	9.4 $\text{ng mL}^{-1}$	8.5 $\text{ng mL}^{-1}$	5.9 $\text{ng mL}^{-1}$
<b>Sample 7</b>	66.9 $\text{ng mL}^{-1}$	63.9 $\text{ng mL}^{-1}$	56.7 $\text{ng mL}^{-1}$
<b>Sample 8</b>	1.2 $\text{ng mL}^{-1}$	0.9 $\text{ng mL}^{-1}$	Not detected

The results show that the developed immunosensor managed to interpolate all the samples and transcribe a proposed concentration of cTnT in the samples. It should be noted however that although the calibration function managed to estimate the concentrations of cardiac troponin in the unknown samples, the accuracy is questionable. This is because the limit of quantification, which was calculated as the mean of the blank plus 10 times the standard deviation, was far much higher than the calculated limit of detection. In general more and more high sensitivity assays find themselves on this conundrum (F.D.A, 2001). Statistically significant replications would need to be done to validate the effectiveness of the immunosensor. The CV for the developed immunosensor was superior to that of the QCM but higher than that of the laboratory analyser at Bedford Hospital. There was a difference in the actual estimations of the cTnT in the samples between all the three methods. Figure 4.18 shows the correlation between the performances of the developed immunosensor for cTnT in comparison to (A) hospital analyser and (B) QCM-1 analyser. The three methods used makeshift specimens with 75% serum spiked with unknown concentrations of cTnT. The results show that although the developed immunosensor had more standard error (12% CV) than the hospital analyser (5% CV) there was a good correlation on the results obtained using the two methods ( $R^2$  0.991). This means that despite some calibration differences between the two methods they had similar capabilities in distinguishing between different concentrations of cTnT. The QCM-1 method had a relatively high standard of error between the specimens (14% CV) and its lower limit of detection was higher in comparison to the electrochemical sensor. The QCM method was developed over a short period of time (2 months) and as such was not fully optimised thus it is difficult to ascertain its actual limitations.

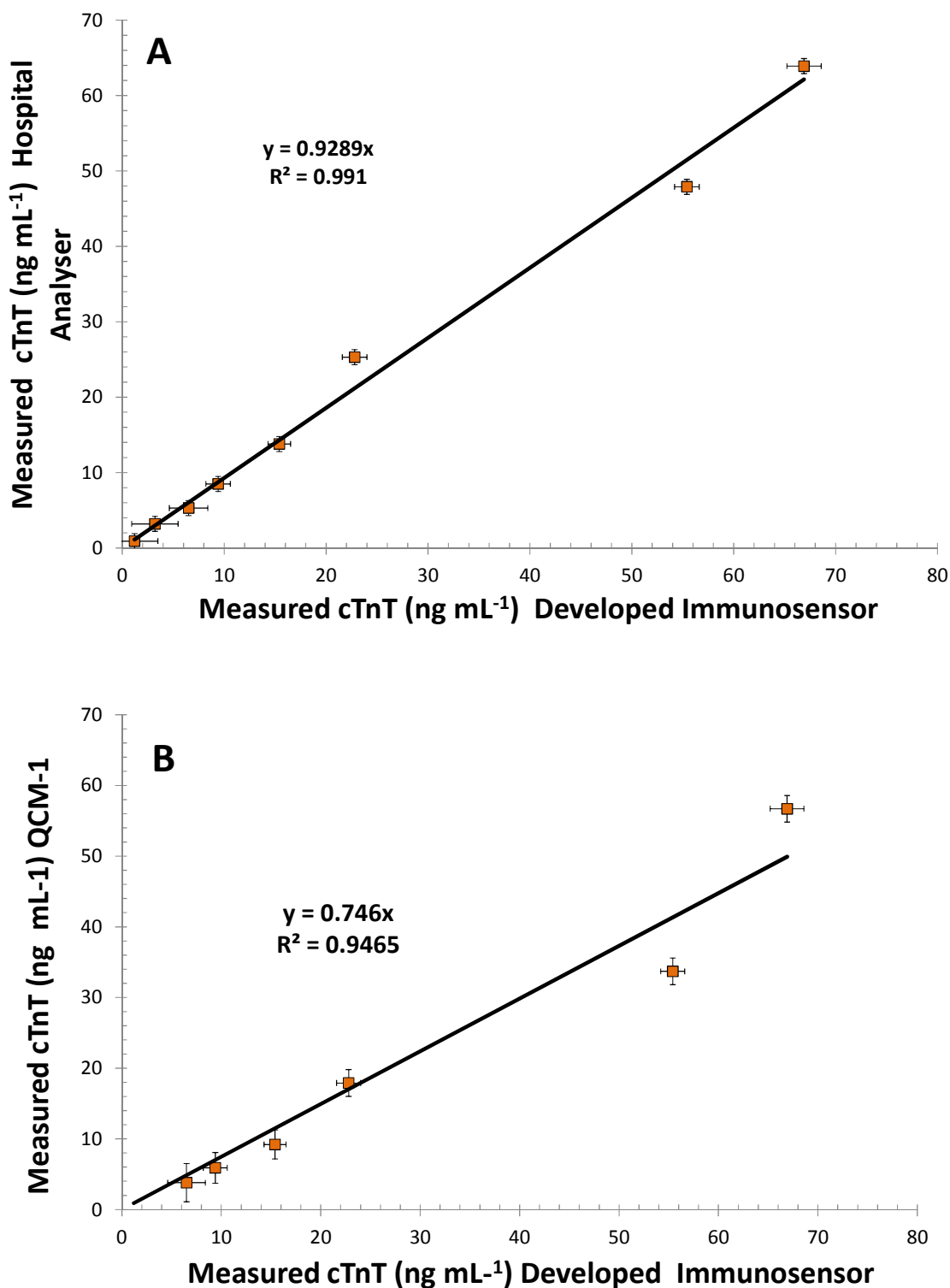


**Figure 4.18:** Correlation plots showing the performance of the developed biosensor for cTnT against two other detection methods. Results from a hospital analyser (A) and QCM-1 analyser (B) were compared with those of the gold nanoparticle enhanced immunosensor. Bars indicate standard deviation.

## 4.5 Conclusions

An electrochemical immunosensor based on gold- nanoparticles and self-assembled monolayers SAMs for enhanced sensitivity was developed for the detection and analysis of cTnT in partly diluted serum samples. Screen printed gold electrodes with gold working electrodes were modified with 11-MUA to make surfaces suitable for covalent immobilisation of the capture antibody using the EDC/NHS chemistry. The covalent coupling enabled higher numbers of correctly orientated coating antibodies that helps in increasing the sensitivity of the assay. Incremental development was done in the development of the cardiac troponin immunosensor the first assay set up was based on the passive adsorption and conjugated detection antibodies and resembled that developed for CRP assay described in Chapter 3. This assay set up did not achieve much in terms of increasing sensitivity with a lower limit of detection LOD of 2.12 ng mL<sup>-1</sup> and a maximum Coefficient of variance (CV) of 10.9%.

Further development to the assay setup was done with the use of self-assembled monolayers on the gold working electrode. An improvement on the method of generating self-assembled monolayers using 11-MUA was made. In the new method there was limited exposure of the electrodes to the solvents which had been identified to be causing problems in earlier work done on CRP immunosensor. Precautions to prevent rapid evaporation of the 11-MUA solution before the monolayer was created were done with the use of refrigeration and moisture tubs. Successful modification of the working electrodes was achieved and this was confirmed through cyclic voltammetry and contact angle measurements. The EDC/NHS chemistry was used to aid the covalent coupling of the coating antibodies in a manner described in previous literature (Van Delden *et al.*, 1996).

The effects of covalent coupling were evidently fruitful as observed with an increase in maximum signal generated by the assay from (-2.98  $\mu\text{A}$  for the passive adsorption) to (-4.78  $\mu\text{A}$  on the covalent coupled assay). The LOD also improved significantly from 2.12 to 1.14  $\text{ng mL}^{-1}$ . The next step in the development process was incorporating the use of conjugated gold nanoparticles on the assay set up to improve on sensitivity. A 60nm gold nanoparticles were coated with HRP followed by the detection antibody 7E7 using passive adsorption method. The conjugation of the gold nanoparticles was quality checked using high salt concentration and examining for flocculation. The QCM-1 was also initially used for the checking of the conjugation of the antibodies on to the gold since it was an automated technique. Gold nanoparticles are capable of allowing more quantities of the detection reagents to be localised thus increasing the potential for enhanced signal output to occur in low antigen concentrations (Ansari *et al.*, 2010; Saha *et al.*, 2012). This has an advantage of lowering the limit of detection which is particularly important for the cTnT assay that has small antigen concentrations in baseline samples  $\leq 0.03 \text{ ng mL}^{-1}$ .

The clinical reference ranges for cTnT are defined by the ability of an assay to detect 99% of laboratory baseline values. This equates to lower limit of detection levels of around  $0.03 \text{ ng mL}^{-1}$ . To achieve such high sensitivity a lot of development has to be done on the assay that incorporates techniques which helps to achieve this. The use of the gold nanoparticles significantly lowered the limit of detection further to  $0.51 \text{ ng mL}^{-1}$  on buffer and 0.58 in 75% serum standards. This assay was comparable to other reported assays that used screen printed electrodes for detecting cTnT (Silva *et al.*, 2010) but may have been outperformed by other reports of SPR based immunosensors (Dutra *et al.*, 2007). A standard curve was made with commercial serum to mimic the actual conditions of use. The interference posed by the serum samples was too much that it grossly affected the sensor performance. Other researchers have discovered that there is limited matrix effect on screen printed electrodes but

their research did not incorporate the use of SAMs which may have aided in this (Kadir and Tothill, 2010). Earlier work by colleagues had proven that a 75% serum dilution with PBS Tween and some additives was sufficient in reducing the nonspecific binding due to the protein matrix in serum (Uludag and Tothill, 2010). This method was adopted in the hope that should a immunosensor be made it will be ready for proper serum samples provided there was a dilution step to counteract the matrix effect. The current strides made on the electrochemical immunosensor have achieved a limit of detection  $0.58 \text{ ng mL}^{-1}$  with a dynamic range spanning to  $100 \text{ ng mL}^{-1}$ . Although this is not enough to satisfy the diagnostic requirements of the cTnT for cardiovascular diseases, it could be used for screening high-end cardiac events.

The performance of the developed immunosensor has been proven better than other biosensor methods like the QCM and the in-house ELISA methods. When analysing unknown concentrations of cTnT in samples the QCM-1 gave relatively high standard of error between the specimens (14% CV) and its lower limit of detection was high. The correlation results on 75% spiked commercial serum samples show that although the developed immunosensor had more standard error than the hospital analyser there was a good correlation on the results obtained using the two methods ( $R^2$  0.991). This means that despite some calibrations differences between the two methods they had similar capabilities in distinguishing between different concentrations of cTnT. The development of the immunosensor needs further optimisation to reach diagnostic ranges, however current performance is sufficient for screening high end cardiovascular events, as well as demonstrate proof of concept for a simultaneous immunosensor for the detection of cardiovascular diseases using screen printed electrodes.

## CHAPTER 5

### STABILITY OF THE IMMOBILISED ANTIBODIES ON THE IMMUNOSENSOR SURFACE



## **5 Stability of the Immobilised Antibodies on the Immunosensor Surface**

### **5.1 Introduction**

The stabilisation of proteins is of great interest in a number of biosensor applications where shelf life during storage and operation are required. The main problems often encountered in the development of commercial biosensors is the stabilisation of enzymes and other proteins used in the bioactive layer (Gibson, 1999; McAteer *et al.*, 1999; Jawaheer *et al.*, 2002). Immunosensors often use high value proteins such as antibodies, analytical enzymes and as such, there is a need to employ effective stabilisation technology in an attempt to curb cost associated with denaturing and lack of activity of the often-expensive biomolecules (Fernandez-Lafuente *et al.*, 1999). Most proteins are easily affected by their microenvironment and this can either antagonise or enhance their activity, this is more so during use or storage. The sensor developed in this project can offer good examples of how several factors can affect both the shelf and operational stability of the immunosensor devices and these include; storage temperature, humidity, contact with other reagents or device surfaces, and operational conditions such as voltage. In such situations, the stability of the biosensor as a whole is desired and the focus of stabilisation is not limited to biomolecules (antibodies and enzymes used) but generally includes everything including the inks and the electrodes, therefore effective methods of stabilisation are needed to enhance the stability and retain the performance of the biosensor (Jawaheer *et al.*, 2002).

#### **5.1.1 Types of biosensor stability**

For a biosensor to be successful it has to be stable during storage (shelf life stability) and also during use (operational stability). Shelf stability is defined as the improvement of activity retention of an enzyme, protein, diagnostic or device when stored under specified conditions after manufacture (Gibson, 1999). This

is an important parameter particularly for the commercialisation of adaptable materials that are capable of degrading over time, a good example of shelf stability is evident in the pharmaceutical industry where medications have a use by date indicated on the packaging. The same principle is often observed on simple diagnostics applications like the lateral flow devices for example the pregnancy tests, where the product is guaranteed for a specific duration from the date of manufacture. The shelf stability of a biosensor is often one of the crucial factors on deciding commercial viability of a developed biosensor (Fernandez-Lafuente *et al.*, 1999). Operational stability on the other hand is the retention of activity of a protein or enzyme when it is actually in its intended use. This is often crucial when an analytical device incorporate a reusable sensor that needs to achieve a relatively long lifetime. However, although both shelf-stability and operating stability are important parameters in biosensor development, shelf-stability is usually the more crucial parameter (Gibson, 1999). This is because in some cases the operational stability is irrelevant for example in the manufacture of disposable single use biosensors like those developed in this project.

### **5.1.2 Mechanisms of the Inactivation and Preservation of Proteins**

Several well-varied mechanisms are responsible for the inactivation of proteins and enzymes. The simple unfolding of the structure (denaturing) represents a small proportion of the methods by which enzymes and proteins inactivate (McAteer *et al.*, 1999). Table 5-1 gives an overview of the different types of inactivation mechanisms (Gibson, 1999).

**Table 5-1:** Methods of Inactivation of Proteins.

<b>Inactivation Due to Chemistry of Protein Changing</b>	<b>Inactivation Due to Other Changes</b>
Hydrolysis	Unfolding
Deglycosylation	Loss of Cofactors
Imide Formation	Protein Aggregation
Cyclisation	Poisoning-Irreversible Inhibition
Oxidation / Photooxidation	Proteolysis
Disulphide Bridges Formation	Substrates of Microorganisms

Most proteins including enzymes can deactivate in a number of different ways depending on the conditions and there are strong possibilities that several deactivation mechanisms may occur simultaneously. A wide variety of techniques can be employed to influence the stability of proteins for biosensor applications. Table 5-2 gives a summary of some of the methods that are currently used in industry (Gibson, 1999).

**Table 5-2:** Summary of Methods of Protein Stabilisation

<b>Physico-Chemical Methods</b>	<b>Additives/ Media Engineering</b>
Physical Entrapment	Salts/ Including Buffers
Chemical Modification	Metal Ions
Cross Linking	Polymers
Protein Engineering	Solvents
Immobilisation on Other Supports- Electrodes	Water Modifiers-Sugars & polyhydric Alcohols

The experiments described in this chapter focus on the methods highlighted in orange in Table 5-2 . The immobilisation of proteins offers many functional advantages for the construction of a biosensor. However, besides the generic functional need for proteins like antibodies or enzymes to be immobilised in biosensor development, there are often inadvertent stability advantages that come with the immobilisation of proteins on biosensor surfaces (Pessela *et al.*, 2004).

This chapter will discuss methods for stabilisation of biomaterials used in electrochemical immunosensor applications with particular reference to shelf life stability of immobilised antibodies. The immunosensors developed in earlier work described in Chapters 3 and 4, utilise proteins in the form of antibodies for both capture and detection functions as well as enzymes in the form of HRP. There is need to preserve these bio molecules and ensure that they are fully functional at the time of analysis. Two techniques investigated in this work will be discussed and these were aimed at improving the stability of the immobilised antibody. The use of self-assembled monolayers, and a commercial stabilising agent Stabiliguard® (Diarect, Germany) were employed.

## 5.2 Materials

Potassium Chloride (KCl), Potassium Ferricyanide ( $K_3Fe(CN)_6 \cdot 3H_2O$ ), TMB (3, 3', 5, 5'- tetramethylbenzidine hydrochloride), PBS (phosphate buffered saline) containing 0.137 M sodium chloride, and phosphate buffer, 0.01 M, pH 7.4 in tablet form, citrate phosphate buffer (0.05 M, pH 5.5) tablets. Hydrogen peroxide, sodium hydroxide (NaOH) and sodium chloride (NaCl), bovine serum albumin (BSA), 11-mercaptoundecanoic acid (11-MUA) were purchased from Sigma-Aldrich (Dorset, UK). Samples of Stabilicoat® were supplied from Surmodics through their distributor Diarect , UK. Micropipettes were purchased from Eppendorf, UK. Pipette tips and 1.5 mL tubes, Potassium chloride (KCl) were purchased from Fisher Scientific (Loughborough, UK). Primary (batch 1c11), secondary antibody (batch 9g6 HRP conjugated) and (7E7 non conjugated), and human cTnT (Molecular Weight (MW) = 36 kDa) were obtained from (Abcam, Cambridge, UK). Skimmed milk protein, (KPL Ltd, Gaithersburg, USA ).

Reverse Osmosis (RO, Ultrapure) water ( $18\text{ M M}\Omega\text{cm}^{-1}$ ) was obtained from Milli-Q water system (Millipore Corp., Tokyo, Japan). Glassware and volumetric materials were of analytical grade. Gold nanoparticles with a diameter ranges from 20-100 nm were purchased from BBInternational Ltd (Cardiff, UK). An incubator/shaker from Labsystem iEMS® was used for temperature control incubation. The electrodes used in this project were the JD type designed by Cranfield University and fabricated using the facilities at DuPont (Bristol, UK). The gold working electrode was circular with a  $0.226\text{ cm}^2$  planar area, a complementary carbon counter electrode and an Ag/AgCl reference electrode. The substrate material used is PET 125  $\mu\text{m}$  Autotype HT5. The carbon electrode has an approximate dried thickness of 7  $\mu\text{m}$ , while the gold and Ag/AgCl electrodes both have an approximate thickness of 18  $\mu\text{m}$ . The encapsulation of 5036 blue had an approximate thickness dried of 4  $\mu\text{m}$ . Inks used in the construction of the sensors are BQ221 carbon ink, BQ331 gold ink and the 5880 Ag/AgCl and are available from DuPont (Bristol, UK). Autolab Electrochemical Analyser with general-purpose electrochemical software GPES 4.9 was purchased from Metrohm (Utrecht, Netherlands). The electrodes were connected to an edge connector and then connected to the electrochemical analyser using a modified connector (Maplin UK).

### 5.3 Methods

There were three stabilisation methods that were investigated for their potential to increase the performance span of the immunosensor over time. The use of self-assembled monolayers, a commercial stabilising agent Stabiliguard® (Direact, Germany) and Trehalose (a natural alpha-linked disaccharide) were investigated for their ability to improve the stability of immobilised antibodies. Immunosensors were made in big batches were coated and blocked using the three techniques. A reference immunosensor batch was made using passively absorbed antibody that had no stabilisation mechanism employed. All the immunosensors used for this work were for the cardiac troponin t assay cTnT

as it had a wide breath of assay design. For enhanced reproducibility, the assay format used was the classic sandwich that did not employ the use of gold nanoparticles but detection with HRP conjugated mouse monoclonal anti cTnT (7E7) antibody. This was to eliminate any batch to batch variation associated with the conjugation of gold nano-particles especially when a new batch had to be made for every time measurement due to their lack of stability.

### **5.3.1 Method for preparing immunosensors using passive adsorption**

Immunosensors for cTnT optimise of the coating and detection antibody for cTnT assay on bare screen-printed gold for passive adsorption were made using the method described in Section 4.4.2.1 .The electrodes were first baked at a temperature of 120 °C for 30 minutes, washed and rinsed with distilled water to remove any particle contamination. The working electrode was then coated with a drop of 10 µL of mouse monoclonal anti cTnT (90 µg mL<sup>-1</sup> of 1C11) dissolved in 0.05 M carbonate-bicarbonate buffer pH 9.6 and allowed to incubate for 2h at 37 °C in a moist environment. The electrode surface was then gently washed with phosphate buffer saline with 0.05% Tween 20 (PBS-T), two times, rinsed with distilled water and air-dried with nitrogen. The working electrodes surface was then blocked for 30 minutes at 37 °C. The blocking solution was a 1:10 skimmed milk dilution in PBS. The electrodes were then gently dried again with a nitrogen gun and split into three batches that were stored in different conditions.

### **5.3.2 Method for preserving immunosensors using covalent immobilisation**

This was done using the procedure described in Section 4.3.3.1. The electrodes were baked in an oven for 120 °C for 30 min before being plasma cleaned in oxygen free nitrogen at 50w for 2.5 minutes (Emitech K 1050X, EM Technologies, Kent, UK), at a power of 50 W with a bleed vacuum trip of  $3 \times 10^{-1}$  mbar and an ashing time of 1 minute. After this, the working electrode was coated with 2 x 50µL of 4mM 11-MUA placed three hours apart in an overnight incubation step at 4 °C in darkness. This allowed the 11-MUA to form a self-assembled monolayer on the sensor surface. Two solutions a 400 mM EDC and 100 mM NHS solution in deionized water were premixed 1:1 and applied to the working electrode surface immediately after mixing them (30 µL and incubating for 10 min). The electrodes were then washed in PBS-T and the capture antibody (10 µL of 90 µg mL<sup>-1</sup> mouse monoclonal anti cTnT 1C11) dissolved in 0.05 M carbonate-bicarbonate buffer pH 9.6 was added and allowed to incubate on the sensor surface for 2h at 37 °C in a moist environment. The electrodes were then washed and blocked, first for 10 min with 50 µL of 1M ethanol amine solution and then further blocking was done by covering with 50 µL 10% milk blocking proteins (KPL) dissolved in PBS for 30 min at 37 °C. The electrodes were then gently dried again with a nitrogen gun and split into three batches that were stored in different conditions.

### **5.3.3 Method for preserving Immunosensors using Stabiliguard®**

Immunosensors were prepared using the procedures for both passive adsorption described in Section 5.3.1 and covalent immobilisation described in Section 5.3.2 with a couple of modifications. Stabiliguard ® (50 µL of neat solution was used for the blocking instead of using 10 % milk protein. The blocking time was cut from 30 min to 10 min but all the other parameters remained the same for both methods. These were the recommended parameters for the use of Stabiliguard for preserving the functionality and shelf life of immobilised antibodies.

### 5.3.4 Batching and Storage of Immunosensors

The three types of immunosensors were made and stored so that each type had three batches of electrodes stored in different temperature and humidity environments. One batch was stored in petri dishes wrapped in foil at 4°C, another batch was stored in petri dishes wrapped in foil at room temperature and a third batch was stored in petri dishes wrapped in foil inside a vacuum desiccator with silica gel beads

### 5.3.5 Analysis of the Functionality of the Immobilised Antibodies

The immunosensors were analysed over time to check for the functionality of the immobilised antibodies using electrochemical measurements. The analysis was done for 1, 3, 7, 14, 28, 60, 90 days after the making of the immunosensor for each of the sensor type and storage condition. The analysis was done by Premixing the antigen (50  $\mu\text{L}$  of cTnT) with the detection antibody HRP conjugated anti cTnT to give a final concentration of 50  $\text{ng mL}^{-1}$  antigen concentration and 60  $\mu\text{g mL}^{-1}$  of conjugated mouse monoclonal anti human cardiac troponin t antibody. The mixture was *incubated to premix for 1hr* min on a rotter away from sunlight. It was then added (20  $\mu\text{L}$ ) in triplicates to the blocked electrodes and incubated for 1hr min at 37°C. The electrodes were then washed and connected to an edge connector, which is connected with a multi-channel AUTOLAB electrochemical instrument. All measurements were performed by adding 100  $\mu\text{L}$  of 4 mM TMB and 0.06 %  $\text{H}_2\text{O}_2$  in 0.05 M citrate phosphate buffer plus 0.1 M KCL with chronoamperometry methods at -200 mV constant current and run for 200 s to 300 s using electrochemical GPES 4.7 software.



## 5.4 Results and Discussion

### 5.4.1 Stabilisation of immobilised antibodies

In this study, two methods were used for the antibody immobilisation on the sensor surface that is the passive and covalent immobilisation techniques. Unlike passive immobilisation that is relatively simple and relies on the adsorption of the antibodies on the sensor covalent techniques requires a series of steps that modify the surface to increase the efficiency of the immobilisation process. This has been reported to have an enhanced stabilising effect on the covalently immobilised antibodies (Wink *et al.*, 1997; Altintas *et al.*, 2012). A commercial reagent for stabilisation of immobilised proteins (stabiliguard) was also investigated. Although the constituents of the reagent are aclosely guarded commercial secret, research has shown the usefulness of water modifiers in the preservation of immobilised proteins. The use of polyalcohols, polyelectrollytes or a combination of both is consistent in most stabilisation products currently on the market. Polyalcohols include polyhydric molecules like sugars, sugar alcohols and other more exotic substituted sugar molecules. These modify the water environment surrounding a protein by competing for and replacing the free water (A.E.T Ltd, 2012). This has an effect of modifying the hydration shell of the protein in and confers protection to the protein while maintaining 3D structure and biological activity .The storage of biological materials in the presence of these polyalcohol molecules is suitable stabilisation of both solution based and dehydrated proteins with preserved biological activity. Polyelectrolytes on the other hand include numerous polymers of varying size charge and structure. The interactions between proteins and these polymers are electrostatic based on the charge groups. They are capable of forming large protein-polyelectrolyte complexes that retain full biological activity of the proteins. The important aspect on the use of these is the need for precision in calculating the stoichiometry of protein/polymer binding which is critical factor for maintaining enzyme activity in stabilised formulations (A.E.T Ltd, 2012).

There is a strong chance that the composition of Stabiliguard® is a combination of both polyalcohol's and polyelectrolytes. The combination of the two has the advantage of having polyelectrolyte molecules binding to a large protein molecule and the smaller polyalcohol molecules fitting in within the matrix generated by the protein/polyelectrolyte complex as shown in Figure 5.1. This has a net effect of improved protein protection that will make it retain the function for longer periods.

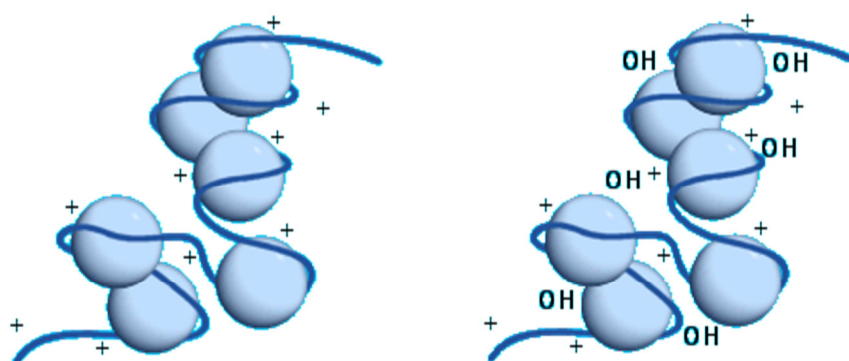


**Figure 5.1:** The effect of combined polyelectrolytes and Polyhydroxyl compounds in stabilising immobilised proteins. Polyelectrolytes promotes the formation of soluble protein - polyelectrolyte complexes, polyhydroxyl compounds can then penetrate the structure more effectively leading to stabilisation (A.E.T Ltd, 2012).

However, as mentioned before the actual constituents of the reagent are protected intellectual property. Self-assembled monolayers have been shown to increase the shelf life and functionality of immobilised proteins (Srisombat et al., 2011). In this experiment self-assembled monolayers were made using alkanethiol group chemical 11-mercaptopundecanoic acid (11-MUA) purchased from Sigma-Aldrich UK. They were made by the treating the working electrode with 2 x 50  $\mu\text{L}$  of 4 mM 11-MUA placed three hours apart in an overnight incubation step at 4°C in darkness. The EDC/NHS chemistry was then used to activate the functionalised surface and immobilisation of the antibodies followed. Figure 5.2 shows both the effect SAMs and Stabiliguard® on preserving the functionality of the immunosensor over time.

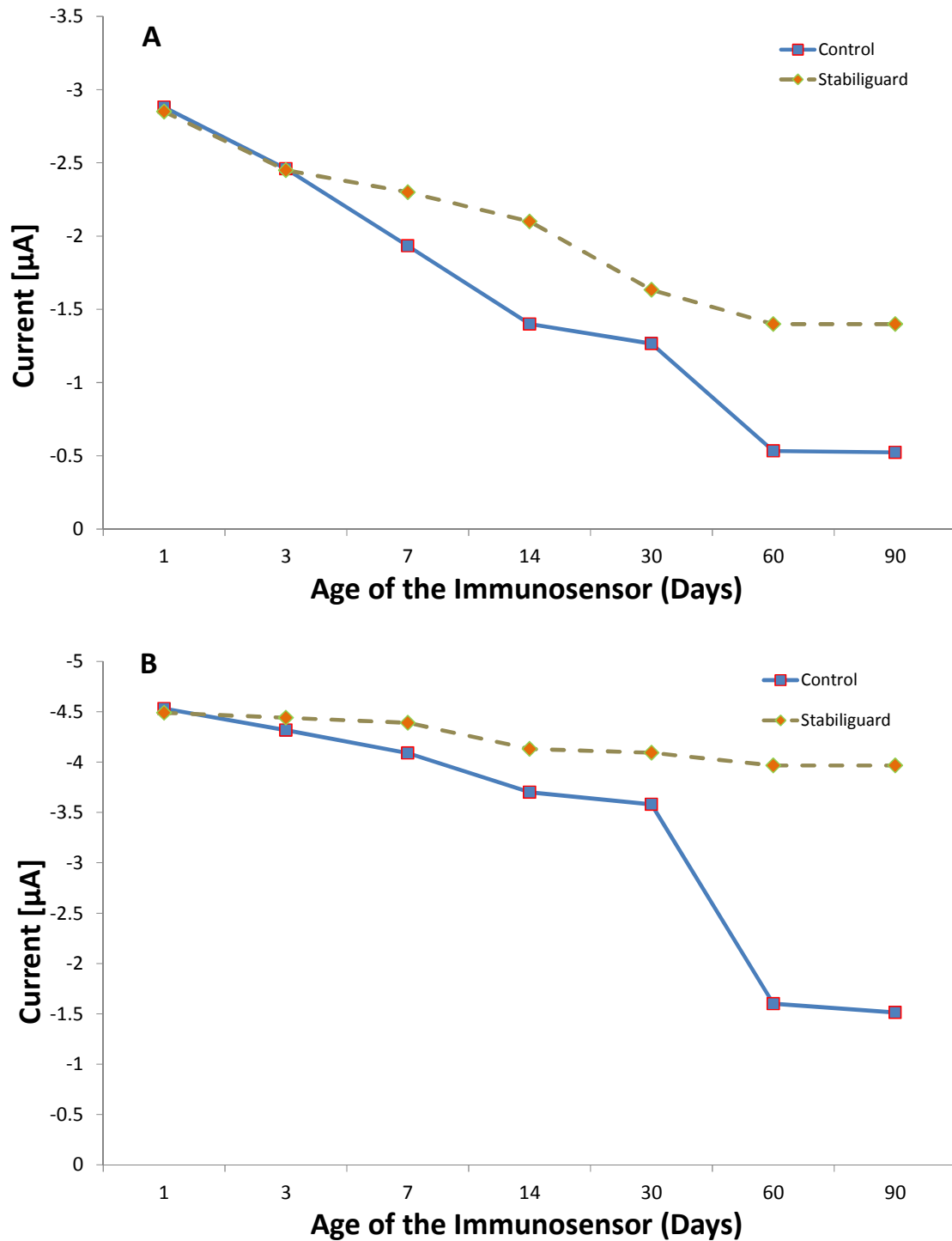


**Figure 5.2:** Effect of Stabiliguard® on preserving the functionality of immobilised antibodies on (A) passively adsorbed and (B) covalently immobilised using 11-MUA self-assembled monolayers. Each of the two setups had a Stabiliguard® stabilised and un stabilised variables and performance was compared over immunosensors stored in a variety of environments (4°C, room temperature and vacuum dessicator), n=9.

Although optimisation of the concentration of antibodies for covalent immobilisation on the actual cTnT assay recommended a lower concentration ( $60\text{ }\mu\text{g mL}^{-1}$ ) than that for covalent immobilisation ( $90\text{ }\mu\text{g mL}^{-1}$ ) the procedure for this experiment required uniform concentration of the immobilised antibody and thus the optimum for the passive adsorption was used ( $90\text{ }\mu\text{g mL}^{-1}$ ). The results show that there is significant retained functionality of the immobilised antibody for longer if Stabiliguard® is used as a replacement for the blocking agent. This is evident in both passively immobilised

Figure 5.2 (A) and SAM modified immunosensors Figure 5.2 (B). The results also showed that there is increased protein stability on immunosensors with self-assembled monolayers (covalent coupling). This is shown by the low gradient on the drop of activity compared to that of passive immobilised immunosensors; this was observed on both immunosensor types with or without Stabiliguard®. Although the Immunosensors with SAMs had an advantage of higher signals, they did not rapidly lose signals in a manner exhibited by the immunosensors without SAMs

#### **5.4.1 The environmental conditions**

The environmental conditions during the storage and transportation of bio reactive products play an important role in their functionality and shelf life. Environmental factors like humidity, temperature, and air exposure all offer potential obstacles in the functionality of biomaterials. In this experiment, batches of different immunosensors for cardiac troponin t were made and stored in different conditions. They were then analysed over time to find out which environmental conditions were favourable for the storage of immunosensors as well as to evaluate the methods of protein stabilisation that had been used on them. Three environmental conditions were investigated which included storing the electrodes in a refrigerated environment at  $4^{\circ}\text{C}$ , at room temperature, and in a vacuum. Figure 5.3 show the effect of different storage conditions on the performance of immunosensors with passively adsorbed antibodies over time.

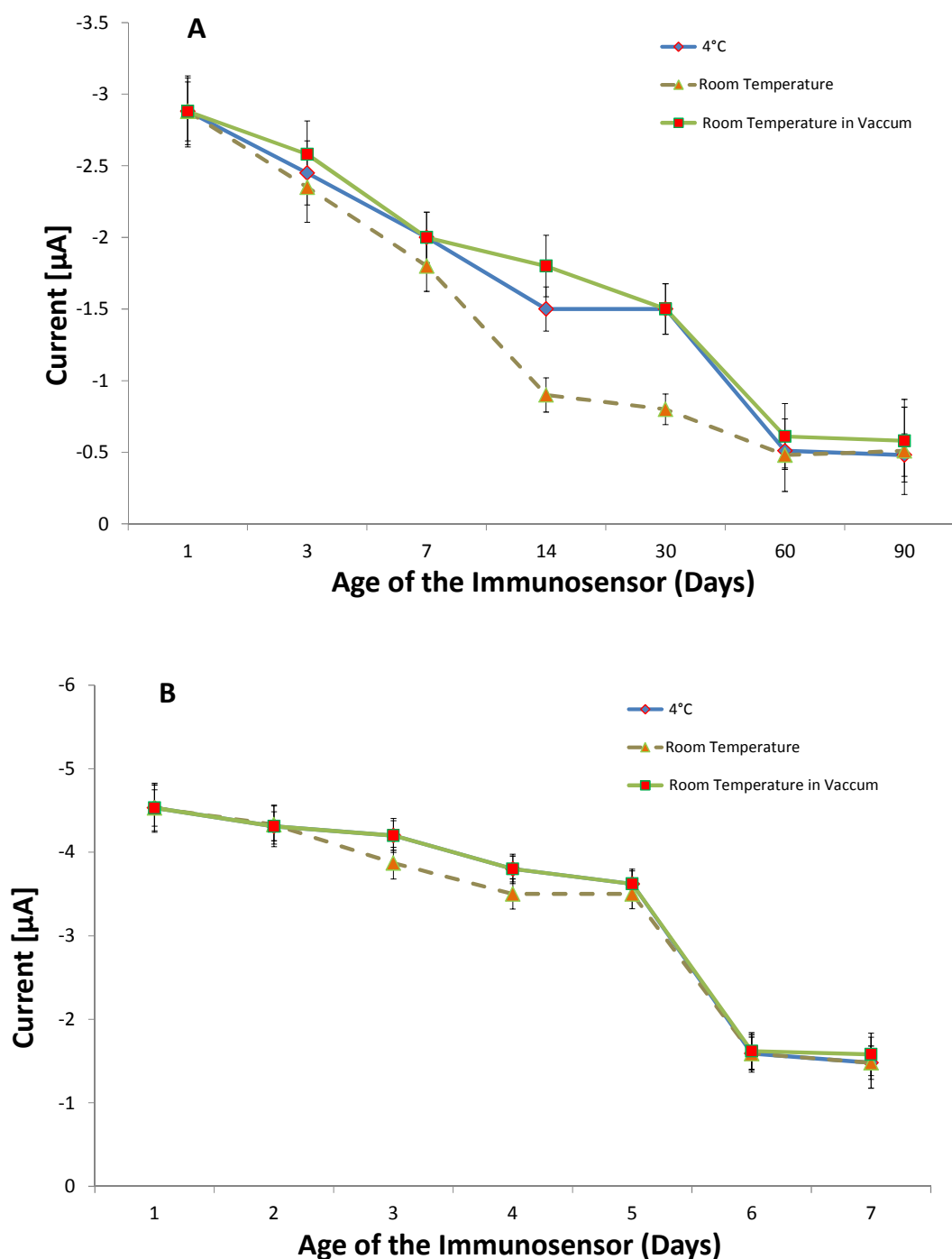


**Figure 5.3** The effect of different storage conditions on the performance of immunosensors with (A) passively immobilised (B) covalently immobilised antibodies. Batches of immunosensors were stored in different conditions and analysed.  $n=3$ ,  $CV=12.2\%$ , Error bars represent standard deviation.

The results show a typical trend of deterioration in signal with immunosensor age. This was expected, as the immunosensors used did not have any mechanism for stabilisation of the immobilised antibodies. However, the immunosensors that were kept at room temperature deteriorated faster than the ones kept in the fridge and in the vacuum. The average showed that the vacuum preserved the immunosensors better than the fridge but due to the high margin of error exhibited by the experiment in general the advantage could not be validated. The same was done on different types of immunosensors and the obtained results are summarised in Figure 5.4. The results show different immunosensor performance after storage for up to a period of 90 days in different conditions (a) refrigerated at 4°C, (b) room temperature (c) room temperature in a vacuum. The results showed corresponding information to that given by Figure 5.3; the general trend shows that there is increased deterioration on immunosensors that were left on room temperature. Refrigeration and vacuum improve the life span of the immunosensor and Stabiliguard® significantly help in retaining functionality of the immobilised antibodies for longer.

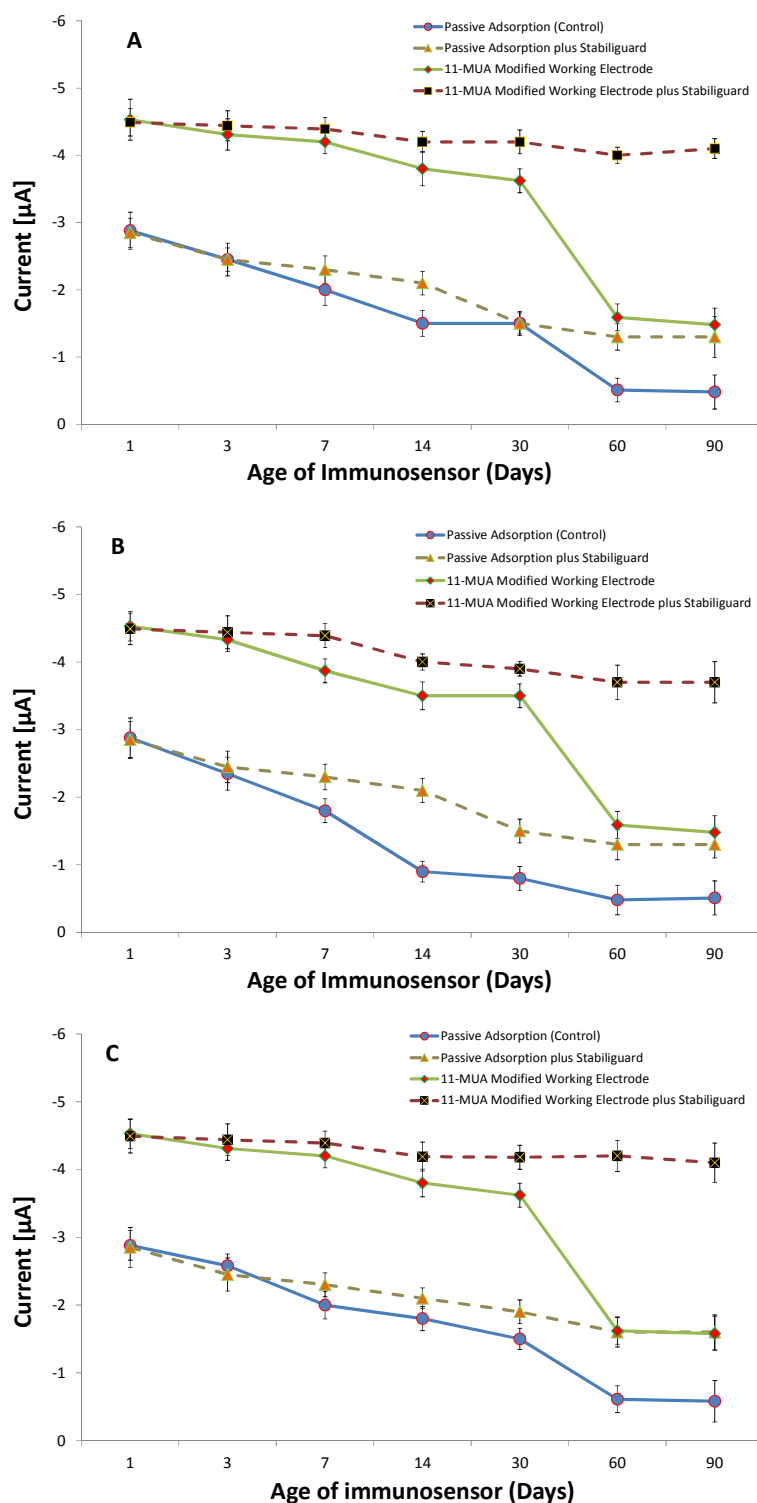


**Figure 5.4** The effect of time on the performance of various immunosensor compositions for cardiac troponin t stored at different conditions over 90 days. Immunosensors were stored at (A) 4°C (B) room temperature (C) room temperature in a vacuum.

## 5.5 Conclusion

The stability of proteins on biosensor surfaces is crucial to the feasibility of any commercialisation prospects. This factor is crucial and can make or break the business viability of any biosensor product. In this Chapter, the use of water modifiers in the stabilisation of immobilised antibodies has been shown using a commercial product Stabiliguard®, (Surmodics, USA). Although the actual chemical composition of the product is proprietary, the evidence suggested that it was effective in preserving protein functionality for longer periods possibly using a combination of polyelectrolytes and Polyhydroxyl compounds (de Cordt *et al.*, 1994). The use of Stabiliguard® made a difference on both passively immobilised and covalently immobilised antibodies using self-assembled monolayers. In both cases there was continued improved signal compared to immuno sensors without the stabilisation agent. Furthermore, the gradient of the drop of activity with time was less than that observed on immunosensors without the stabilisation agent, this was consistent with findings from other researchers (Wu and Grainger, 2006). The use of self-assembled monolayers has been demonstrated to have a positive impact on the stabilisation of the immobilised proteins (Wink *et al.*, 1997; Altintas *et al.*, 2012). Although SAMs were used in the assay for other benefits, including improved signals due to controlled antibody orientation, they were evaluated for their role in stabilising immobilised reagents to maintain prolonged functionality. Monolayers of 11-mercaptoundecanoic acid (11-MUA) were made on the gold surface and immobilisation of antibodies was carried out using the procedure described in Section 0. When compared to immunosensors with antibodies immobilised via passive adsorption, the immunosensors with SAMs had more retained functionality over time. There was a significant resistance in the drop of performance over time for the immunosensors with SAMs compared to passively adsorbed antibody ones. The comparison of the two types of immunosensors was tricky in the regard that the immunosensors with SAMs had a higher starting signal compared to the passively adsorbed, due to the benefits of improved packing (Mrksich and Whitesides, 1996). However



considering this and using the performance-time gradient, it was demonstrated that SAMs are capable of improving the stability of immobilised antibodies and even perform better at this when used with other water modifying agents that enhance protein stability.

The effect of environment on the immunosensor performance, with particular reference to storage conditions was also investigated in this work. Immunosensors for cTnT were made and batches were stored in three environmental conditions that included storing the electrodes in a refrigerated environment at 4°C, at room temperature, and in a vacuum. The performance of the electrodes from each of the batches was assayed with a uniform mixture of premixed antigen and antibody and then analysed using amperometry. The results showed a typical trend of decreasing in signal as the immunosensor aged in all of the three storage environments and for all the types of immunosensors. The data showed that the immunosensors that were kept at room temperature deteriorated faster than the ones kept in the fridge and in the vacuum. The immunosensors stored at room temperature showed the steepest decline in signal with time compared to the other two storage conditions. This could have been due to temperature and exposure to other factors like humidity. Data showed that the vacuum preserved the immunosensors better than the fridge (4°C) but due to the high margin of error exhibited by the experiment in general the advantage could not be validated. The experiment had limitations imposed on the time that was investigated, and the frequency of the measurement. More information may have been collected if there were more closely spaced periods for performance analysis. This however was not economically feasible, as it would have entailed the making and usage of a lot of electrodes and reagents. More work need to be done in this area to improve the stability of immobilised bio regents like antibodies as it is crucial for commercialisation.

## CHAPTER 6

### FINAL DISCUSSION AND CONCLUSION

## **6 Final Discussion and Conclusions**

### **6.1.1 Overview**

This thesis covers the development of two immunosensors based on the enzymatic electrochemical transduction of modified screen-printed gold electrodes. The immunosensors were developed to detect two cardiovascular markers cardiac Troponin T (cTnT) and C-reactive protein (CRP). The immunosensor development started at investigating various components for the electrodes and some manufacturing parameters that were appropriate for producing high performance electrodes. The best electrodes were then adopted for use in the development of the immunosensors. The combined use of self-assembled monolayers and gold nano-particles for enhancing signal in detecting cTnT is new technology that has been shown to increase sensitivity of electrochemical assays. A new method for the development of self-assembled monolayers on screen-printed electrodes without compromising the functionality of the electrodes was proposed. The development of immunosensors for the two cardiac markers cTnT and CRP gave a platform for proof of concept in the development of a multi marker electrochemical detection biosensors as the two electrodes could be combined on the same analyser and give signal from the same sample.

### **6.1.2 Fabrication and Characterisation of Screen-printed Electrodes**

The fabrication of high quality electrodes is the foundation of the development of competent electrochemical biosensors. In this report aspects of the fabrication process were investigated with particular reference to investigating compatible ink combinations and optimum curing conditions. The actual compositions of the inks are proprietary information and this provides restrictions to what can be discussed regarding its composition. However,

superior electrode performance was noted on electrodes with better carbon notably the JD type of electrodes.

This is because the carbon usually constitutes more than 80 per cent of the total ink coverage on an electrode (Cui *et al.*, 2001b; Morrin *et al.*, 2003). This is because besides being used for the counter electrode it is also used for tracking the other electrodes to complete the circuit. Electrochemical and immuno assay evaluations were done to characterise the different electrodes and identify optimum performers. Cyclic voltammetry is a key tool in the characterisation of electrodes (Garcia-Gonzalez, 2008). It was used to define the electrode's activity as well as to calculate the percentage of the available area on the working electrode. Experiments were conducted to evaluate the effect of different curing conditions on the performance of the electrode. The curing conditions of an electrode play a major role in the rate and cost of production of electrodes (Hobby, 1997). Different techniques are constantly being investigated to improve the production process by finding fast and cheaper curing alternatives.

Although infra-red drying is a faster and cheaper method than the conventional oven drying (Morrin *et al.*, 2003). The results showed that the conventional drying resulted in better performing electrodes. The findings of the electrochemical results were confirmed with imaging. The results from the scanning electron microscope showed that although the same ink was used for the working electrodes there were differences in the surface composition of the electrodes after curing them differently. This may have been caused by temperature variations and humidity conditions during the curing process (Cui *et al.*, 2001a; Grennan *et al.*, 2001). The E-SEM showed a clear difference in both the chemical composition and the morphology of the constituent particles on the gold surface. The amount of the exposed gold on the infra-red dried sensors (65.34%) was less than that from the conventionally dried electrodes (84.8%).

This may explain the superior electrochemical behaviour of the conventionally dried electrode as shown by the cyclic voltammetry and the immuno assay results. Although the IR drying may have commercial advantages on speeding the production line, it is evident that this has an impact on the quality.

### **6.1.3 Development of an Electrochemical Immunosensor for C-Reactive Protein**

An electrochemical immunosensor based on screen-printed gold electrodes was developed for the detection of C reactive protein. CRP has evolved from being a postulated marker that can possibly predict cardiovascular events and mortality to a proven direct partaker in the pathogenesis of atherosclerotic cardiovascular disease (Bisoendial *et al.*, 2010; Nagai *et al.*, 2011). This direct relationship makes it a suitable marker for inclusion on as part of a multi marker cardiac immunosensor panel. Biomarkers work better as a panel of several biomarkers so that they can complement each other in aiding diagnosis (Apple, 2007)

The electrochemical transduction method adopted for the measurement of the immunosensor signal was adopted earlier work done on the same electrodes to develop an immunosensor for the detection of salmonella (Salam and Tothill, 2009). Measurements were performed by adding 100  $\mu\text{L}$  of 4 mM TMB and 0.06%  $\text{H}_2\text{O}_2$  in 0.05 M citrate phosphate buffer plus 0.1 M KCL combined in a 1:1 ratio, with chronoamperometry methods at -200 mV constant potential. Electrochemical noise from the reagents was also investigated and thus the parameters prescribed in literature were adopted for use on this immunosensor. Electrodes that performed better (JD) in the characterisation, experiments were adopted for the development of the immunosensor. Immuno assays were developed and optimised on the microplate before being transferred for use on

the immunosensor. The direct transfer of plate-based assays on to the screen-printed electrode presented some challenges. Unlike the microwells that can easily accommodate 300  $\mu\text{L}$ , the screen-printed gold working electrode surface can hold a maximum of 35  $\mu\text{L}$  before the liquid overflows to other electrodes (Kadir and Tothill, 2010).

The most effective concentration of the coating antibody on the screen-printed electrode was 60  $\mu\text{g mL}^{-1}$ , which was exactly ten times the concentration on the plate based assay, however less volumes were needed. The highest peak response to a standardized antigen concentration was at 60  $\mu\text{g mL}^{-1}$  coating antibody concentration. It was observed that there was a characteristic tailing of the curve with concentrations of the coating antibody above 60  $\mu\text{g mL}^{-1}$ . This could be attributed to steric hindrance and other factors associated with the change in behaviour of highly concentrated antibodies (Law, 1996; Zhu *et al.*, 2003; Salam and Tothill, 2009). While the prospect of increasing signal with increasing the concentration of the antibodies were plausible, trade-offs were made to take into account the performance and costs relationship. The detection antibody exhibited similar characteristics as shown on the optimisation of the capture where there was increasing signal with increasing concentration of the antibody. The data showed that the concentration of 30  $\mu\text{g mL}^{-1}$  was the optimum for the detection antibody. The investigation of finding out the best method for the detecting the antigen showed that there are better results if the antigen is premixed with the detection antibody before being exposed to immobilised capture antibody. This is because both the antigen and the detection antibody are free in solution they have a better chance of binding (Law, 1996; D'Orazio, 2003; Zhu *et al.*, 2003). Passive adsorption was used in the immobilisation of the capture antibody on the gold working electrode. This was because the required sensitivity for the CRP assay was not stringent and could easily be achieved using passive adsorption. However, attempts were made to covalently immobilise antibodies using self-assembled monolayers SAMs. These were made using 11-mercaptoundecanoic acid (11-MUA), and 3,3-dithiodipropionic acid (DTDPA).

The action of thiol groups on metal surfaces results in the formation of semi covalent bonds on the electrode surface (Srisombat *et al.*, 2011; Altintas *et al.*, 2012). SAMs have been reported to cause improved antibody performance and stability on the sensor surface (Love *et al.*, 2005; Li *et al.*, 2009). However, in the development of CRP immunosensor the method of depositing SAMs interfered with other electrodes and since the CRP immunosensor had achieved its operational parameters this avenue was not pursued further.

The clinical reference ranges for CRP assay are  $\geq 1 \mu\text{g mL}^{-1}$  low risk,  $1-3 \mu\text{g mL}^{-1}$  is medium risk and  $\leq 3 \mu\text{g mL}^{-1}$  is high risk (Di Napoli *et al.*, 2005; McBride, 2008). The performance of the CRP immunosensor was able to achieve diagnostically relevant parameters. The developed electrochemical immunosensor was highly specific and had a LOD of  $2.6 \text{ ng mL}^{-1}$  and spanning up to  $100 \text{ ng mL}^{-1}$ , this translated to a dynamic range of  $0.52 \mu\text{g mL}^{-1}$  to  $20 \mu\text{g mL}^{-1}$  after compensating for the 200x dilution. This result was comparable to other electrochemical immunosensors for CRP that has been reported in literature (Zhou *et al.*, 2010; Shaolin *et al.*, 2011) and even had better limit of detection when compared to other reported CRP immunosensors assays (Zhu *et al.*, 2003).

Performance of the developed immunosensor was compared to that of an in-house developed ELISA and a commercial ELISA, using some spiked commercial serum samples. The performance of the commercial ELISA was superior to both the electrochemical immunosensor and the in-house optimised ELISA. This is because the commercial ELISA had the lowest calculated lower limit of detection of  $1.1 \text{ ng mL}^{-1}$ , unlike  $1.91 \text{ ng mL}^{-1}$  for the in-house ELISA and  $2.2 \text{ ng mL}^{-1}$  achieved by the immunosensor.

A correlation curve was plotted using randomly spiked samples between a commercial ELISA kit a correlation with a  $R^2$  value of 0.998 was achieved. The in-house immunosensor had an  $R^2$  value of 0.999 against the commercial ELISA. The data for comparing the showed no statistical difference in performance, to conclude a CRP immunosensor based on electrochemical transduction was developed and it performed comparably to a commercial kit.

#### **6.1.4 The Development of a Gold Nanoparticle Enhanced Immunosensor for Cardiac Troponin T**

An electrochemical immunosensor based on gold nanoparticles and self-assembled monolayers SAMs for enhanced sensitivity was developed for the detection of cardiac Troponin T (cTnT) in partly diluted serum samples. Cardiac Troponins (T and I) are cardiac isoforms of contractile proteins of the myofibril that are very specific for cardiac injury. Due to their great sensitivity and specificity for myocardial cell damage, cardiac troponins have been considered as the “gold standard” for AMI diagnosis (Alpert *et al.*, 2000; Babuin, 2005). As such they would be a suitable biomarker for inclusion in an multi marker panel alongside other markers like CRP.

The clinical reference ranges for cTnT are defined by the ability of an assay to detect 99% of laboratory baseline values. This equates to lower limit of detection levels of around  $0.03 \text{ ng mL}^{-1}$ . To achieve such high sensitivity a lot of development has to be done on the assay that incorporates techniques which helps to achieve this. Screen-printed gold electrodes with gold working electrodes similar to those used on The CRP immunosensor were modified with 11-mercaptoundecanoic acid (11-MUA) to make self-assembled monolayers (SAMs). This was to facilitate covalent immobilisation of the capture antibody using the EDC/NHS chemistry (Van Delden *et al.*, 1996).



The covalent coupling enabled higher numbers of correctly orientated coating antibodies that helps in increasing the sensitivity of the assay (Law, 1996; Chaki and Vijayamohanan, 2002). Incremental development was done in the development of the cardiac troponin immunosensor the first assay set up was based on the passive adsorption and conjugated detection antibodies and resembled that developed for CRP assay described in Chapter 3. This assay set up had a lower limit of detection LOD of  $2.12 \text{ ng mL}^{-1}$  and a maximum Coefficient of variance (CV) of 10.9%.

Further development to the assay setup was done with the use of self-assembled monolayers on the gold working electrode. As discussed earlier SAMs and have been reported to cause improved antibody performance and stability on the sensor surface (Love *et al.*, 2005; Li *et al.*, 2009), this was particularly useful in the detection of cTnT assay that has small antigen concentrations in baseline samples  $\leq 0.03 \text{ ng mL}^{-1}$  (Jaffe *et al.*, 2006). A new method of generating self-assembled monolayers on the gold working electrode using 11-MUA was developed. The method has limited exposure of the electrodes to the solvents. Exposure to solvents had been identified to cause problems with electrode performance in earlier work done on CRP immunosensor. Precautions to prevent rapid evaporation of the 11-MUA solution before the monolayer were made with the use of refrigeration and moisture tubs. Successful modification of the working electrodes was achieved and this was confirmed through cyclic voltammetry and contact angle measurements. The EDC/NHS chemistry was used to aid the covalent coupling of the coating antibodies in a manner described in previous literature (Van Delden *et al.*, 1996).

Increased signal were achieved on immunosensors with covalent immobilisation and the LOD was significantly lowered 2.12 to 1.14 ng mL<sup>-1</sup>. The next step in the development process was incorporating the use of conjugated gold nanoparticles on the assay set up to improve on sensitivity. This has been reported to have a remarkable effect in improving the sensitivity of the assay through signal amplification (Ansari *et al.*, 2010; Suprun *et al.*, 2011; Saha *et al.*, 2012; Li *et al.*, 2009). Gold nanoparticles were conjugated to HRP and the detection antibody 7E7 using passive adsorption method. Gold nanoparticles are capable of allowing more quantities of the detection reagents to be localised thus increasing the potential for enhanced signal output to occur in low antigen concentrations (Ansari *et al.*, 2010; Saha *et al.*, 2012). This has an advantage of lowering the limit of detection that is particularly important for the cTnT assay

The use of the gold nanoparticles significantly lowered the limit of detection further to 0.51 ng mL<sup>-1</sup> on buffer and 0.58 in 75% serum standards. This assay was comparable to previously reported assays that used screen printed electrodes for detecting cTnT (Silva *et al.*, 2010). The interference posed by the serum samples was too much that it grossly affected the sensor performance. Earlier work by colleagues had proven that a 75% serum dilution with PBS Tween and some additives was sufficient in reducing the nonspecific binding due to the protein matrix in serum (Uludag and Tothill, 2010) and this was adopted for the use on the immunosensor to counteract the matrix effect. A limit of detection 0.58 ng mL<sup>-1</sup> was achieved which fell short of the new requirements for the diagnosis of cardiovascular disease using cTnT. However, the immunosensor can have other applications in the screening of suspected cardiac events. Other researchers have reported achieving better limits of detection with immunosensors that utilise other assay set-ups. The use of streptavidin microsphere modified screen printed electrodes managed to achieve LOD of 0.2 ng mL<sup>-1</sup> (Silva *et al.*, 2010).

Other transduction mechanisms like surface Plasmon resonance SPR have been reported to detect cTnT to a LOD of  $0.05 \text{ ng mL}^{-1}$  (Dutra *et al.*, 2007), and the use of QCM has been reported to detect cardiac troponin t to a limit of detection of  $0.003 \text{ ng mL}^{-1}$  (Fonseca *et al.*, 2011) although some researchers reported higher LOD of  $5 \text{ ng mL}^{-1}$  (Wong-ek *et al.*, 2010). Commercial assays for the detection of cardiac Troponin T are based on mostly optical methods and have already been summarised in Table 1-3.

Comparisons were made between the developed immunosensor with a hospital analyser. The correlation results on 75% spiked commercial serum samples show that although the developed immunosensor had more standard error than the hospital analyser there was a good correlation ( $R^2$  0.991) on the results obtained using the two methods. This indicates that despite some calibrations differences between the two methods they had similar capabilities in distinguishing between different concentrations of cTnT. The development of the immunosensor needs further optimisation to reach diagnostic ranges, however current performance is sufficient to demonstrate proof of concept and screening purposes. The shelf stability of a biosensor is often one of the crucial factors on deciding commercial viability of a developed biosensor (Fernandez-Lafuente *et al.*, 1999). In this Chapter, investigations on to the preservation of immobilised antibodies were done using self-assembled monolayers (SAMs) and a commercial product Stabiliguard® which contain a combination of polyelectrolytes and polyhydroxyl compounds. The use of self-assembled monolayers has been demonstrated to have a positive impact on the stabilisation of the immobilised proteins (Wink *et al.*, 1997; Altintas *et al.*, 2012). Although SAMs were used in the assay for other benefits, including improved signals due to controlled antibody orientation, they were evaluated for their role in stabilising immobilised reagents to maintain prolonged functionality. The results showed that both the use of SAMs and the application of Stabiliguard® effectively preserved the functionality of the immunosensor.

## 6.2 Future Work

There are a lot of interesting areas in immunosensor development that may be investigated further in future work. These span the whole spectrum of interrelated areas including sensor fabrication, to integration of immunosensors with compatible microfluidic devices. In the sensor fabrication area, there are major restrictions as current sensor compositions, inks and curing methods are withheld by manufacturers as either protected intellectual property, or commercial secrets aimed at gaining competitive advantage. Should resources appear and information barriers be broken, more work could be done on the investigating the inclusion of other materials on the electrode. This can help to investigate performance of electrodes absent of secret ingredients and identify key parameters for enhanced screen printed electrode performance. Investigating the benefits of incorporating other rare metals like platinum may have been attempted in this work if time and resources had permitted, the inclusion of masking compounds that prevent electrode degradation during rapid curing is also a potential minefield for future studies. On the fabrication processes, it may have been worthwhile to look at the effect of other environmental conditions like humidity, as well as increasing the array of curing temperatures and conditions that were investigated. There is also the possibility of investigating different ink thicknesses and evaluating if there were any economic and performance benefits associated with using small ink quantities to make microelectrodes. Another interesting area that may need to be explored in the future is to compare the screen-printed electrodes against others fabricated with other methods including inkjet printed using the same materials.

The technical set up of the immunosensors can benefit from other non-antibody based molecules like aptamers and molecular imprinted polymers. These molecules have been demonstrated to provide remarkable interactions with antigens with specificities and sensitivities often superior to those of traditional antibodies. Although gold nanoparticles were not used in the CRP assay this can be explored in future to improve the assay sensitivity. The conjugation of the gold nanoparticles in the cardiac Troponin T assay was done passively, this

is an uncontrolled process that results in variation and decreases assay capability.

The potential of covalently immobilising the detection antibodies and the HRP on the nanoparticles using coupling chemistries like EDC/HNS would help standardise the assay. The improvements on the use of EDC/NHS chemistries on the immunosensor were demonstrated and thus such improvements can be enjoyed if the gold nanoparticles were conjugated in a similar manner.

The development of an integrated sub circuit for both the C-reactive protein and cardiac Troponin T capable of simultaneous detection would be a good way forward. This is because most clinical results from cardiac markers are more useful if they are part of a panel of several markers providing several a set of results from a single sample. This helps the doctors to give a more accurate diagnosis as well as lowering turnaround times as well as maximising output from samples. The integration of the immunosensors to a micro fluidic device capable of controlling sample and substrate movement will progress the work further towards becoming a commercial product.

### 6.3 Final Conclusions

The overall results achieved in this study include the development immunosensors for the detection of c ardiac markers that can easily be integrated to form a multi marker panel.

Key Achievements of this study are listed below

- The investigation of the best curing methods and suitable ink combinations for the development of screen-printed of electrodes with enhanced performance.
- The development and optimisation of an ELISA assay for C reactive protein which can detect diagnostically relevant CRP concentrations in serum with comparable measurement to a commercial alternative
- The development and optimisation of an immunosensor for C reactive protein using screen-printed gold electrodes, capable of detecting diagnostically relevant ranges of CRP in serum with comparable measurement to a commercial alternative
- The development of an ELISA assay for Cardiac Troponin T
- The development and optimisation of an immunosensor for cardiac Troponin T using screen-printed gold electrodes.
- The development of a method for modifying the sensor surface with self-assembled monolayer in a sensor friendly way
- The optimisation and preservation of the immunosensor performance for cardiac Troponin T using self-assembled monolayers.
- The amplification of the detection signal using gold nanoparticles on the cardiac troponin immunosensor
- The investigation of methods for enhancing immuno sensor shelf life

The main objective of the development of a multi sensor for the detection of biomarkers for cardiovascular disease has been met.

## REFERENCES

## REFERENCES

- A.E.T Ltd.(2012), *Mechanisms of protein stabilisation*, available at: [http://www.gwent.org/aet\\_protein\\_stabilisation.html](http://www.gwent.org/aet_protein_stabilisation.html).
- Abbott.(2011), *Integrating i-STAT into Your Electronic Systems*, available at: <http://www.abbottpointofcare.com/Products-and-Services/Integrating-iSTAT>, Accessed 20 November, 2011
- Ackerson, C.J., Jadzinsky, P.D., Jensen, G.J. & Kornberg, R.D.(2006)," Rigid, Specific, and Discrete Gold Nanoparticle/Antibody Conjugates", *Journal of the American Chemical Society*, 128,2635-2640.
- Adame, I.M., De Koning, P.J.H., Lelieveldt, B.P.F., Wasserman, B.A., Reiber, J.H.C. & Van Der Geest, R.J.(2006)," An integrated automated analysis method for quantifying vessel stenosis and plaque burden from carotid MRI images - Combined postprocessing of MRA and vessel wall MR", *Stroke*, 37,2162-2164.
- Ahmed, N., Dawson, M., Smith, C. & Wood, E. (eds.) (2007), *Biology of Disease*, Taylor and Francis, New York
- Ahmed, N., Dawson, M., Smith, C., Wood, E. (ed.) (2007), *Biology of Disease*, Taylor and Francis, New York
- Alderman, C.J., Bunyard, P.R., Chain, B.M., Foreman, J.C., Leake, D.S. & Katz, D.R.(2002)," Effects of oxidised low density lipoprotein on dendritic cells: a possible immunoregulatory component of the atherogenic micro-environment?", *Cardiovascular Research*, 55,806-819.
- Allender, S., Peto, V., Scarborough, P., Boxer, A., Rayner, M., Leal, J., Fernandez, R. & Gray, A. 2008a. European Cardiovascular Statistics 2008. *European Cardiovascular Statistics 2008*. Oxford: British Heart Foundation Health Promotion Group.
- Allender, S., Scarborough, P., O'flaherty, M. & Capewell, S.(2008b)," Patterns of coronary heart disease mortality over the 20th century in England and Wales: Possible plateaus in the rate of decline", *BMC Public Health*, 8,148.
- Alpert, J.S., Thygesen, K., Antman, E. & Bassand, J.P.(2000)," Myocardial infarction redefined--a consensus document of The Joint European Society of Cardiology/American College of Cardiology Committee for the redefinition of myocardial infarction", *American Journal of College Cardiology*, 36,959-969.
- Altintas, Z., Uludag, Y., Gurbuz, Y. & Tothill, I.(2012)," Development of surface chemistry for surface plasmon resonance based sensors for the detection of proteins and DNA molecules", *Analytica Chimica Acta*, 712,138-144.



- Alvarez, M.J.B., Abedul, M.T.F. & Garcia, A.C.(2002)," Flow amperometric detection of indigo for enzyme-linked immunosorbent assays with use of screen-printed electrodes", *Analytica Chimica Acta*, 462,31-37.
- Alvarezicaza, M. & Bilitewski, U.(1993)," Mass-Production of Biosensors", *Analytical Chemistry*, 65,A525-A533.
- Ambrosi, A., Airò, F. & Merkoçl, A.(2009)," Enhanced Gold Nanoparticle Based ELISA for a Breast Cancer Biomarker", *Analytical Chemistry*, 82,1151-1156.
- Amrita, U.(2012), *Immunology Virtual Lab*, available at: <http://amrita.vlab.co.in/?sub=3&brch=69>.
- Anand, I.S., Latini, R., Florea, V.G., Kuskowski, M.A., Rector, T., Masson, S., Signorini, S., Mocarelli, P., Hester, A., Glazer, R. & Cohn, J.N.(2005)," C-reactive protein in heart failure: prognostic value and the effect of valsartan", *Circulation*, 112,1428-1434.
- Anand, S.S. & Yusuf, S.(2010)," C-reactive protein is a bystander of cardiovascular disease", *European Heart Journal*, 31,2092-2096.
- Anderson, L.(2005)," Candidate-based proteomics in the search for biomarkers of cardiovascular disease", *Journal of Physiology*, 563,23-60.
- Ansari, A.A., Alhoshan, M., Alsalhi, M.S. & Aldwayyan, A.S.(2010)," Prospects of nanotechnology in clinical immunodiagnostics", *Sensors*, 10,6535-6581.
- Apple, F.S.(2007)," Cardiac troponin monitoring for detection of myocardial infarction: newer generation assays are here to stay", *Clinica Chimica Acta*, 380,1-3; discussion 245-246.
- Arya, S.K., Chornokur, G., Venugopal, M. & Bhansali, S.(2010)," Antibody functionalized interdigitated [small mu ]-electrode (ID[small mu ]E) based impedimetric cortisol biosensor", *Analyst*, 135,1941-1946.
- Avrameas, S.(1969)," Coupling of enzymes to proteins with glutaraldehyde", *Immunochemistry*, 6 43-52.
- Azzazy, H., Christenson Rh.(2002)," Cardiac markers of acute coronary syndromes: is there a case for point-of-care testing?", *Clinical Biochemistry*, 35,13–27.
- Babuin L, J.A.(2005)," Troponin:the biomarker of choice for the detection of myocardial injury", *Canadian Medical Association Journal*, 173,1191-1202.
- Babuin, L., Jaffe As (2005)," Troponin: the biomarker of choice for the detection of myocardial injury", *Canadian Medical Association Journal*, 173,1191–1202.

- Bard, J.F., L. R (2001), *Electrochemical Methods: Fundamentals and Applications*, John Wiley and Sons,
- Biosite.(2009), *Triage ® Cardiac Panel*, available at: <http://www.biosite.com/products/cardiac.aspx>
- Bisoendial, R.J., Matthijs, B., Menno, V., Erik, S.G. & Kastelein, J.P.(2010)," C-reactive protein is a mediator of cardiovascular disease", *European Heart Journal*, 31,2087–2095.
- Bolduc, O.R. & Masson, J.-F.O.(2008)," Monolayers of 3-Mercaptopropyl-amino Acid to Reduce the Nonspecific Adsorption of Serum Proteins on the Surface of Biosensors", *Langmuir*, 24,12085-12091.
- Braunwald, E.(1997)," Shattuck lecture--cardiovascular medicine at the turn of the millennium: triumphs, concerns, and opportunities", *New England Journal of Medicine*, 337,1360-1369.
- Braunwald, E.(2008)," Medical Progress: Biomarkers in Heart Failure", *New England Journal of Medicine*, 358,2148-2159.
- Breathnach, C.S. & Westphal, W.(2006)," Early detectors of the heart's electrical activity", *Pace-Pacing and Clinical Electrophysiology*, 29,422-424.
- Brogan, G.X., Jr., Friedman, S., Mccuskey, C., Cooling, D.S., Berrutti, L., Thode, H.C., Jr. & Bock, J.L.(1994)," Evaluation of a new rapid quantitative immunoassay for serum myoglobin versus CK-MB for ruling out acute myocardial infarction in the emergency department", *Annals of Emergency Medicine*, 24,665-671.
- Brown, D.A., Breit, S. N., Buring, J., Fairlie, W. D., Bauskin, A. R., Liu, T. And Ridker, P. M.(2002)," "Concentration in Plasma of Macrophage Inhibitory Cytokine-1 and Risk of Cardiovascular Events in Women: A Nested Case-Control Study"", *Lancet*, 359,2159-2163.
- Bunde, R.L., Jarvi, E.J. & Rosentreter, J.J.(1998)," Piezoelectric quartz crystal biosensors", *Talanta*, 46,1223-1236.
- Cai, J.M., Hatsukami, T.S., Ferguson, M.S., Kerwin, W.S., Saam, T., Chu, B.C., Takaya, N., Polissar, N.L. & Yuan, C.(2005)," In vivo quantitative measurement of intact fibrous cap and lipid-rich necrotic core size in atherosclerotic carotid plaque - Comparison of high-resolution, contrast-enhanced magnetic resonance imaging and histology", *Circulation*, 112,3437-3444.
- Chaki, N.K. & Vijayamohanan, K.(2002)," Self-assembled monolayers as a tunable platform for biosensor applications. ", *Biosensors and Bioelectronics*, 17,1-12.
- Chen, X., Wang, Y., Zhou, J., Yan, W., Li, X. & Zhu, J.-J.(2008)," Electrochemical Impedance Immunosensor Based on Three-

- Dimensionally Ordered Macroporous Gold Film", *Analytical Chemistry*, 80,2133-2140.
- Choi, S. & Chae, J.(2010)," Methods of reducing non-specific adsorption in microfluidic biosensors", *Journal of Micromechanics and Microengineering*, 20,1-9.
- Christenson, R.a.A., Hme.(1998)," Biochemical markers of the acute coronary syndromes", *Clinical chemistry*, 44,1855–1864.
- Clark, L.C., Jr. & Lyons, C.(1962)," Electrode systems for continuous monitoring in cardiovascular surgery", *Annals New Yourk Academy of Sciences*, 102,29-45.
- Cotran, R., Kumar, V. & Collins, T. (1999), *Pathologic Basis of Disease*, W.B. Saunders Company., Philadelphia.
- Cotran R, K.V., Collins T (1999), *Pathologic Basis of Disease*, W.B. Saunders Company., Philadelphia.
- Cui, G., Yoo, J.H., Lee, J.S., Yoo, J., Uhm, J.H., Cha, G.S. & Nam, H.(2001a)," Effect of pre-treatment on the surface and electrochemical properties of screen-printed carbon paste electrodes", *Analyst*, 126,1399-1403.
- Cui, J.B., Robertson, J. & Milne, W.I.(2001b)," Improved electron emission from carbon film using a resistive layer", *Journal of Applied Physics*, 89,3490-3493.
- D'orazio, P.(2003)," Biosensors in clinical chemistry", *Clinica Chemica Acta*, 334,41-69.
- Da Silva, S.H. & Moresco, R.N.(2011)," Cardiac biomarkers for assessment of acute coronary syndrome", *Biomarcadores cardíacos na avaliação da síndrome coronariana aguda*, 21,132-142.
- Darain, F., Park, S.U. & Shim, Y.B.(2003)," Disposable amperometric immunosensor system for rabbit IgG using a conducting polymer modified screen-printed electrode", *Biosensors and Bioelectronics*, 18,773-780.
- Davies, R.J., Eapen, S. S. And Carlisle, S. J (2007 ), *Handbook of biosensors and biochips*, John Wiley, Chichester, West Sussex, England.
- De Cordt, S., Hendrickx, M., Maesmans, G. & Tobback, P.(1994)," The influence of polyalcohols and carbohydrates on the thermostability of  $\alpha$ -amylase", *Biotechnology and Bioengineering*, 43,107-114.
- Decaterina, R., Libby, P., Peng, H.B., Thannickal, V.J., Rajavashisth, T.B., Gimbrone, M.A., Shin, W.S. & Liao, J.K.(1995)," Nitric-Oxide Decreases Cytokine-Induced Endothelial Activation - Nitric-Oxide Selectively Reduces Endothelial Expression of Adhesion Molecules and Proinflammatory Cytokines", *Journal of Clinical Investigation*, 96,60-68.

- Di Napoli, M., Schwaninger, M., Cappelli, R., Ceccarelli, E., Di Gianfilippo, G., Donati, C., Emsley, H.C.A., Forconi, S., Hopkins, S.J., Masotti, L., Muir, K.W., Paciucci, A., Papa, F., Roncacci, S., Sander, D., Sander, K., Smith, C.J., Stefanini, A. & Weber, D.(2005)," Evaluation of C-reactive protein measurement for assessing the risk and prognosis in ischemic stroke - A statement for health care professionals from the CRP pooling project members", *Stroke*, 36,1316-1329.
- Dickason, R.R., Huston, M.M. & Huston, D.P.(1994)," Enhanced detection of human IL-5 in biological fluids utilizing murine monoclonal antibodies which delineate distinct neutralizing epitopes", *Cytokine*, 6,647-656.
- Dutra, R.F. & Kubota, L.T.(2007)," An SPR immunosensor for human cardiac troponin T using specific binding avidin to biotin at carboxymethyl-dextran-modified gold chip", *Clinica Chimica Acta*, 376,114-120.
- Dutra, R.F., Mendes, R.K., Lins Da Silva, V. & Kubota, L.T.(2007)," Surface plasmon resonance immunosensor for human cardiac troponin T based on self-assembled monolayer", *Journal of Pharmaceutical and Biomedical Analysis*, 43,1744-1750.
- Dzyadevych, S.V., Arkhypova, V.N., Soldatkin, A.P., El'skaya, A.V., Martelet, C. & Jaffrezi-Renault, N.(2008)," Amperometric enzyme biosensors: past, present and future.", *Innovation et technologie en biologie et médecine (ITBMRBM)*, 29,171-180.
- Ellertsen, I., Petri, H.M., Bäck, M.(2011)," Atherosclerosis, inflammation and leukotrienes", *Michael Quarterly*, 8,514-522.
- Emdin, M., Passino, C. And Clerico, A.(2011)," "Natriuretic Peptide Assays Revisited: Do we need Pro-B-type Natriuretic Peptide?""", *Journal of the American College of Cardiology*, 57,1396-1398.
- Engvall, E., And Perlman, P.(1971)," "Enzyme-linked immunosorbent assay (ELISA). Quantitative assay of immunoglobulin G""", *Immunochemistry*, 8,871-874.
- Erlenkotter, A., Kottbus, M.,Chemnitius, G.C.(2000)," Flexible amperometric transducers for biosensors based on a screen printed three electrode system", *Journal of Electroanalytical Chemistry*, 481 82-94.
- F.D.A.(2001), *Guidance for Industry Bioanalytical Method Validation*, available at: <http://www.fda.gov/downloads/Drugs/.../Guidances/ucm070107.pdf>.
- Fernandez-Lafuente, R., Rodríguez, V., Mateo, C., Penzol, G., Hernandez-Justiz, O., Irazoqui, G., Villarino, A., Ovsejevi, K., Batista, F. & Guisán, J.M.(1999)," Stabilization of Multimeric Enzymes via Immobilization and Post-Immobilization Techniques", *Journal of Molecular Catalysis B: Enzymatic*, 7.

- Fernandez-Ortiz, A., Meyer, B., Chesebro, J.H., Fuster, V. & Badimon, J.J.(1995)," Potential applications of iontophoresis for local drug delivery of vascular diseases", *Journal of Interventional Cardiology*, 8,420-426.
- Fonseca, R.a.S., Ramos-Jesus, J., Kubota, L.T. & Dutra, R.F.(2011)," A Nanostructured Piezoelectric Immunosensor for Detection of Human Cardiac Troponin T", *Sensors*, 11,10785-10797.
- Freymuth, P. & Sauebray, G.(1963)," Ausheilung von Bestrahlungsschäden in Quarz-Schwingkristallen", *Journal of Physics and Chemistry of Solids*, 24,151-155
- Furuya, M., Haramura, M. & Tanaka, A.(2006)," Reduction of nonspecific binding proteins to self-assembled monolayer on gold surface", *Bioorganic & Medicinal Chemistry*, 14 537-543.
- Galan-Vidal, C.A., Muñoz, J., Dominguez, C., Alegret, S.(1998)," Glucose biosensor strip in a three electrode configuration based on composite and biocomposite materials applied by planar thick film technology", *Sensors and Actuators*, B,257–263.
- Garcia-Cardena, G., Comander, J., Anderson, K.R., Blackman, B.R. & Gimbrone, M.A.(2001)," Biomechanical activation of vascular endothelium as a determinant of its functional phenotype", *Proceedings of the National Academy of Sciences of the United States of America*, 98,4478-4485.
- Garcia-Gonzalez, R., Fernandez-Abedul, M.T., Pernia, A .,Costa-Garcia, A.(2008)," Electrochemical characterization of different screen-printed gold electrodes", *Electrochimica Acta*, 3242–3249.
- Gauthier, T.W., Scalia, R., Murohara, T., Guo, J.P. & Lefer, A.M.(1995)," Nitric oxide protects against leukocyte-endothelium interactions in the early stages of hypercholesterolemia", *Arteriosclerosis Thrombosis and Vascular Biology*, 15,1652-1659.
- Gerszten, R.E. & Wang, T.J.(2008)," The search for new cardiovascular biomarkers", *Nature*, 451,949-952.
- Gibson, T.D.(1999)," Biosensors:The Stability Problem", *Analysis*, 27,630-638.
- Gomes-Filho, S.L.R., Dias, A.C.M.S., Silva, M.M.S., Silva, B.V.M. & Dutra, R.F. A carbon nanotube-based electrochemical immunosensor for cardiac troponin T", *Microchemical Journal*.
- Gosser, D.K. 1993. Cyclic Voltammetry: Simulation and Analysis of Reaction Mechanisms. New York.
- Grant, S.A., Lichlyter, D.J., Pierce, M.E., Boettcher, L. & Soykan, O.(2004)," Investigation of a FRET immunosensor technique for the detection of cardiac troponin T and I", *Sensor Letters*, 2,58-63.

- Gray, H., Dawkins, K., Morgan, J., Simpson, I. (2002a), *Lecture Notes on Cardiology* Blackwell Publishing, Oxford.
- Gray H, D.K., Morgan J, Simpson I. (2002), *Lecture Notes on Cardiology* Blackwell Publishing, Oxford.
- Gray, J.(2002b)," Treating isolated systolic hypertension prevented major cardiovascular events across strata of risk in older patients", *Journal of American College of Physicians*, 137,4.
- Grennan, K., Killard, A.J. & Smyth, M.R.(2001)," Physical characterizations of a screen-printed electrode for use in an amperometric biosensor system", *Electroanalysis*, 13,745-750.
- Grocott, H.P., White, W.D., Morris, R.W., Podgoreanu, M.V., Mathew, J.P., Nielsen, D.M., Schwinn, D.A. & Newman, M.F.(2005)," Genetic polymorphisms and the risk of stroke after cardiac surgery", *Stroke*, 36,1854-1858.
- Hanson, G., Nilson, J.(2008)," Introduction: Atherosclerosis as inflammation: A controversial concept becomes accepted.", *Journal of Internal Medicine*, 263,462-463.
- Hao, R., Wang, D., Zhang, X., Zuo, G., Wei, H., Yang, R. & Zhang, Z.(2009)," Rapid detection of Bacillus anthracis using monoclonal antibody functionalized QCM sensor", *Biosensors and Bioelectronics*, 24,1330-1335.
- Hennessey, H., Afara, N., Omanovic, S. & Padjen, A.L.(2009)," Electrochemical investigations of the interaction of C-reactive protein (CRP) with a CRP antibody chemically immobilized on a gold surface", *Analytica Chimica Acta*, 643,45-53.
- Heurich, M.a.K., M. K. And Tothill, I.E. .(2011)," An electrochemical sensor based on carboxymethylated dextran modified gold surface for ochratoxin A analysis", *Sensors and Actuators B: Chemical*, 156,162-168.
- Heuser, J.(1999), *A Scan of two video prints of a sclerotic artery*, available at: <http://lexikon.freenet.de/Koronarangiografie>.
- Hobby, A.(1997), *Printing thick film hybrids* available at: [http://www.gwent.org/gem\\_thick\\_film.html](http://www.gwent.org/gem_thick_film.html).
- Hochholzer, W., Morrow, D. A. And Giugliano, R. P.(2010a)," "Novel Biomarkers in Cardiovascular Disease: Update 2010"", *American Heart Journal*, 160 583-594.

- Hochholzer, W., Morrow, D. A. And Giugliano, R. P.(2010b)," Novel Biomarkers in Cardiovascular Disease: Update 2010", *American Heart Journal*, 160,583-594.
- Hu, S.Q., Xie, J.W., Xu, Q.H., Rong, K.T., Shen, G.L. & Yu, R.Q.(2003)," A label-free electrochemical immunosensor based on gold nanoparticles for detection of paraoxon", *Talanta*, 61,769-777.
- Huether, S. & Mccance, K. (2004), *Understanding Pathophysiology.* , Mosby Incorporated, St. Louis.
- Invitrogen.(2012), *Antibody-Structure-and-Classification*, available at: <http://www.invitrogen.com/site/us/en/home/References/Molecular-Probes-The-Handbook/Technical-Notes-and-Product-Highlights/Antibody-Structure-and-Classification.html>.
- Iwanaga, Y.a.M., S.(2010)," Heart Failure, Chronic Kidney Disease,and Biomarkers--An Integrated Viewpoint", *Journal of the Japanese Circulation Society*, 74,1274-1282.
- Iwasaki, Y., Horiuchi, T. & Niwa, O.(2001)," Detection of electrochemical enzymatic reactions by surface plasmon resonance measurement", *Analytical Chemistry*, 73,1595-1598.
- Jaffe, A.S., Babuin, L. & Apple, F.S.(2006)," Biomarkers in acute cardiac disease: the present and the future", *Journal of American College Cardiology*, 48,1-11.
- Jawaheer, S., White, S.F., Rughooputh, S.D.D.V. & Cullen, D.C.(2002)," Enzyme stabilisation using pectin as a novel entrapment matrix in biosensors ", *Analytical Letters*, 35,2077-2091.
- Jeremias, A., Gibson C.M.(2005)," Narrative review: alternative causes for elevated cardiac troponin levels when acute coronary syndromes are excluded. ", *Annals International Medicine*, 142,786-791.
- Jongh-Leuvenink, J., Bouter, A.S., Marcelis, J.H., Schellekens, J. & Verhoef, J.(2005)," Cross-reactivity of monoclonal antibodies against lipopolysaccharides of gram-negative bacteria", *European Journal of Clinical Microbiology & Infectious Diseases*, 5,148-151.
- Jubete, E., Loaiza, O.A., Ochoteco, E., Pomposo, J.A., Grande, H., Rodr, #237 & Guez, J.(2009)," Nanotechnology: A Tool for Improved Performance on Electrochemical Screen-Printed (Bio)Sensors", *Journal of Sensors*, 2009.
- Kadir, M.K. & Tothill, I.E.(2010)," Development of an electrochemical immunosensor for fumonisins detection in foods", *Toxins (Basel)*, 2,382-398.
- Kannel, W.B., Castelli, W.P. & Gordon, T.(1979)," Cholesterol in the prediction of atherosclerotic disease. New perspectives based on the Framingham study", *Annals of International Medicine*, 90,85-91.

- Kawaguchi, T., D.R. , Shankaran, S.J., Kima, K.V., Gobi, K., Matsumoto, K., Toko, N. & Miura, N.(2007)," Fabrication of a novel immunosensor using functionalized self assembled monolayer for trace level detection of TNT by surface plasmon resonance", *Talanta*, 72 554–560.
- Kemeny, D.M. & Chantler, S. (1989), "*An Introduction to ELISA*", John Wiley & Sons Ltd, Oxford, UK.
- Kempf, T., Horn-Wichmann, R., Brabant, G., Peter, T., Allhoff, T., Klein, G.,Drexler, H., Johnston, N., Wallentin, L. And Wollert, K. C.(2007)," "Circulating Concentrations of Growth-Differentiation Factor 15 in Apparently Healthy Elderly Individuals and Patients with Chronic Heart Failure as Assessed by a New Immunoradiometric Sandwich Assay"", *Clinical chemistry*, 53,284-291.
- Kempf, T., Sinning, J. -M., Quint, A., Bickel, C., Sinning, C., Wild, P. S.,Schnabel, R., Lubos, E., Rupprecht, H. J., Münzel, T., Drexler, H.,Blankenberg, S. And Wollert, K. C.(2009)," "Growth-Differentiation Factor-15 for Risk Stratification in Patients with Stable and Unstable Coronary Heart Disease: Results from the AtheroGene Study"", *Circulation Cardiovascular Genetics*, 2,286-292.
- Khan, S.Q., Dhillon, O. S., O'brien, R. J., Struck, J., Quinn, P. A., Morgenthaler, N. G., Squire, I. B., Davies, J. E., Bergmann, A. And Ng, L. L.(2007 )," "C-terminal Provasopressin (Copeptin) as a Novel and Prognostic Marker in Acute Myocardial Infarction: Leicester Acute Myocardial Infarction Peptide (LAMP) Study"", *Circulation*, 115,2103-2110.
- Kimseng, K. & Meissel, M.(2001), *Short overview about the ESEM Environmental Scanning Electron Microscope*, available at: <http://www.calce.umd.edu/TSFA/ESEM.pdf>,Accessed 2/12/2001.
- Kohler, G., Milstein, C.(1976)," Derivation of specific antibody producing tissue culture and tumor lines by cell fusion", *European Journal of Immunology*, 6,511-519.
- Kumar, G. & Prabhu, K.N.(2007)," Review of Non-Reactive and Reactive Wetting of Liquids on Surfaces", *Advances in Colloid and Interface Science.*, 133,61-89.
- Kwon, H.J., Peiper, S.C., Kang, K.A.(2003)," Fiber optic immunosensors for cardiovascular disease diagnosis: quantification of Protein C, Factor V Leiden, and cardiac Troponin T in plasma", *Oxygen Transport to Tissue Volume Xxiii*, 115-119.
- Laing, S., Ellis, M. & Greenhalgh, R. 1991. Who should be investigated for occult atherosclerotic disease? Occult Atherosclerotic Disease. *Occult Atherosclerotic Disease*. Dordrecht: Academic Publishers.



- Law, B. (1996), *Immunoassay: A Practical Guide*, Taylor and Francis,, London.
- Lee, B.K., Kwon, H.M., Hong, B.K., Park, B.E., Suh, S.H., Cho, M.T., Lee, C.S., Kim, M.C., Kim, C.J., Yoo, S.S. & Kim, H.S.(2001)," Hemodynamic effects on atherosclerosis-prone coronary artery: wall shear stress/rate distribution and impedance phase angle in coronary and aortic circulation", *Yonsei Medical Journal*, 42,375-383.
- Li, J., Liu, R. & Yu, J.( 2009)," A gold electrode modified with self-assembled diethylenetriaminepentaacetic acid via charge-based discrimination", *Analytical sciences the international journal of the Japan Society for Analytical Chemistry*, 25,1289-1293.
- Licka, M., Zimmermann, R., Zehelein, J., Dengler, T.J., Katus, H.A. & Kubler, W.(2002)," Troponin T concentrations 72 hours after myocardial infarction as a serological estimate of infarct size", *Heart*, 87,520-524.
- Liedberg, B., Nylander, C. & Lundstrom, I.(1995)," Biosensing with surface plasmon resonance--how it all started", *Biosensors and Bioelectronics*, 10,i-ix.
- Liu, X., Wu, H., Zheng, Y., Wu, Z., Jiang, J., Shen, G. & Yu, R.(2010)," A Sensitive Electrochemical Immunosensor for  $\alpha$ -Fetoprotein Detection with Colloidal Gold-Based Dextrin Enzyme Complex Amplification", *Electroanalysis*, 22,244-250.
- Love, J.C., Estroff, L.A., Kriebel, J.K., Nuzzo, R.G. & Whitesides, G.M.(2005)," Self-Assembled Monolayers of Thiolates on Metals as a Form of Nanotechnology", *Chemical Reviews*, 105,1103-1170.
- Luo, X., Morrin, A., Killard, A.J. & Smyth, M.R.(2006)," Application of Nanoparticles in Electrochemical Sensors and Biosensors. ", *Electroanalysis*., 18,319 – 326.
- Luppa, P.B., Müller, C., Schlichtiger, A. & Schlebusch, H.(2011 )," Point-of-care testing (POCT): Current techniques and future perspectives", *Trends in Analytical Chemistry*, 30,887-898.
- Mackay, J., Mensah, G.A., Mendis, S., Greenlund, K. & World Health Organization. (2004), *The atlas of heart disease and stroke*, World Health Organization, Geneva.
- Males, R.G., Stephenson, J. & Harris, P.(2001)," Cardiac markers and point-of-care testing: a perfect fit", *Critical Care Nursing Quarterly*, 24,54-61.
- Mao, K., Wu, D., Li, Y., Ma, H., Ni, Z., Yu, H., Luo, C., Wei, Q. & Du, B.(2012)," Label-free electrochemical immunosensor based on graphene/methylene blue nanocomposite", *Analytical Biochemistry*, 422,22-27.
- Martin, M.J., Browner, W.S., Wentworth, D., Hulley, S.B. & Kuller, L.H.(1986)," Serum-Cholesterol, Blood-Pressure, and Mortality - Implications from a Cohort of 361 662 Men", *Lancet*, 2,933-936.

- Martins, J.T., Li, D.J., Baskin, L.B., Jialal, I. & Keffer, J.H.(1996)," Comparison of cardiac troponin I and lactate dehydrogenase isoenzymes for the late diagnosis of myocardial injury", *American Journal of Clinical Pathology*, 106,705-708.
- Masson, J.F., Obando, L., Beaudoin, S. & Booksh, K.(2004)," Sensitive and real-time fiber-optic-based surface plasmon resonance sensors for myoglobin and cardiac troponin I", *Talanta*, 62,865-870.
- Mcateer, K., Simpson, C.E., Gibson, T.D., Gueguen, S., Boujtita, M. & Murr, M.(1999)," Proposed Model for Shelf-Life Prediction of Stabilised Commercial Enzyme-Based Systems and Biosensors", *Journal of Molecular Catalysis B:Enzymatic*, 7.
- Mcbride, J.M.a.C., M.A.(2008)," A high sensitivity assay for the inflammatory marker C-Reactive protein employing acoustic biosensing", *Nanobiotechnology*, 6,1-8.
- Mcdonnell, B., Hearty, S., Leonard, P. & O'kenedy, R.(2009)," Cardiac biomarkers and the case for point-of-care testing", *Clinical Biochemistry*, 42,549-561.
- Mcdonnell, J.M.(2001)," Surface plasmon resonance: towards an understanding of the mechanisms of biological molecular recognition", *Current Opinion in Chemical Biology*, 5,572-577.
- Melanson, S.F. & Tanasijevic, M.J.(2005)," Laboratory diagnosis of acute myocardial injury", *Cardiovascular Pathology*, 14,156-161.
- Mendelson, Y. (2000), *Optical Sensors*, CRC Press LLC, Boca Raton.
- Meyer, M.H., Hartmann, M. & Keusgen, M.(2006)," SPR-based immunosensor for the CRP detection--a new method to detect a well known protein", *Biosensors and Bioelectronics*, 21,1987-1990.
- Miller, M., Zhan, M. & Havas, S.(2005)," High attributable risk of elevated C-reactive protein level to conventional coronary heart disease risk factors: the Third National Health and Nutrition Examination Survey", *Archives of Internal Medicine*, 165,2063-2068.
- Mohammed, M.I. & Desmulliez, M.P.Y.(2011)," Lab-on-a-chip based immunosensor principles and technologies for the detection of cardiac biomarkers: A review", *Lab on a Chip - Miniaturisation for Chemistry and Biology*, 11,569-595.
- Morrin, A., Killard, A.J. & Smyth, M.R.(2003)," Electrochemical characterization of commercial and home-made screen-printed carbon electrodes", *Analytical Letters*, 36,2021-2039.
- Mrksich, M. & Whitesides, G.M.(1996)," Using self-assembled monolayers to understand the interactions of man-made surfaces with proteins and

- cells", *Annual Review of Biophysics and Biomolecular Structure*, 25,55-78.
- Murray, C.J. & Lopez, A.D.(1997)," Global mortality, disability, and the contribution of risk factors: Global Burden of Disease Study", *Lancet*, 349,1436-1442.
- Muskopf, S.(2012), *Biology Corner: Anatomy, Circulatory Images*, available at: <http://www.biologycorner.com/anatomy/circulatory/images/ecg03.gif>.
- Nagai, T., Anzai, T., Kaneko, H., Mano, Y., Anzai, A., Maekawa, Y., Takahashi, T., Meguro, T., Yoshikawa, T. & Fukuda, K.(2011)," C-reactive protein overexpression exacerbates pressure overload-induced cardiac remodeling through enhanced inflammatory response", *Hypertension*, 57,208-215.
- Newman, J.D. & Turner, A.P.F.(1994)," Biosensors - the Analysts Dream", *Chemistry & Industry*, 374-378.
- Noh, M.F. & Tothill, I.E.(2006)," Development and characterisation of disposable gold electrodes, and their use for lead(II) analysis", *Analytical and Bioanalytical Chemistry*, 386,2095-2106.
- Novak, K.(1998)," Cardiovascular disease increasing in developing countries", *Nature Medicine*, 4,989-990.
- O'dwyer, C., Gay, G., Viaris De Lesegno, B. & Weiner, J.(2004)," The Nature of Alkanethiol Self-Assembled Monolayer Adsorption on Sputtered Gold Substrates", *Langmuir*, 20,8172-8182.
- O'regan, T., Pravda, M., O'sullivan, C.K., and Guilbault, G.G.(2003)," 'Development of Biosensor Array for Rapid Detection of Cardiac Markers: Immunosensor for Detection of Free Cardiac Troponin I'", *Analytical Letters*, 36,1903-1920.
- Oh, B.K., Lee, W., Chun, B. S., Bae, Y. M., Lee, W. H. & Choi, J. W.(2005)," The fabrication of protein chip based on surface plasmon resonance for detection of pathogens.", *Biosensors and Bioelectronics*, 20,1847–1850.
- Open University.(2010), *Understanding Cardiovascular Disease*, available at: <http://open.jorum.ac.uk/xmlui/bitstream/handle/123456789/972/PreviewIndexBitstream?sequence=122>, Accessed 15 January 2010.
- Osborne, M.D., Seddon, B.J., Dryfe, R.a.W., Lagger, G., Loyall, U., Schafer, H. & Girault, H.H.(1996)," Excimer laser-induced electrochemical activity in carbon ink films", *Journal of Electroanalytical Chemistry*, 417,5-15.
- Panteghini, M.(2004)," Role and importance of biochemical markers in clinical cardiology", *European Heart Journal*, 25,1187-1196.
- Panteghini, M., Cuccia, C., Pagani, F. & Turla, C.(1998)," Comparison of the diagnostic performance of two rapid bedside biochemical assays in the

- early detection of acute myocardial infarction", *Clinical Cardiology*, 21,394-398.
- Park, I., Kima, D.K., Adanyi, N., Varadi, M. & Kim, N.(2004)," Development of a direct-binding chloramphenicol sensor based on thiol or sulfide mediated self-assembled antibody monolayers", *Biosensors and Bioelectronics*, 19,667-674.
- Parker, C.O., Lanyon, Y.H., Manning, M., Arrigan, D.W. & Tothill, I.E.(2009)," Electrochemical immunochip sensor for aflatoxin M1 detection", *Analitical Chemistry*, 81,5291-5298.
- Pepys, M.B. & Hirschfield, G.M.(2003)," C-reactive protein: a critical update (vol 111, pg 1805, 2003)", *Journal of Clinical Investigation*, 112,299-299.
- Perkins, E.A. & Squirrell, D.J.(2000)," Development of instrumentation to allow the detection of microorganisms using light scattering in combination with surface plasmon resonance", *Biosensors and Bioelectronics*, 14,853-859.
- Pessela, B.C.C., Mateo, C., Fuentes, M., Vian, A., García, J.L., Carrascosa, A.V., Guisán, J.M. & Fernández-Lafuente, R.(2004)," Stabilization of a Multimeric  $\beta$ -Galactosidase from *Thermus* sp. Strain T2 by Immobilization on Novel Heterofunctional Epoxy Supports Plus Aldehyde-Dextran Cross-Linking", *Biotechnology Progress*, 20,388-392.
- Péterfi, Z.(2000)," Comparison of blocking agents for an ELISA for LPS", *Journal of Immunoassay*, 21,341-354.
- Piras, L. & Reho, S.(2005)," Colloidal gold based electrochemical immunoassays for the diagnosis of acute myocardial infarction", *Sensors and Actuators, B: Chemical*, 111-112,450-454.
- Pumera, M., Castañeda, M.T., Pividori, M.I., Eritja, R., Merkoçi, A. & Alegret, S.(2005)," Magnetically Triggred Direct Electrochemical Detection of DNA Hybridization Using Au67 Quantum Dot as Electrical Tracer", *Langmuir*, 21,9625-9629.
- Rajesh, Sharma, V., Tanwar, V.K. & Biradar, A.M.(2010)," Electrochemical Impedance Immunosensor for the Detection of C-Reactive Protein in Aqueous Solution", *Sensor Letters*, 8,362-369.
- Reichlin, T., Hochholzer, W., Stelzig, C., Laule, K., Freidank, H., Morgenthaler, N. G., Bergmann, A., Potocki, M., Noveanu, M., Breidthardt, T., Christ, A., Boldanova, T., Merki, R., Schaub, N., Bingisser, R., Christ, M. And Mueller, C.(2009)," "Incremental Value of Copeptin for Rapid Rule Out of Acute Myocardial Infarction"", *Journal of the American College of Cardiology*, 54,60-68.

- Ricci, F., Giulia, V., Micheli, L. & Palleschi, G.(2007)," A review on novel developments and applications of immunosensors in food analysis. ", *Analytica Chimica Acta*, 111–129.
- Ricci, F., Giulia Volpe, Laura Micheli, Giuseppe Palleschi.(2007)," A review on novel developments and applications of immunosensors in food analysis", *Analytica Chimica Acta*, 605,111–129.
- Rifai, N.a.R., P. M.(2001)," High-sensitivity C-Reactive Protein: A Novel and Promising Marker of Coronary Heart Disease", *Clinical chemistry*, 47,403-411.
- Ross, R.(1999)," Atherosclerosis is an inflammatory disease", *American Heart Journal*, 138,S419-420.
- Ross, R. & Harker, L.(1976)," Hyperlipidemia and atherosclerosis", *Science*, 193,1094-1100.
- Sabban, S. 2011. *Development of an in vitro model system for studying the interaction of Equus caballus IgE with its high- affinity FcεRI receptor*. PhD, University of Sheffield.
- Saha, K., Agasti, S.S., Kim, C., Li, X. & Rotello, V.M.(2012)," Gold nanoparticles in chemical and biological sensing", *Chemical Reviews*, 112,2739-2779.
- Salam, F. & Tothill, I.E.(2009)," Detection of Salmonella typhimurium using an electrochemical immunosensor", *Biosensors and Bioelectronics*, 24,2630-2636.
- Santos, E.M., Araujo, A.N., Couto, C.M., Montenegro, M.C., Kejzlarova, A. & Solich, P.(2004)," Ion selective electrodes for penicillin-G based on Mn(III)TPP-Cl and their application in pharmaceutical formulations control by sequential injection analysis", *Journal of Pharmaceutical and Biomed Analysis*, 36,701-709.
- Sattler, K.J., Woodrum, J.E., Galili, O., Olson, M., Samee, S., Meyer, F.B., Zhu, X.Y., Lerman, L.O. & Lerman, A.(2005)," Concurrent treatment with renin-angiotensin system blockers and acetylsalicylic acid reduces nuclear factor kappaB activation and C-reactive protein expression in human carotid artery plaques", *Stroke*, 36,14-20.
- Schreiber, F.(2000)," Structure and growth of self-assembling monolayers", *Progress in Surface Science*, 65,151-257.
- Schroeder, A.P. & Falk, E.(1996)," Pathophysiology and inflammatory aspects of plaque rupture", *Cardiol Clin*, 14,211-220.
- Schulz, R. & Heusch, G.(2011)," C-reactive protein: just a biomarker of inflammation or a pathophysiological player in myocardial function and morphology?", *Hypertension*, 57,151-153.

- Schumacher, J.T.(2001)," Direct Electron Transfer Observed for Peroxidase to Screen-Printed Graphite Electrodes", *Electroanalysis*, , . 13,779–785.
- Scirica, B.M., Cannon, C. P., Sabatine, M. S., Jarolim, P., Sloane, S., Rifai, N., Braunwald, E., Morrow, D. A. And for the Prove It-Timi 22 Investigators.(2009)," Concentrations of C-Reactive Protein and B-Type Natriuretic Peptide 30 Days after Acute Coronary Syndromes Independently Predict Hospitalization for Heart Failure and Cardiovascular Death", *Clinical chemistry*, 55,265-273.
- Sentandreu, M., Aubry, L., Toldrá, F. & Ouali, A.(2007)," Blocking agents for ELISA quantification of compounds coming from bovine muscle crude extracts", *European Food Research and Technology*, 224,623-628.
- Shahar, E., Chambless, L.E., Rosamond, W.D., Boland, L.L., Ballantyne, C.M., Mcgovern, P.G. & Sharrett, A.R.(2003)," Plasma lipid profile and incident ischemic stroke: the Atherosclerosis Risk in Communities (ARIC) study", *Stroke*, 34,623-631.
- Shan, D., Wang, S., He, Y. & Xue, H.(2008)," Amperometric glucose biosensor based on in situ electropolymerized polyaniline/poly(acrylonitrile-coacrylic acid) composite film. ", *Materials Science and Engineering*, 213-217.
- Shaolin, Z., Hankun, Z., Ning, G. & Yuting, C.(2011)," A Renewable C Reactive Protein Amperometric Immunosensor Based on Magnetic Multiwalled Carbon nanotubes Probes Modified Electrode", *Applied Mechanics and Materials*, 80-81.
- Sigma-Aldrich.(2012), *11-Mercaptoundecanoic Acid*, available at: [http://www.sigmaaldrich.com/catalog/ProductDetail.do?D7=0&N5=SEARCH\\_CONCAT\\_PNO%7CBRAND\\_KEY&N4=705241%7CALDRICH&N25=0&QS=ON&F=SPEC](http://www.sigmaaldrich.com/catalog/ProductDetail.do?D7=0&N5=SEARCH_CONCAT_PNO%7CBRAND_KEY&N4=705241%7CALDRICH&N25=0&QS=ON&F=SPEC).
- Silva, B.V.M., Cavalcanti, I.T., Mattos, A.B., Moura, P., Sotomayor, M.D.P.T. & Dutra, R.F.(2010)," Disposable immunosensor for human cardiac troponin T based on streptavidin-microsphere modified screen-printed electrode", *Biosensors and Bioelectronics*, 26,1062-1067.
- Solanki, P.R., Kaushik, A., Agrawal,V., and Malhotra, B (2011)," Nanostructured metal oxide-based biosensors", *NPG Asia Materials*, 17–24
- Spichiger-Keller, U.E. (1998), *Chemical sensors and biosensor for the medical and biological applications*, Wiley-VCH, Weinheim.
- Srisombat, L., Jamison, A.C. & Lee, T.R.(2011)," Stability: A key issue for self-assembled monolayers on gold as thin-film coatings and nanoparticle protectants", *Colloids and Surfaces A: Physicochemical and Engineering Aspects*, 390,1-19.

- Stoeva, S.I., Lee, J.-S., Smith, J.E., Rosen, S.T. & Mirkin, C.A.(2006)," Multiplexed Detection of Protein Cancer Markers with Biobarcode Nanoparticle Probes", *Journal of the American Chemical Society*, 128,8378-8379.
- Stoiser, B., Mörtl, D., Hülsmann, M., Berger, R., Struck, J., Morgenthaler, N. G.,Bergmann, A. And Pacher, R.(2006)," "Copeptin, a Fragment of the Vasopressin Precursor, as a Novel Predictor of Outcome in Heart Failure"", *European Journal of Clinical Investigation*, 36,771-778.
- Storrow, A.B. & Gibler, W.B.(1999)," The role of cardiac markers in the emergency department", *Clinica Chemica Acta*, 284,187-196.
- Sun, H., Koike, T., Ichikawa, T., Hatakeyama, K., Shiomi, M., Zhang, B., Kitajima, S., Morimoto, M., Watanabe, T., Asada, Y., Chen, Y.E. & Fan, J.(2005)," C-reactive protein in atherosclerotic lesions: its origin and pathophysiological significance", *American Journal of Pathology*, 167,1139-1148.
- Sun, X., Du, S., Wang, X., Zhao, W. & Li, Q.(2011)," A label-free electrochemical immunosensor for carbofuran detection based on a sol-gel entrapped antibody", *Sensors (Basel)*, 11,9520-9531.
- Suprun, E.V., Shilovskaya, A.L., Lisitsa, A.V., Bulko, T.V., Shumyantseva, V.V. & Archakov, A.I.(2011)," Electrochemical immunosensor based on metal nanoparticles for cardiac myoglobin detection in human blood plasma", *Electroanalysis*, 23,1051-1057.
- Szmitko, P.E., Wang, C.H., Weisel, R.D., De Almeida, J.R., Anderson, T.J. & Verma, S.(2003)," New markers of inflammation and endothelial cell activation: Part I", *Circulation*, 108,1917-1923.
- Thevenot, D.R., Toth, K., Durst, R.A. & Wilson, G.S.(2001)," Electrochemical biosensors: recommended definitions and classification", *Biosensors and Bioelectronics*, 16,121-131.
- Thim, T., Hagensen, M.K., Bentzon, J.F. & Falk, E.(2008)," From vulnerable plaque to atherothrombosis", *Journal of International Medicine*, 263,506-516.
- Tong, S., Marjono, B., Brown, D. A., Mulvey, S., Breit, S. N., Manuelpillai, U.,and Wallace, E. M.(2004)," "Serum Concentrations of Macrophage Inhibitory Cytokine 1 (MIC 1) as a Predictor of Miscarriage"", 363, 9403.
- Tothill, I.E.(2009)," Biosensors for cancer markers diagnosis", *Seminars in Cell & Developmental Biology*, 20,55-62.
- Tothill, I.E. & Turner, A.(1998)," Biosensors :new developments and oppotunities in the diagnosis of livestock diseases.", *International Atomic Energy Agency*, 79-94.

- Tothill, I.E. & Turner, A. (2003), "Biosensors", in: Benjamin Caballero, Liuz Trugo & Finglas, P. (editors.), *Encyclopedia of food sciences and nutrition*, (2<sup>nd</sup> ed), Academic Press, p. 250-264.
- Turner, A.P.(1998)," Array of hope for biosensors in Europe", *Nature Biotechnology*, 16,824.
- Turner, A.P.F., Karube, I. & Wilson, G.S. (1987), *Biosensors : Fundamentals and applications*, Oxford University Press, Oxford.
- Uludag, Y. 2010. *Development of an Affinity Sensor for Prostate Cancer Diagnosis*. PhD, Cranfield.
- Uludag, Y. & Tothill, I.E.(2010)," Development of a sensitive detection method of cancer biomarkers in human serum (75%) using a quartz crystal microbalance sensor and nanoparticles amplification system", *Talanta*, 82,277-282.
- Van Delden, C.J., Bezemer, J.M., En Gbers, G.H.M. & Feijen, J.(1996)," Poly(ethylene oxide)-modified Carboxylated Polystyrene Latexes - Immobilization Chemistry and Protein Adsorption", *Journal of Biomaterials Science Polymer Edition*, 8, 251-268.
- Van Heusden, F. 2011. *A Novel Quartz-Crystal Microbalance Based Sensor For The Detection Of Cardiovascular Disease Markers*. Master of Science, Cranfield.
- Vaughan, R.D., O'sullivan, C.K. & Guilbault, G.G.(1999)," Sulfur based self-assembled monolayers (SAM's) on piezoelectric crystals for immunosensor development", *Fresenius' Journal of Analytical Chemistry*, 364,54-57.
- Velasco-Garcia, M.N. & Mottram, T.(2003)," Biosensor Technology addressing Agricultural Problems", *Biosystems Engineering*, 84,1-12.
- Verma, S. & Anderson, T.J.(2002)," Fundamentals of endothelial function for the clinical cardiologist", *Circulation*, 105,546-549.
- W.H.O.(2011a), *The Atlas of Heart Disease and Stroke*, available at: [http://www.who.int/cardiovascular\\_diseases/resources/atlas/en/](http://www.who.int/cardiovascular_diseases/resources/atlas/en/).
- W.H.O.(2011b), *Cardiovascular Disease (CVDs) Fact Sheet*, available at: <http://www.who.int/mediacentre/factsheets/fs317/en/index.html>.
- W.H.O.(2011c), *International Statistical Classification of Diseases and Related Health Problems*, available at: <http://apps.who.int/classifications/apps/icd/icd10online/>.



- Wang, J., Pamidi, P.V.A.(1995)," Disposable screen printed electrodes for monitoring hydrazines", *Talanta*, 42,463–467.
- Warwick, M.J. (1996), "Standerdisation of immunoassays", in: Brian, L. (editor) *Immunoassay, A Practical Guide*, (5<sup>th</sup> ed), Tylor and Francis Ltd, London. p. 160.
- Warwick, M.J. (1996 ), "Standardisation of immunoassays", in: Brian, L. (editor) *Immunoassay, A Practical Guide*, Taylor & Francis Ltd., London. p. 160.
- Wild, D. (2000), *Immunoassay Handbook*, Nature Pulishing Group, London.
- Wink, T., J. Van Zuilen, S., Bult, A. & P. Van Bennekom, W.(1997)," Self-assembled Monolayers for Biosensors", *Analyst*, 122,43R-50R.
- Wong-Ek, K., Chailapakul, O., Nuntawong, N., Jaruwongrunsee, K. & Tuantranont, A.(2010)," Cardiac Troponin T Detection Using Polymers Coated Quartz Crystal Microbalance as a Cost-effective Immunosensor.", *Biomedizinische Technik*, 55,279-284.
- Wong-Ek, K., Chailapakul, O., Prommas, J., Jaruwongrunsee, K., Nuntawong, N., and Tuantranont, A 2009. Active Implants and Biosensors *In: Medicine*, G.M.-a.N.I. (ed.) *World Congress on Medical Physics and Biomedical Engineering*. Munich.
- Wu, A.H.(2005)," Markers for early detection of cardiac diseases", *Scandinavian Journal of Clinical Laboratory Investigations Suppliment*, 240,112-121.
- Wu, P. & Grainger, D.W.(2006)," Comparison of hydroxylated print additives on antibody microarray performance", *Journal of proteome research*, 5,2956-2965.
- Yusuf, S., Reddy, S., Ounpuu, S. & Anand, S.(2001)," Global burden of cardiovascular diseases: part I: general considerations, the epidemiologic transition, risk factors, and impact of urbanization", *Circulation*, 104,2746-2753.
- Zhang, Y.X., Cliff, W.J., Schoefl, G.I. & Higgins, G.(1999)," Coronary C-reactive protein distribution: its relation to development of atherosclerosis", *Atherosclerosis*, 145,375-379.
- Zhou, F., Lu, M., Wang, W., Bian, Z.-P., Zhang, J.-R. & Zhu, J.-J.(2010)," Electrochemical Immunosensor for Simultaneous Detection of Dual Cardiac Markers Based on a Poly(Dimethylsiloxane)-Gold Nanoparticles Composite Microfluidic Chip: A Proof of Principle", *Clinical chemistry*, 56,1701-1707.
- Zhu, J.J., Xu, J.Z., He, J.T., Wang, Y.J., Miao, Q. & Chen, H.Y.(2003)," An electrochemical immunosensor for assays of C-reactive protein", *Analytical Letters*, 36,1547-1556.

## APPENDIX A- PUBLICATIONS

### Papers

**W M Fakanya**, I E. Tothill, “Electrochemical Immunosensors for the Detection of the Inflammatory Marker C-Reactive Protein” In preparation

**W M Fakanya**, I E Tothill “The development of an electrochemical multi-marker biosensor for the detection of cardiovascular disease”, In preparation

F. Vanheusden **W.M Fakanya**, I.E Tothill “The detection of cardiac troponin T using a Quartz Crystal Microbalance Sensor Amplified with Nanoparticles”, In preparation

### Conference Posters and Presentation

**W M Fakanya**, I E. Tothill, “A Multi Marker Immunosensor for Cardiovascular Disease Detection”, poster presentation, Biosensors 2012 (Cancun, Mexico) conference, 15-18.05.2012

**W M Fakanya**, I E. Tothill, “Electrochemical Biosensors for the Detection of Cardiovascular Disease”, Oral presentation, Canfield Health Conference, 23.09.2011

**W M Fakanya**, I E. Tothill, “Point of care Sensors for Cardiovascular Disease Diagnosis”, Oral presentation, Translational Medicine Research Meeting, (Gloucester, UK), 04.03.2011

**W M Fakanya**, E. Maryns ,I E. Tothill, “Point of care Sensors for Cardiovascular Disease Diagnosis”, Oral presentation, Dupont Visit (Cranfield , UK), 21.05.2010

# A Multi Marker Immunosensor for Cardiovascular Disease Detection

Fakanya W. and Tothill I.E\*

Cranfield Health, Cranfield University, Cranfield, Bedfordshire, MK43 0AL, UK

## Introduction

Cardio Vascular Disease (CVD) has been listed as one of the premier causes of death worldwide (The World Health Organization (WHO)). CVD accounts for up to 17.5 million annual deaths globally. Research has shown that the information from biomarkers such as Creatine Kinase-MB (CK-MB), Myoglobin, Cardiac Troponin T & I and C reactive protein (CRP) can be crucial not only for diagnosis but also prognosis of CVD. Due to the low specificity and sensitivity of some of the biomarkers, multi marker assessment approaches have been proven to be the most effective in the diagnosis of cardiovascular diseases. Early intervention has been linked to an improved mortality rates and cost effective management of health care services, hence, the need to develop effective versatile multi marker sensor for point-of care testing. This paper describes the development of an electrochemical immunosensor system that can simultaneously detect low concentrations of several cardiac markers in serum samples with sensitivity using nanoparticles.

## Sensor Development

Immunoassays were first developed for C-reactive protein (CRP) and Cardiac Troponin T biomarkers. The assays were optimized in ELISA plates before being transferred to the gold electrodes for the biosensor development. Electrochemical measurements were conducted based on the use of HRP as the enzyme label and TMB /  $H_2O_2$  as the substrate mixture (Figure 1).

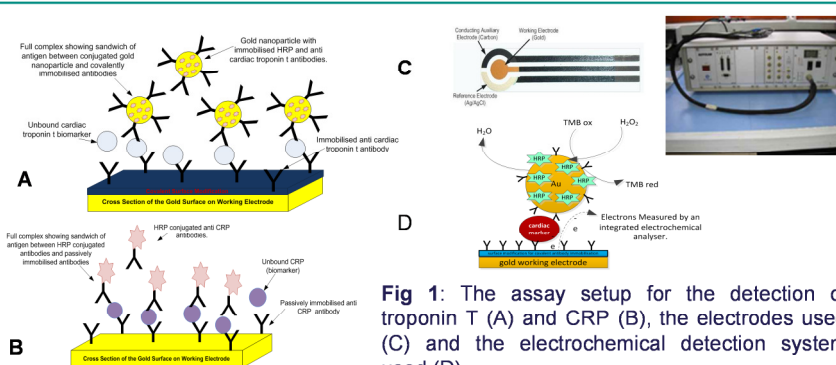


**Fig 1:** The assay setup for the detection of troponin T (A) and CRP (B), the electrodes used (C) and the electrochemical detection system used (D).

## Results

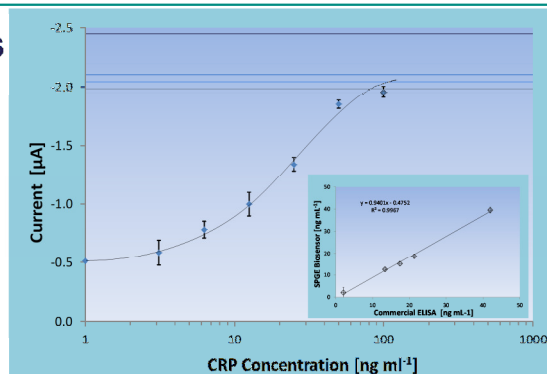


**Fig 2:** Current vs. CRP concentration on the screen-printed gold electrodes. The insert shows correlation of the sensor analysis with a commercial ELISA kit of unknown samples.

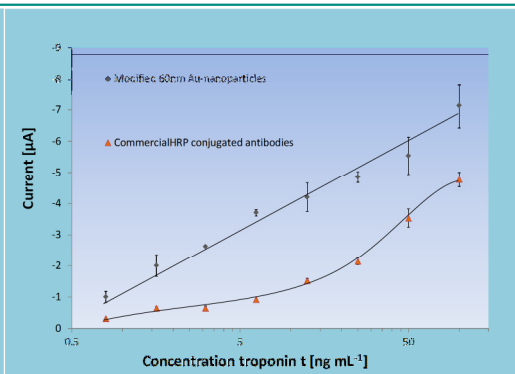


**Fig 3:** Comparison of the sensor signals for troponin T assay with and without the use of gold nanoparticles signal enhancement.

## Conclusions

Immunoassays were developed and optimized for both, the cardiac troponin T and CRP on the electrodes surface. A detection limit of  $2.6 \text{ ng mL}^{-1}$  was achieved for the CRP assay and this was well suited to satisfy the diagnostic range subject to suitable sample dilution (Figure 2). A good correlation was then achieved with a commercial ELISA kit for measuring CRP in serum with  $R^2$  99.7 (Figure 2 insert). Assays were also developed for troponin T and sensitivity was enhanced through the use of gold nanoparticles (Figure 3). The detection limit for cardiac troponin T assay was  $1.1 \text{ ng mL}^{-1}$  and when the assay was enhanced with the use of gold nanoparticle a detection limit of  $0.51 \text{ ng mL}^{-1}$  was achieved. The current troponin values are still higher than the required diagnostic range, but assay optimization is still being conducted to improve it. Other biomarkers will also be considered for the multisensor development.

## Acknowledgements

w.m.fakanya@cranfield.ac.uk

The authors would like to thank DuPont UK Limited (the Microcircuit Materials) for collaborative work in the fabrication of the gold screen-printed sensors and NHS Bedford hospital (pathology department) for analysing troponin t samples.